AD-A076 610 LOCKHEED-GEORGIA CO MARIETTA F/G 1/3
AERODYNAMIC INVESTIGATION OF C-141 LEADING EDGE MODIFICATION FO--ETC(U)
JUN 79 W T BLACKERBY , P R SMITH F09603-77-A-0204
UNCLASSIFIED LG78ER0233-VOL-1 AFFDL-TR-79-3059-VOL-1 NL

1 OF 2
AD A076610

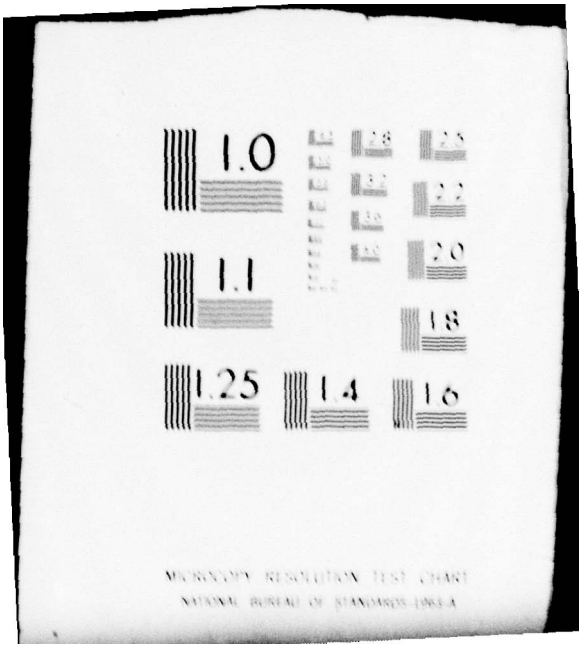
1.0
1.1
1.25
1.4
1.6
2.0
1.8
MICROCOPY RESOLUTION TEST CHART
NATIONAL BUREAU OF STANDARDS 1963-A

AFFDL-TR-79-3059
VOLUME I

LEVEL II

AERODYNAMIC INVESTIGATION OF C-141 LEADING EDGE MODIFICATION FOR CRUISE DRAG REDUCTION

W. T. Blackerby
P. R. Smith

Lockheed-Georgia Company
86 South Cobb Drive
Marietta, Georgia 30063

JUNE 1979

Final Report June 1977 to September 1978

Approved for public release; distribution unlimited

AIR FORCE FLIGHT DYNAMICS LABORATORY
AIR FORCE SYSTEMS COMMAND
WRIGHT-PATTERSON AIR FORCE BASE, OHIO 45433

NOTICE

When Government drawings, specifications, or other data are used for any purpose other than in connection with a definitely related Government procurement operation, the United States Government thereby incurs no responsibility nor any obligation whatsoever; and the fact that the government may have formulated, furnished, or in any way supplied the said drawings, specifications, or other data, is not to be regarded by implication or otherwise as in any manner licensing the holder or any other person or corporation, or conveying any rights or permission to manufacture, use, or sell any patented invention that may in any way be related thereto.

This report has been reviewed and cleared for open publication and/or public release by the appropriate Office of Information (OI), in accordance with AFR 190-17 and DODD 5230.9. There is no objection to unlimited distribution of this report to the public at large, or by DDC to the National Technical Information Service.

This technical report has been reviewed and is approved for publication.

Robert A. Large

ROBERT A. LARGE, Capt, U.S.A.F.
Project Engineer/Technical Monitor

Eric K. Lindberg

ERIC K. LINDBERG, Maj, U.S.A.F.
Chief, Aerodynamics & Airframe Branch

FOR THE COMMANDER:

PETER J. BUTKEWICZ, Col, USAF
Chief, Aeromechanics Division
Air Force Flight Dynamics Laboratory

AIR FORCE/56780/18 September 1979 — 100

SECURITY CLASSIFICATION OF THIS PAGE (When Data Entered)

REPORT DOCUMENTATION PAGE

READ INSTRUCTIONS BEFORE COMPLETING FORM

1. REPORT NUMBER: AFFDL-TR-79-3059-Vol-1	2. GOVT ACCESSION NO.
3. RECIPIENT'S CATALOG NUMBER	
4. TITLE (and Subtitle): AERODYNAMIC INVESTIGATION OF C-141 LEADING EDGE MODIFICATION FOR CRUISE DRAG REDUCTION, Volume 1.	5. TYPE OF REPORT & PERIOD COVERED: Technical / Final (Technical Rept.) June 1977 – Sept 1978
	6. PERFORMING ORG. REPORT NUMBER: LG78ER0233-VOL-1
7. AUTHOR(s): W. T. Blackerby, P. R. Smith	8. CONTRACT OR GRANT NUMBER(s): F09603-77-A-0204-0010
9. PERFORMING ORGANIZATION NAME AND ADDRESS: Lockheed-Georgia Company, 86 South Cobb Drive, Marietta, Georgia 30063	10. PROGRAM ELEMENT, PROJECT, TASK AREA & WORK UNIT NUMBERS: 2404-10-02 (17) 10
11. CONTROLLING OFFICE NAME AND ADDRESS: Air Force Flight Dynamics Laboratory (FXM), Wright Patterson AFB, Ohio 45433	12. REPORT DATE: June 1979
	13. NUMBER OF PAGES: 171
14. MONITORING AGENCY NAME & ADDRESS (if different from Controlling Office) (12) 172	15. SECURITY CLASS. (of this report): Unclassified
	15a. DECLASSIFICATION DOWNGRADING SCHEDULE

16. DISTRIBUTION STATEMENT (of this Report)

Approved for public release; distribution unlimited

17. DISTRIBUTION STATEMENT (of the abstract entered in Block 20, if different from Report)

18. SUPPLEMENTARY NOTES

19. KEY WORDS (Continue on reverse side if necessary and identify by block number)

C-141, Drag Reduction, Fuel Savings, Leading Edge Modification, Wing Design, Transonic, Wing Modification, Wing Drag Rise, Airfoil Drag Rise, Wing Pressure Distributions.

20. ABSTRACT (Continue on reverse side if necessary and identify by block number)

A study of the aerodynamic design and high speed wind tunnel investigation of wing leading edge modifications for cruise drag reduction on the C-141 aircraft has been completed. Also investigated were the effects of a wing swept tip extension and trailing edge anti-drag bodies. These modifications were tested in the AEDC 16-Foot Transonic Facility, using a 0.044 scale C-141B model, to determine the effects on C-141 cruise aerodynamic characteristics and wing chordwise pressure distributions. Design of the leading edge modifications was based on the use of transonic wing (over)

DD FORM 1 JAN 73 1473 EDITION OF 1 NOV 65 IS OBSOLETE

SECURITY CLASSIFICATION OF THIS PAGE (When Data Entered)

210 065

theory, transonic airfoil theory and experience previously gained with a two-dimensional airfoil leading edge modification program. Force data results were analyzed to determine the effects on C-141 cruise drag, drag rise characteristics and cruise performance. Correlations were made with transonic theory using the measured chordwise pressure distributions. A fuel and cost savings evaluation was made of the selected leading edge configuration based on measured and predicted cruise performance improvements.

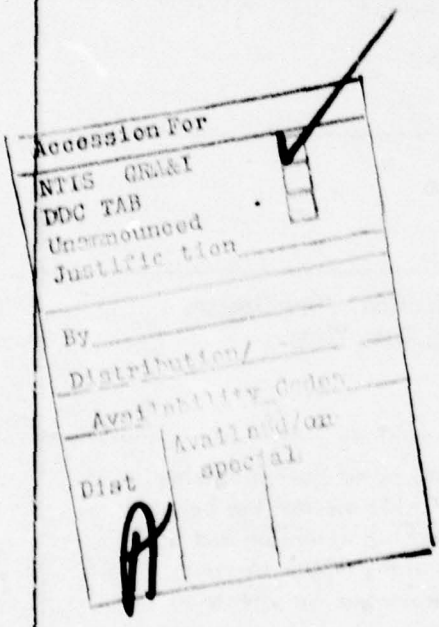

FOREWORD

This is the final report on the aerodynamic design, test and analysis of modified wing leading edges for cruise drag reduction on the C-141 aircraft. This work was performed by the Lockheed-Georgia Company, Marietta, Georgia, under Contract No. F09603-77-A-0204-0010 for the Air Force Flight Dynamics Laboratory. The studies and wind tunnel testing were accomplished between June 1977 and September 1978.

This report is published in two volumes. Volume I covers the aerodynamic design approach for modifying an existing 0.044 scale C-141B model for high speed tests at the AEDC 16-Foot Transonic Facility, the analysis and correlation of the wind tunnel results and a fuel and cost savings evaluation of the performance improvements due to the selected leading edge modification. Volume II contains the details of the wind tunnel model, the test program and plotted wind tunnel test results.

Mr. J. D. Wallace was the Program Manager and W. T. Blackerby was the Technical Leader. The wing leading edge modification design was accomplished by P. R. Smith and M. E. Carlton. The technology base for this program, in the form of transonic analysis and numerical optimization methods for wings and airfoils, was developed by the Advanced Flight Sciences Department at Lockheed-Georgia.

The authors wish to thank J. P. Perdue for assistance in conducting the wind tunnel test and W. F. LaBozzetta for assisting with the analysis of the wind tunnel results and preparation of the final report.

Technical direction for this program was provided by Mr. J. K. Johnson of the Air Force Flight Dynamics Laboratory/FXM.

This report is also identified as LG78ER0233 for Lockheed Corporation's internal control purposes.

TABLE OF CONTENTS

TABLE OF CONTENTS (CONT'D)

LIST OF ILLUSTRATIONS

LIST OF ILLUSTRATIONS (CONT'D)

LIST OF ILLUSTRATIONS (CONT'D)

LIST OF ILLUSTRATIONS (CONT'D)

LIST OF ILLUSTRATIONS (CONT'D)

LIST OF TABLES

LIST OF SYMBOLS

$A_{1, 2, 3, 4}$	Coefficients of independent variable in leading edge curve fit polynomial, upper surface
$B_{1, 2, 3, 4}$	Exponents of independent variable in leading edge curve fit polynomial, upper surface
BL	Butt line
b	Wing span
$C_{1, 2}$	Coefficients of independent variable in leading edge curve fit polynomial, lower surface
C_D	Drag coefficient
C_{D_C}	Compressibility drag coefficient
$C_{D_{MIN}}$	Minimum drag coefficient
C_{D_W}	Wave drag coefficient
C_L	Lift coefficient
$C_{L_{TAIL-OFF}}$	Tail-off lift coefficient
C_M	Pitching moment coefficient
$C_{M_{c/4}}$	Pitching moment coefficient about the quarter chord
C_P	Pressure coefficient
$C_{P_{MIN}}$	Minimum pressure coefficient
C_P^*	Critical pressure coefficient for M = 1

LIST OF SYMBOLS (CONT'D)

c	Chord
$\bar{c}$	Average chord
c_d	Section drag coefficient
c_l	Section lift coefficient
c_{l_i}	Section design lift coefficient
FRL	Fuselage reference line
FS	Fuselage station
L/D	Lift to drag ratio
LE	Leading edge
M	Mach number
MAC	Mean aerodynamic chord
M(L/D)	Cruise range parameter
MOD	Modification
q	Dynamic pressure
R_k	Reynolds number based on height, k
R_N	Reynolds number
WL	Water line

WS	Wing station
X/C, x/c	Non-dimensional chordwise location
x	Chordwise distance
x_l	Chordwise distance, lower surface
x_{NOSE}	Chordwise location of leading edge point
Y/C, y/c	Non-dimensional ordinate
y	Ordinate or vertical location
y_l	Lower surface ordinate
y_o	Ordinate at leading edge
y_u	Upper surface ordinate
2D	Two-dimensional
3D	Three-dimensional
α	Angle of attack
Δ	Incremental
η	Non-dimensional semi-span location
Λ	Sweep angle
Λ_{EFF}	Effective sweep angle based on local flow

WIND TUNNEL MODEL CONFIGURATION SYMBOLS

B^{12}	Fuselage - C-141B base; basic C-141A fuselage with 280 inch full scale extensions
K^{19}	Pylons - engine nacelles
N^{8}	Nacelles - flow through, with inlet spinners
P^{4}	Aerial refueling pod-prototype production
W^{12C}	Wing-basic high/low speed W^{12} steel wing with removable leading edge (forward 12% chord). 3 panels each semi-span
W^{35}	Wing - W^{12C} with 3-D CONMIN leading edge
W^{36}	Wing - W^{12C} with 2-D test airfoil leading edge
Z^{a2}	Antenna fairing - located on top of fuselage, aft of wing
Z^{f1}	Anti-shock bodies - flap track fairing type, wing trailing edge, 8 per semi-span
Z^{f2}	Anti-shock bodies - flap track fairing type, wing trailing edge, 4 per semi-span
Z^{G21}	Wheel well fairing
Z^{t6}	Wing tip - swept, chord/span ratio = 1.33
Z^{W7}	Wing-fuselage fillet - C-141A production

WIND TUNNEL MODEL CONFIGURATION SYMBOLS (CONT'D)

S^1	$B^{12}{}_K{}^{19}{}_N{}^8{}_P{}^4{}_Z a2_Z G21_Z W7$
S^2	$B^{12}{}_P{}^4{}_Z a2_Z G21_Z W7$

SUMMARY

A research program has been conducted to investigate the potential for cruise drag reduction for several modifications to the C-141 wing leading edge.

The program consisted of the aerodynamic design of two alternate leading edge contours, fabrication of necessary model components, a high speed wind tunnel test, analysis and correlation of the test results, and an evaluation of the effects on C-141 cruise performance, fuel and cost savings.

Two design approaches were employed during the aerodynamic design of the leading edge candidates. One design was based on application of a 3-D numerical optimization scheme coupled with an inviscid full potential code. An alternate leading edge was designed using previous experience gained during a 2-D leading edge investigation. In the latter case the ordinates from a successfully tested C-141 2-D leading edge modification were scaled to fit several control stations on the wing with linear lofting between stations.

The test was conducted at the Arnold Engineering Development Center 16-Foot Transonic Wind Tunnel in April 1978. Analysis of the test data led to the selection of the 3-D design leading edge as the preferred configuration. In addition to high speed evaluation of the leading edges, two other drag reduction concepts were evaluated: swept wing tips and wing trailing edge anti-drag bodies.

A drag reduction goal of from 5 to 7 percent of total cruise drag was established for the modified leading edge designs, based on previous 2-D test results and theoretical predictions. As tested, the selected leading edge (3-D design) produced only about one-half the design goal. This result is shown to be consistent with the fact that the fabricated model contours for the leading edges differed from the design in such a way as to lessen the measured drag improvement. By correlating theoretically predicted drag with experimental 2-D and 3-D drag as a function of the upper surface

ordinate at two percent chord, it is shown that the predicted drag reduction would be achieved for the design leading edge contours. Accordingly, performance improvements are presented for both the leading edge modification as tested and as predicted. As tested, an increase in the long range cruise parameters, M(L/D), of 2.4 percent was obtained. Based on the correlation, an improvement in M(L/D) of 5.7 percent is projected for the design leading edge modification.

Increased cruise speed is also an important result for the modified leading edges. The test results show a $\Delta M = 0.015$ increase in cruise speed and a predicted increase of 0.03 is indicated. This effect provides an additional potential benefit of increased productivitiy for the C-141.

Substantial drag reductions were shown for the swept tip and anti-drag body configurations. The swept tip modification provides a 17 count reduction in induced drag at cruise with further reductions in compressibility drag at high Mach numbers. The anti-drag bodies improve the drag rise characteristics beyond the normal cruise Mach number. Increased cruise speed for both the swept wing tip and anti-drag bodies are indicated, with potential productivity improvements.

Cost and fuel savings analyses for the selected leading edge demonstrate that the savings for high utilization aircraft such as the C-141 are impressive. Assuming no increase in productivity, the predicted leading edge would save 25 million gallons of fuel per year for the C-141 fleet. With productivity increases, a total of over 43 million gallons of fuel are saved. On a cash flow basis, assuming a fuel cost of 60 cents per gallon, the former case would save almost $15 million in fuel costs per year. Including the productivity increase, the fuel cost savings would reach nearly $25 million annually. Over the remaining life of the C-141 fleet, the accrued savings could reach over 800 million gallons of fuel and approximately a half billion dollars of fuel costs.

SECTION I
INTRODUCTION

Requirements for efficient transonic performance of aircraft continues to lead aerodynamicists to explore new concepts and apply emerging technology to the design of future fuel-efficient aircraft. The aerodynamicist also must recognize the importance of applying such technology to improve the performance of current production aircraft where practical. In particular, aircraft such as the C-141A, which utilizes approximately 15% of the total Air Force fuel allotment, should be continually evaluated against a framework of advancing technology to identify and develop modifications with pay-off potential.

Lockheed-Georgia has given special attention to several concepts which could reduce the C-141 cruise drag and hence lower fuel consumption. One concept which appears feasible is to modify the wing leading-edge contour, forward of the front spar, to reduce the subsonic creep drag and premature compressibility drag.

The C-141A wing was designed in the early 1960's prior to the development of advanced technology "peaky" airfoils and the recent "supercritical" airfoil types. As a result, the C-141A wing airfoil sections are not as aerodynamically efficient as those that would be designed today. The C-141A aircraft is characterized by a significant amount of drag increase prior to the onset of drag divergence and Lockheed-Georgia studies indicate that a major portion of this drag is associated with the wing.

Recent airfoil research on peaky and supercritical airfoils has demonstrated the importance of the upper and lower surface chordwise pressure distributions in the design of high-speed airfoils. In particular, attention has been focused on pressures over the region from the upper surface leading edge back to the airfoil crest. In this region, several characteristics of the pressure distribution,

such as the amount of leading-edge suction, the shape of the recompression region aft of the minimum pressure, and the pressure at the crest, are related to the development of creep drag, pre-shock drag losses, and premature shock formation. Flight and wind tunnel measurements of the C-141 chordwise wing pressure demonstrate the non-existence of favorable leading edge suction at cruise conditions. Since the C-141 has no leading edge high lift device, the region forward of the front spar (12% chord) could be modified at low cost with a possible reduction of 5 to 7 percent in cruise drag. Consequently, the C-141 wing represents an excellent candidate for application of redesign efforts based on advanced technology methods.

Lockheed-Georgia researchers, in conjunction with the Air Force Flight Dynamics Laboratory and researchers at NASA/Ames have been studying ways to improve the C-141 wing aerodynamics. Several efforts have resulted. An independent Research and Development Program at Lockheed-Georgia investigated the use of viscous transonic airfoil theory to design small leading edge contour changes to improve a two-dimensional C-141 airfoil. These concepts were experimentally verified at the Lockheed-Georgia Compressible Flow Facility.

Following this, a research contract was awarded by AFFDL to Lockheed-Georgia to apply these concepts to investigate three-dimensional application of leading edge modifications to the C-141 wing. An existing large scale (0.044) model of the C-141B was chosen for use in an experimental program to evaluate the relative merits of the modified leading edges. This report, in two volumes, presents the results of this program, including the design, wind tunnel test data, data analysis and correlation studies. Volume I gives summary results of the wind tunnel test, data analysis and correlation with theoretical predictions. Volume II contains the details of the test facility, model configuration, program and procedures, and the basic wind tunnel test data.

SECTION II

AERODYNAMIC DESIGN

1. BACKGROUND - TWO-DIMENSIONAL DESIGN AND TEST

Drag Characteristics for the C-141A, as determined from both flight and wind tunnel tests, exhibit an increasing drag with increasing Mach number throughout the subsonic Mach number range. These characteristics are summarized in Figure 1. The wind tunnel results in Figure 1 reveal that the basic airfoil and wing also experience subsonic drag rise, or creep drag, of the same order of magnitude as that of the airplane.

Previous studies to determine the source of the C-141 wing creep drag characteristic indicate that the problem is not related to induced drag changes or premature flow separation as Mach number increases. Attention has, therefore, been directed toward the more likely source of increased profile drag due to viscous and pressure losses.

Independent Research and Development (IRAD) studies were initiated at the Lockheed-Georgia Company to understand more fully the relationships between pressure distributions and the creep drag phenomena as they occur on 2-D airfoils such as that of the C-141A.

Initial efforts were directed toward comparing the creep drag and drag rise characteristics of a number of recently developed supercritical airfoils with the characteristics of more conventional airfoil shapes such as the C-141 airfoil. In addition to the well known trailing edge cusp region effects, another geometric characteristic, leading edge contour, emerged as an important determinant of airfoil drag rise performance. An example of this is shown in Figure 2. The two research airfoils are essentially the same except over the forward 15 percent chord. The peaky leading edge characteristic results in a moderate pressure peak with a weaker shock

development which is further aft than the shock on the airfoil without the leading edge peak.

The influence of the leading edge peak is evidenced throughout the Mach number range, causing improved creep drag as well as drag rise performance. Since the pressure distribution and drag characteristics of the C-141 wing are similar to those exhibited by the non-peaky airfoil in Figure 2, it was reasoned that a re-design of the upper surface of a C-141 airfoil to provide a more favorable pressure distribution should produce an accompanying drag reduction. Therefore, the IRAD studies were expanded to include the design, test and analysis of a series of leading edge modifications to a two-dimensional C-141 airfoil model. For the C-141, practical considerations restrict the extent of modification to the forward 12% chord, thus limiting the amount of drag reduction which might be achieved.

An existing 2-D model of an airfoil equivalent to the C-141 wing at η = 0.389, previously fabricated for testing in the Lockheed-Georgia Company Compressible Flow Wind Tunnel (CFWT), was cut at the 12% chord location and modified to accept a removable leading edge. A replacement leading edge was constructed using the original airfoil ordinates to provide a baseline airfoil for comparison.

A number of designs were developed using manual iteration of the viscous airfoil theory of Bauer, et al.[1] One design was also determined during a cooperative effort with NASA/Ames using the 2-D CONMIN method which was under development at Ames.[2] [3] This latter design procedure also verified the previous modifications to the leading edge contour determined from the manual iteration scheme using the viscous theory.

Results for the baseline and two of the modified leading edges are summarized in Figure 3. The 2-D CONMIN leading edge, LE 6, uses the existing lower surface shape and is thus a more practical modification. Several larger pertubations, such as LE 3A, were included in the program to provide a range of leading edge shapes. Figure 3(b)

illustrates relative changes of the flow over the leading edges and demonstrates that weaker shock formations were achieved with the modifications. The drag rise data of Figure 3(c) shows the substantial improvement of both LE 6 and 3A over the baseline. Although the expected reductions in creep drag at the low and intermediate Mach numbers ($M < 0.65$) did not materialize, creep drag is lessened for $M > 0.65$ and an increase in drag divergence Mach number of approximately 0.02 is achieved. At $M_{2D} = 0.73$, corresponding to a cruise Mach number of 0.775, a drag reduction of 11 counts is indicated. For most conditions evaluated during the study, LE 6 proved to be as good or better than any of the others, thus verifying the capability of the CONMIN design approach and also emphasizing that the modification may be simply applied to the upper surface only.

At the section lift coefficients which correspond to the equivalent 2-D local lift coefficients at cruise on the mid and outer span portions of the C-141 wing, drag reductions of 11 to 16 counts were typical. Since 15 counts of drag represents about 6 percent of the C-141 cruise total, a design goal of 5 to 7 percent drag reduction for the wing was adopted as a standard for the aerodynamic design.

2. DESIGN METHODOLOGY

Three leading edge modifications were designed for the current study, from which two were selected for model fabrication and testing in conjunction with the basic C-141 leading edge. The first modification was designed using a Lockheed-Georgia version of 2-D CONMIN, extended to permit a wider range of design variables. A three-dimensional numerical optimization scheme under development by Hicks, similarly extended in scope, was employed to obtain a second leading edge modification. The third leading edge was based on the best of the 2-D modifications tested in the Lockheed-Georgia CFWT.

Analysis of the resulting 2-D equivalent airfoils was accomplished using the Bauer 2-D viscous transonic code. The leading edge modification based on the 3-D design code was further analyzed with the

Bailey-Balhaus and Jameson 3-D inviscid transonic wing codes. A summary of the design procedure is shown in block diagram form in Figure 4. Details of the individual design methods are given in the following sections.

a. 2-D CONMIN Approach

Analytical 2-D transonic flow computer codes have been generally available for several years, the most prominent, perhaps, being the Bauer et. al. code[1], known at Lockheed-Georgia as the TAP Program. Comparable design codes are currently under development. An excellent code has been developed by Carlson[4], which computes the airfoil ordinates required to match the input pressure distribution. This method, however, requires the prior definition of the leading edge, and is therefore unsuitable for the current application.

An alternative approach has been introduced by Hicks[5] which involves the use of numerical optimization of the airfoil contours to achieve the desired aerodynamic characteristics while maintaining constraints on specified variables. The method known as 2-D CONMIN, is based on the constraint-minimization scheme of Vanderplaats[6] which employs the Method of Feasible Directions as the basic optimization algorithm. Evaluation of the objective and constraint functions is made using the inviscid mode of the TAP program, and the main calling program is supplied by the individual user to satisfy his own requirements. This method was adopted for one of the theoretical leading edge modifications in the current study.

Two control stations on the wing were chosen for the 2-D modification - WS 373 (η = 0.389) on the inboard panel, and WS 761 (η = 0.793) on the outboard panel. These stations were chosen because they corresponded to those at which model test chordwise pressure distributions were available[7], and were typical of the sections on their respective wing panels. The presence of significant three-dimensional flow effects prevented optimization of the root and tip sections.

It was necessary to convert the three-dimensional basic wing sections into equivalent 2-D ordinates. This was accomplished using simple sweep corrections based on the sweep angle of the chord location at which the upper surface shock occurs at the 3-D design point represented by M = 0.775 and C_L = 0.50. Examination of the model test pressure distribution indicated that the shock occurs at approximately 50 percent chord, resulting in sweep angles of 18.457 degrees and 22.728 degrees for the inner and outer wing panels respectively. The 3-D wing ordinates and design Mach number were factored in accordance with the simple sweep relationships:

$$(y/c)_{2D} = (y/c)_{3D}/\cos\Lambda$$

$$M_{2D} = M_{3D}\cos\Lambda$$

Selection of the 2-D design lift coefficients was handled in a slightly different manner. The measured 3-D pressure distributions are affected by the presence of the fuselage, pylons and nacelles, which induce a lower surface lift loss not present in the isolated wing case. Thus there is no direct correspondence between the 2-D calculated upper surface pressure distribution and that measured in the wind tunnel for the equivalent 3-D lift coefficient. Since the leading edge modification was limited to the first 12 percent of the wing chord, the desired aerodynamic improvement at the design condition must result from changes in the upper surface pressure distribution and reduction in local Mach number ahead of the shock. It was therefore necessary to insure that the 2-D theory was run at a lift coefficient which would reproduce the 3-D wing upper surface pressure distributions in terms of $C_{P_{MIN}}$, shock strength and shock location. As shown in Figure 5, the 2-D TAP viscous theory provided excellent upper surface pressure correlation with the 3-D test pressures when run at lift coefficients somewhat higher than those obtained by simple sweep corrections. In these figures, the 2-D calculated pressures have been factored by $\cos^2\Lambda$ to retain 2-D to 3-D equivalence.

The next task was to choose curve fit equations for the leading edge contour, whose coefficients and exponents could be perturbed in the optimization process. Based on previous experience, the following equations were selected:

Upper Surface

$$y_u = y_o + A_1 x^{B1} + A_2 x^{B2} + A_3 x^{B3} + A_4 x^{B4} = y_o + \sum_{n=1}^{4} A_n x^{Bn}$$

Lower Surface

$$y_l = C_1 x^{B_{AV}} + C_2 x + y_o$$

where $B_{AV} = (B_1 + B_2 + B_3 + B_4)/4$

Initial exponent values were input as follows:

$$B_1 = 0.4;\ B_2 = 0.7;\ B_3 = 1.0;\ B_4 = 2.0;\ y_o = 0$$

These resulted in the following coefficients required to fit the basic C-141 2-D airfoil leading edge upper surface:

$\underline{\eta = 0.389}$

$A_1 = 0.084335;\ A_2 = 0.15273;\ A_3 = -0.15281;\ A_4 = -0.030996$

$C_1 = -0.200977;\ C_2 = .194520$

$\underline{\eta = 0.794}$

$A_1 = 0.06877;\ A_2 = 0.27321;\ A_3 = -0.28619;\ A_4 = -0.032942$

$C_1 = -0.200105;\ C_2 = 0.243282$

The calling program SUB1 was written at Lockheed-Georgia to define C_D/C_L as the objective function to be minimized and to constrain the following variables:

$$C_L \geq 0.74$$
$$-0.3 \leq C_M \leq +0.3$$
$$-0.01 \leq y_o \leq +0.01$$

Design variables which could be perturbed were:

$$A_1, A_2, B_1, B_2, B_3, B_4, y_o, \alpha, M, x_{NOSE}$$

The A_3 and A_4 coefficients were computed by the program to permit the modified leading edge upper surface contour to match the ordinate and slope of the basic airfoil at the front beam location. Similarly the C_1 and C_2 coefficients were calculated to match the lower surface front beam ordinate and slope.

Preliminary runs with the 2-D CONMIN code indicated that the A_1 and A_2 coefficients were less powerful than the other design variables. Mach number was held constant at the 2-D design value, since the program tended to want to reduce it below the design condition in minimizing the C_D/C_L objective function. Attempts to vary the chord length by varying X_{NOSE} led to the conclusion that the basic chord length gave the lowest value of C_D/C_L at or near the design conditions. Accordingly the final runs which defined the leading edge modification were made with six design variables, i.e., the four exponents, y_o, and angle of attack.

The optimized leading edges are shown in Figure 6. At both control stations the upper surface was raised above the basic contour due primarily to positive values of y_o of approximately 0.5 percent chord.

A comparison of the modified and basic theoretical 2-D inviscid pressure distributions as computed by 2-D CONMIN for the η = 0.389 station is given in Figure 7. The computed section wave drag coefficient for the modified leading edge was reduced by 20 counts at the 2-D design lift coefficient. The modified pressure distribution features increased leading edge suction, followed by an isentropic

recompression which resulted in a reduced shock strength. A similar improvement resulted at the $\eta = 0.793$ outboard wing control station.

The complete three-dimensional wing was obtained by linear lofting the leading edge from the existing root section through the $\eta = 0.389$ modified section to obtain an extrapolated wing break section. From the break station the leading edge was then linear lofted through the $\eta = 0.793$ modified section to obtain an extrapolated tip section.

The contract called for the design and test of two modified leading edges. Comparison of the 2-D CONMIN modification with the 3-D CONMIN modification described in Section II.2.c. showed close similarities in ordinates, theoretical pressure distributions and drag coefficients. Accordingly, the 2-D CONMIN airfoil was subordinated to the 2-D test airfoil described in the next section in the selection process of the modifications to be tested.

b. 2-D Test Airfoil Approach

During the IRAD studies, discussed in Section II.1., a total of four leading edges were tested and compared with the basic C-141 airfoil. The most promising modification based on analysis of the test results was identified as LE 6. Unlike the other test airfoils, which had been derived by trial and correction methods using the TAP analysis program, LE 6 had been designed using an early version of the 2-D CONMIN numerical optimization scheme described in the previous section. This version, which was extended to include additional design variables during the current study as described in Section II.2.a., retained the same lower surface and y_o value of the basic airfoil. As a candidate for one of the two leading edge modifications to be tested, the choice of a three-dimensional leading edge based on the LE 6 2-D airfoil had three major advantages:

1) The airfoil retained the same lower surface as that of the basic C-141.

2) As such it was a distinct alternative from the other numerically optimized leading edges.

3) The 2-D airfoil had already been successfully tested, and the 2-D test data was available for correlation with the subsequent 3-D test data, thus permitting an assessment of pure 3-D effects.

Since LE 6 was a modification of the basic section at η = 0.389, it was necessary to derive a comparable section at the η = 0.793 control station. This was accomplished by using the following relationship:

$$y_{u_{(\eta = .793)_{MOD}}} = (y_{u_{LE\ 6}} \times y_{u_{(\eta = .793)_{BASIC}}})/y_{u_{(\eta = .389)_{BASIC}}}$$

The three-dimensional wing was then lofted using the method described in Section II.2.a. The model designation for this wing design is W^{36}.

c. 3-D CONMIN Approach

The Vanderplaats CONMIN scheme has recently been applied to the numerical optimization of three-dimensional wings[8]. The method was extended for application to the design of a third modified leading edge candidate. Procedurally, the 3-D CONMIN scheme is similar to that for 2-D CONMIN described in Section II.2.a. The major advantage of the 3-D scheme is its ability to account for the 3-D effects at the root and tip, which is not possible with a purely 2-D method.

The number of design variables was increased to permit curve fitting of the leading edge at a maximum of four control stations. Stations at the root, WS = 113, (η = 0.118), break, WS = 426 (η = 0.445) and tip, WS = 958 (η = 1.0) were used in the present study. The flow program used to calculate the objective function and constraints was the 3-D full potential inviscid code of Jameson (FLO 22).[9]

The form of the curve fit equations used for the leading edge upper surface were identical to those for 2-D CONMIN:

$$y_{u(k)} = y_o + \sum_{n=1}^{4} A_{(n,\,k)} x^{B(n,\,k)}$$

where k = index of wing station

$$y_{l(k)} = y_o + C_1 x^D + C_2 x$$

Initial exponent values were input as follows:

$$B_{(1,\,k)} = 0.2;\ B_{(2,\,k)} = 0.6;\ B_{(3,\,k)} = 1.0;\ B_{(4,\,k)} = 1.0$$

A calling program was written to define C_{D_W}/C_L as the objective function to be minimized and to constrain the following variables:

$$C_L \leq 0.60$$

$$-0.015 \leq y_{o_1} \leq .01$$

$$-0.01 \leq y_{o_2} \leq .013$$

$$-0.01 \leq y_{o_3} \leq .01$$

Design variables which could be perturbed were:

A_1, A_2, B_1, B_2, B_3, B_4, D, y_o at each wing station plus angle of attack.

The A_1, A_2, C_1, C_2 variables were computed by the program to permit leading edge matching at the full scale design conditions of M = 0.77 and C_L = 0.46. The wave drag computed by the inviscid FLO 22 code was virtually zero. Accordingly, a Mach number of 0.79 was input to give the CONMIN scheme a large enough value of C_{D_W}/C_L on which to optimize. The final computer run which established the leading edge

modification was made with thirteen design variables, i.e., B_1, B_2, D and Y_O at each station, and angle of attack.

The resulting optimized leading edges at each station are shown in Figure 8. At the root station the nose was lowered relative to the basic leading edge. This result takes into account the 3-D wing centerline effects and could only be obtained using a 3-D optimization scheme. At the break and tip stations the nose point was raised in a manner similar to that obtained by 2-D CONMIN. The inviscid pressure distributions computed by the 3-D CONMIN flow program are presented in Figure 9. The theoretical wave drag is reduced from 51 counts to 42 counts. This wing design is designated W^{35}.

3. ADDITIONAL DRAG REDUCTION CONCEPTS

Two additional wing modifications were included in the wind tunnel test portion of this study to evaluate additional drag reduction potential for the C-141 aircraft. These two modifications were: swept wing tips (extended span), and a series of wing trailing edge bodies called anti-drag bodies spaced across the wing. The necessary model components for these configurations were provided at the expense of the Lockheed-Georgia Company and the test time was included in the overall test program with the agreement and cooperation of the Air Force Flight Dynamics Lab. Design considerations for these two modifications are discussed in the next two sections.

a. Wing Swept Tips

The rationale for the employment of swept wing tips on the C-141 wing is two-fold. First, the obvious increase in aspect ratio reduces the induced drag for a given wing lift coefficient. Simultaneously, the overall lowering of the wing loading for a given total lift should tend to reduce shock losses on the wing at the higher cruise speeds. The second objective of the wing tip modification is to sweep the leading edge to counter the tendency for the isobars on the present wing to become unswept at the tip. The amount of extension and sweep was determined for this C-141 wing

application based on experience with similar applications on the Lockheed C-5A wing. The tip planform is sketched in Figure 10.

b. Wing Anti-Drag Bodies

Lockheed-Georgia experience with development tests on the C-5A flap-track fairings indicated that such fairings could be designed to provide a net drag reduction notwithstanding the increased profile drag due to the fairings themselves. Analysis of the C-5A results show that the major effect at cruise speeds must be a reduction in shock strength due to an effective change in camber. For application to the C-141 wing an approach to design of a set of anti-drag bodies, similar to flap-track fairings, was devised as follows: Assuming that a favorable change in 2-D camber could be applied to the 3-D wing by means of properly sized anti-drag bodies, use was made of the 2-D TAP airfoil analysis program to determine the effects of changes in camber. To increase the aft camber in a manner which could be approximately represented by isolated bodies at the trailing edge, a lower surface modification was devised as shown in Figure 11(a). The lower surface ordinates were modified by the addition of thickness which varied from zero at X/C = 0.65 to 2 percent at the trailing edge. Figure 11 (b) shows the effect on the theoretical pressure distribution. In comparison with the basic airfoil, the higher aft loading permits a reduction in section angle of attack from 2.7 degrees to 0.9 degrees. This results in a decrease in upper surface shock strength coupled with a rearward shock movement, which reduces the section compressibility drag from 24 counts to 5 counts.

The increase in lower surface trailing edge thickness of 2 percent chord was converted into a spanwise cross-sectional area distribution at the trailing edge. To ensure a reasonable representation of this distribution with adequate spacing to prevent local channel flow interference effects, a total of eight bodies on each wing was chosen, with the most outboard body located at the inboard edge of the aileron. Figure 12 shows a sketch of the body locations on the wing.

SECTION III
WIND TUNNEL DATA ANALYSIS

1. GENERAL

Presentation of the basic wind tunnel data for the various configurations tested is to be found in Volume II of this report. Summary curves, comparison plots and discussion of the principal analytical results are presented in this section.

Volume II also contains a detailed description of the wind tunnel facility, model, instrumentation, test conditions, schedule and data reduction. The test was conducted at the Arnold Engineering Development Center 16-foot Transonic Facility in April 1978 and is designated as Test TF-481. The model was a 0.044 scale C-141B with an internal balance for 6-component force measurement and pressure instrumentation for four stations on the wing. The forward 12% chord of the wing was removed and three new sets of leading edges were fabricated, one set to replace the baseline C-141 leading edge and two modified sets for evaluation. Structural break locations and the locations of the four pressure measuring stations are shown on the model wing planform sketch in Figure 13. Locations of the nacelle and anti-drag body centerlines are also shown in Figure 13.

2. MODIFIED LEADING EDGE RESULTS

a. Transition Fixing

Previous test results on a two-dimensional C-141 airfoil, modified in a manner and amount similar to that used for this program, indicate that the increased leading edge suction of the modified airfoil compared to the baseline produces a forward shift in natural transition location. This is illustrated in Figure 14. The favorable pressure gradient over the leading edge of the modified airfoil extends only to about 2-3 percent chord, whereas the basic airfoil has a favorable gradient (no peak) almost to the shock. Thus the

transition would be expected to be further forward on the modified leading edge. The fixed transition/free transition drag comparisons of Figure 14 show a larger increment between fixed and free drag levels at the lower test Reynolds number for the basic airfoil. This is characteristic of a further aft extension of the laminar boundary layer on the basic airfoil relative to the modified. Analytical results for these two airfoils using viscous transonic theory such as TAP substantiate this effect. The significance of this transition phenomenon is that the additional drag associated with the more extensive turbulent boundary layer on the modified airfoil obscures the effectiveness of the modification as a drag reduction device. Therefore, careful attention to the details of transition fixing technique and verification of transition location are important aspects of any experimental evaluation of leading edge modifications as described here.

Several different methods were employed during AEDC TF-481 in order to minimize transition location differences and any possible correction to the data for transition. These are discussed in Volume II. The results of the analyses described in Volume I show that the model contour differences between the basic and modified leading edges were smaller than planned, therefore any possible transition correction would be insignificant and a single method was selected for the leading edge drag evaluation. The preferred method, coded as Method D in Volume II, consists of a light application of Ballotini glass beads in a narrow band (0.05 inches wide) located 0.7 inches from the leading edge. This method is based on the work by Braslow[10], for a critical roughness Reynolds number criterion $R_K \geq 600$. Because of time limitations during the test, all three leading edge configurations were not tested using each of the methods. Method D was used on the baseline and W^{35} leading edges but not on W^{36}. The leading edge results for W^{36} are based on transition fixation using Method C which is similar to Method D except that the transition band is located at a constant percent chord location near the leading edge.

Experiments at AEDC, reported by Keeney[11], establish a preferred technique for visually substantiating the location of transition at the AEDC 16T facility. This method is a sublimation technique wherein a film of fluorescent oil is sprayed over the wing

surface and under ultraviolet lighting, the variation in film thickness caused by the shearing action of the boundary layer gives an indication of transition. Based on AEDC experience[11], a solution of fluorene/trichloroethane (trico) was selected for sublimation checks during the C-141 testing.

Fixed and free transition results at approximately the cruise condition (M = .77, $\alpha = 1^{\circ}$) are shown for the basic wing and modified wing W^{35} in Figure 15. In these photos, the white areas over the leading edge indicate where the solution has not sublimed and the boundary layer is still laminar. The 12% chord break line can be seen in all these photos and is a good reference line. For the fixed transition cases, the grit line can also be seen. Transition on the basic wing is seen to occur naturally at or aft of the 12% chord location whereas, for W^{35} natural transition is generally ahead of the 12% line. In both cases, the grit strip successfully moves transition forward to the strip. Again, the actual location of transition (fixed) on W^{35} may be slightly ahead of the basic wing. This is as expected but the differences are quite small and no correction for transition is indicated.

b. Chordwise Pressure Distribution Comparisons

Chordwise pressure distributions at the four spanwise pressure stations for the base (W^{12C}) and 3-D modified (W^{35}) wings are compared in Figures 16 through 19 for M = 0.7, 0.75, 0.77 and 0.79. An angle of attack of approximately 1.2°, corresponding to C-141 cruise conditions, was chosen for these comparisons.

The effect of the inboard leading edge droop, designed into W^{35} by the 3-D CONMIN method, can be seen in the $\eta = 0.193$ pressure data. Since this apparently does not improve the transonic flow development on the model, future design permutations would not include this characteristic. The comparisons at $\eta = 0.418$ indicate that the increased leading edge peak of W^{35} does occur over the middle part of the wing with a corresponding favorable effect on the flow. This effect is quite localized as can be seen by examination of the results

at η = 0.637 and 0.793. The pressure distributions for the base and W^{35} wings are very similar at these two stations. Therefore, the improvement area for W^{35} is limited to between about η = 0.3 and η = 0.55. Since it is known that the compressibility drag on the C-141 wing at cruise extends from η = 0.3 to about η = 0.85, these data indicate that less than half of the critical area is favorably affected.

c. Effect of Pylon/Nacelles on Chordwise Pressure Distributions

The pylon/nacelles-off configuration was incorporated into the test program primarily to provide a source of clean-wing pressure data for correlation of 3-D wing transonic codes. No degradation of the leading edge effects due to the pylon/nacelles is anticipated but these data also should offer insight into that possibility.

Figures 20 and 21 compare chordwise pressure distributions for the base wing and W^{35}, with and without pylon/nacelles installed on each wing. These data show that the effect of the pylon/nacelles is essentially the same on both wings. A lower surface loading change is obvious on the two inboard stations. Since these two pressure measuring stations are at least one nacelle diameter away from the nacelles, see Figure 13, any severe localized pressure disturbances are somewhat attenuated. Results for the two outboard stations are surprising in that lower surface effects have almost completely attenuated, however, the upper surface loading for a constant angle of attack has been decreased and the shock moved forward by the addition of the pylon/nacelles.

Comparisons are made in Figure 22 of W^{12C} and W^{35} chordwise pressure distributions for the pylon/nacelles-off configuration. These data show leading edge effects which are the same as those observed previously with the pylon/nacelles installed. Therefore, although the pylon/nacelles evidently have a slightly unfavorable effect on the basic wing flow development, there is no degradation of the leading edge effect.

d. Aerodynamic Characteristics

(1) Repeatability

The importance of data accuracy, especially the drag force measurement, cannot be over emphasized in an evaluation of this type where small increments between configurations are to be measured. The accuracy of the data acquisition is discussed in some detail in the report documenting the test data by Spurlin of AEDC[12]. Balance uncertainties of ± 7 to 10 drag counts are quoted for the Mach number and angle of attack corresponding to the cruise range for the C-141. During Test TF-481 the accuracy, as evidenced by the final results, was considerably better than this. Figure 23 illustrates how this conclusion can be made. In Figure 23, repeat runs are shown for the baseline configuration, one set taken at the start of the test and the second set taken near the end of the test. The repeatibility within a run as well as from run-to-run, is excellent, about ± 1 to 3 drag counts. For most configurations, a large number of data points were taken, with repeats at $\alpha = 0$, so that inaccuracy due to scatter may be minimized by judicious fairing of the data. Therefore, the accuracy for the results reported here are believed to be within 1 to 2 drag counts between configurations. Accuracy of the lift and pitching moment data are seen to be close to the limits given by Spurlin[12], ± 0.002 for C_L and ± 0.0005 for C_M, except at the high C_L/M combination where shock location repeatability becomes a significant factor affecting both lift and pitching moment.

(2) Lift, Drag and Pitching Moment Characteristics

Lift, drag and pitching moment characteristics for the base wing, W^{12C}, and modified wing W^{35} are compared in Figure 24. The leading edge modification has no significant effect on the aerodynamics at M = 0.7 where most of the differences are seen to be within the accuracy of the test data. At higher Mach numbers, as exemplified by the M = 0.79 data on Figure 24, some improvement is noted, starting at approximately $C_L = 0.4$. A lift increase, at constant angle of attack, is accompanied by a drag decrease at constant lift coefficient. This is due to the improved supersonic flow development over the wing with the modified leading edge described above. At $\alpha = 1.2^{\circ}$,

the lift increase is 0.01 and at C_L = 0.5, the drag reduction is approximately 9 to 10 drag counts. The nose down pitching moment shift (ΔC_M = -.005) associated with the change is considered insignificant, as it represents less than 0.1 of a degree of stabilized trim change for the C-141.

(3) Drag Rise Characteristics

Drag rise summaries for the base wing and W^{35} for a range of lift coefficients are shown in Figures 25 and 26. These data were interpolated from the drag polars contained in Volume II at constant lift coefficient. A comparison is made in Figure 27 of the drag rise for both wings at three lift coefficients near the cruise value. Since these data are tail-off and untrimmed, the cruise lift coefficient is approximately 0.5, corresponding to a trimmed airplane lift coefficient at cruise of 0.46. The low speed drag level remains essentially unchanged whereas a decrease in creep drag between M = 0.7 and M = 0.76 and an improved drag divergence Mach number is evidenced. Similar data for the pylon/nacelles-off configuration are shown in Figures 28, 29 and 30. The comparison of Figure 30 shows an improvement due to the wing modification which is close to that observed in Figure 27. This result increases confidence in the indicated benefits of W^{35} and also implies that the pylon/nacelle installation does not adversely affect the leading edge aerodynamic improvement.

Drag rise results for W^{36} and the base are summarized in Figures 31, 32 and 33. Improvements in the drag rise characteristics of W^{36}, relative to W^{12C}, similar to those observed for W^{35} can be noted. However, the magnitude of the effects are less than for W^{35}. This is believed due to several factors. First, the amount of leading edge change associated with W^{36} was less than W^{35} by design and the results were anticipated to be intermediate to W^{35}. Second, as noted in Section III, 2, a, W^{36} was not tested using the selected transition fixing technique and thus the comparison basis is not the same. This represents an unknown factor which could be unfavorable to the W^{36} leading edge effect. For these reasons, the W^{35} leading edge was selected as the preferred configuration. Accordingly, all the theoretical correlations and pay-off evaluations detailed subsequently in this report are based on the W^{35} leading edge modification.

e. Incremental Drag and Pitching Moment

Incremental drag and pitching moment coefficients for the selected leading edge, W^{35}, are summarized in Figure 34 for constant values of tail-off untrimmed lift coefficient. Since no corrections are believed necessary, these data are increments taken directly from the plotted results of Volume II. Scatter, amounting to ± 0.0001 in C_D and ± 0.001 in C_M have been faired out in Figure 34 to provide systematic variations with C_L and Mach number. At a typical cruise point for the C-141, approximately M = 0.77 and $C_{L_{TAIL-OFF}} = 0.5$, the W^{35} modification reduces drag by about 5 counts. This increases to over 9 counts at M = 0.79. Pitching moment changes are seen to be less than -0.005 over the cruise range.

3. AERODYNAMIC CORRELATION OF LEADING EDGE EFFECTS

a. Comparison of Theoretical and Measured Wing Ordinates

Fabrication of the basic and two modified leading edges was accomplished by applying a standard method for model wing construction to shape the forward 12 percent of the wing. This method consisted of the use of wing station templates at several spanwise control stations, shown on Figure 13, fit to the existing wing aft of the 12 percent chord location. The templates for each station were based on theoretical ordinates for the C-141 wing aft of 12 percent chord combined in each case with the appropriate theoretical ordinates for the leading edge portion. Previous experience with the template/control station procedure at the Lockheed-Georgia Model Shop has resulted in model accuracies of 0.001 to 0.002 inches.

Validation of the wing ordinates with each leading edge in place shows that for this application the procedure was successful for the leading edges inboard of the wing planform break, ($\eta \approx 0.43$). However, for the outboard wing, significant deviations from theoretical

contours were found. Measurements were made along the pressure instrumented stations for each leading edge in order to compliment the correlation process. Comparisons of these measured contours and their theoretical or design counterparts are made in Figures 35, 36 and 37. The basic wing agreement at η = 0.418 is within 0.002 inches and this is typical of the results for all three leading edges inboard of η = 0.418. As can be seen, the deviations on all three leading edges vary considerably for the outboard stations. Generally, the basic leading edge is fuller than the theoretical by as much as 0.02 inches, and the modified leading edges are undercut by as much as 0.02 inches. Although these are small deviations, which might not be critical over the mid-chord to trailing edge regions of a wing, they represent critical differences for a leading edge study of this type. Figure 38 illustrates the magnitude of the problem. Basic and W^{35} contours are compared for both the theoretical and measured ordinates at η = 0.793. At this station, 0.01 inches amounts to 0.13 percent chord for the model, and since both contours have moved toward each other by approximately that amount, then the overall difference between the basic and modified leading edges has decreased by 0.26 percent. This represents about half of the difference which was intended by the W^{35} design change at the η = 0.793 station. Similar comparisons for W^{36} and for the other measured stations show that the trends of Figure 38 are typical for both leading edges for the entire outer wing panel.

b. Comparison of Theoretical and Measured Pressure Distributions - Equivalent 2-D Method

Correlations are made in this section of the experimental pressures measured during the test and theoretical predictions based on the 2-D viscous transonic code, TAP[1]. The equivalent 2-D method is employed, as discussed in Section II, wherein an effective sweep angle is used to convert the 3-D wing ordinates to equivalent 2-D sections for theoretical analysis. The measured pressure coefficients are also ratioed to their 2-D counterpart for comparison with the TAP results. This process was used during the design phase of this study to analyze the flow characteristics of the modified airfoil shapes at various stations on the model wing. In order to verify the procedure,

it is important that the test results be similarly analyzed. If it can be shown that 2-D transonic theory can be used to predict the effect of relatively small changes in leading edge contour on the flow development and associated drag, then the equivalent 2-D approach is a very useful interim method for the aerodynamicist until 3-D viscous transonic codes become economically feasible and well proven.

Two types of comparisons are made in this section. The first group of comparisons relates to the degree of success achieved with the TAP program in matching the chordwise pressure distribution shapes, shock location, shock strength, etc. The second group is included to compare the leading edge effects predicted by the theory for both the design and measured wing ordinates. For the first group, an iterative process is followed to find the TAP lift coefficient, which provides the best match of the experimental upper surface pressure distribution. This implies that any fuselage and nacelle over-pressure effects are relegated to the lower surface. While this may not in fact be true, by matching the upper surface loading the proper wave drag can be determined and a close simulation of the boundary layer effects made. The second group of comparisons is made for a constant lift coefficient and Mach number using the TAP theoretical predictions. In this way the leading edge effects can be systematically compared.

The C-141 wing, because of its high aspect ratio, moderate sweep angle and relatively low taper ratio, represents a good candidate for correlation using the equivalent 2-D method. It is recognized, however, that 3-D effects dominate the pressure distributions at the root and tip. Accordingly, the 2-D investigation has been limited to the wing stations from $\eta = 0.418$ to $\eta = 0.793$.

Results for the first group of correlations, are given in Figures 39 and 40. The comparisons for the three outboard stations on the basic wing, shown in Figure 39, are typical of the high degree of accuracy attainable with the TAP theory. Theoretical predictions are shown for both the design and measured model wing ordinates. At the

η = 0.418 station, where the measured ordinates are very close to the design ordinates, no difference in the pressure distribution is predicted and the theoretical pressures match the measured values quite well. The conventional airfoil characteristic of a collapsed peak is obvious in the η = 0.418 data. Shock location is predicted exactly in Figure 39 and the suppressed shock strength in the experimental data is probably a residual effect of the inboard lambda shock sometimes noticed on the C-141 wing at this station. The theory predicts the shape of the lower surface pressure distribution but an almost constant overpressure of ΔC_p = 0.15 results from the upper-surface matching.

A noticeable difference is seen between the two theoretical upper surface pressure distributions over the leading edges of the two most outboard stations, η = 0.637 and 0.793. Predictions for the design ordinates show a shape similar to the η = 0.418 distribution and to previous wind tunnel and flight test pressure data for the outboard portion of the C-141 wing, whereas, the TAP theory for the measured ordinates shows increased leading edge suction, relative to the design ordinate case.

Although the increased leading edge suction has an important influence on the transonic flow development, the significance to be gained from these comparisons is the remarkable agreement between the experimental pressure over the leading edges and those predicted for the measured ordinates. Of note also are the facts that the TAP theory predicts the shock location to within 2 or 3 percent chord and the shock strength for these outboard stations. The lower surface pressure distribution shapes are also duplicated at both stations with some residual over-pressure along the entire chord length. It is surprising to observe that the over-pressure effect has not attenuated significantly even at the η = 0.793 station.

The comparisons of Figure 39 are repeated in Figure 40 for the modified leading edge W^{35}. The results and conclusions are quite similar, except in this case the TAP data for the measured ordinates

show decreased leading edge suction relative to the design ordinate case for the two outboard stations. Again, a more favorable agreement is achieved between the measured ordinate TAP theory and the experimental data. These results give added confidence to the capability of the TAP program to monitor the effects of the relatively small leading edge shape differences involved in this study.

After having established that the TAP theory can predict the flow over the tested wing shapes, including the effect of small differences in local contour, the theory was used to compare leading edge effects for both the measured and design ordinate cases. These comparisons were made for a series of constant Mach number/lift coefficient conditions for several spanwise stations on the wing.

Typical results are shown in Figures 41, 42 and 43. In Figure 41(a) can be seen the expected differences in leading edge characteristics at η = 0.793 which were designed into the modified leading edges. The 2-D conditions, M_{2D} = 0.73 and c_1 = 0.75, correspond to 3-D conditions of M = 0.79 and C_L = 0.5. These conditions are slightly above cruise conditions (M = 0.77 and C_L = 0.46), but were selected to ensure that the comparisons were made somewhat into the drag rise where wave drag differences can be seen more clearly. The actual leading edge differences at η = 0.793 are shown in Figure 41(b) for the same conditions using the measured ordinates as input to the TAP theory. The results are as expected. The differences have been decreased in each case, partly due to the increased ordinates on the base leading edge and partly due to the decreased ordinates on the measured modified leading edges. Similar results for η = 0.637 are shown in Figure 42. These data show that, for the outboard portion of the wing, the actual leading edge effects are approximately one-half of the desired effects. Additional evidence of these results is presented in the Figure 43 comparisons for M_{2D} = 0.71, M_{3D} = 0.77.

c. Comparison of Predicted and Measured Drag Results

Having established that the transonic airfoil theory accurately predicts the shock location and strength for the C-141 wing on an equivalent 2-D basis, it now remains necessary to investigate how well the corresponding drag predictions compare with the test results. In this section, TAP theoretical drag is compared with the experimental results for the wing modified leading edges as well as previously tested 2-D airfoil modified leading edges. The drag used for these comparisons is, for the TAP case the incremental wave drag calculated by the theory, and for the experimental data, an incremental drag taken from some nominal low speed level (M = 0.7) where compressibility effects are minimal.

A convenient parameter was sought which could be used to summarize the effect of leading edge modification on drag. The overlay of leading edge shapes shown in Figure 39 shows that the major geometric difference amongst the leading edges is the vertical displacement of the forward contours. Thus the amount of change between the baseline leading edge shape and any of the modified and/or measured leading edge shapes can best be described by the non-dimensional airfoil ordinate at some forward location on the upper surface. Since the maximum ordinate deviation occurs at approximately the 2 percent chord location, this point was chosen as the best parameter for correlating the leading edge effects on drag.

The results for the 2-D airfoil test are shown in Figure 44. The section lift coefficient of 0.7, chosen for this comparison, is the equivalent 2-D lift coefficient for the mid-span portion of the C-141 wing at the cruise lift coefficient. Test data for two Mach numbers are shown for the baseline airfoil (LE 1) and two modified leading edges (LE 4 and LE 6). A significant decrease in wave drag occurs with increase in upper surface ordinate for both the test airfoils and the theory for LE 6. Average slopes are drawn through the test data to compare with the slope of the theoretical prediction. The theory tends to under-predict the test data, probably because the theoretical prediction only considered wave drag effects, whereas the test data

includes the additional effects of the shock on the boundary layer and associated form drag.

A similar chart, Figure 45, is used to compare the AEDC measured 3-D test results with predictions based on the equivalent 2-D theory. Since the relationship between 3-D and 2-D drag is unknown and the subject of this correlation, a single wing station, $\eta = 0.793$, was chosen as representative of the wing and the variation in leading edge ordinate. Theoretical calculations for both the design and measured ordinate cases for all three leading edges at $\eta = 0.793$ have been plotted and the consistency of the results is quite good. Because of the differences between measured and design ordinates, the range between the design baseline and W^{35} is covered and the slope of compressibility drag versus leading edge ordinate is well established. The test results are plotted at the appropriate measured ordinate for each leading edge. These test drag increments were taken from the wing/fuselage configuration at the cruise lift coefficient and therefore include interference and form drag effects not represented in the 2-D theoretical calculations. Consequently, the theoretical 2-D slope is less than the slope indicated by the 3-D experimental data. This characteristic is similar to that shown in Figure 44, but a closer alignment of slopes exists in Figure 45. Since the $\eta = 0.793$ station is used to represent the entire wing, absolute correlation is not anticipated and would be fortuitous if it occurred. The importance of these comparisons is the consistent trends established by the 2-D theory at $\eta = .793$ and the agreement of the test results with these trends.

d. Drag Reduction for the Design Leading Edge Modification

On the basis of the agreement between the theoretical and experimental drag results detailed in the previous section, and the successful correlation of drag with the airfoil upper surface ordinate, it is possible to determine the drag reduction which would be obtained with the design contours for the leading edge modification.

Figures 44 and 45 have shown that the theory (equivalent 2-D method plus viscous transonic airfoil theory) can be used to conservatively estimate the improvements for the range of leading edge ordinate change investigated. In Figure 45, the measured drag reduction for W^{35} relative to the basic wing is about 7 counts at M = 0.78. Using the conservative theoretical prediction, this reduction would increase to at least 13 counts for the design ordinates as opposed to the model measured ordinates. Recalling, from Section II.1, that the 2-D tests results indicated drag reductions of 11 to 16 counts for sections across the wing, it is reasoned that the drag reduction goal of 5 to 7 percent would have been achieved for the design W^{35} contour.

Consequently, both measured and predicted drag levels have been included in the performance and economic pay-off evaluations presented in Section IV. In order to cover the complete Mach number and lift coefficient range, the 2-D test results were used to determine the aerodynamic data for the design leading edge contours.

4. SWEPT TIP RESULTS

The effects of the swept wing tip on chordwise pressure distributions at the four pressure stations are shown in Figure 46 at the cruise condition, M = 0.77 and $\alpha = 1.2^{\circ}$. Comparisons of the lift, drag and pitching moment characteristics, tip on and off, are presented in Figure 47 for M = 0.77. The additional lift at $\alpha = 1.2^{\circ}$, approximately $\Delta C_L = 0.025$, is primarily concentrated at the tip as the pressure data shows. At $\eta = 0.793$, some indication of a favorable effect on the tip isobars is seen, as the shock has been moved aft approximately 5 percent chord. The expected large savings in wing induced drag due to the 9.5 percent increase in wing span are realized as Figure 47(b) reveals. A slight trim penalty would be encountered by the airplane to offset the nose down pitching moment shift seen in Figure 47(a). At $C_L = 0.5$, the pitching moment increment is $\Delta C_M = -.024$, which corresponds to approximately one-half degree of stabilizer trim change for the C-141.

Drag rise characteristics for the swept tip configuration are plotted in Figure 48 and are compared in Figure 49 with data for the baseline configuration from Figure 33. Drag increments due to the tips are summarized in Figure 50 for constant values of tail-off lift coefficient. These results show that in addition to the induced drag change, an improvement in compressibility drag does occur above about M = 0.76. At C_L = 0.5 and Mach number below 0.76, the induced drag reduction amounts to about 17 drag counts, whereas, at M = 0.79 the drag is reduced by 31 counts, indicating 14 counts less compressibility. This constitutes further evidence that the swept tips are improving the shock losses over the wing, especially at the tip where the isobars on the basic wing become unswept.

Because the swept tip modification alters the wing loading in the region of the tip, the center of pressure for the wing is shifted outboard a significant amount. Figure 51 illustrates this effect. The actual load distribution shape outboard of η = 0.793 is unknown and an extrapolation has been made which approximates the additional lift measured. The location of the wing center of pressure can be determined from the spanwise loads and are shown in Figure 51 for the basic wing and with the swept tip. During the wind tunnel testing several runs were made with only one of the modified tips installed in order to provide asymmetric rolling moment data from which an incremental center of pressure movement could be found. The resulting increments calculated from these data have been applied to the basic wing data and are also shown on Figure 51. The incremental center of pressure at cruise lift is approximately 2.3 percent of the wing semi-span for both methods.

5. ANTI-DRAG BODY RESULTS

Two anti-drag body configurations were tested during the AEDC TF-481 wind tunnel test, one using the baseline wing with eight per side as designed and located on Figure 13, the second using W^{35} with four per side formed by removing every other body starting with the one closest to the fuselage. Chordwise pressures were obtained only

on the eight anti-drag body configuration and typical results are shown in Figures 52 and 53 for constant angle of attack and constant lift coefficient, respectively. It is clear from Figure 52 that the design objective of increasing camber was achieved with the anti-drag bodies. At constant alpha, the upper surface loading is increased substantially for all four pressure stations with the shock moving aft 5 to 10 percent except at the most inboard station. Good carry-over of the upper surface change is evidenced at the η = 0.793 station which is somewhat outboard of the last anti-drag body, see Figure 13. The lower surface load change is more significant inboard and has somewhat attenuated at the η = 0.793 station.

Because of the increased lift associated with the camber effect, the angle of attack for a constant lift coefficient is considerably less. This can be seen in Figure 53. For a constant C_L = 0.5, the alpha is lower by almost a degree. Thus, for constant lift, the upper surface loading is reduced for the anti-drag body configuration relative to the basic wing loading, and the shock has moved aft with reduced strength. A comparison of the η = 0.418 data, Figure 53(b), with the theoretical 2-D data of Figure 11 illustrates how well the 2-D design approach achieved the desired effect.

Force data for the eight and four anti-drag body configurations are compared with the baseline in Figures 54 and 55. The almost constant increase in lift coefficient at all angles of attack, approximately ΔC_L = 0.09 for the eight body case, is further evidence of the camber-increase effect of the anti-drag body design. The lift increase for the four body case, ΔC_L = 0.045, is half that of the eight body case, indicating that the lift effects are somewhat linear. This is not the case for the drag effects. A larger drag increase occurs for the eight body configuration at low C_L's due to the profile drag of the bodies. At higher C_L's, this drag is overcome by the camber effect on the shock losses, so that a net drag reduction occurs at C_L's above about 0.47 in Figure 54(b). Similar data in Figure 55(b) for the four anti-drag body case show that the profile drag penalty at low C_L's is very small, and although the effect on

compressibility is less, the net drag reduction at C_L's around the cruise point is about the same as for the eight body case. At higher loading conditions, the accrued benefits for the eight body configuration are superior to those for the four. Thus, some optimization process is indicated to achieve the maximum improvement with the minimum wing trailing edge modification.

Drag rise characteristics for the eight and four anti-drag body configurations are presented in Figures 56 and 57. Comparisons with the appropriate baseline drag rise are made in Figures 58 and 59 for each anti-drag body configuration. Since the four body case was tested with the W^{35} leading edge, and with free transition, Figure 59 may not reflect the true effect of the four body case on the base, W^{12C} wing. However, assuming that it does, these comparisons show substantial drag savings for both configurations above $M \simeq 0.76$ and $C_L = 0.5$.

Incremental drag data for the two anti-drag body configurations at constant lift coefficient are shown in Figures 60 and 61. Corrections have been applied to these data to account for the Reynolds number effect on skin friction so that the increments correspond to full-scale flight conditions. The effectiveness of the four body configuration is to be noted for $M < 0.78$. The net drag reduction at 0.5 lift coefficient and $M = 0.78$ is about 9 counts which is essentially the same as for the eight body case. Above $M = 0.78$ the four body configuration shows no additional improvement, whereas the compressibility drag reduction for the eight body configuration continues to increase.

Spanwise load distribution and center of pressure data for the eight anti-drag body configuration are presented in Figure 62. The additional camber inboard is seen to cause a redistribution of the load which shifts the center of pressure inboard by approximately 0.8 percent. This represents an additional favorable effect for the anti-drag bodies which might be useful from a structural standpoint.

SECTION IV

PERFORMANCE AND LOADS ANALYSIS

1. SPANWISE LOAD CHANGES DUE TO THE SELECTED LEADING EDGE

Typical spanwise load distributions for the selected leading edge, W^{35}, are compared with the baseline in Figure 63. These comparisons are made for a constant $\alpha = 1.2^{\circ}$ at two cruise Mach numbers. Recalling that the 3-D CONMIN design program "drooped" the leading edge inboard and raised the outboard leading edge, effectively reducing the twist distribution helps explain the results of Figure 63. For a constant lift coefficient, the inboard load is decreased and the outboard load increased slightly. These changes are quite small and the center of pressure would only move outboard less than 0.2 percent of the wing semispan. Since the drooped inboard leading edge is not considered the preferred direction for the inboard leading edge modification, an optimum design would employ no change or a slight increase in the inboard ordinates. Under those circumstances, the load re-distribution would be even less than indicated for these data and would, in either case, be inconsequential to the overall wing loads and have no impact on the wing structure.

2. SUMMARY OF EFFECTS ON C-141B CRUISE PERFORMANCE, PRODUCTIVITY AND MISSION FUEL FOR THE SELECTED LEADING EDGE

In order to determine the net effect of the leading edge modification on C-141 performance, it is necessary to establish the proper baseline performance level, determine the proper wind tunnel results and how to apply these to the baseline, and investigate any corrections to the data necessary for full-scale application. Previous sections have discussed various aspects of these steps and have, in effect, provided the information required to fulfill the performance analysis. This section presents an outline of the information leading to the performance appraisal.

The baseline configuration for the performance evaluation in this study is the C-141B aircraft, as flight tested and reported by Lockheed[13], modified to incorporate the C-141A wing/fuselage fillet fairing. Performance improvements for the leading edge modification are incremental to the performance for this aircraft, herein referred to as the C-141B with "A" fillet.

The leading edge which shows the most promise, based on the AEDC TF-481 results, is the 3D CONMIN or W^{35} leading edge. Since the baseline and W^{35} model contours are known to be different from the design or theoretical shapes, performance improvements for the predicted W^{35} leading edge, as well as the experimental W^{35} leading edge, are included in this summary. For the experimental W^{35}, the actual test drag increments are applied to the C-141B with "A" fillet results for a given Mach number and trimmed lift coefficient. Similarly, the predicted drag increments for W^{35} are applied to the full-scale data.

No corrections are applied to the tested drag increments. Since the geometric changes are so small, the only potential corrections would be due to differences in model transition location for the baseline and W^{35} leading edges, trim drag changes, and any structural considerations affecting drag. In section III.2.a, it was shown that the model transition differences are insignificant and no correction was determined. Pitching moment changes were shown in Figure 24 to require less than 0.1 of a degree of stabilizer trim change between the baseline and W^{35}. Even double this amount, which might occur for the predicted W^{35} leading edge, would represent an insignificant trim drag change. The load distribution effects, shown in Section IV.1., demonstrate that no structural problems would be incurred for the addition of the leading edge modification, and thus no drag penalty is assessed in this area. Finally, the primary drag benefit of the modified leading edge appears to be a compressibility-type improvement. This type of drag reduction is assumed to be independent of scale effects and therefore, the total measured wind tunnel drag increments are applied directly to the full-scale drag.

The cruise lift coefficient for the C-141 is typically 0.46, trimmed, and has been chosen for the cruise summary comparisons. This value corresponds to approximately $C_{L_u} = 0.5$ for the tail-off untrimmed test results reported herein. Figure 64 summarizes the effect of the leading edge modification on the C-141B with "A" fillet drag rise and range parameter, M(L/D), for a constant trimmed $C_L = 0.46$. Two conclusions can be drawn from these results. First, an increase in the range parameter is indicated for both leading edges above M = 0.74. Commensurate with the increased range parameter is an increase in the cruise Mach number. Cruise speed for the C-141B with "A" fillet is M = 0.754 and, assuming that the modified aircraft would cruise at or near the maximum M(L/D) point, an increase in cruise Mach number of about 0.015 is possible for the tested W^{35} configuration and 0.03 for the predicted W^{35}. The corresponding improvements in the range parameter are 2.4 percent for the tested W^{35} and 5.7 percent for the predicted W^{35}.

The combination of reduced drag and increased cruise speed provides a potential for even greater fuel savings than that due just to drag reduction. By taking advantage of the higher speeds, the productivity of the C-141 is increased. In other words, by cruising at the higher speeds indicated in Figure 64, mission time for a given mission, will be reduced accordingly as well as the fuel flow reduction indicated by the range parameter change. A $\Delta M = 0.03$ change is equivalent to about four percent of mission time for a typical long range cruise mission. A summary of the effects of the leading edge modification on C-141 performance, using the predicted and experimental W^{35} drag reduction, is presented in Table 1 for two basic assumptions; first, that the C-141 fleet is maintained at constant flight hours, thus accruing only the drag reduction benefit; and second, that constant productivity is maintained and accumulated benefits from the speed increase are also included. These results are based on the current C-141 peacetime fleet utilization rate of 1170 flight hours per aircraft per year. Penalties to specific fuel consumption for cruise at the higher speeds have been included in these data.

TABLE 1

EFFECT OF LEADING EDGE MODIFICATION
ON FUEL AND FUEL COST SAVINGS

PREDICTED W^{35}

	*FUEL SAVINGS (MILLION GAL/YR)		**FUEL COST SAVINGS (MILLION $/YR)	
	ANNUAL	20 YEARS	ANNUAL	20 YEARS
CONSTANT FLIGHT HOURS	18.4	367.2	8.5	170.0
REDUCED FLIGHT HOURS (CONSTANT PRODUCTIVITY)	29.4	585.3	13.6	271.0

EXPERIMENTAL W^{35}

	*FUEL SAVINGS (MILLION GAL/YR)		**FUEL COST SAVINGS (MILLION $/YR)	
	ANNUAL	20 YEARS	ANNUAL	20 YEARS
CONSTANT FLIGHT HOURS	7.8	156.0	3.6	72.0
REDUCED FLIGHT HOURS (CONSTANT PRODUCTIVITY)	13.9	278.0	6.4	128.7

NOTE. * BASED ON CURRENT PEACETIME UTILIZATION

** BASED ON CURRENT FUEL PRICE = 46.3¢ PER GALLON

From Table 1, the savings are seen to be significant for both assumptions. Based on the leading edge improvements, as tested, a total savings of 7.8 million gallons of fuel per year would be realized after fleet modification and for operating at constant fleet hours. An additional 6.1 million gallons would be saved for operations at the higher cruise speeds and constant productivity. Thus a total savings of 13.9 million gallons of fuel per year would be possible with the selected leading edge (as tested). Table 1 also shows a substantial increase in the fuel savings for performance based on the predicted W^{35} leading edge modification. For constant flight hours, 18.4 million gallons of fuel savings are indicated, increasing to 29.4 million gallons for constant productivity. For each case shown in Table 1, fleet cost savings have been computed for an assumed fuel cost of 46.3 cents per gallon. Installation of the predicted W^{35} leading edge modification would accrue $8.5 million in savings annually for the constant flight hour assumption and almost $13.6 million annually for constant productivity.

The C-141 aircraft is known to have a substantial structural life and, at current utilization rates, the aircraft should be in service for at least 22 more years. Over this time frame, the aerodynamic and performance improvements will have an enormous impact on fuel utilization and cash flow. Figure 65 illustrates the potential savings in fuel which would accrue for the two leading edge configurations over the remaining life of the C-141 fleet. The constant productivity line for the predicted W^{35} leading edge shows that by the end of the projected life, the total savings are over 540 million gallons of fuel.

The potential fuel cost savings are also impressive. Assuming an average cost of 46.3 cents per gallon of fuel (a conservative value based on 1978 prices), cost savings equivalent to the fuel savings can be determined. The results are shown in Figure 66. Within 10 years from the completion of the modification program, the cost savings for the predicted W^{35}/constant productivity case reach nearly 150 million dollars. Over the remaining life, the savings to the Air Force for the C-141B fleet would be approximately one quarter of a billion dollars.

SECTION V

CONCLUSIONS AND RECOMMENDATIONS

A comprehensive analytical and wind tunnel test program has been conducted on several leading edge modifications to the C-141 wing in order to evaluate cruise drag reduction and fuel savings potential for the C-141 fleet. The principal conclusions follow.

a. A successful application of 2-D and 3-D transonic numerical optimization methods (CONMIN) to design improved leading edge contours for the C-141 wing has been demonstrated. The degree of experimental success was limited by differences between the design ordinates and the actual ordinates on the 0.044 scale C-141 model wing as tested at AEDC. Three sets of leading edge designs were developed: one set based on a 3-D CONMIN scheme in conjunction with an inviscid transonic full potential code; another based on a 2-D CONMIN code; and the third was derived by tailoring a successful 2-D shape, previously tested, to the 3-D wing. The first and third sets, designated W^{35} and W^{36}, respectively, were built and tested during this program. The 2-D CONMIN design was similar to the W^{35} leading edge and did not provide an alternative.

b. Excellent correlation of theoretical predictions with the experimental results was achieved. Using an equivalent 2-D approach and a 2-D viscous transonic analysis code, duplication of the test chordwise pressure distributions was obtained for the measured wing ordinates. The capability of the theory to predict subtle differences in leading edge flow development and shock formation due to small perturbations in leading edge shape was demonstrated. In addition to the pressure distribution correlations, the analytical results were also used to derive a correlation of compressibility drag based on the amount of leading edge change. This was done by plotting the predicted wave drag versus the ordinate at 2 percent chord for both the design and measured ordinate airfoils at η = 0.793. Compressibility drag from the test was similarly plotted using the measured ordinate values. Comparison of these results showed that over the measured ordinate range, the test compressibility drag increments between

the baseline and modified leading edges agrees with the predicted wave drag increments.

c. The best leading edge, according to the AEDC test data, is W^{35} for which a drag reduction at cruise of approximately 5 to 9 counts was tested. Because of the high degree of success obtained with correlations, especially the drag/leading edge ordinate comparison, it is concluded that the target drag reduction goal of between 5 and 7 percent cruise drag reduction would have been obtained with the proper leading edge ordinates. Accordingly, performance improvements projected for the optimum leading edge were included in the final results.

d. The leading edge modifications to the C-141 wing increase the amount of leading edge suction, compared to the baseline, and this net thrusting effect tends to reduce creep drag. Additionally, the more favorable leading edge pressures promote a weaker initial shock formation, thus increasing the drag divergence Mach number. For the selected leading edge, W^{35}, a slight reduction in creep drag was obtained above M = 0.7 and the drag divergence was increased by approximately Δ M = 0.01. This combination manifests itself as an improvement in the cruise range parameter, M(L/D), and an associated increase in cruise speed. Relative to the C-141B with 'A' fillet configuration, improvements for the tested and predicted W^{35} leading edges are:

	% M(L/D)	ΔM_{CRUISE}
Tested W^{35}	2.4	0.015
Predicted W^{35}	5.7	0.03

e. The increased cruise speed capability provides a potential benefit with respect to productivity of the C-141. By taking advantage of the higher cruise speed, mission time is decreased, which either reduces the amount of fuel and flight hours for the fleet or increases the total fleet productivity capability.

f. Fuel and cost savings have been projected for the leading edge modification based on the following assumptions:

- Two alternatives are evaluated, one based on constant flight hours, the other based on constant productivity.
- Peacetime C-141 fleet utilization rates of 1170 hours per aircraft per year.
- Fuel price = 46.3 cents/gallon.

The results for the predicted W^{35} are:

	Total Fuel Saved (Gal/Year)	Total Cost Savings ($/Year)
Constant Flight Hours	18,400,000	8,500,000
Constant Productivity	29,400,000	13,600,000

g. Analyses of the incremental chordwise and spanwise load changes due to the leading edge modification indicate that the effects are minimal and should have no significant impact on the wing structure.

h. Two additional wing modification concepts were investigated which show potential for reducing C-141 cruise drag. These were: (1) swept wing tip extensions and (2) trailing edge anti-drag bodies.

In the case of the swept wing tips, substantial drag savings were observed. Wing induced drag at cruise lift was reduced by 17 counts, as expected, by virtue of the 9.5 percent increase in wing span. Improved

drag rise characteristics were also measured which would produce increased cruise speed and productivity benefits similar to those outlined for the leading edge modification.

The anti-drag body configurations performed successfully by increasing wing camber and reducing shock losses as intended. Compressibility drag reductions of 10 to 15 counts are indicated for the M = 0.77 to 0.79 cruise range. Increased cruise speed and improved productivity would also be a benefit from this modification.

In view of the above discussion and conclusions, the following recommendations are submitted:

a. Additional high speed wind tunnel testing should be expeditiously pursued to substantiate fully the predicted aerodynamic improvements for the selected leading edge modification. The model leading edge components should be modified to the correct design ordinates for both the baseline and the two modified leading edges.

b. High speed testing of all three drag reduction concepts (leading edges, swept tips and anti-drag bodies) in various combinations with each other should be accomplished. This process is considered essential to remove the uncertainty of superimposing the individual drag and performance improvements. This is especially cruicial for compressibility type drag changes since these are not likely to be additive.

c. Following the high speed wind tunnel test demonstration of the drag reduction benefits, a program should be initiated to evaluate the structural and economic feasibility of incorporating the drag reduction concepts into the C-141 fleet.

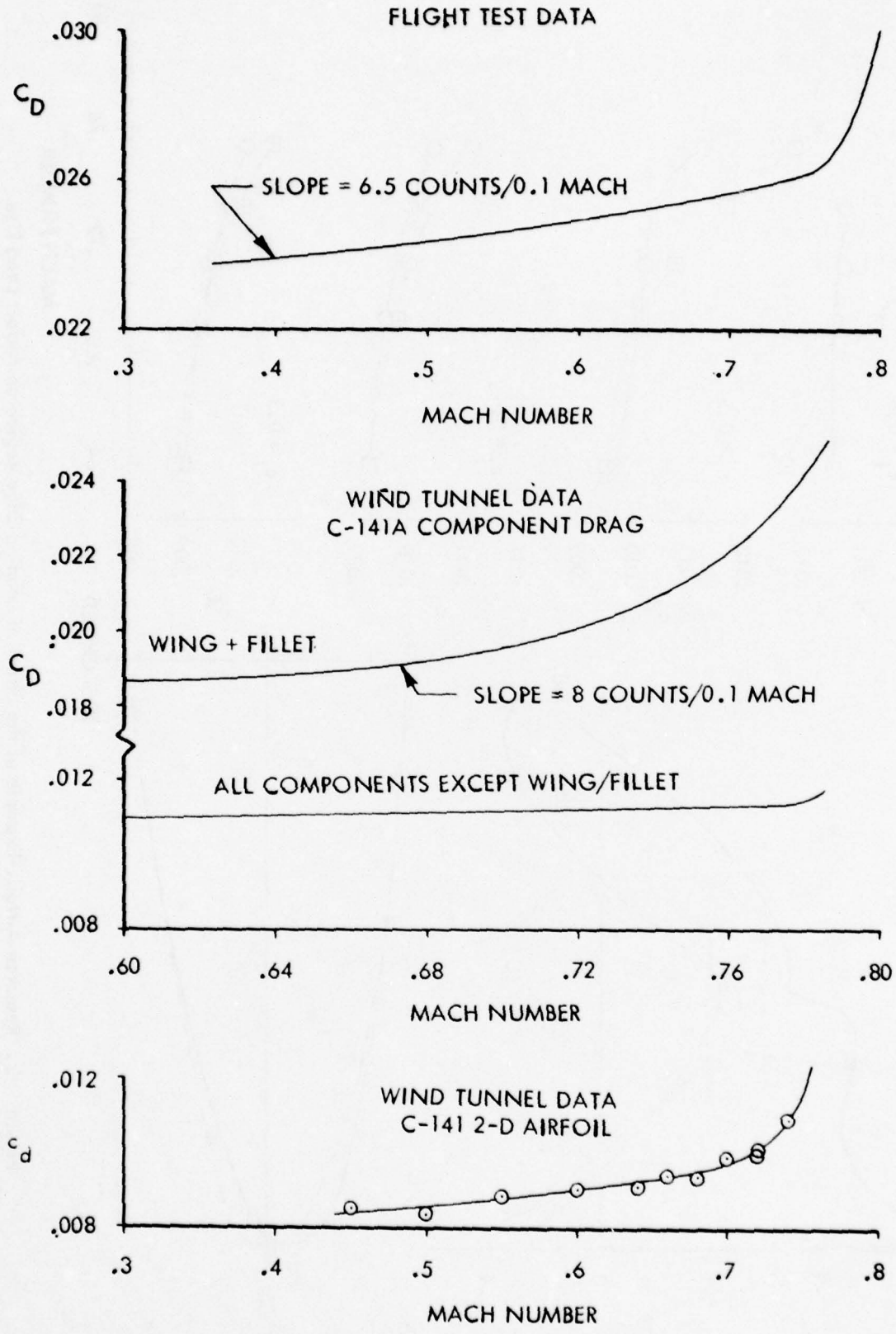

Figure 1. C-141A Drag Characteristics

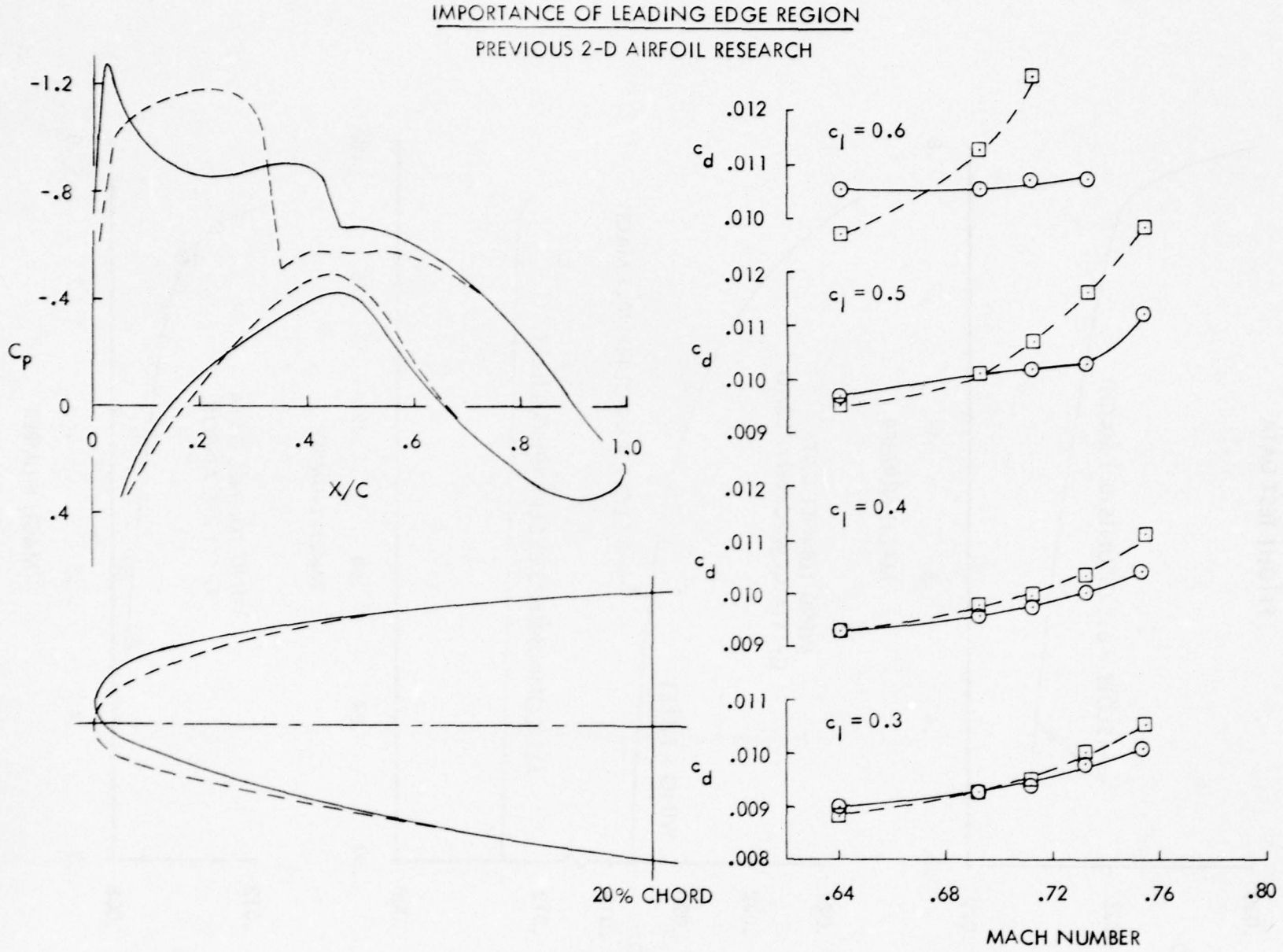

Figure 2. Research Airfoils-Example of the Effect of Leading Edge Region on Airfoil Drag Rise

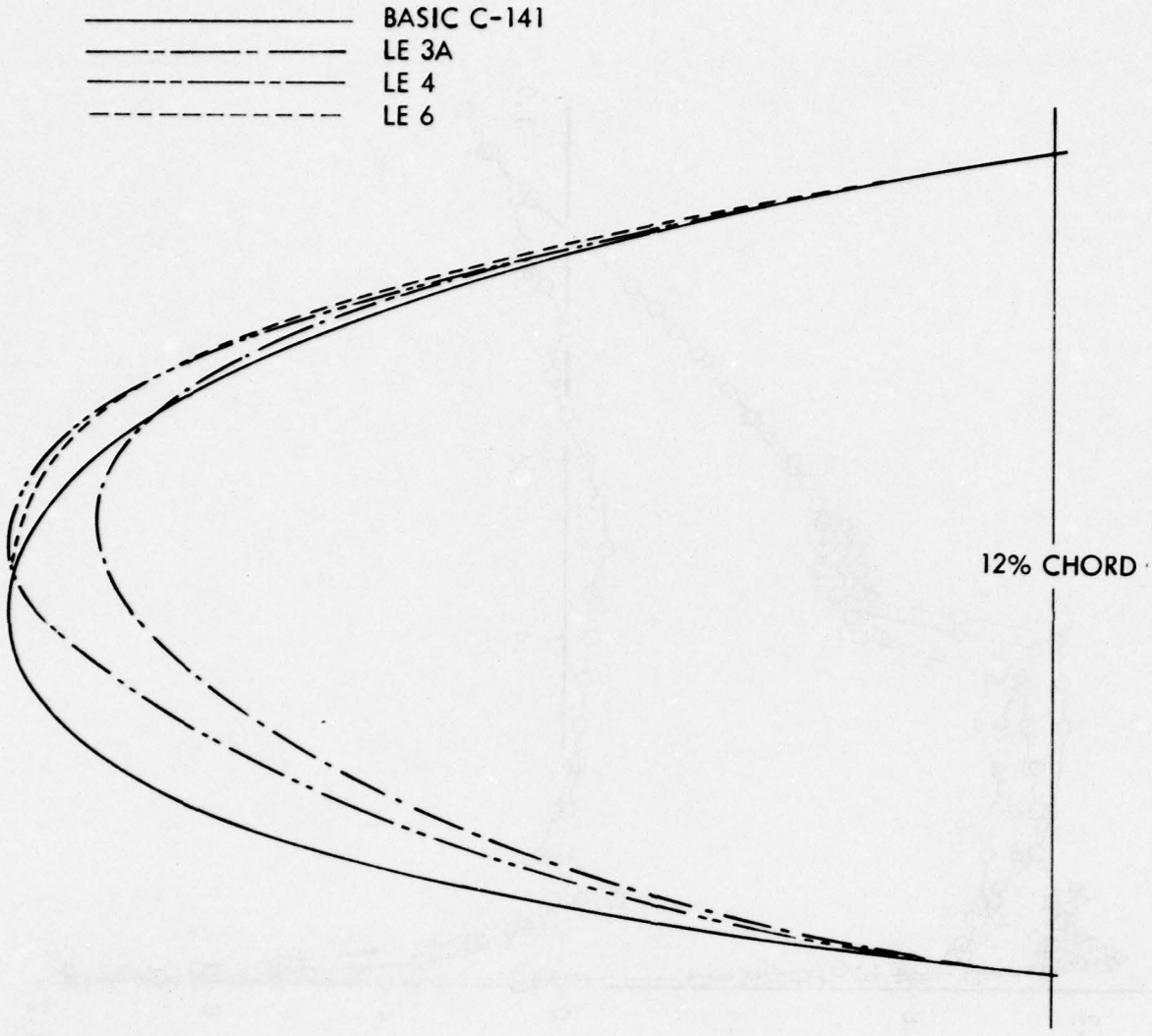

a. Leading Edge Shapes

Figure 3. Results From High Speed Test Evaluation of C-141 2-D Airfoil Leading Edge Modifications

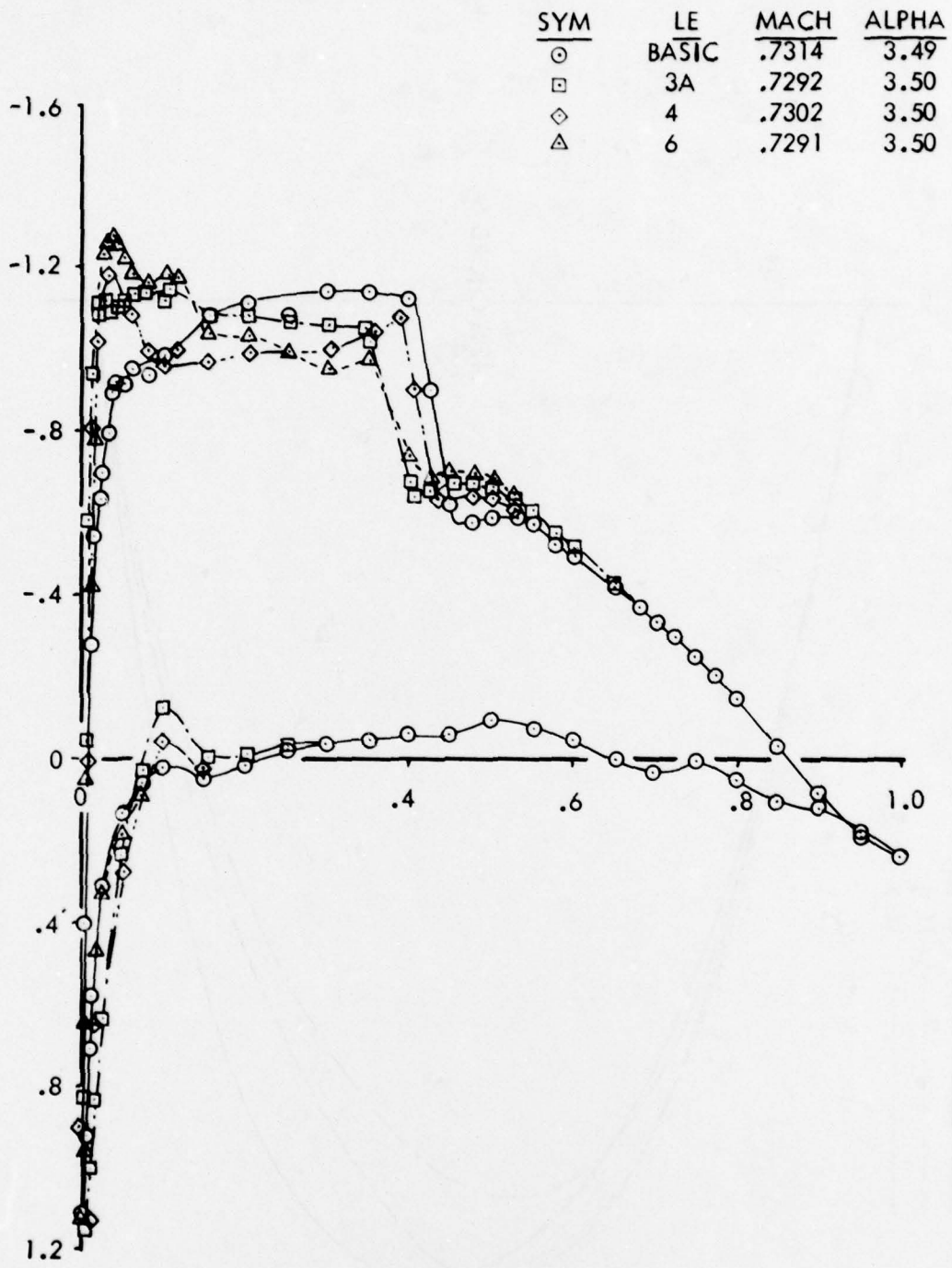

b. Comparison of Experimental Pressure Distributions

Figure 3. Continued

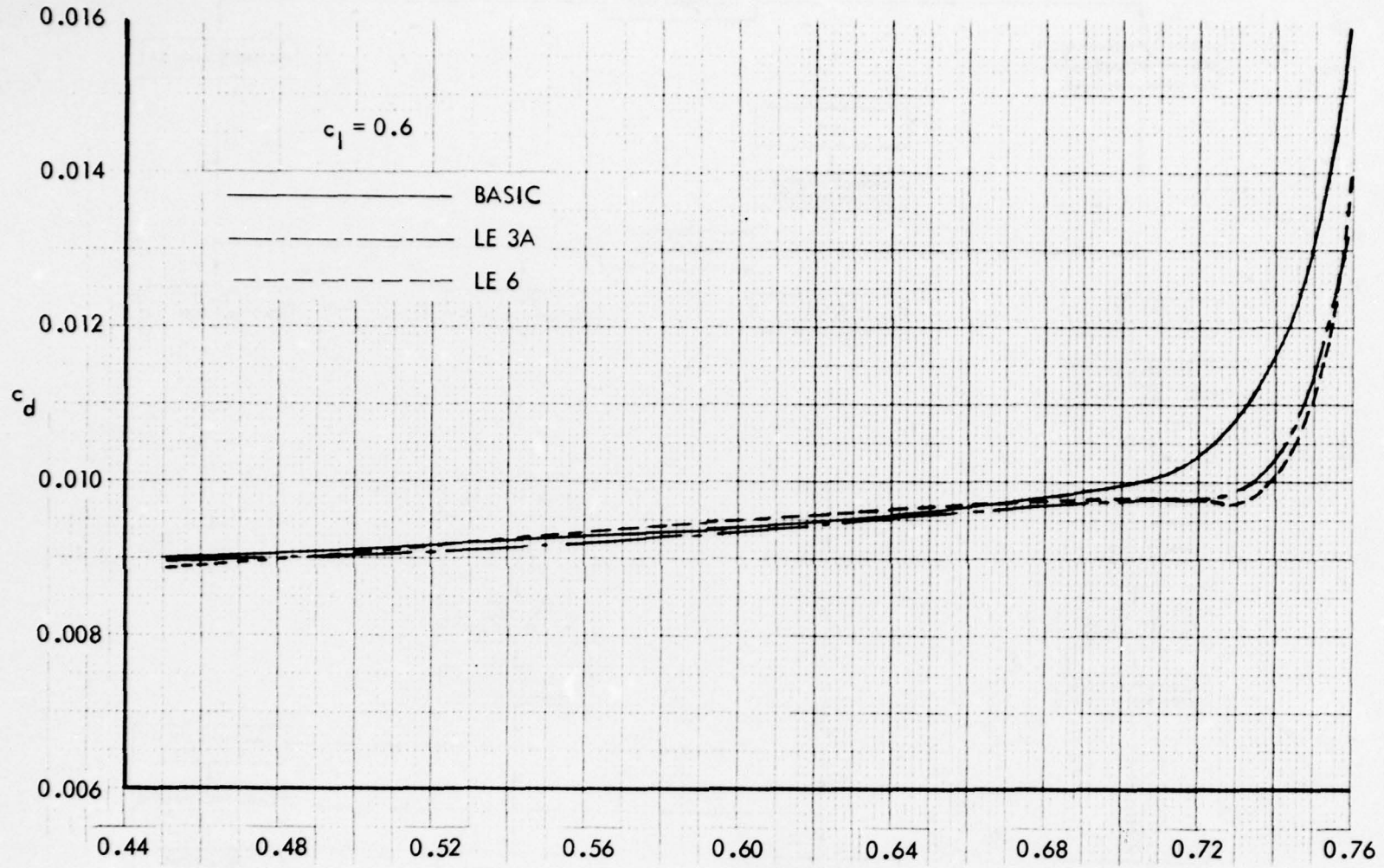

c. Comparison of Drag Rise Characteristics

Figure 3. Concluded

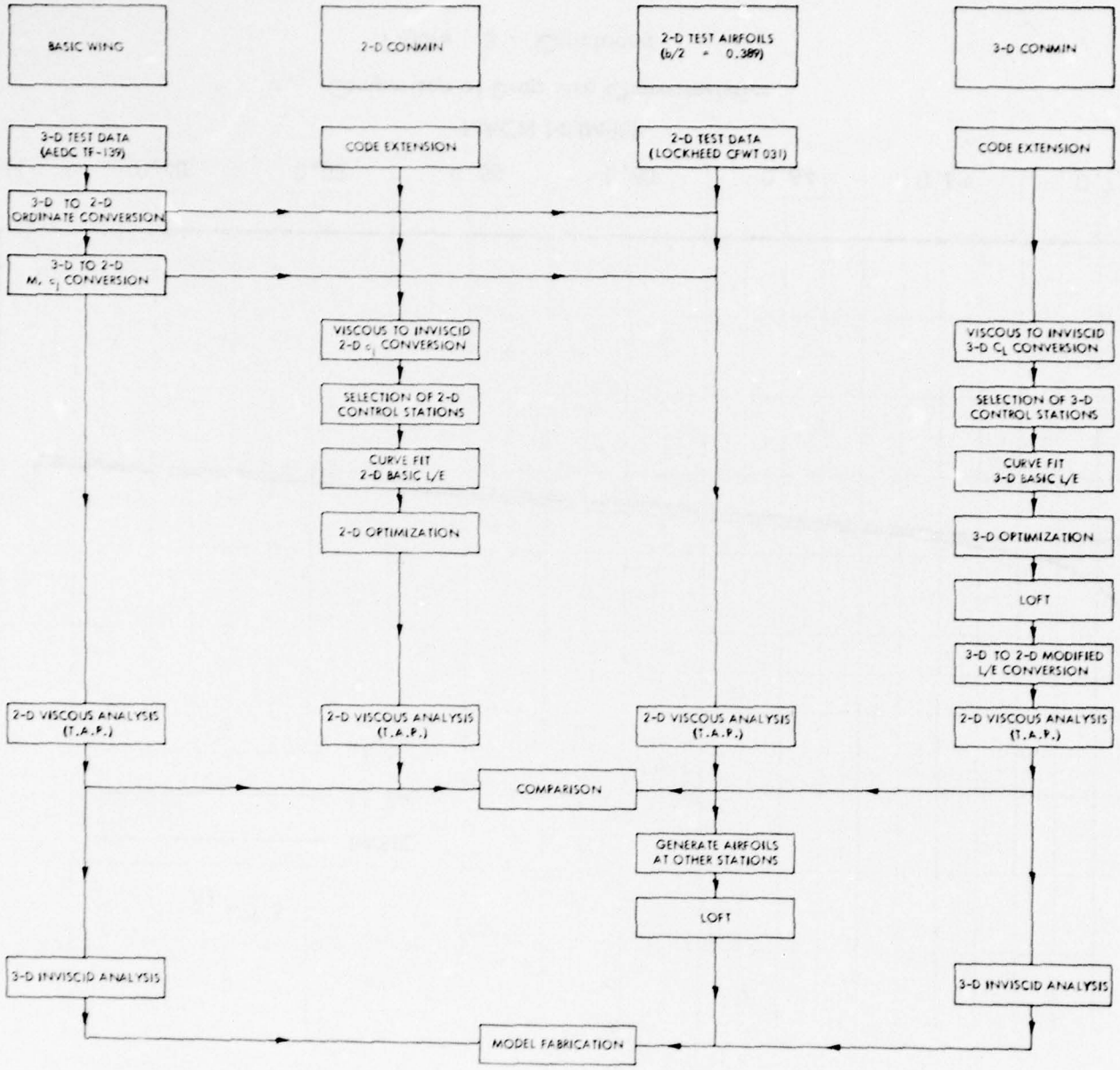

Figure 4. Design Procedure For Leading Edge Modification

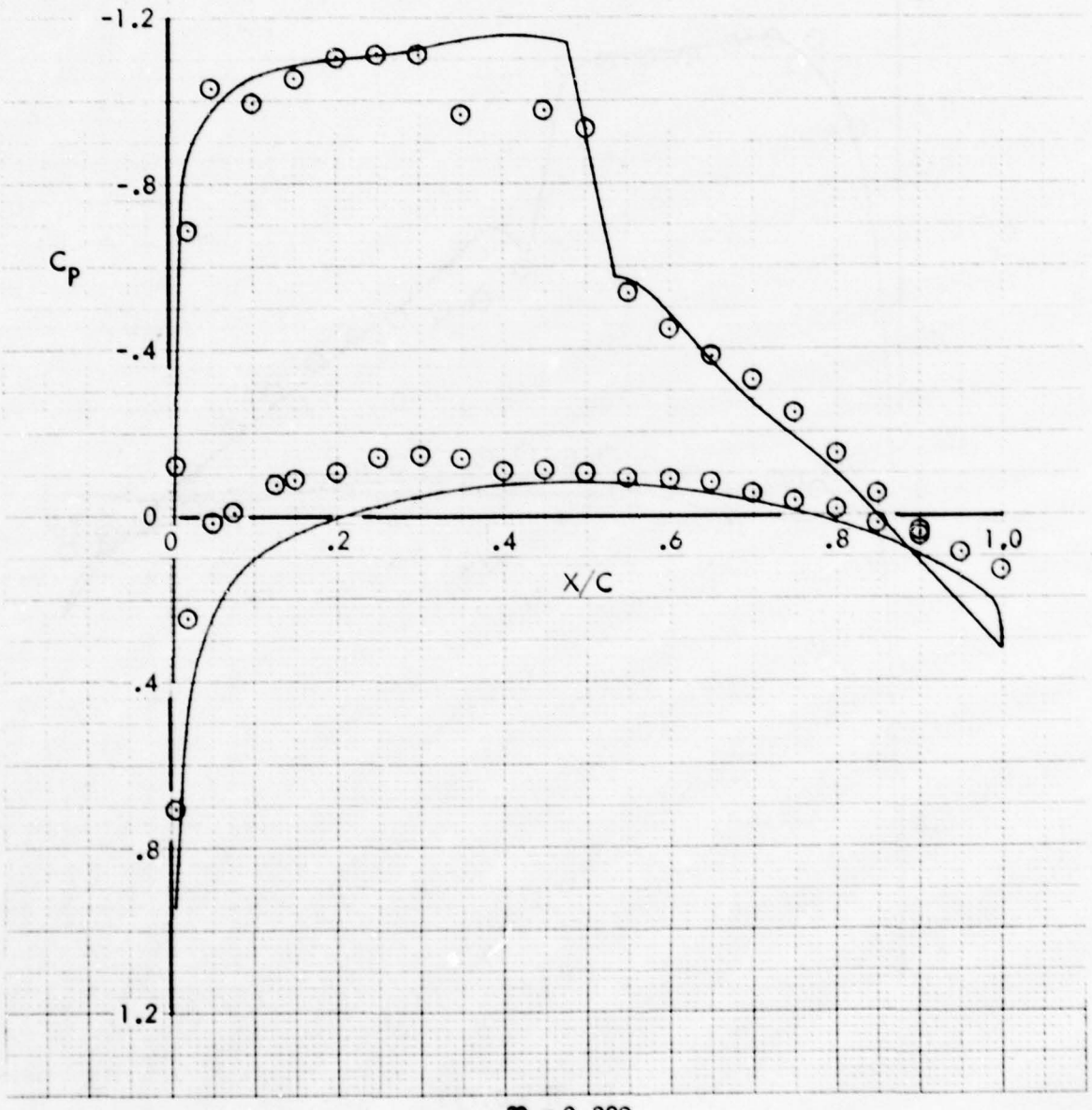

a. $\eta = 0.389$

Figure 5. Comparison of Theoretical (2-D Equivalent) and Experimental 3-D Pressure Distributions

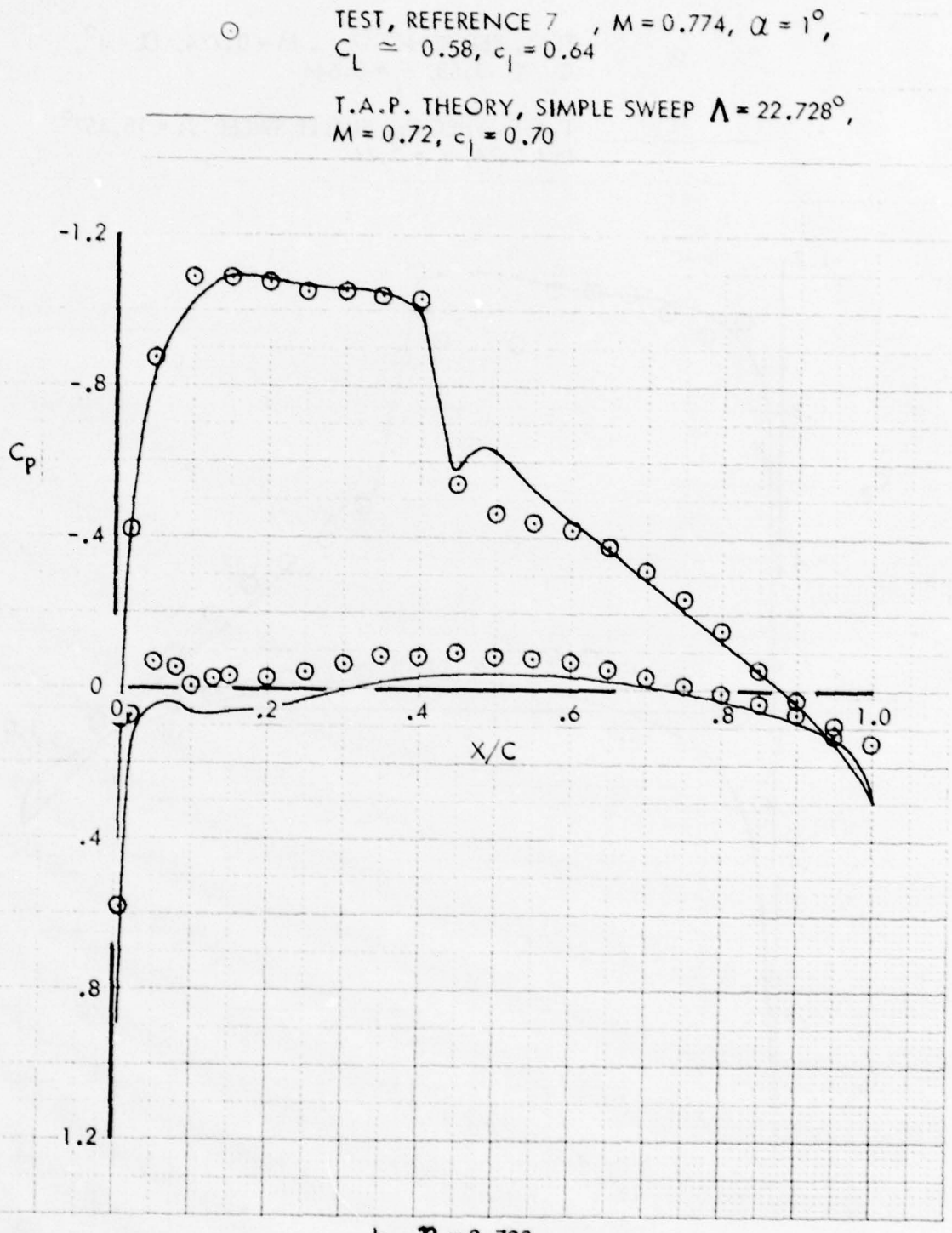

b. $\eta = 0.793$

Figure 5. Concluded

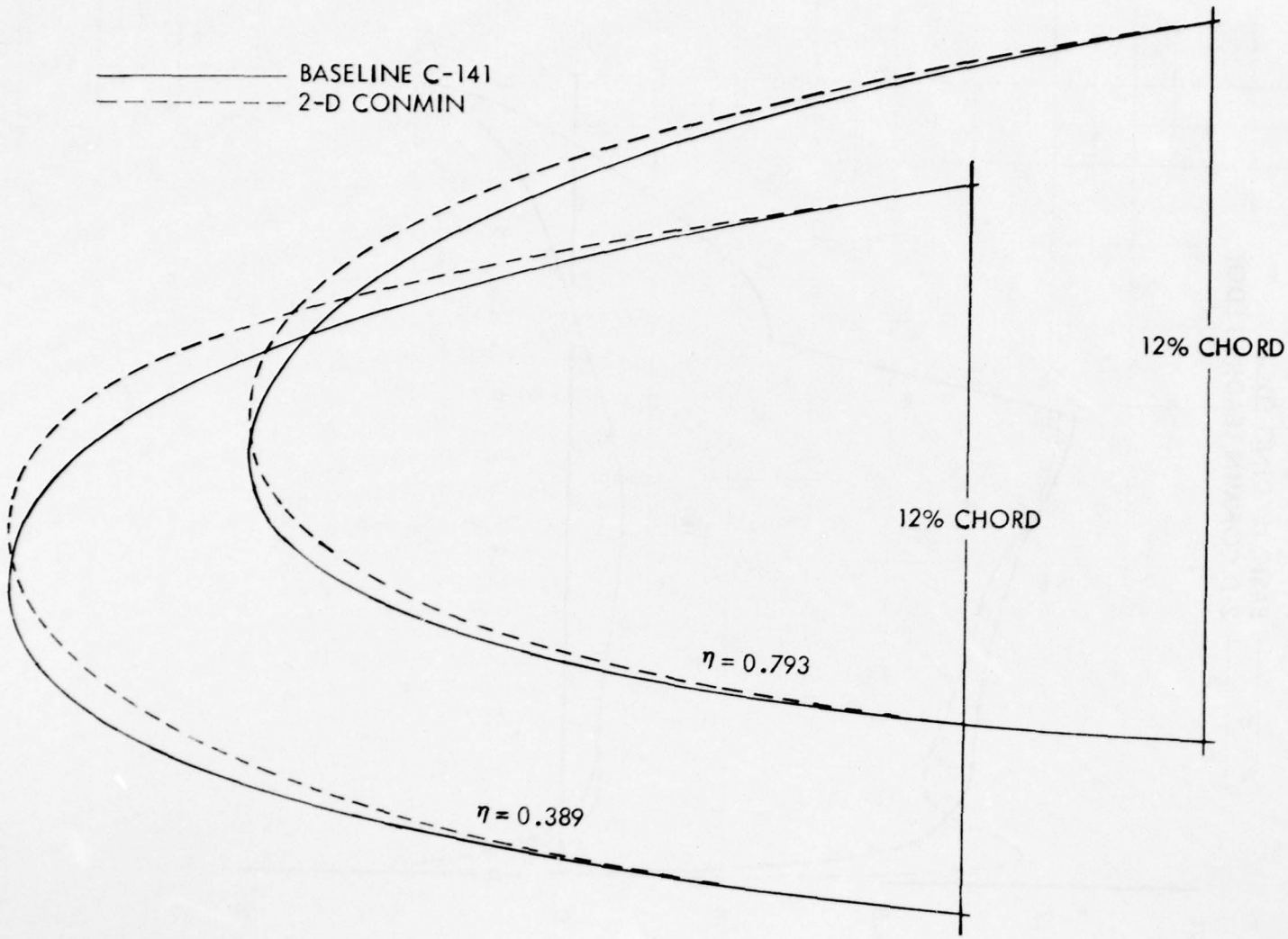

Figure 6. 2-D CONMIN Optimized Leading Edge Modifications

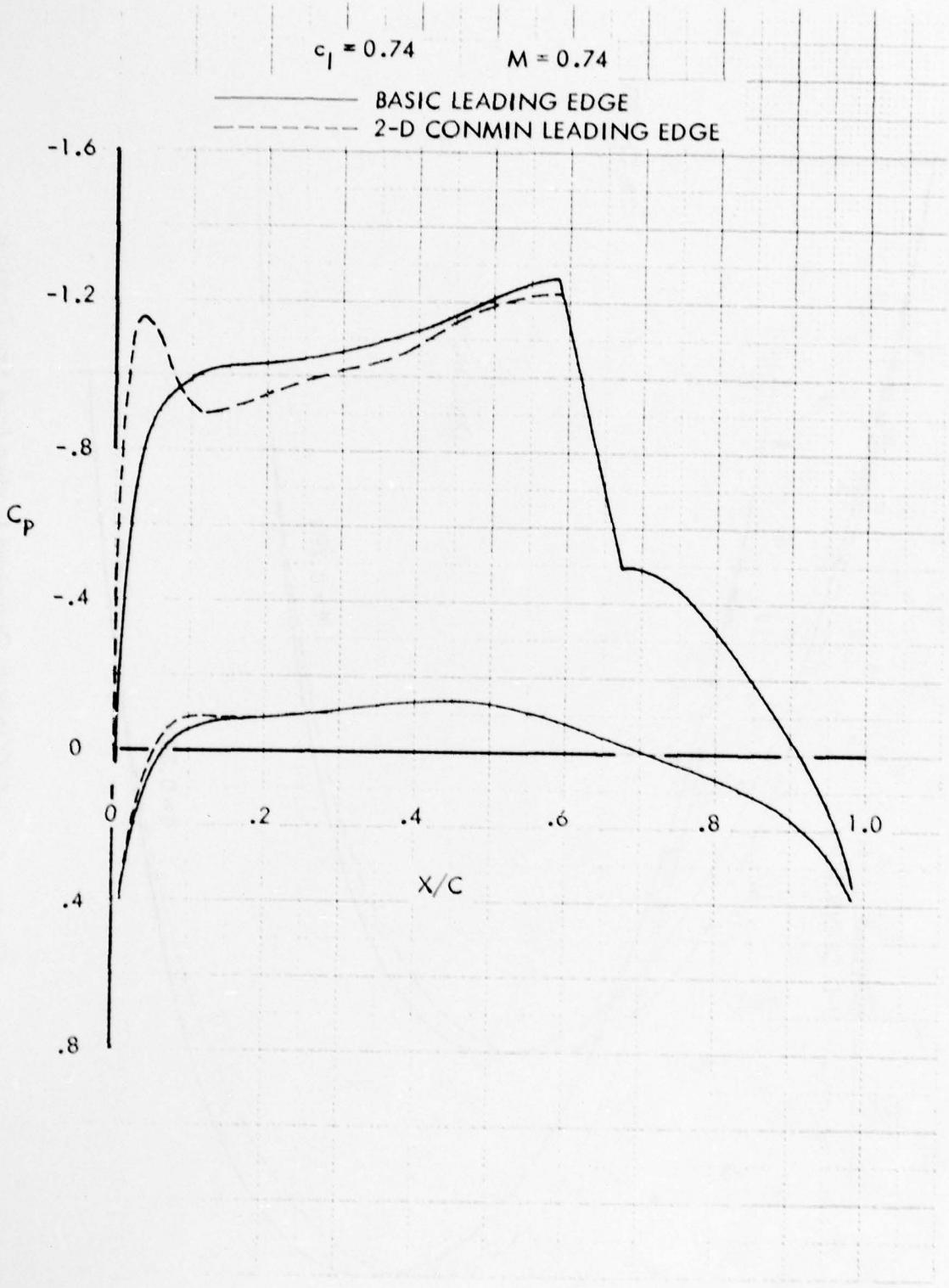

Figure 7. Comparison of the Inviscid Pressure Distributions for the Basic and 2-D CONMIN Leading Edges at η = 0.389

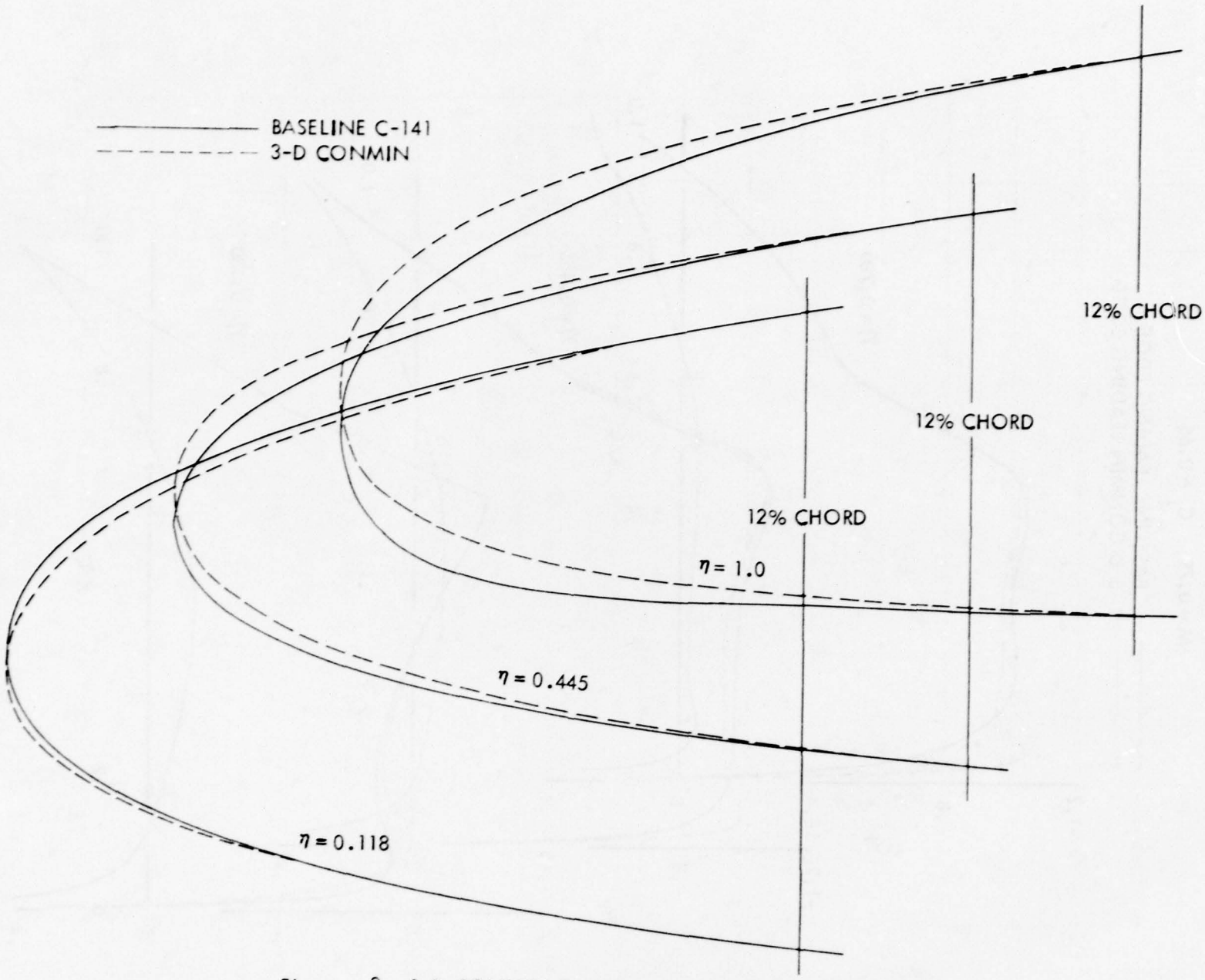

Figure 8. 3-D CONMIN Optimized Leading Edge Modification

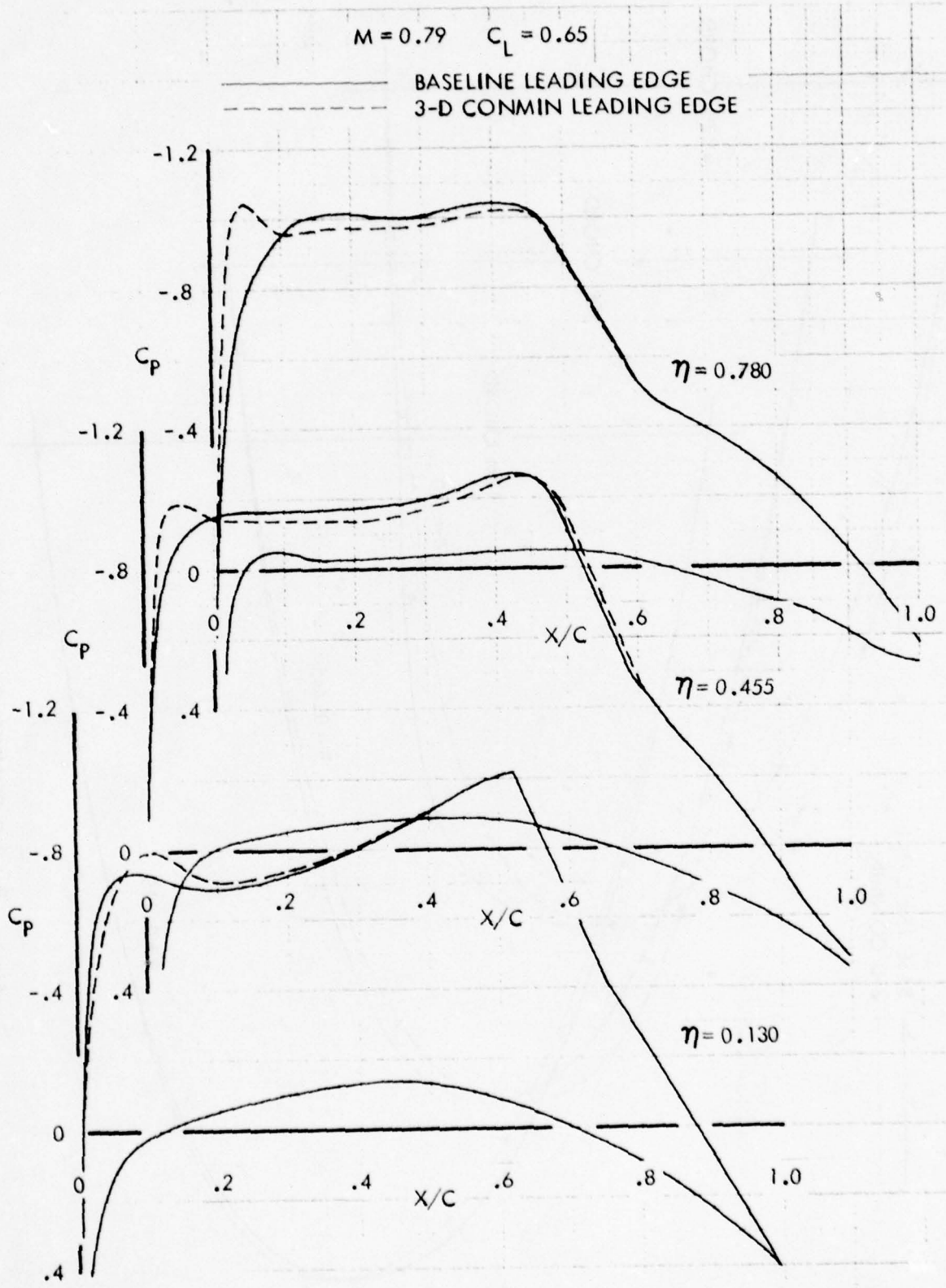

Figure 9. Comparison of the 3-D CONMIN Inviscid Pressure Distribution for the Basic and 3-D CONMIN Leading Edges

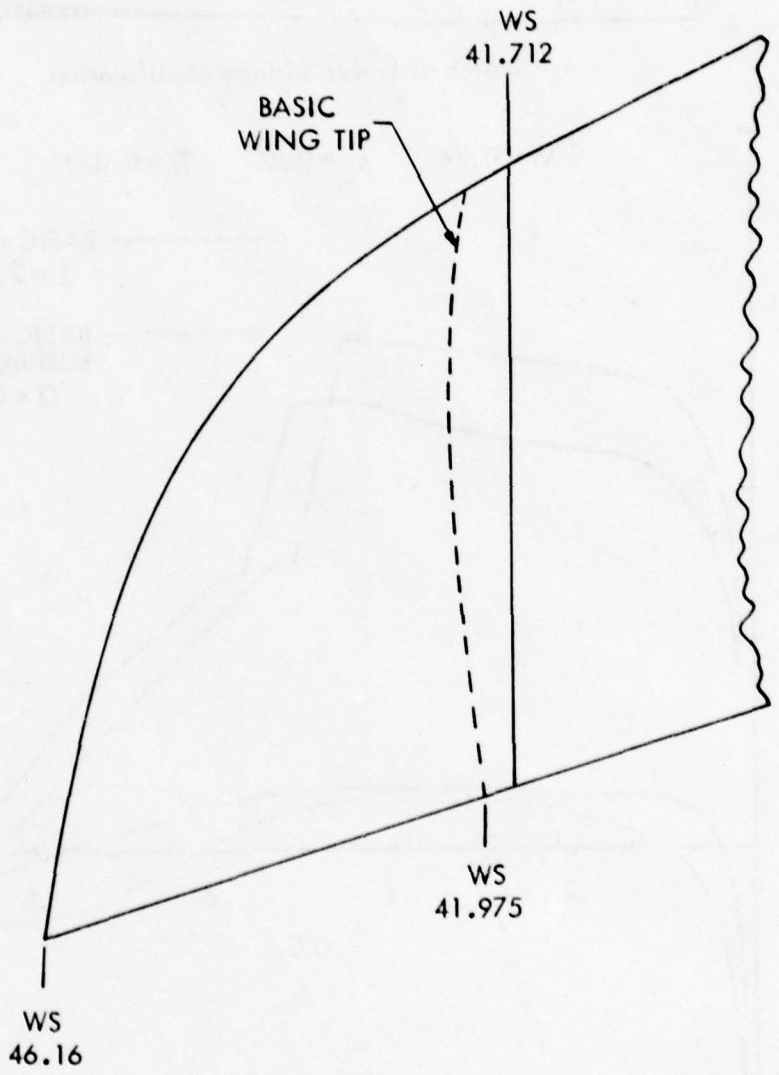

Figure 10 . Swept Wing Tip Extension Planform

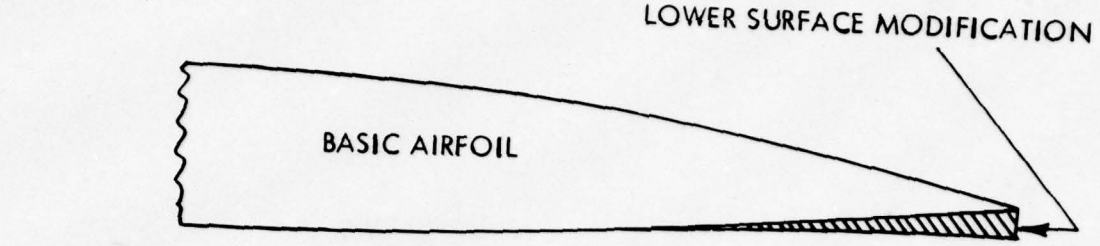

a. Sketch of Lower Surface Modification

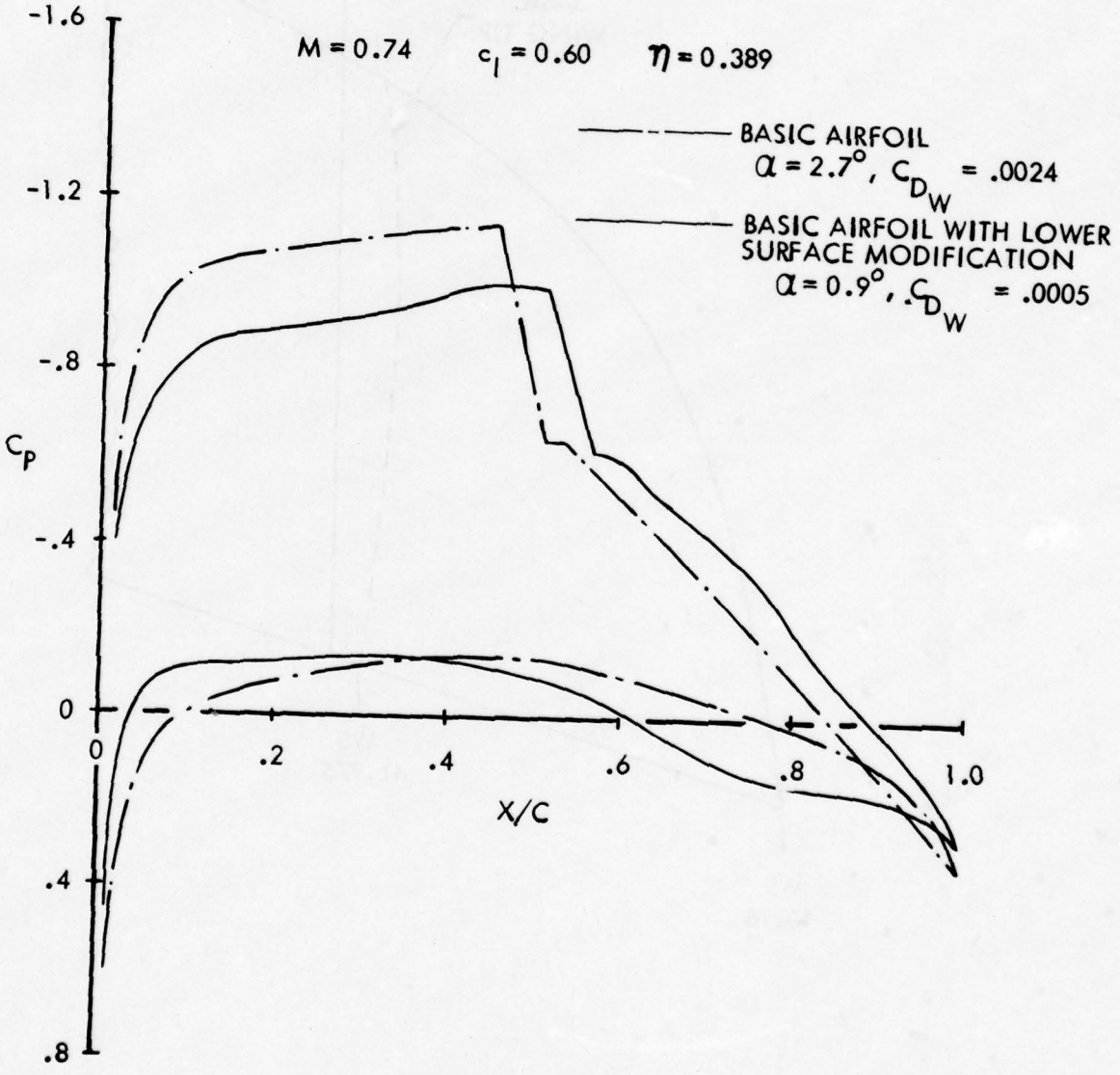

b. Effect on Theoretical Pressure Distribution

Figure 11. C-141 Airfoil Aft Camber Change

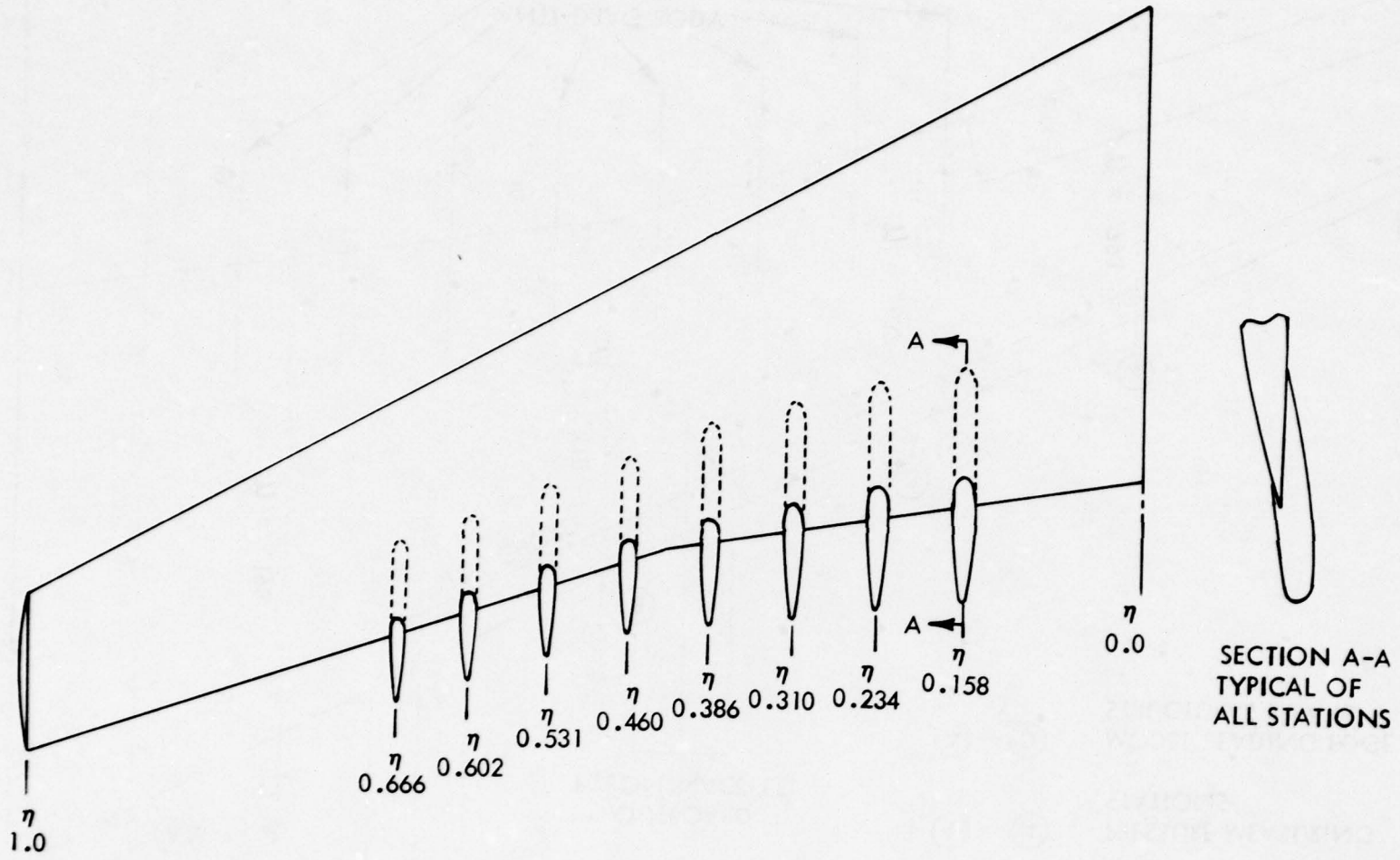

Figure 12 . Sketch of Anti-Drag Body Locations

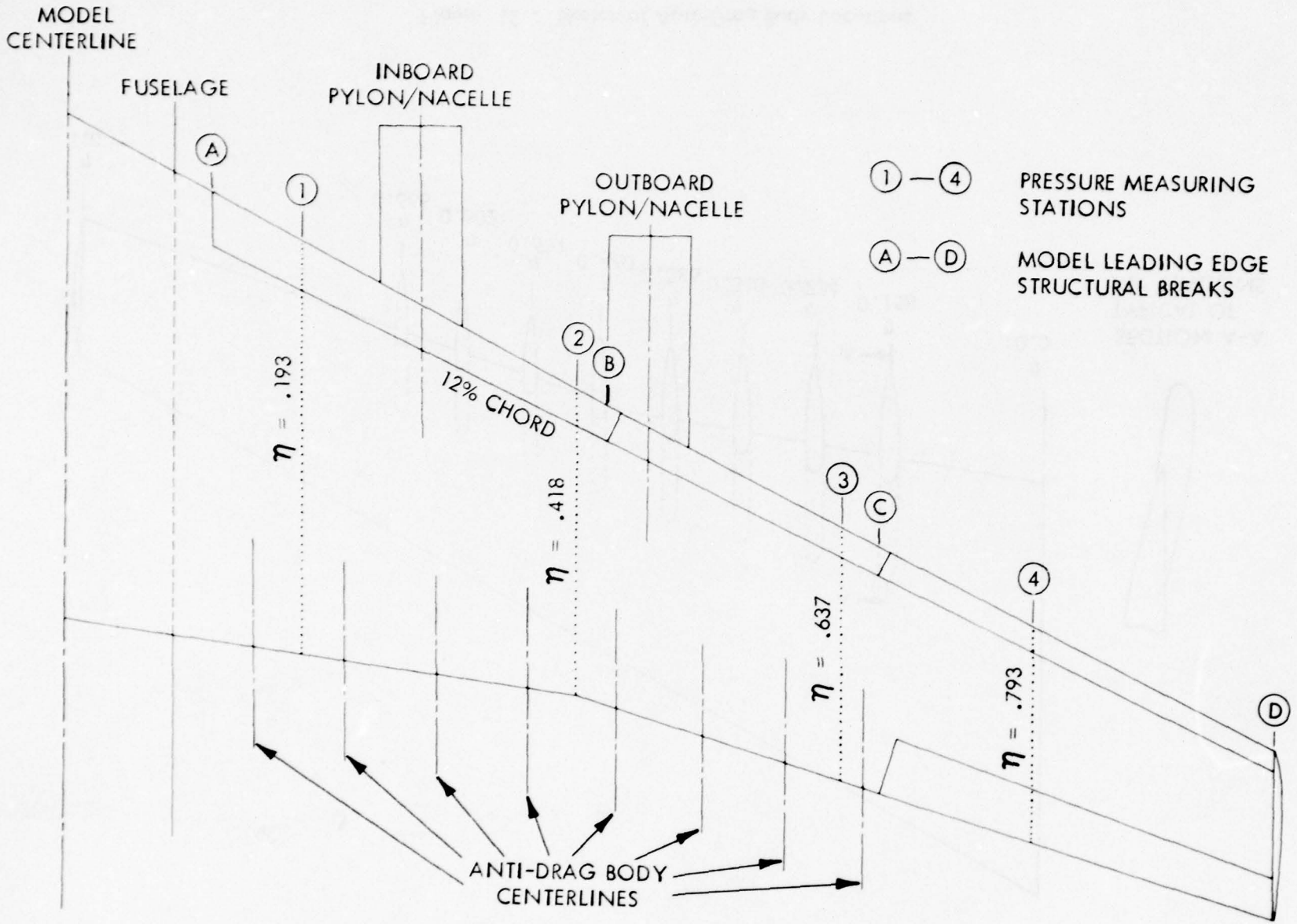

Figure 13. Planform Sketch of 0.044 Scale Model Wing

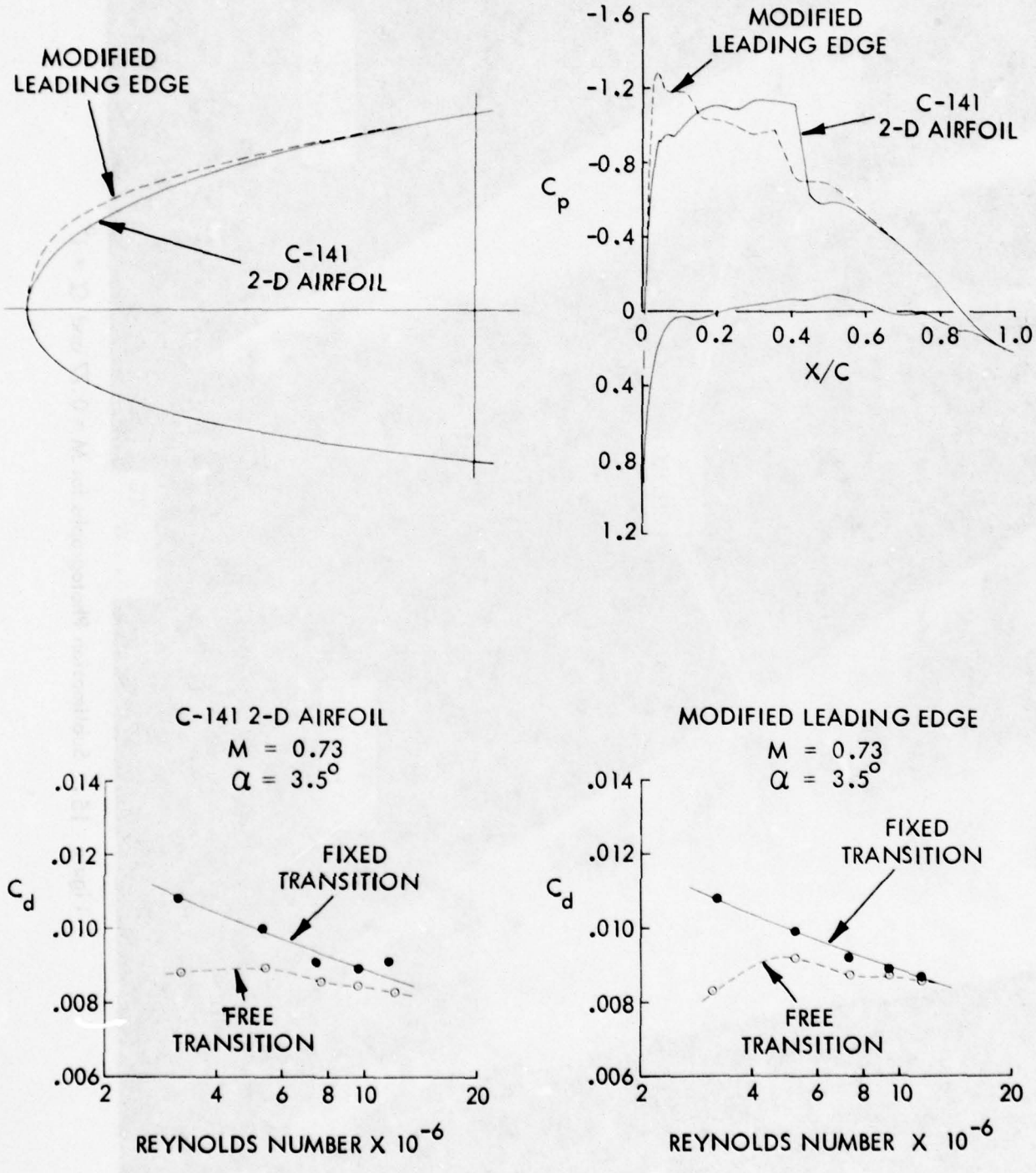

Figure 14. 2-D Airfoil Test Results — Fixed and Free Transition

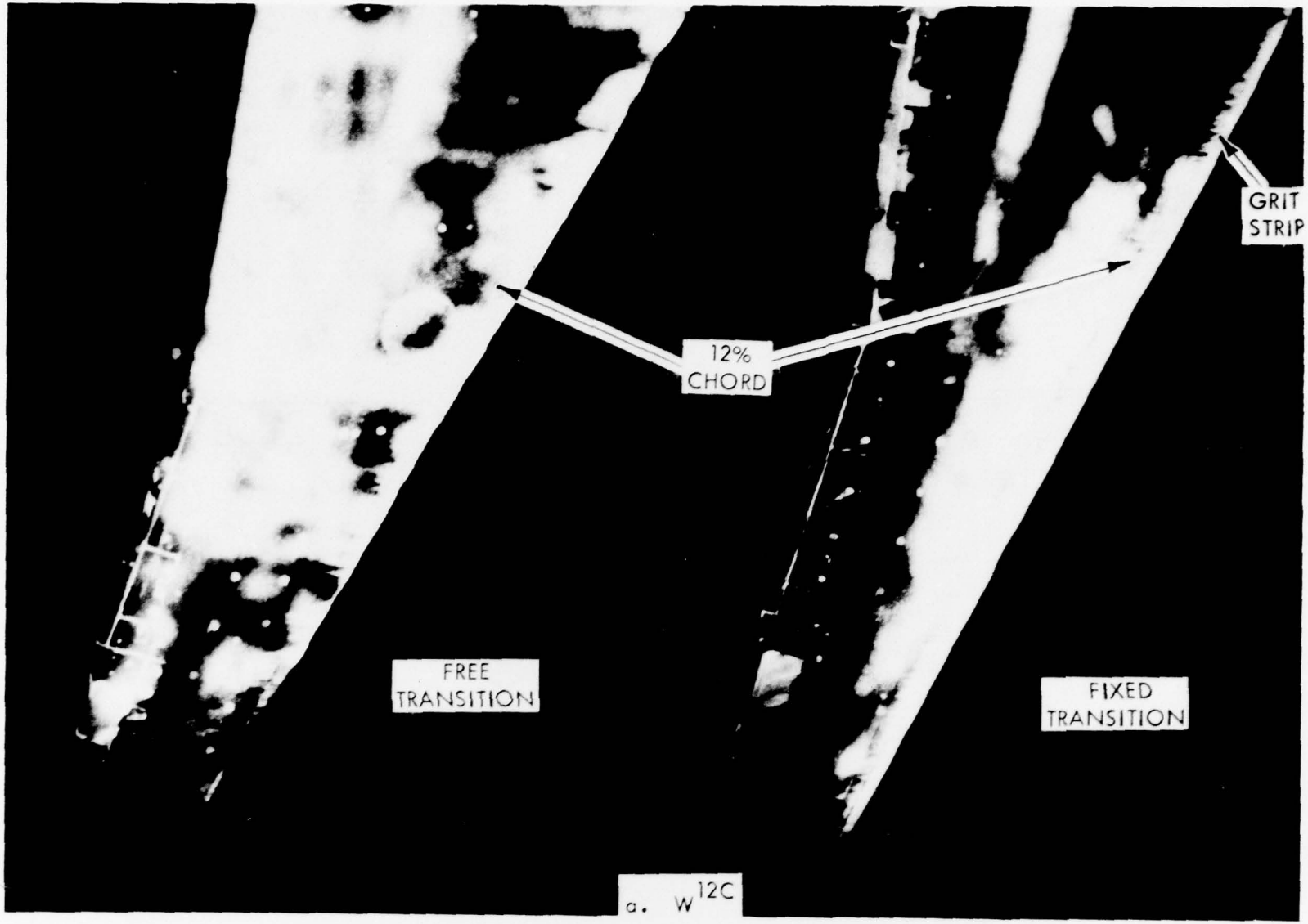

Figure 15. Sublimation Photographs for M = 0.77 and $\alpha = 1^{\circ}$

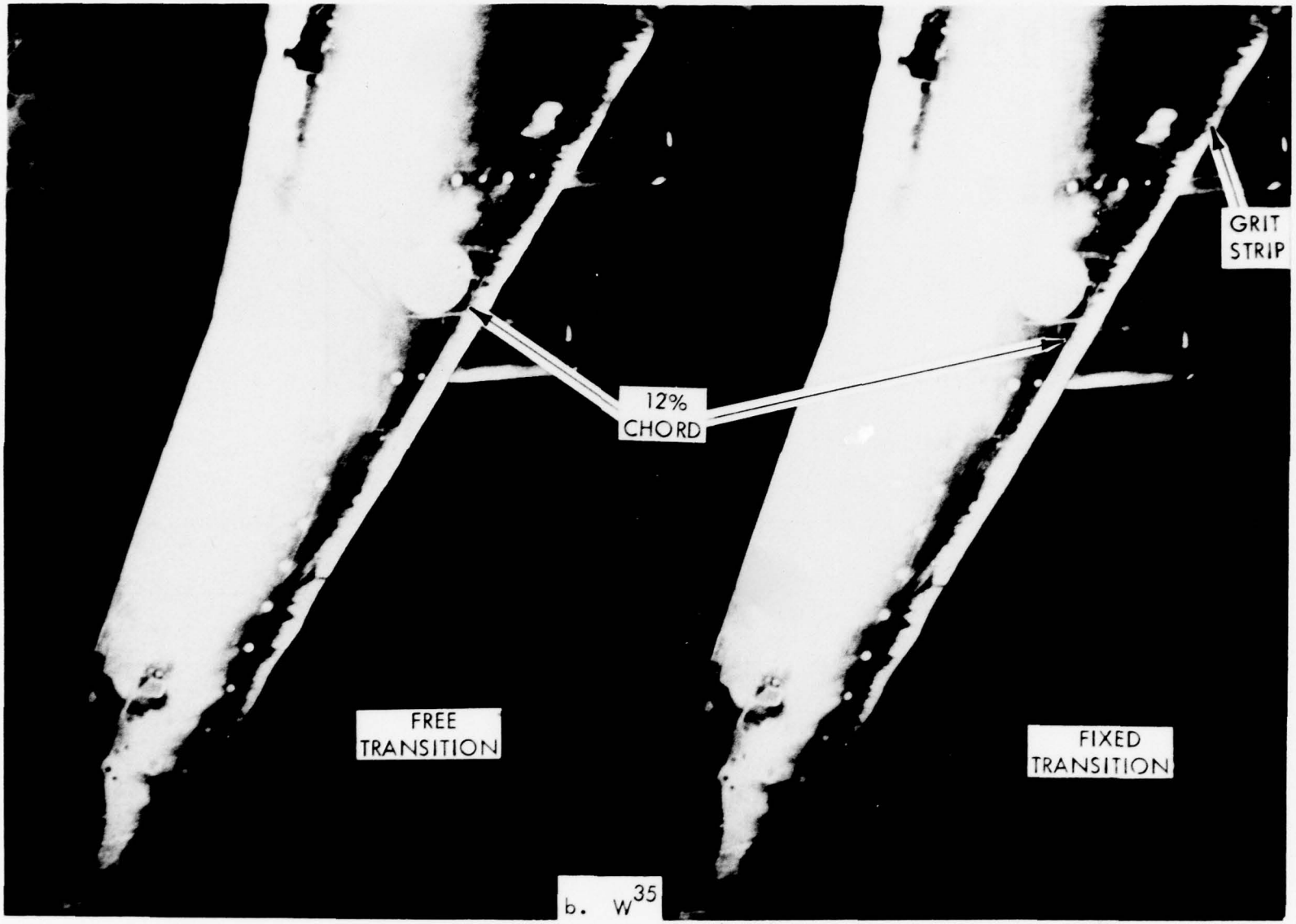

b. W^{35}

Figure 15. Concluded

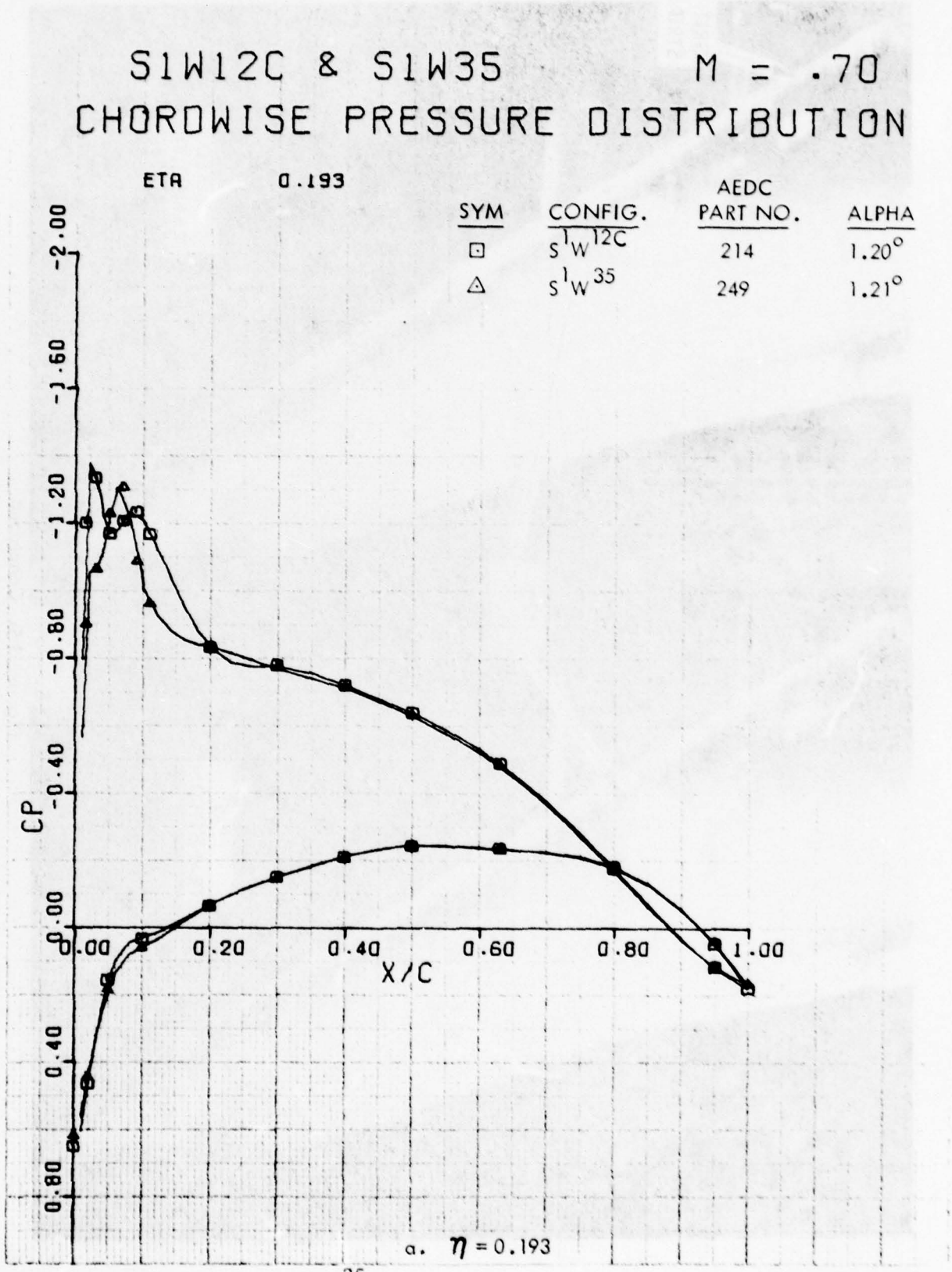

Figure 16. Effect of W^{35} Leading Edge Modification on Chordwise Pressure Distribution at M = 0.7. Pylon/Nacelles On Configuration.

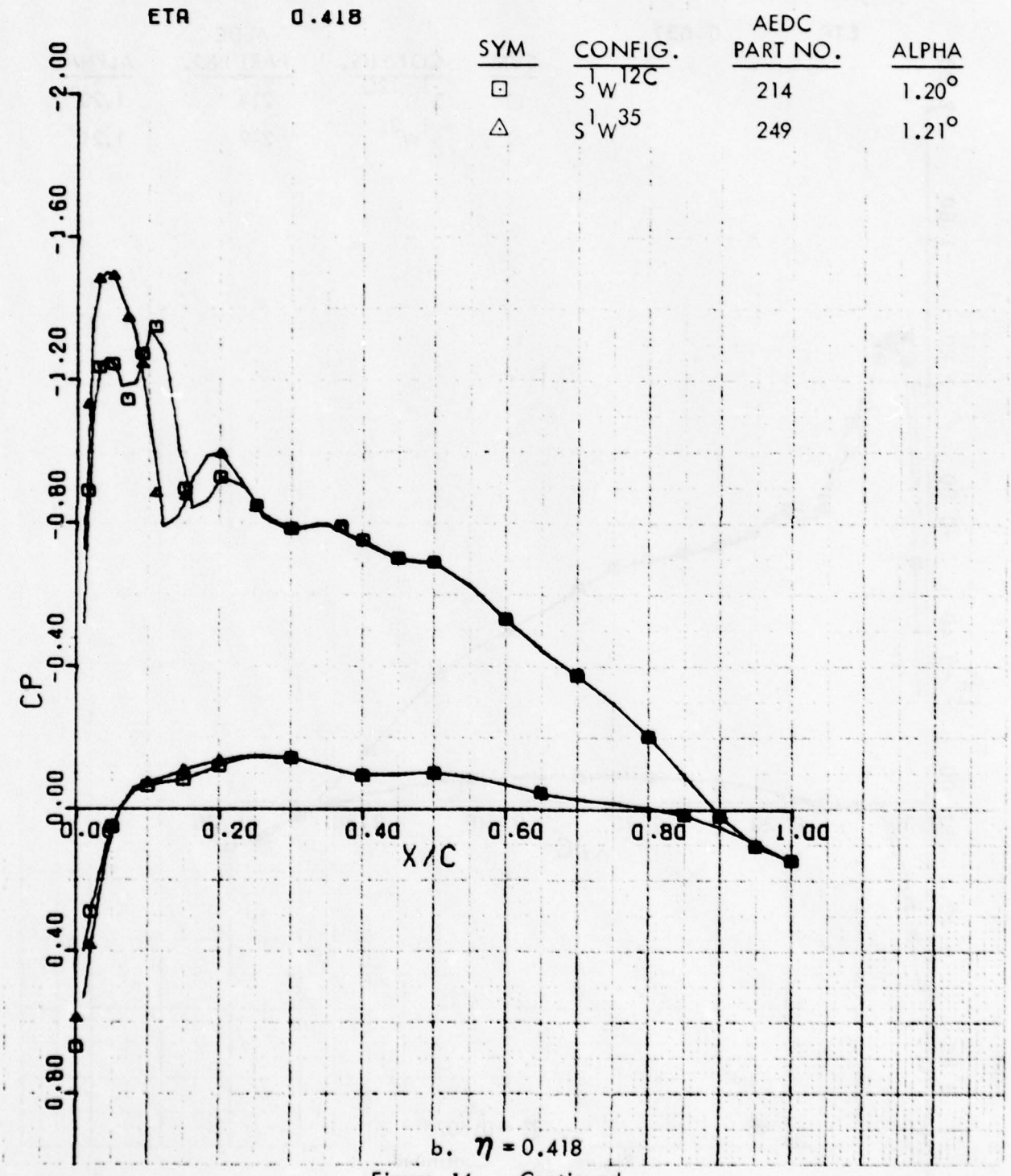

b. $\eta = 0.418$

Figure 16 . Continued

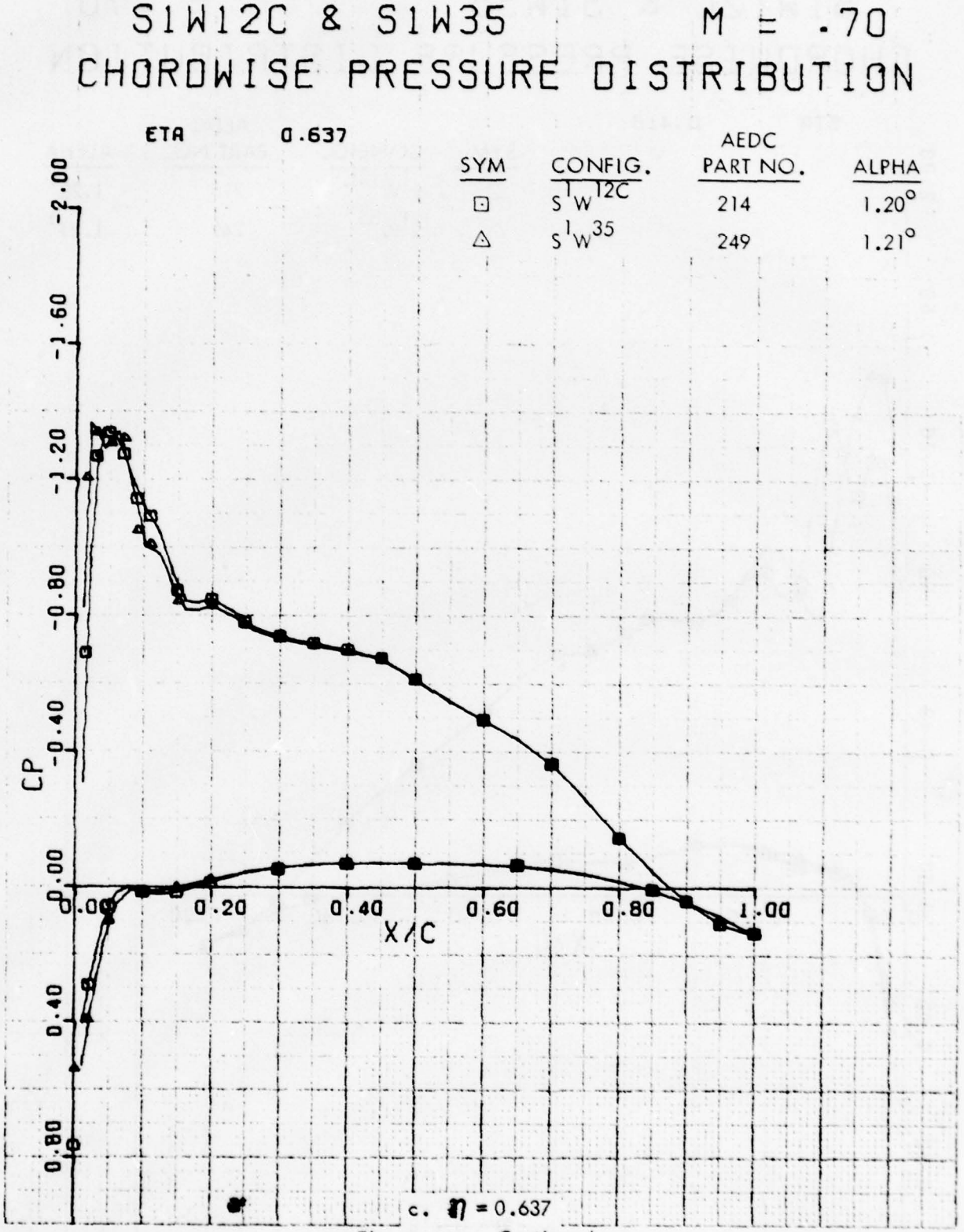

c. $\eta = 0.637$

Figure 16. Continued

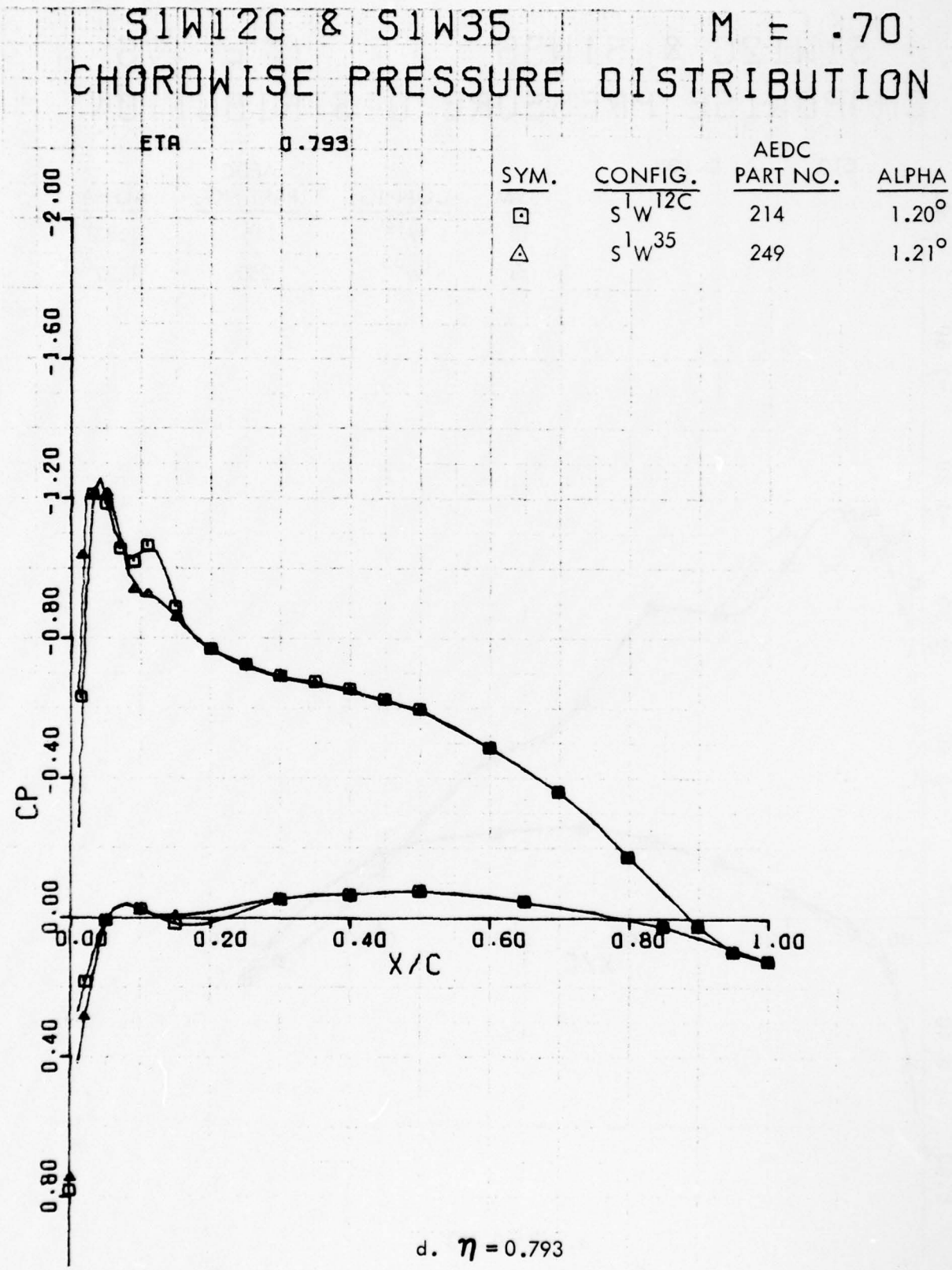

d. $\eta = 0.793$

Figure 16. Concluded

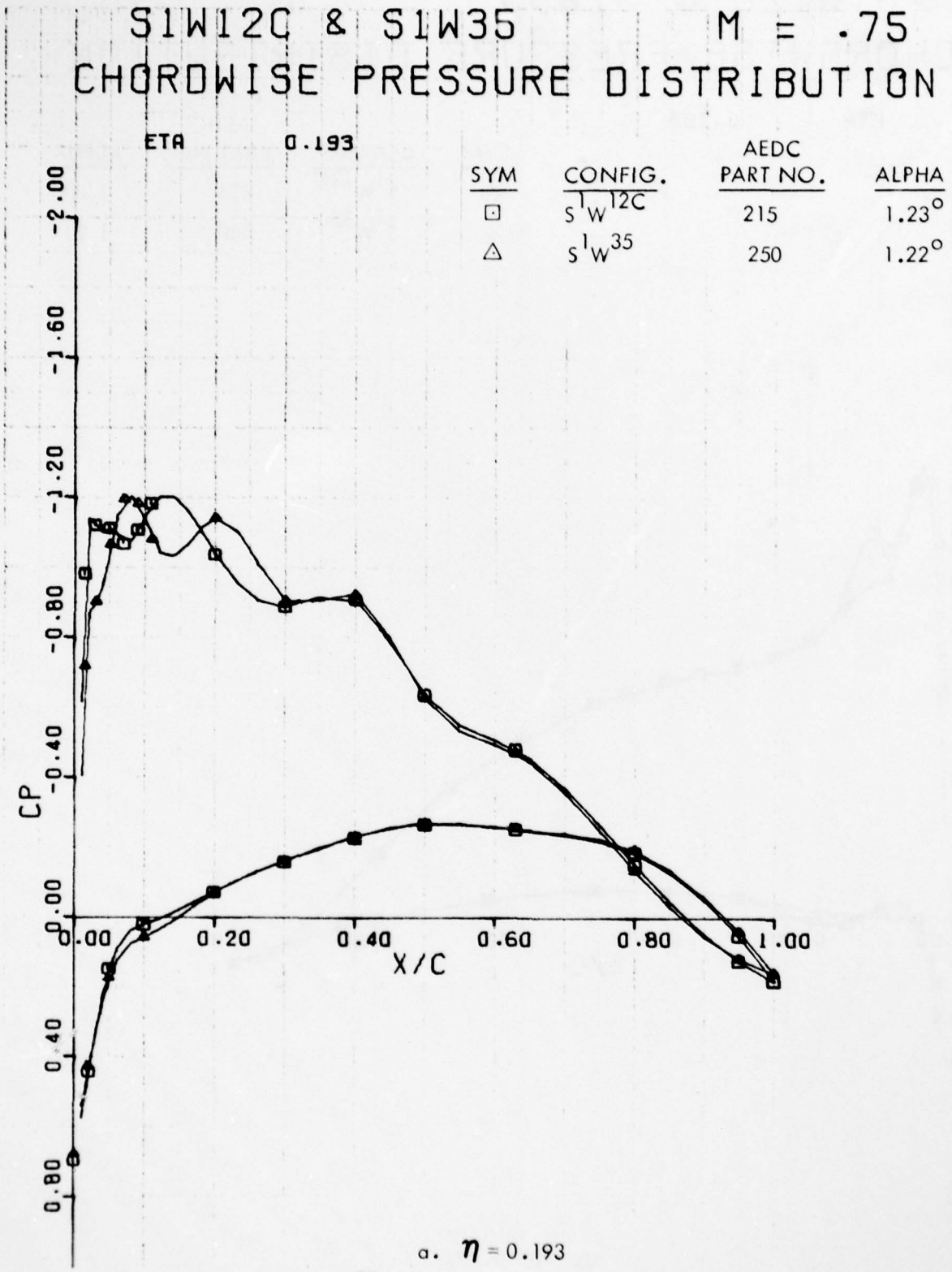

a. $\eta = 0.193$

Figure 17 . Effect of W^{35} Leading Edge Modification on Chordwise Pressure Distribution at M = 0.75. Pylon/Nacelles On Configuration.

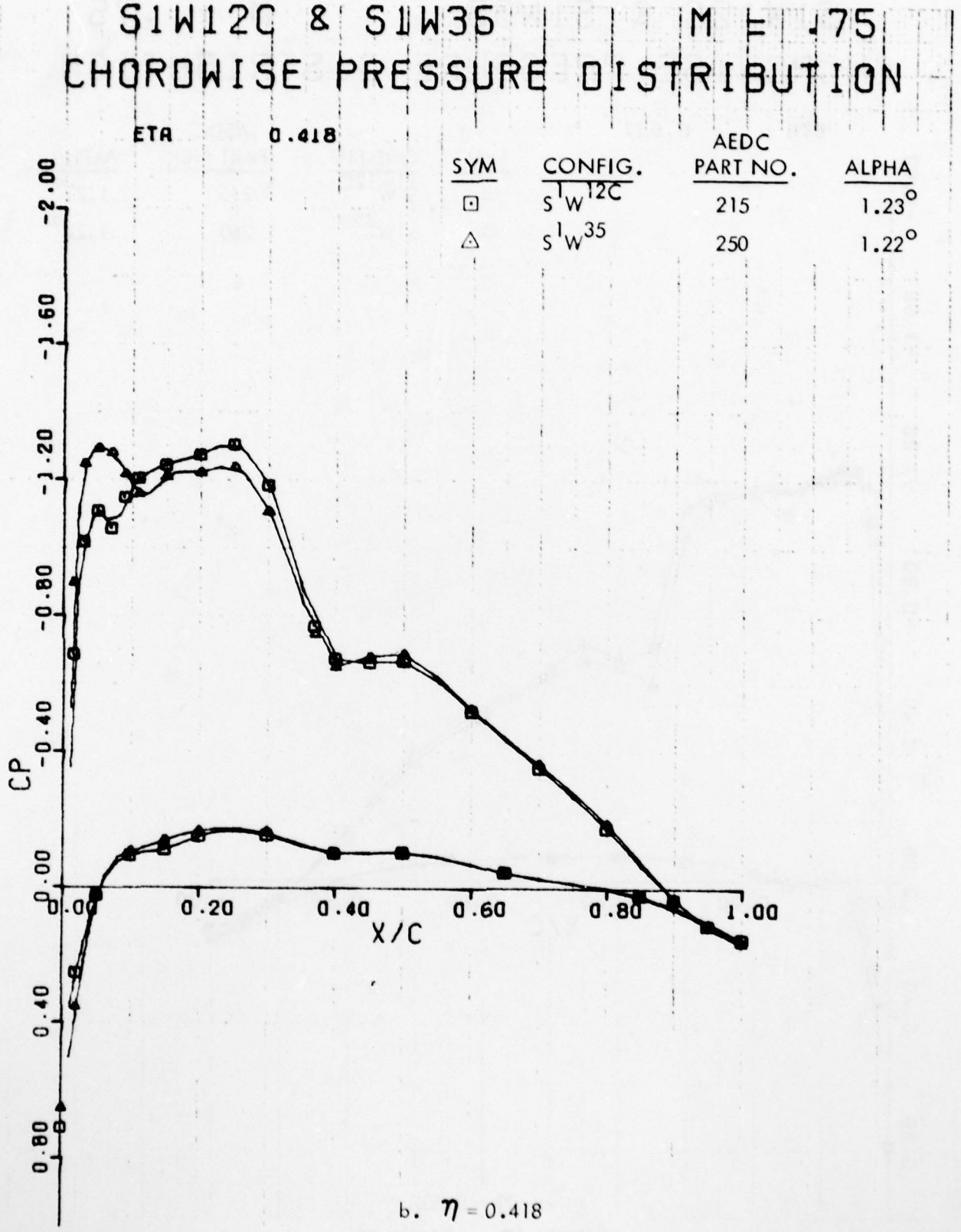

b. $\eta = 0.418$

Figure 17. Continued

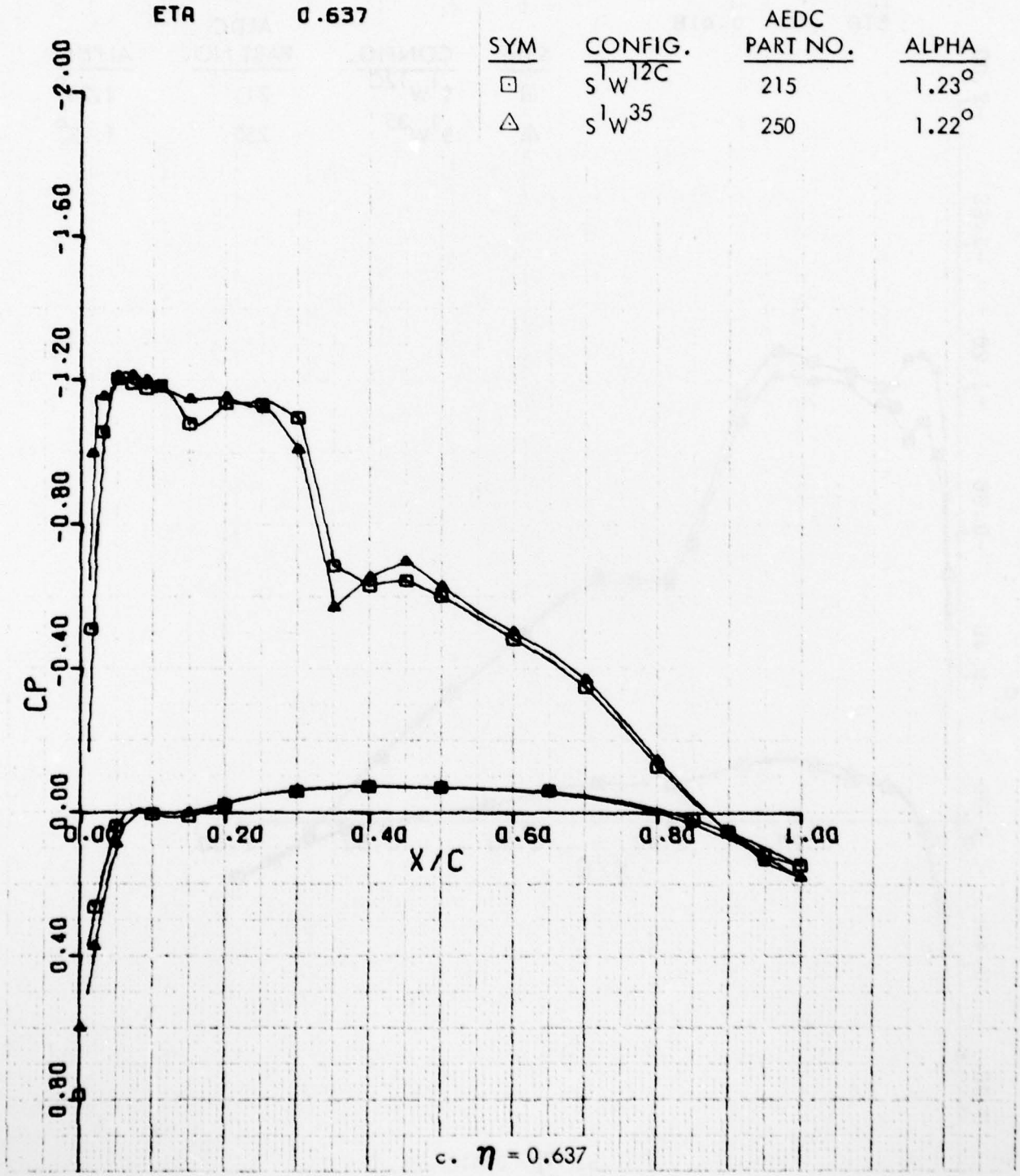

c. η = 0.637

Figure 17. Continued

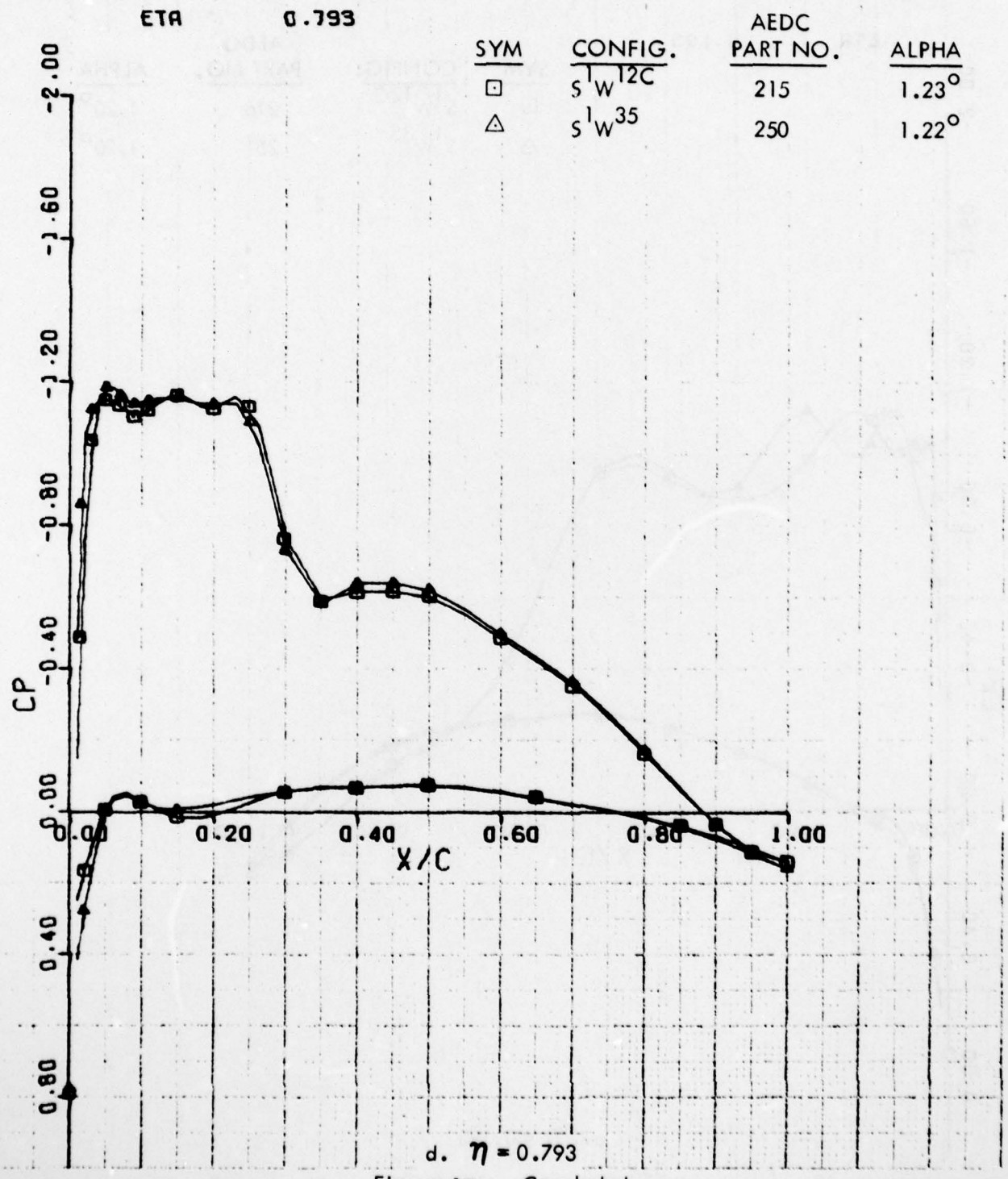

d. $\eta = 0.793$

Figure 17 . Concluded

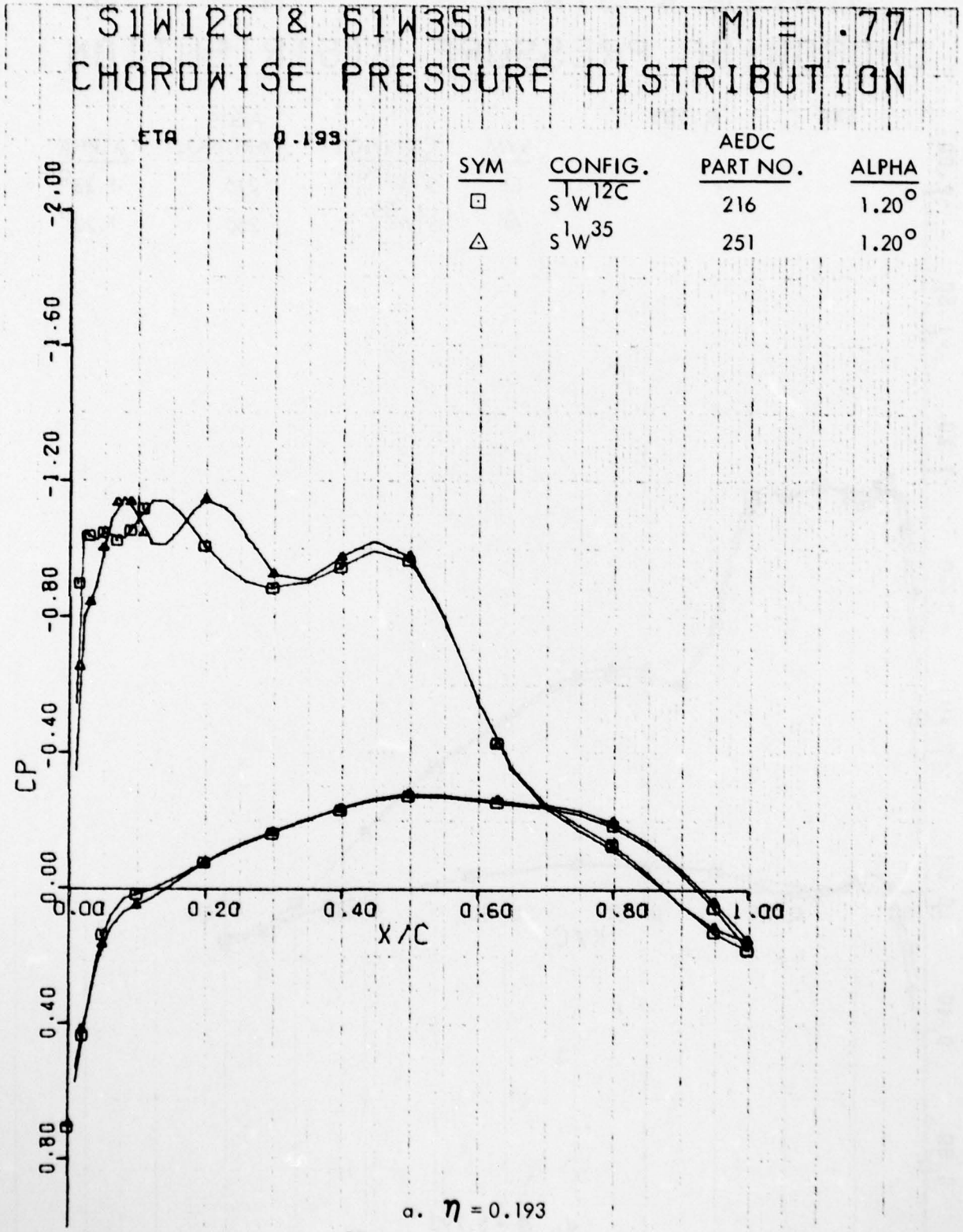

a. $\eta = 0.193$

Figure 18. Effect of W^{35} Leading Edge Modification on Chordwise Pressure Distributions at M = 0.77. Pylon/Nacelles On Configuration.

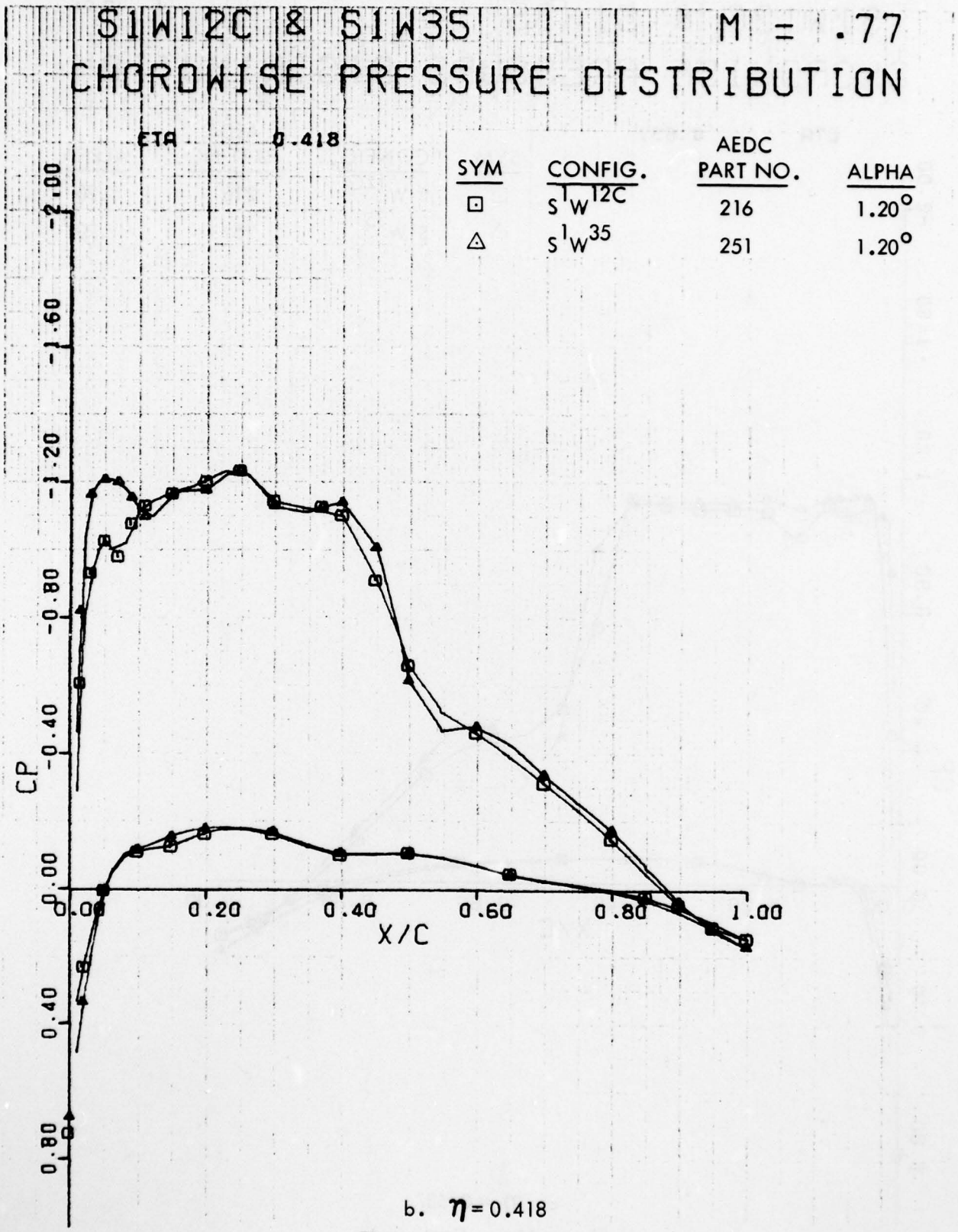

b. $\eta = 0.418$

Figure 18. Continued

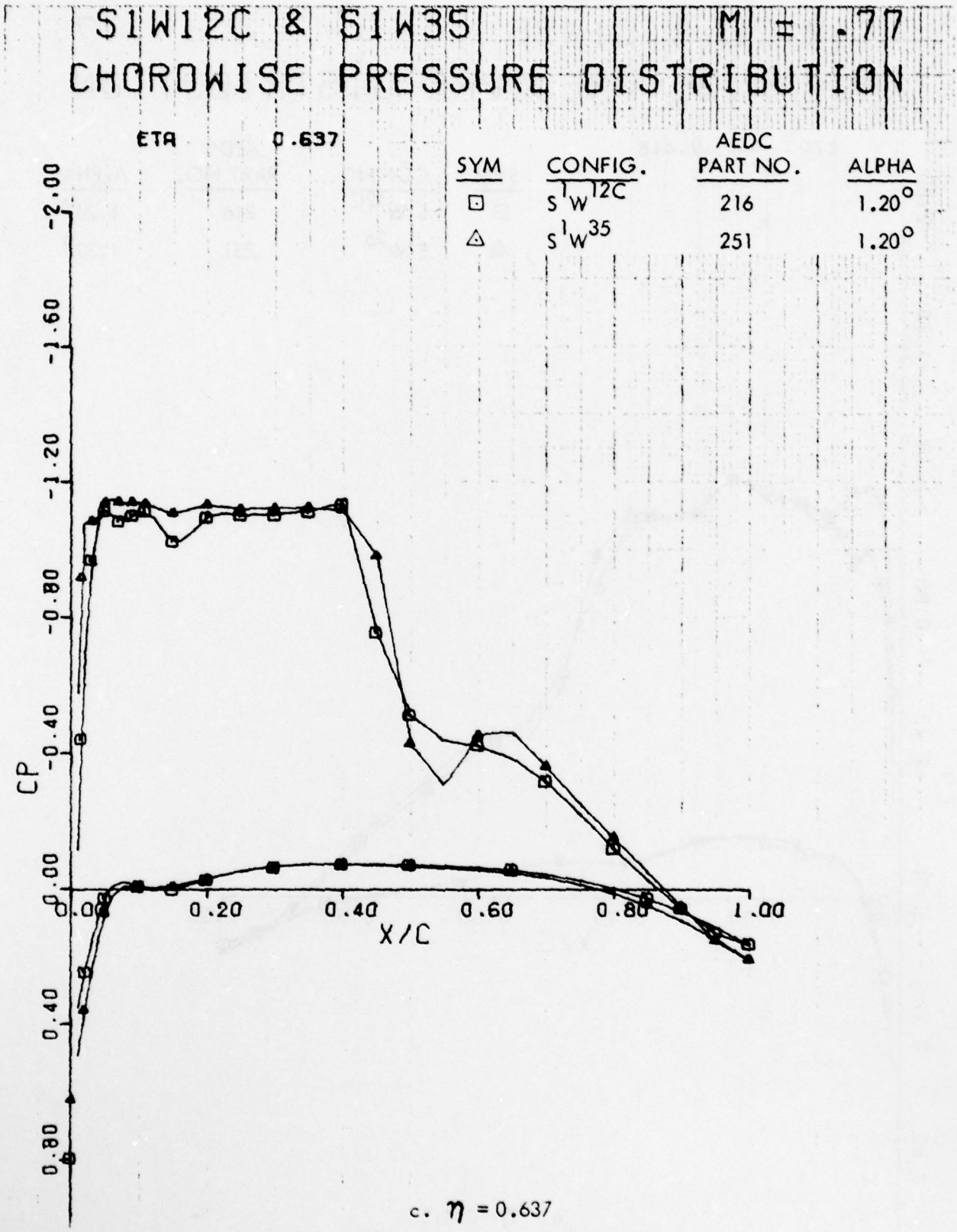

c. $\eta = 0.637$

Figure 18 . Continued

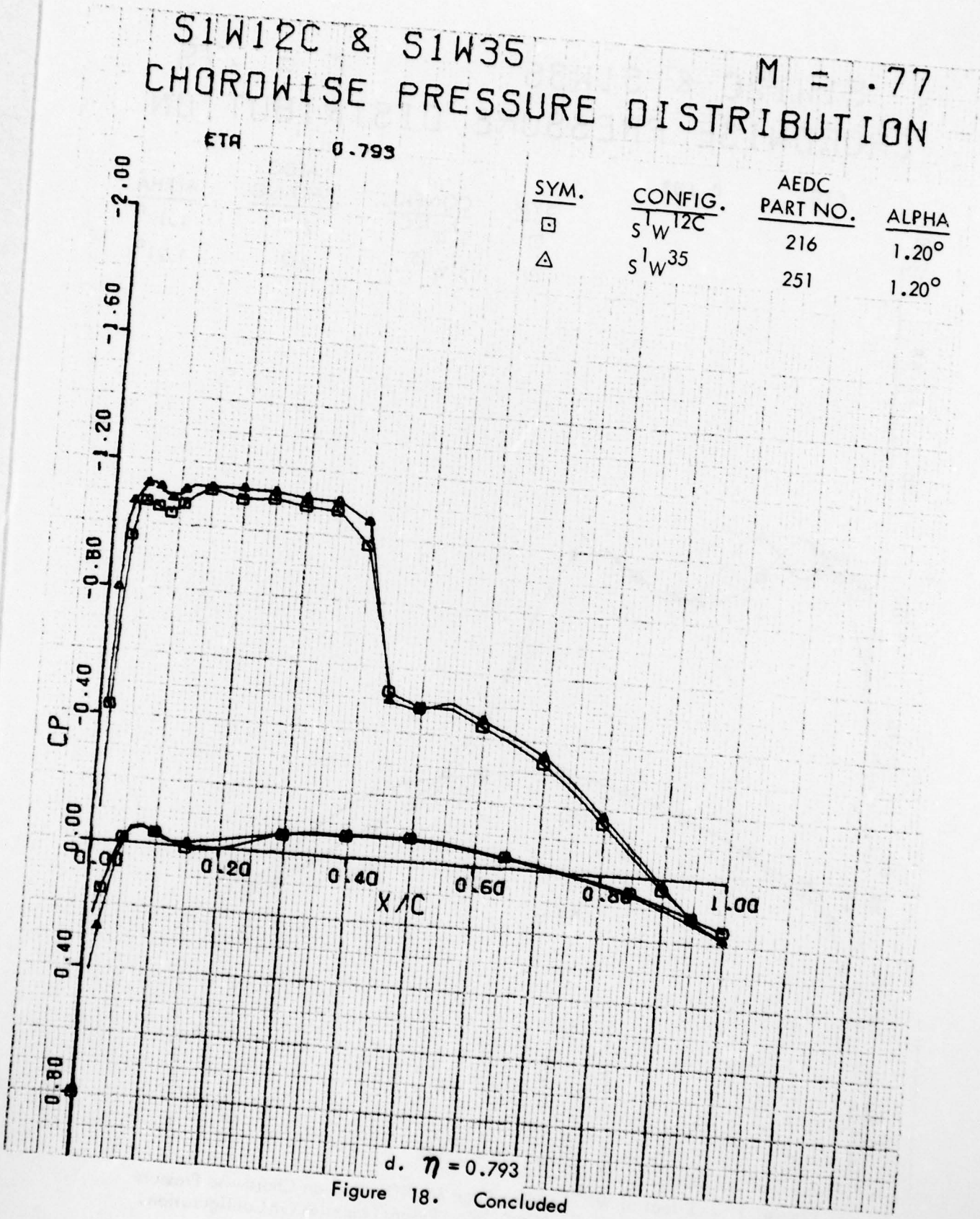

d. $\eta = 0.793$

Figure 18. Concluded

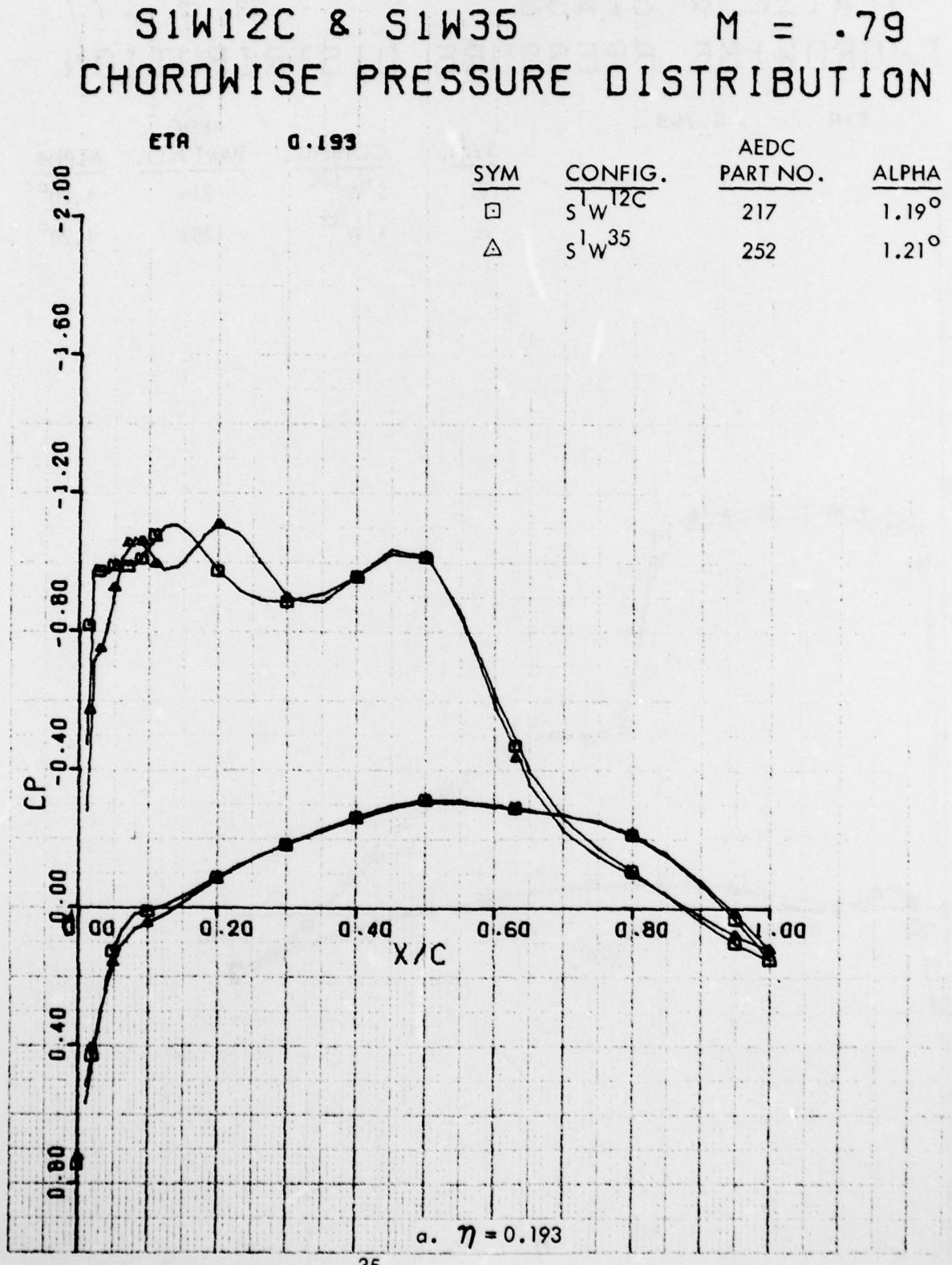

Figure 19. Effect of W^{35} Leading Edge Modification on Chordwise Pressure Distributions at M = 0.79. Pylon/Nacelles On Configuration.

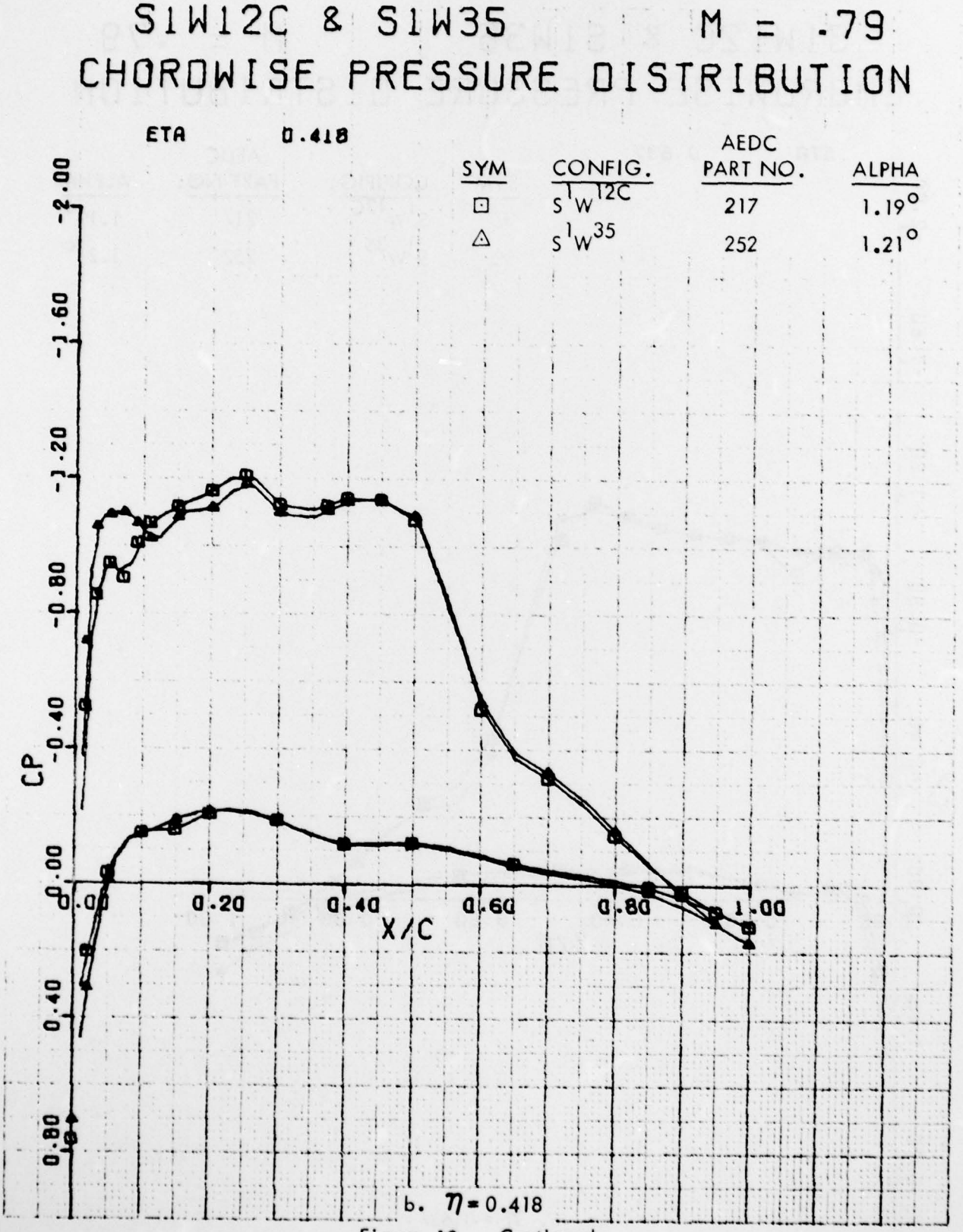

b. $\eta = 0.418$

Figure 19. Continued

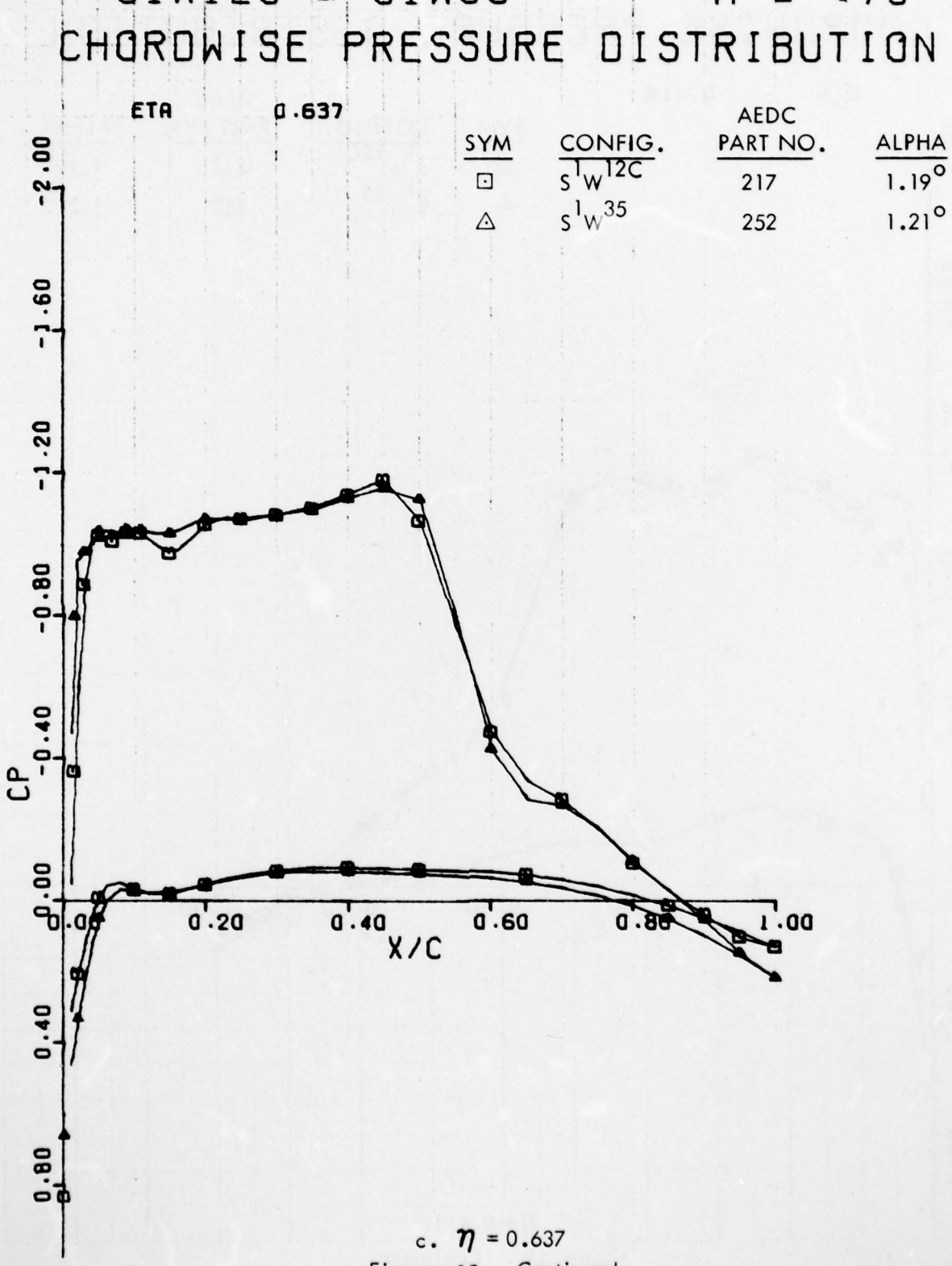

c. η = 0.637

Figure 19. Continued

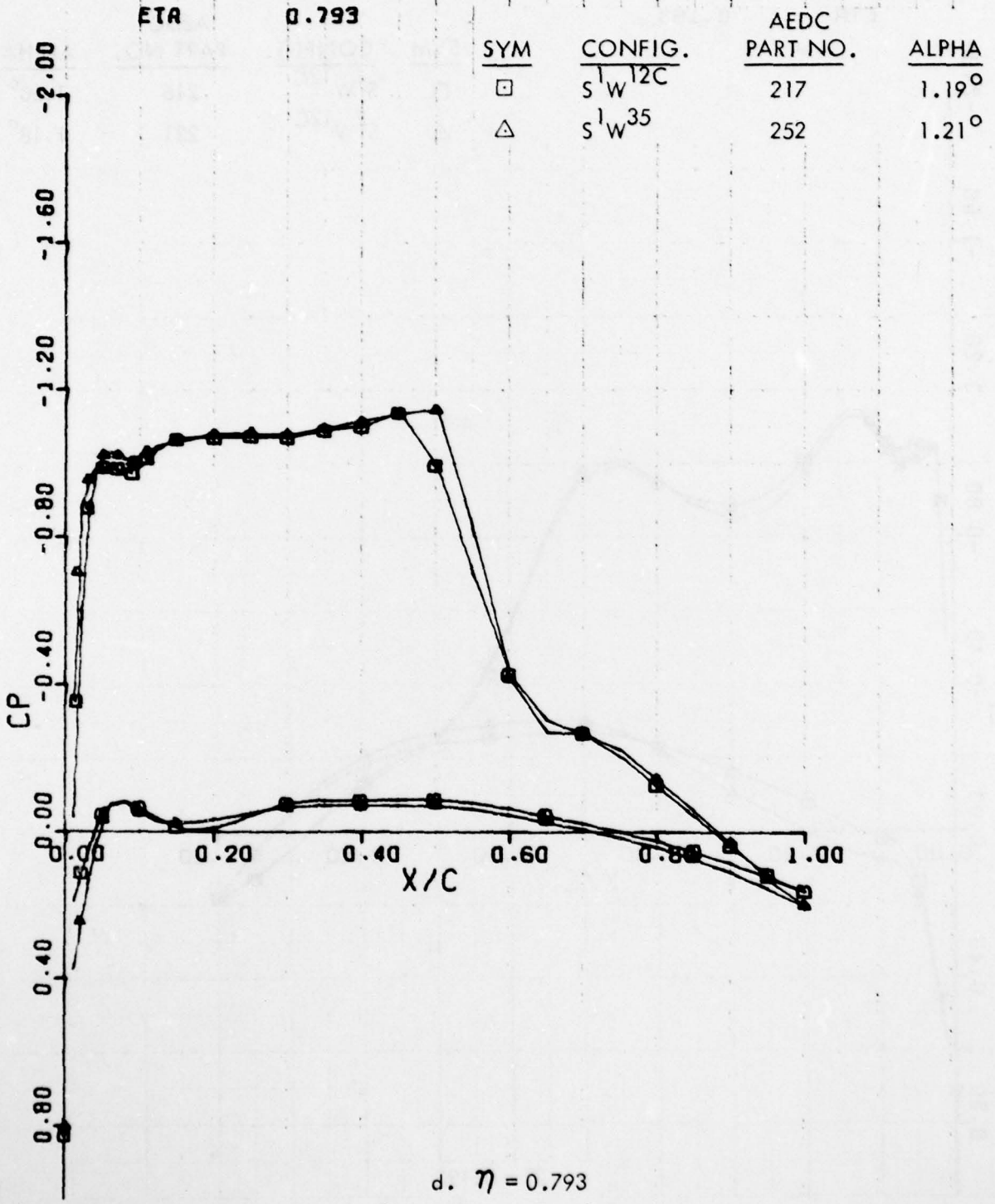

d. $\eta = 0.793$

Figure 19 . Concluded

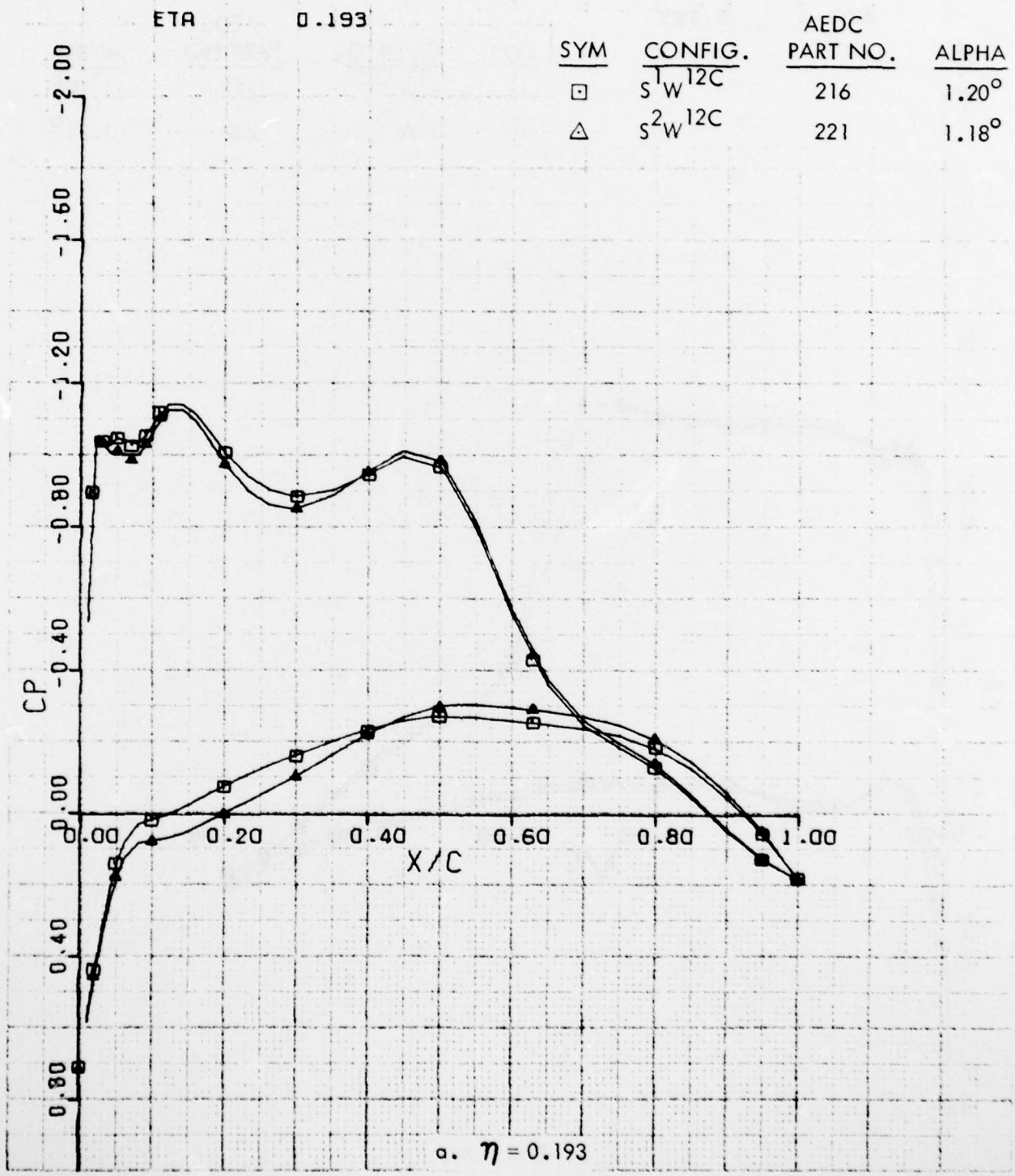

Figure 20. Effect of Pylon/Nacelles on W^{12C} Chordwise Pressure Distributions

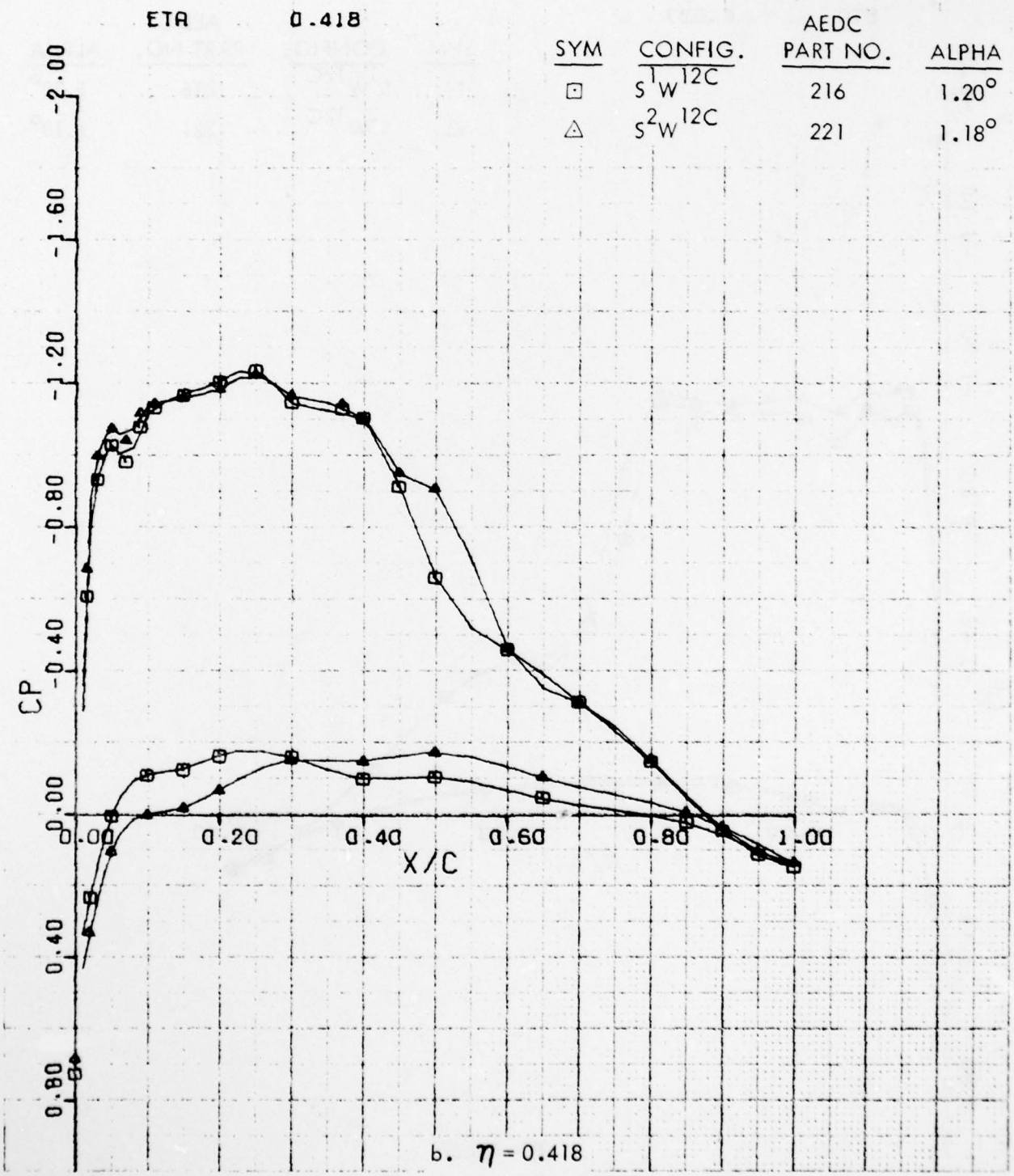

b. $\eta = 0.418$

Figure 20 . Continued

AD-A076 610 LOCKHEED-GEORGIA CO MARIETTA F/G 1/3
AERODYNAMIC INVESTIGATION OF C-141 LEADING EDGE MODIFICATION FO--ETC(U)
JUN 79 W T BLACKERBY , P R SMITH F09603-77-A-0204
UNCLASSIFIED LG78ER0233-VOL-1 AFFDL-TR-79-3059-VOL-1 NL

2 OF 2
AD
A076610

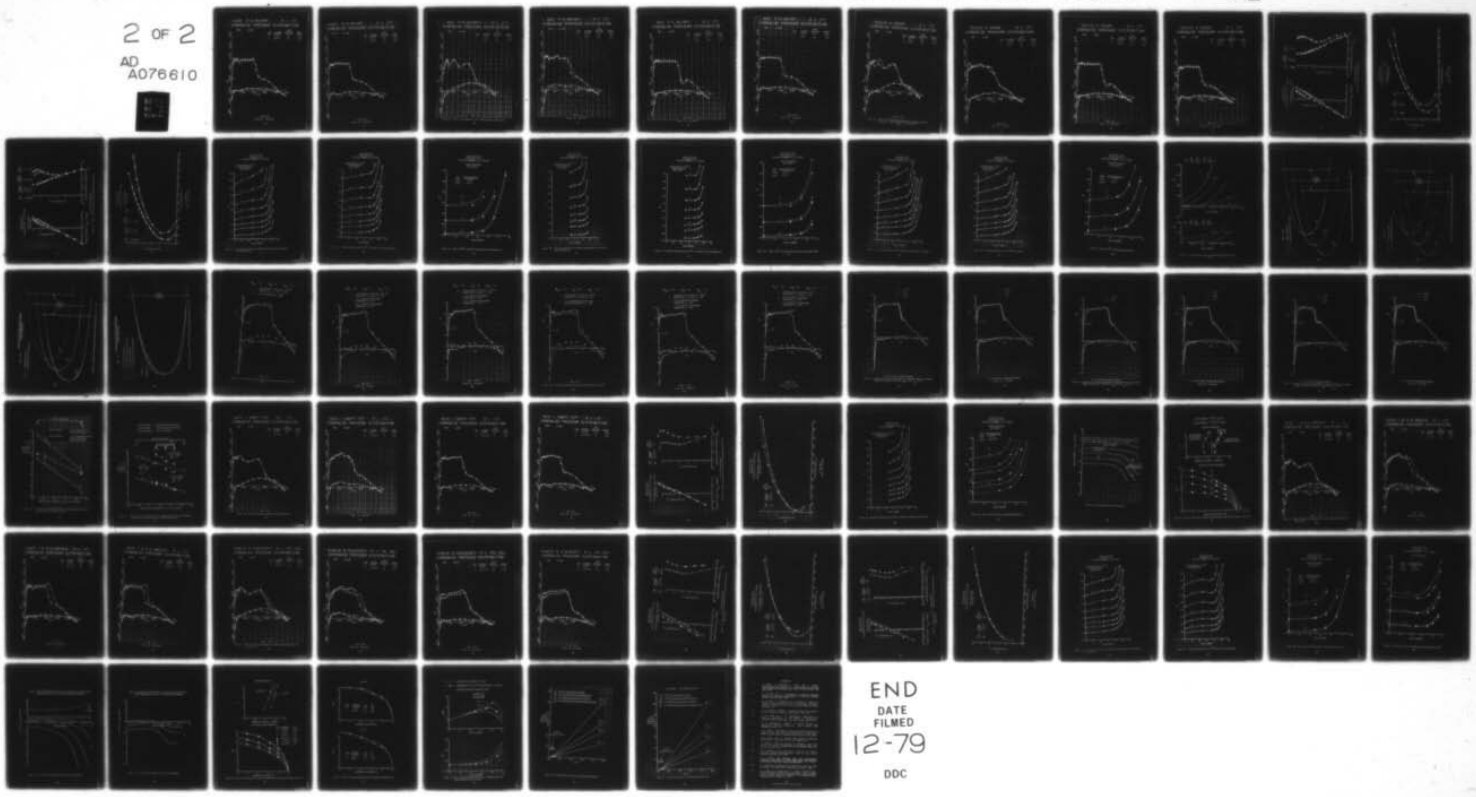

END
DATE
FILMED
12-79
DDC

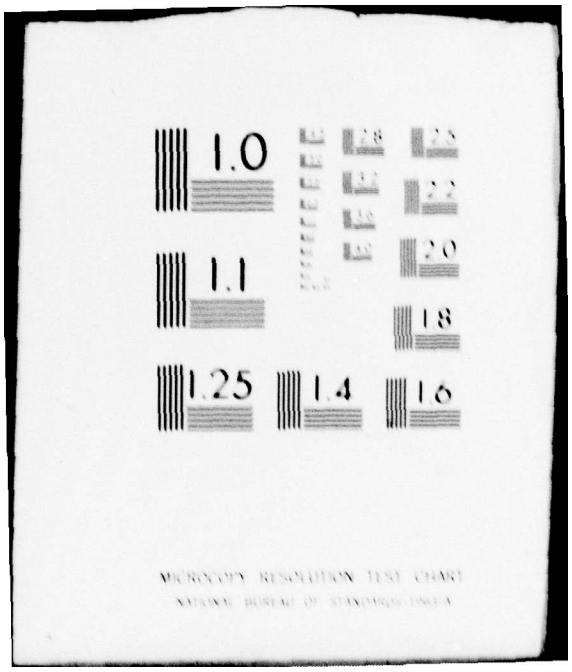
1.0
1.1
1.25
1.4
1.6
2.0
1.8
MICROCOPY RESOLUTION TEST CHART
NATIONAL BUREAU OF STANDARDS-1963-A

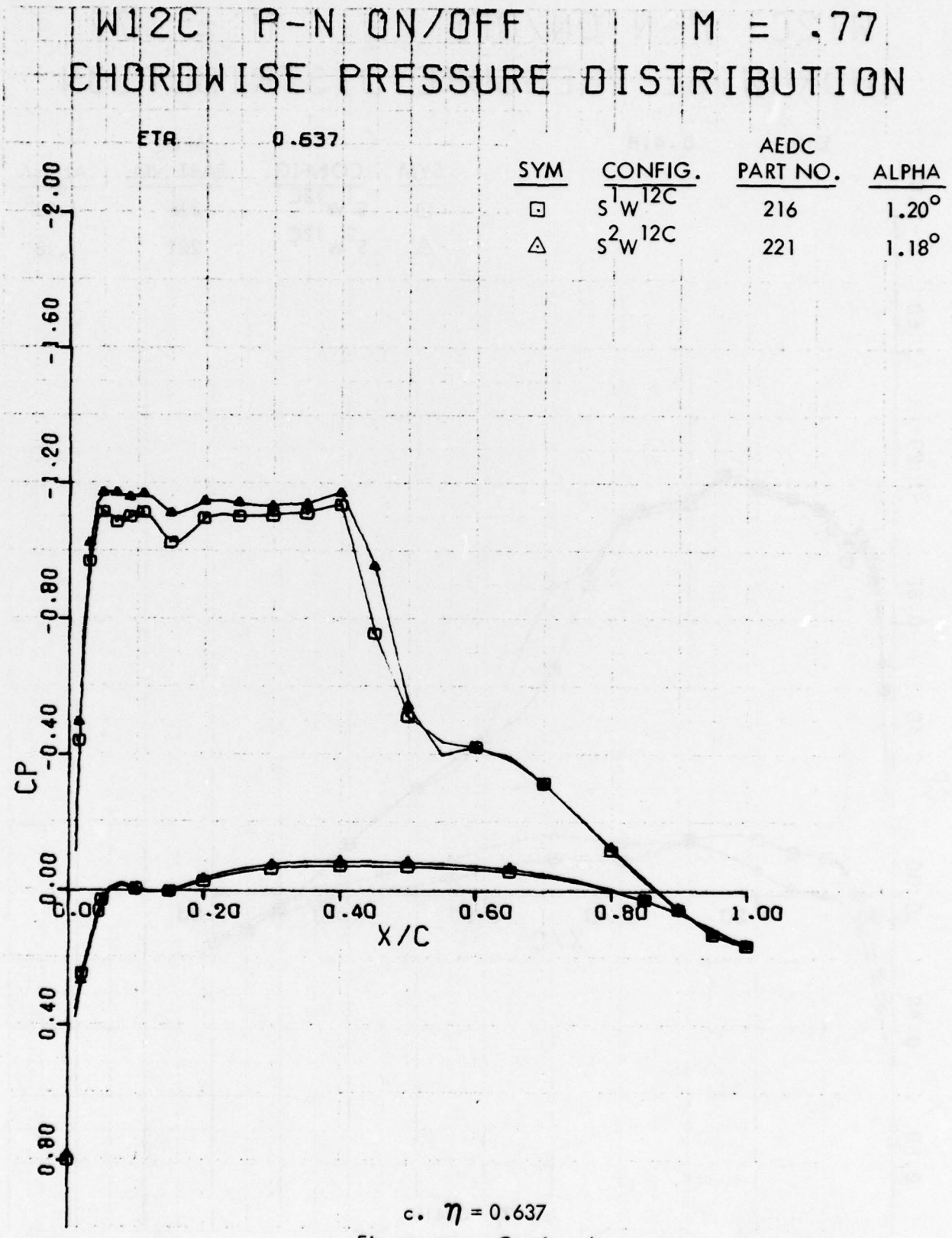

c. $\eta = 0.637$

Figure 20 . Continued

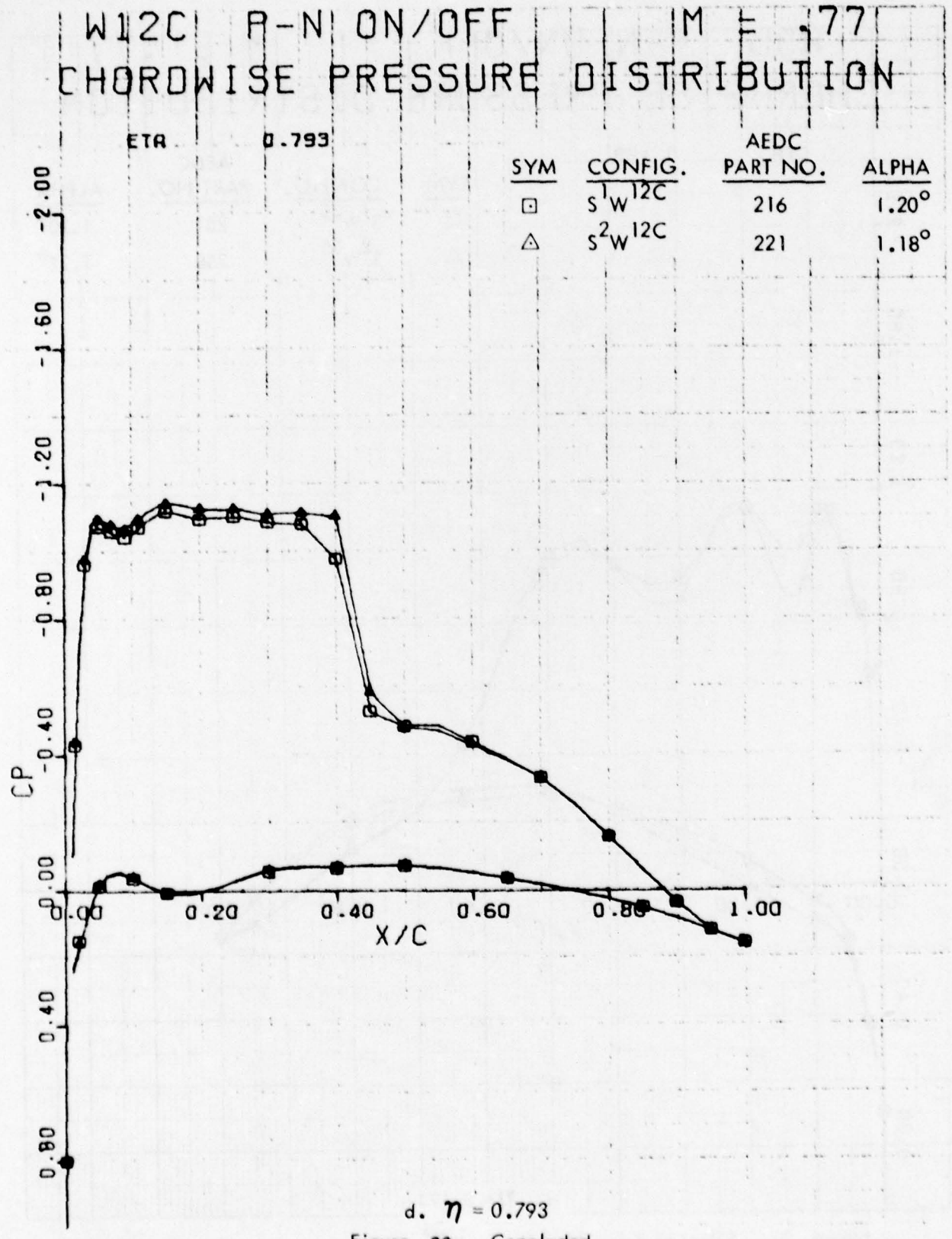

d. $\eta = 0.793$

Figure 20. Concluded

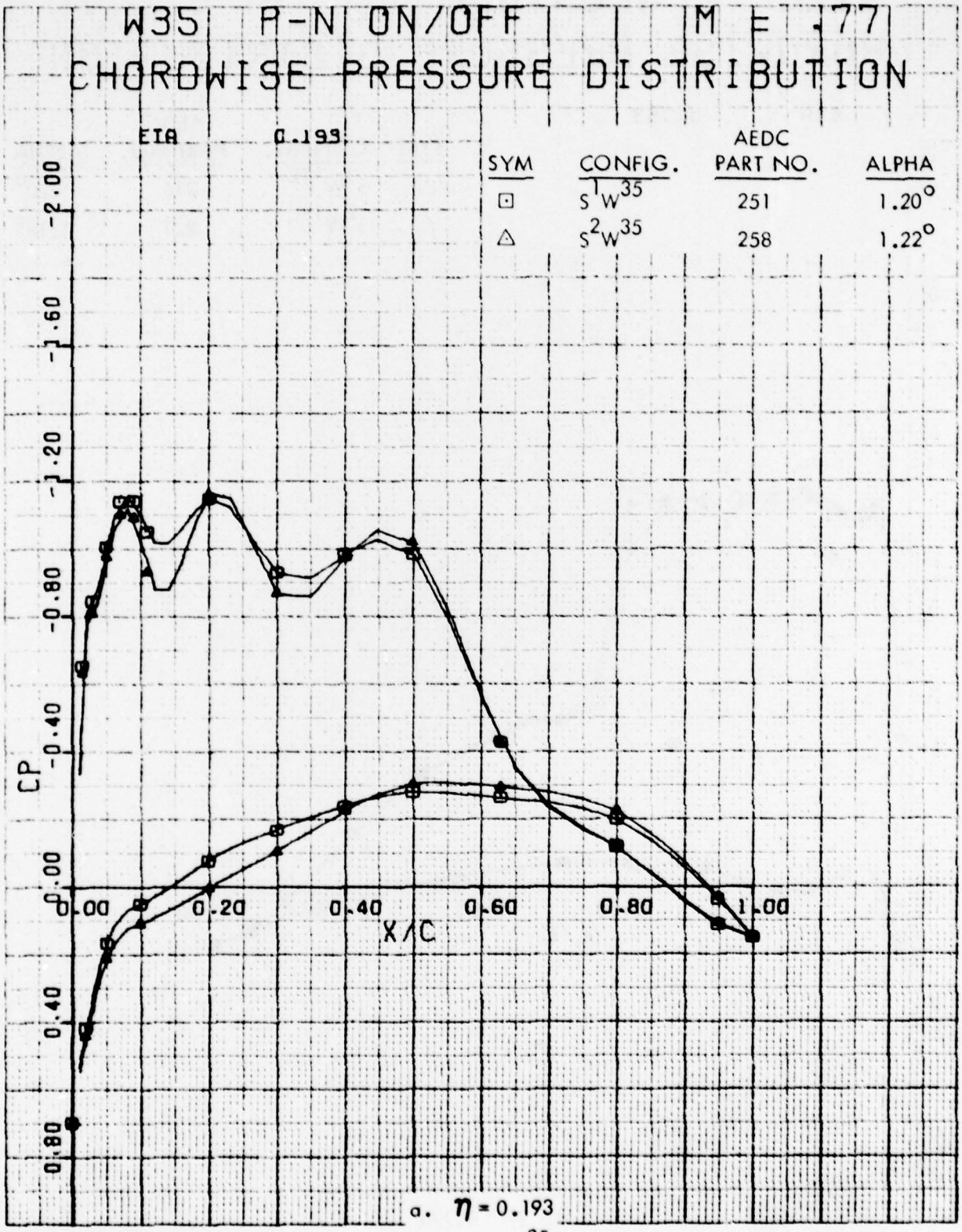

Figure 21. Effect of Pylon/Nacelles on W^{35} Chordwise Pressure Distributions

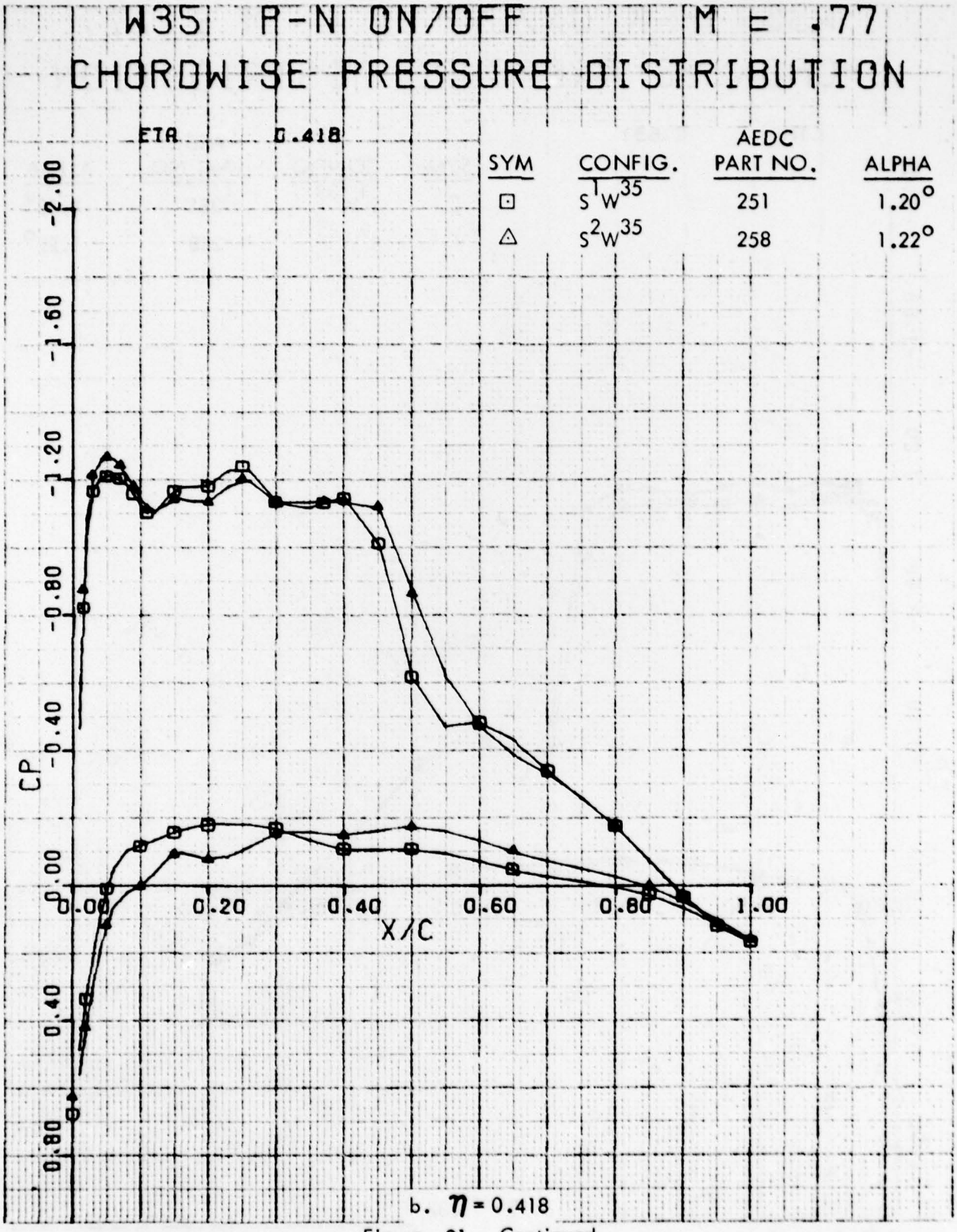

b. $\eta = 0.418$

Figure 21. Continued

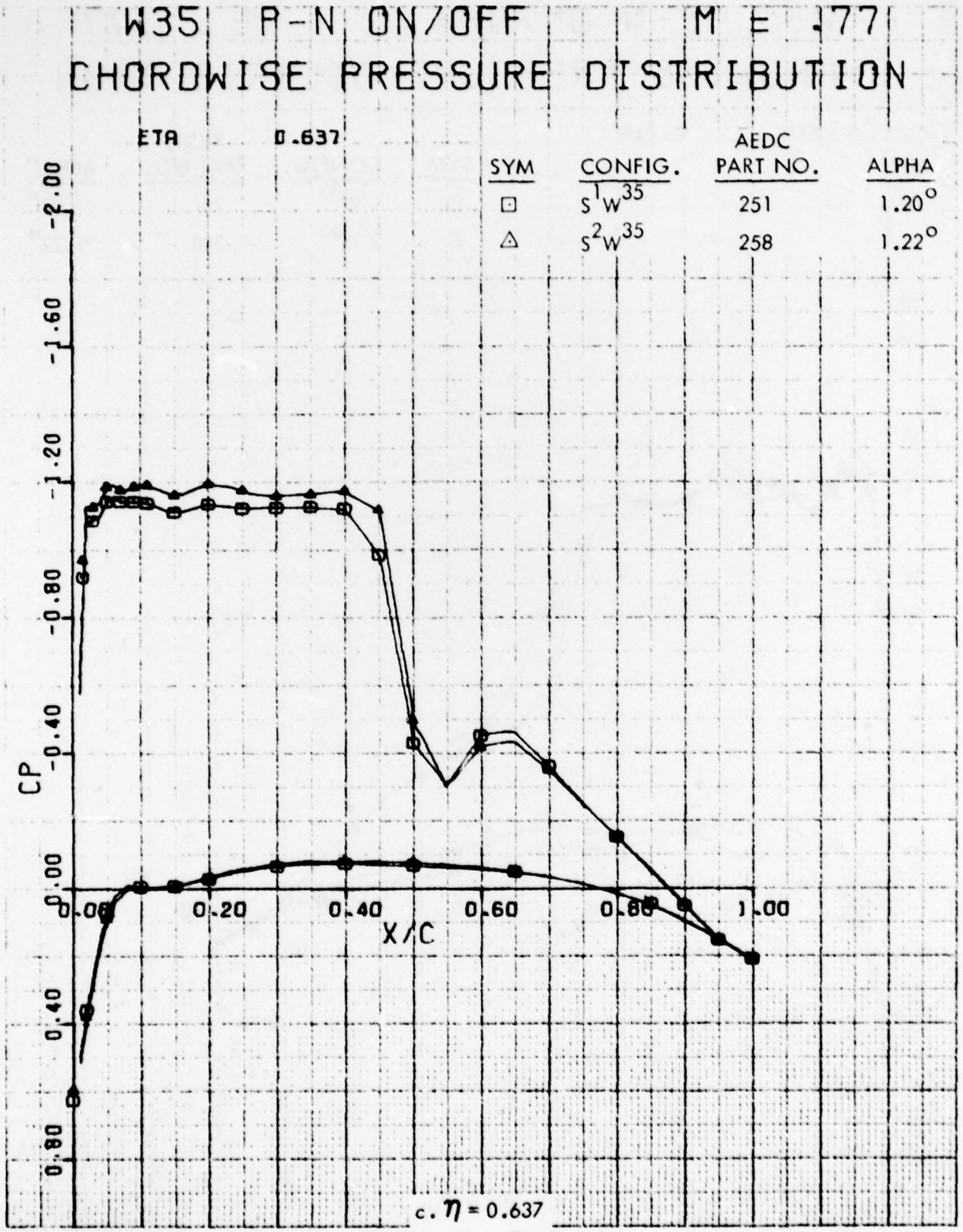

c. $\eta = 0.637$

Figure 21. Continued

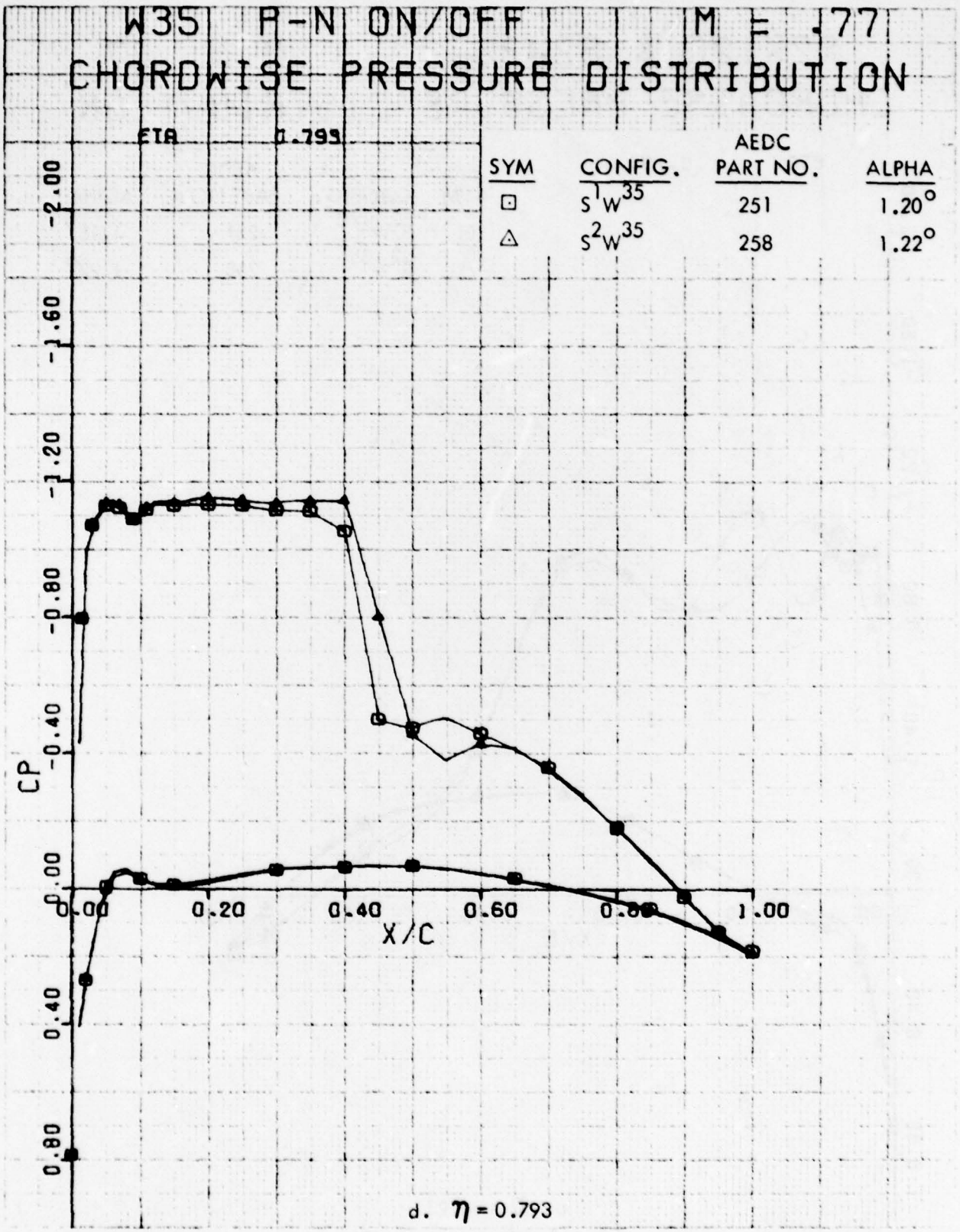

d. $\eta = 0.793$

Figure 21. Concluded

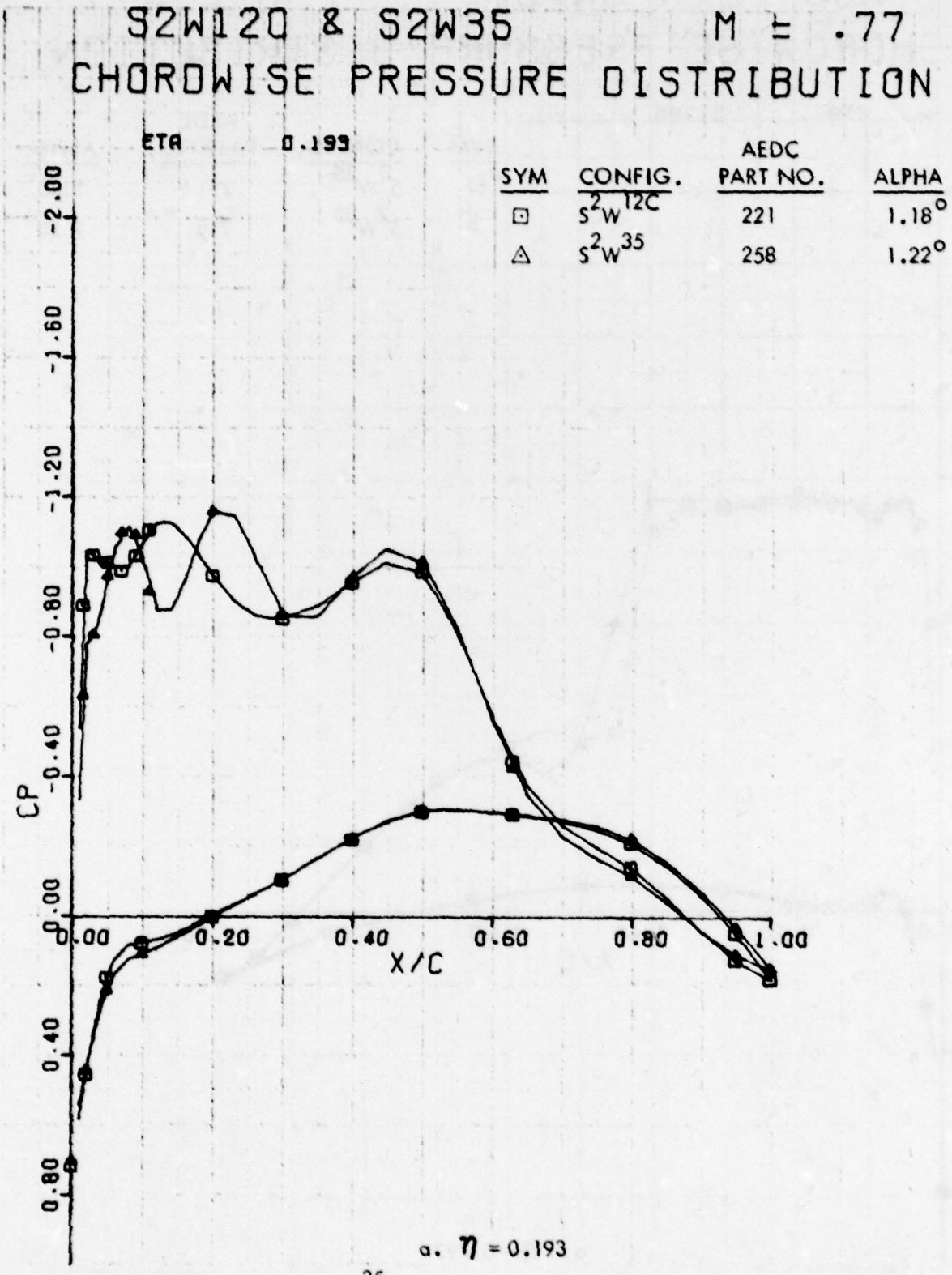

a. $\eta = 0.193$

Figure 22. Effect of W^{35} Leading Edge Modification on Chordwise Pressure Distributions. Pylon/Nacelles Off Configuration.

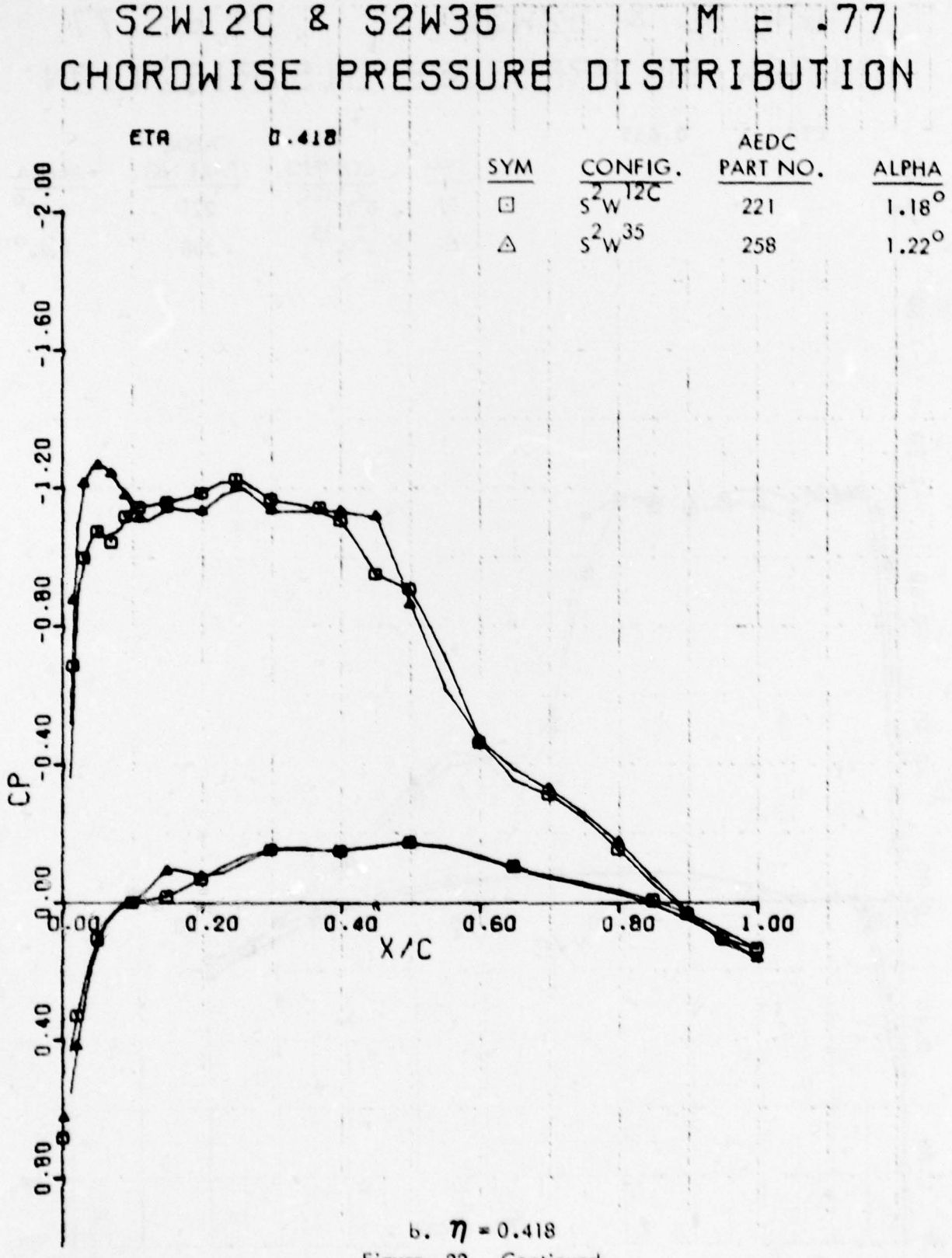

b. $\eta = 0.418$

Figure 22. Continued

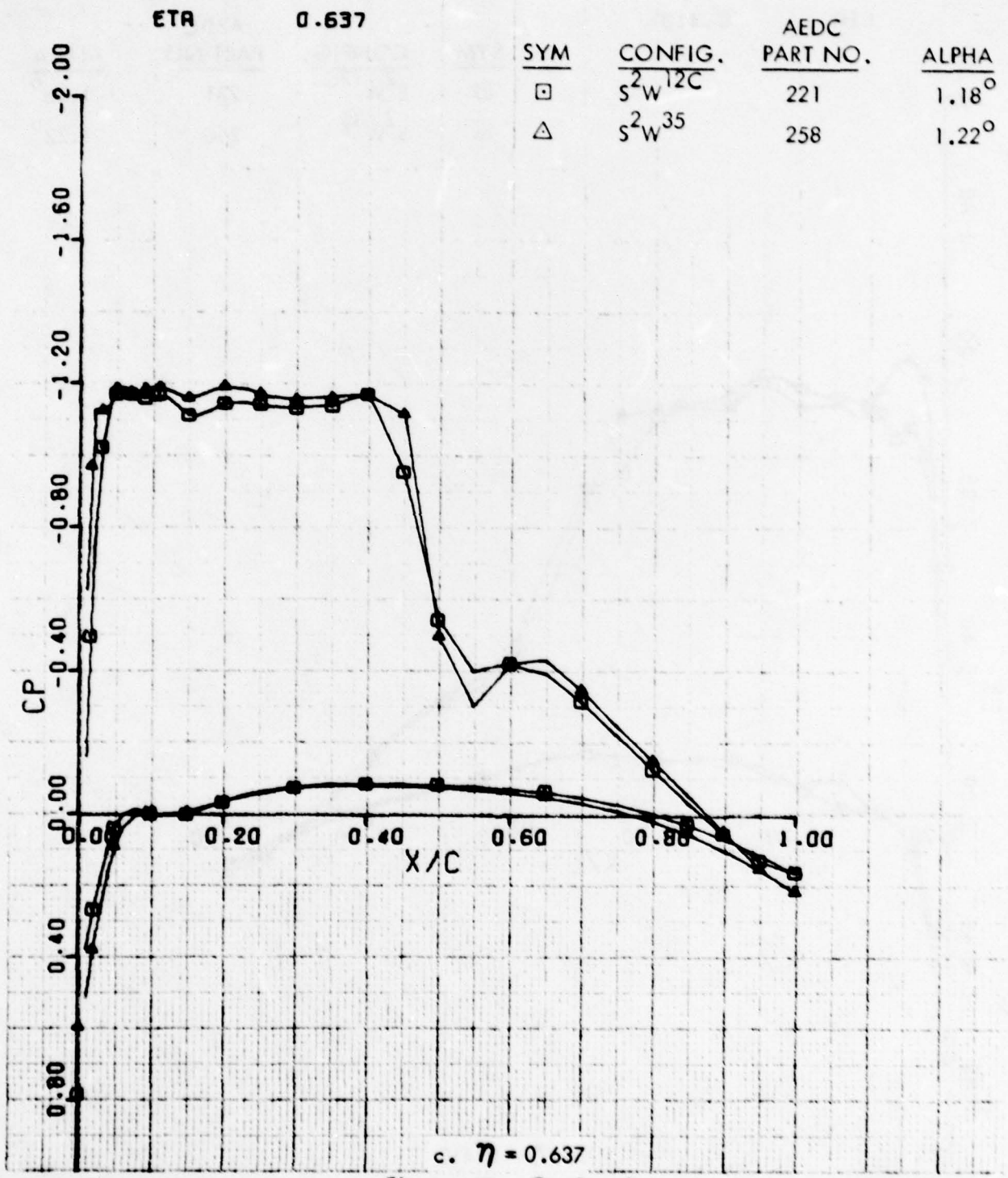

c. $\eta = 0.637$

Figure 22. Continued

S2W12C & S2W35 M = .77
CHORDWISE PRESSURE DISTRIBUTION

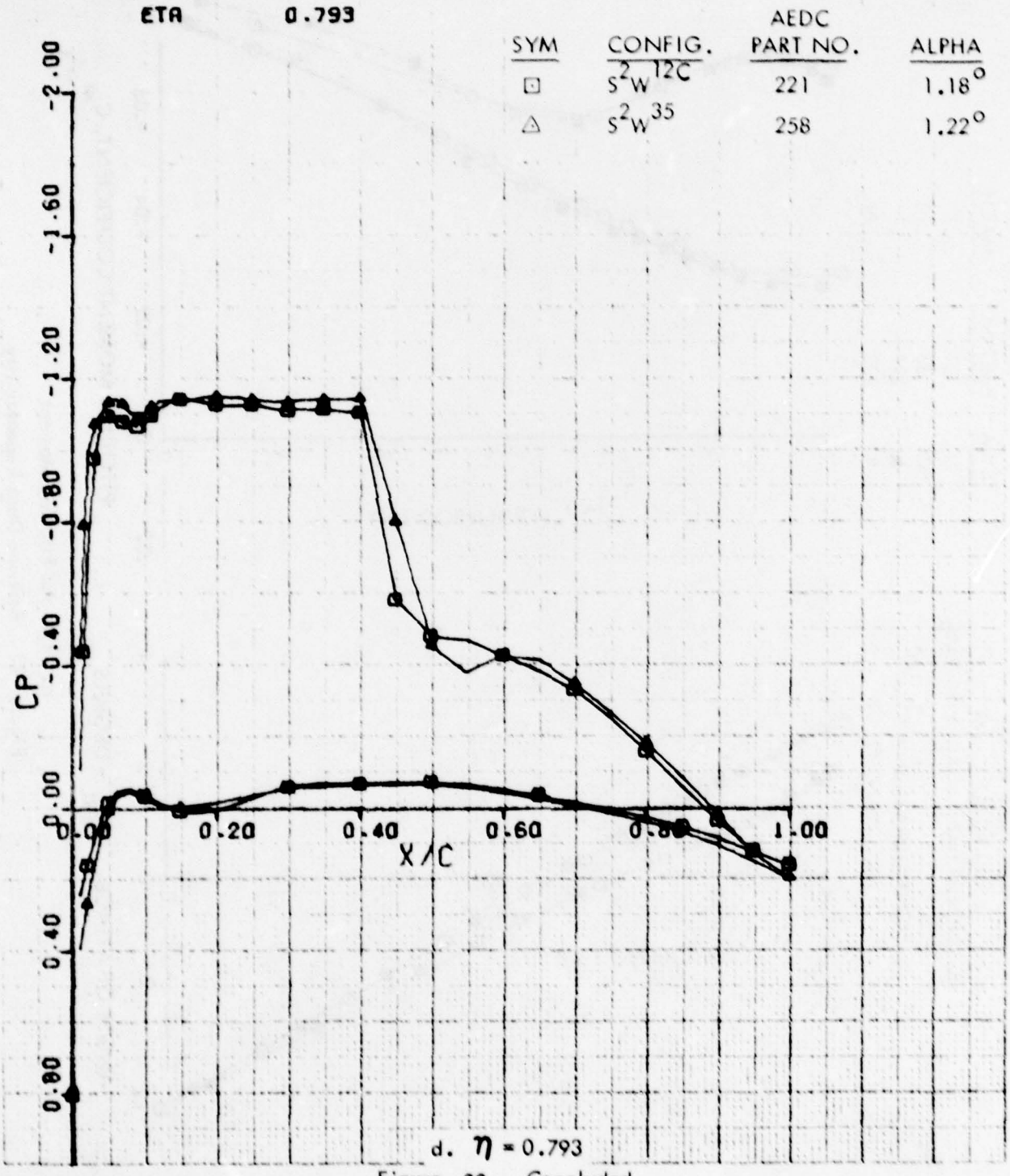

d. $\eta = 0.793$

Figure 22. Concluded

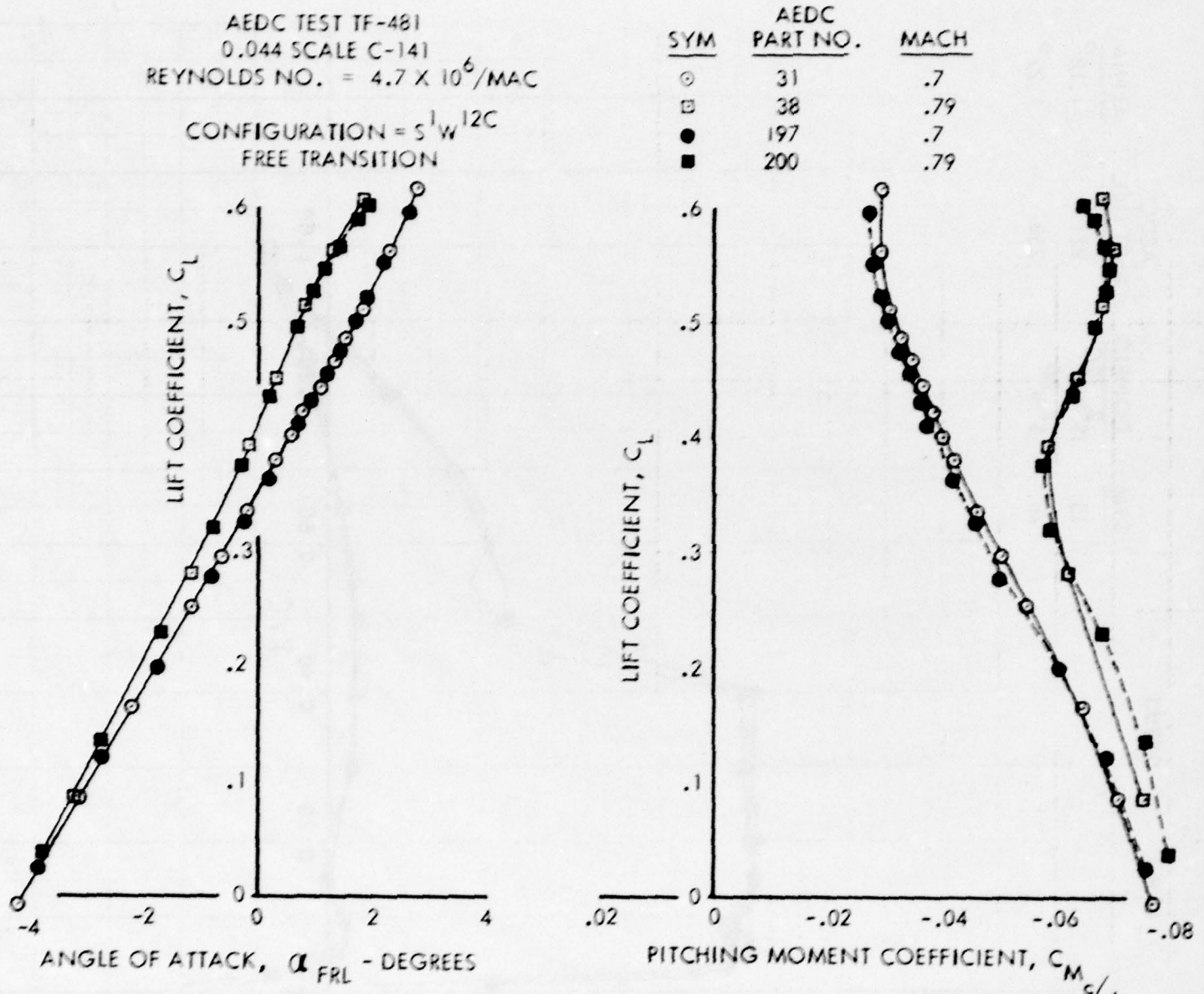

a. Lift and Pitching Moment

Figure 23. Baseline Data Repeatability

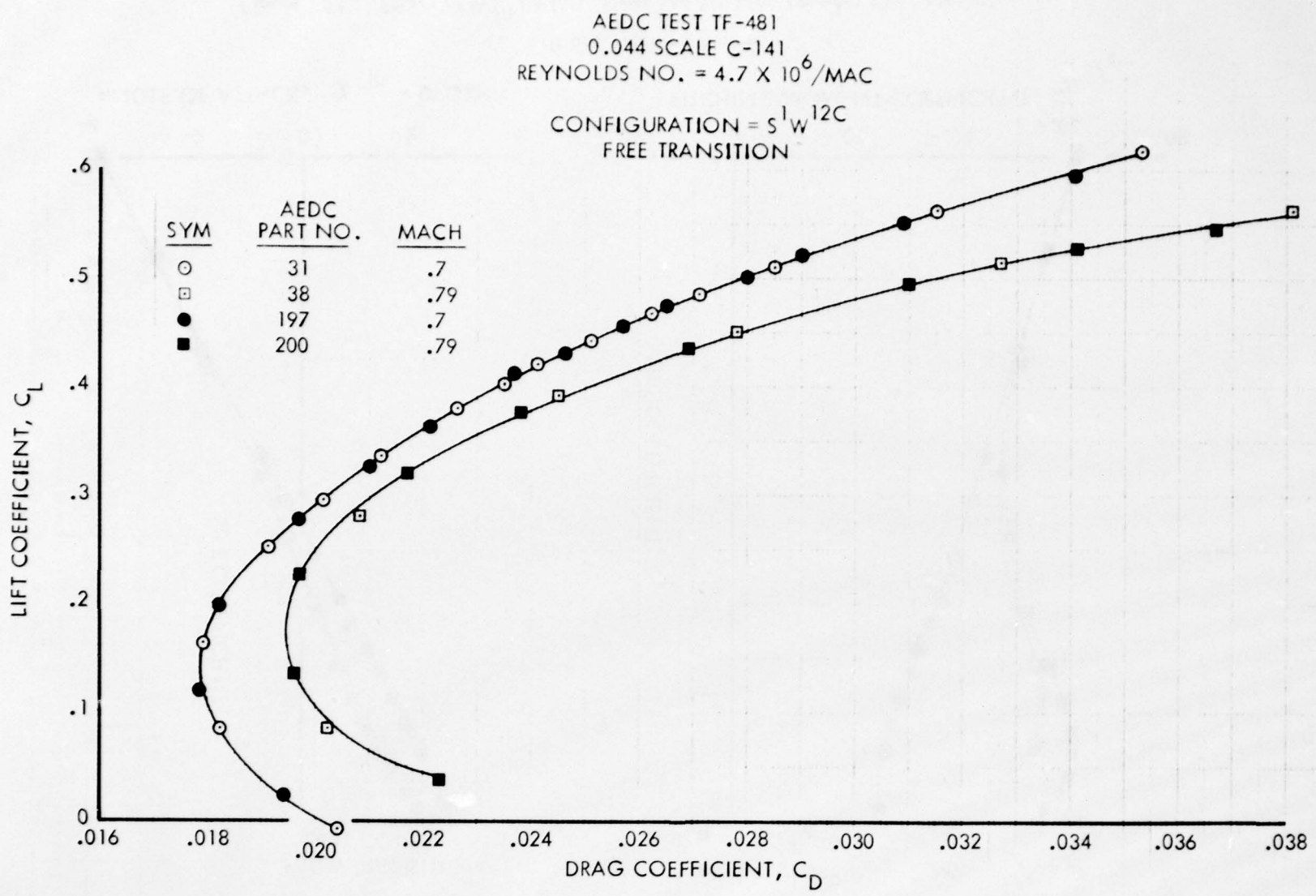

b. Drag Polar

Figure 23. Concluded

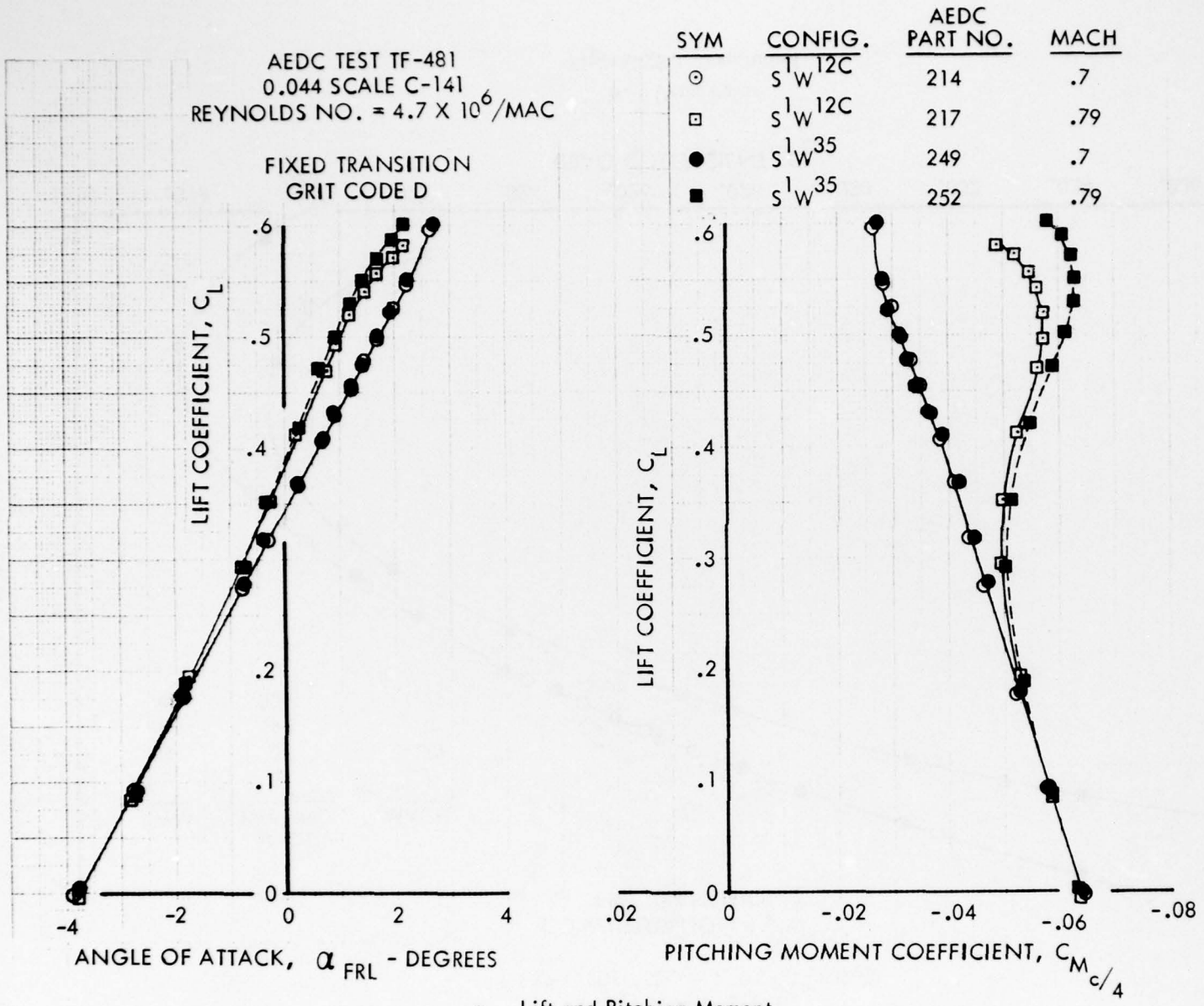

a. Lift and Pitching Moment

Figure 24. Effect of W^{35} on Lift, Drag and Pitching Moment Characteristics

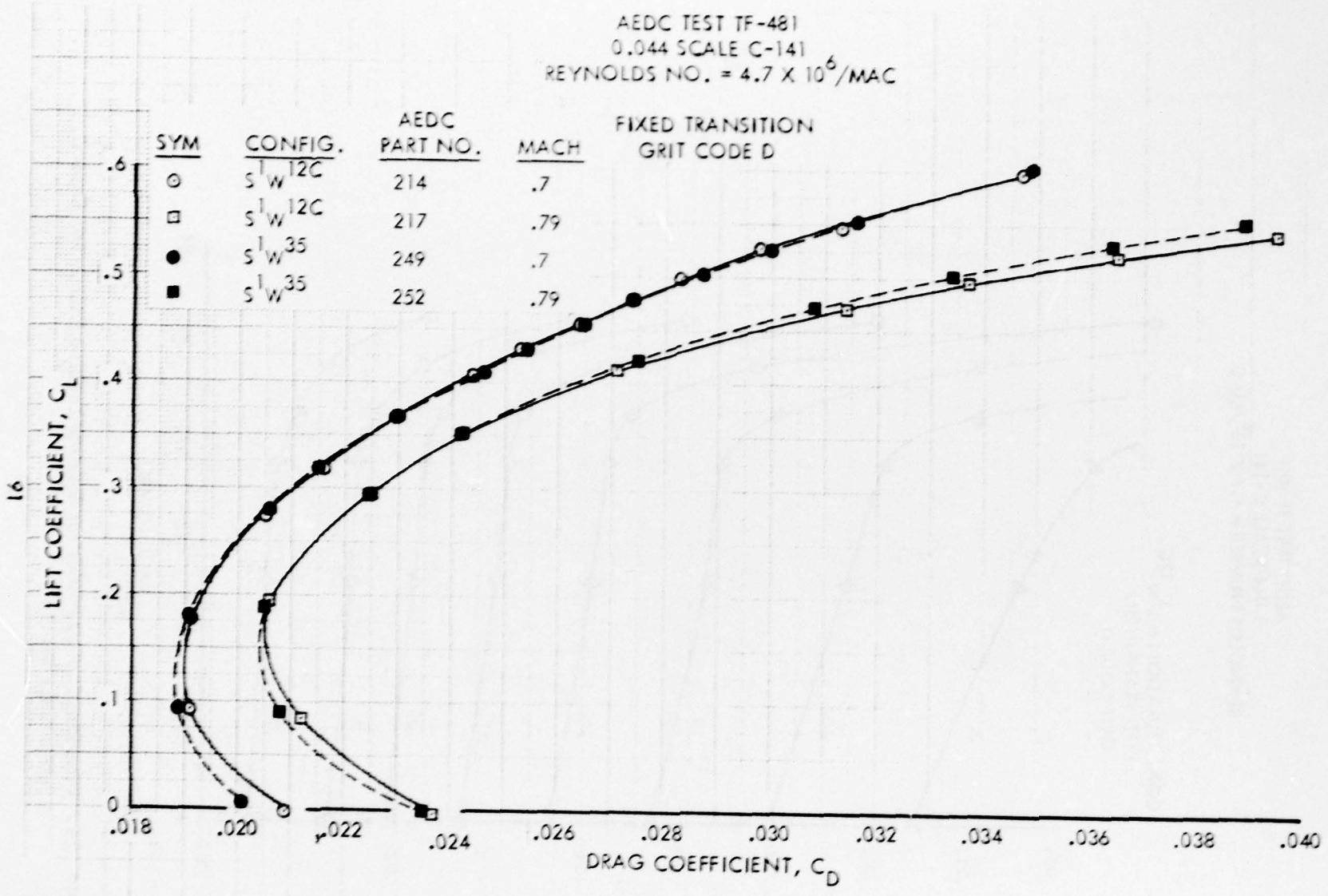

b. Drag Polar

Figure 24. Concluded

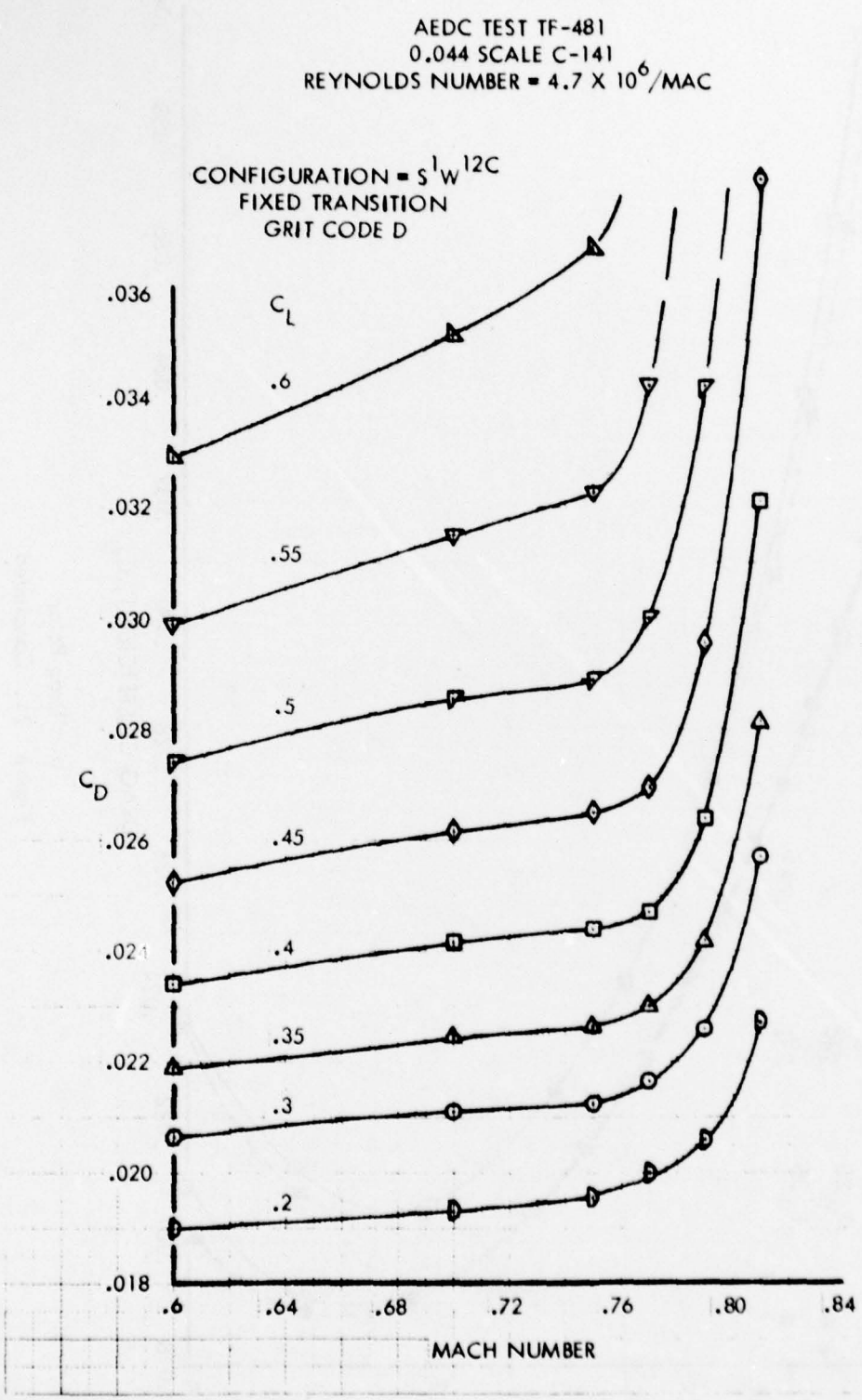

Figure 25. Drag Rise Characteristics for Baseline Leading Edge, Grit Code D, Pylon/Nacelles On

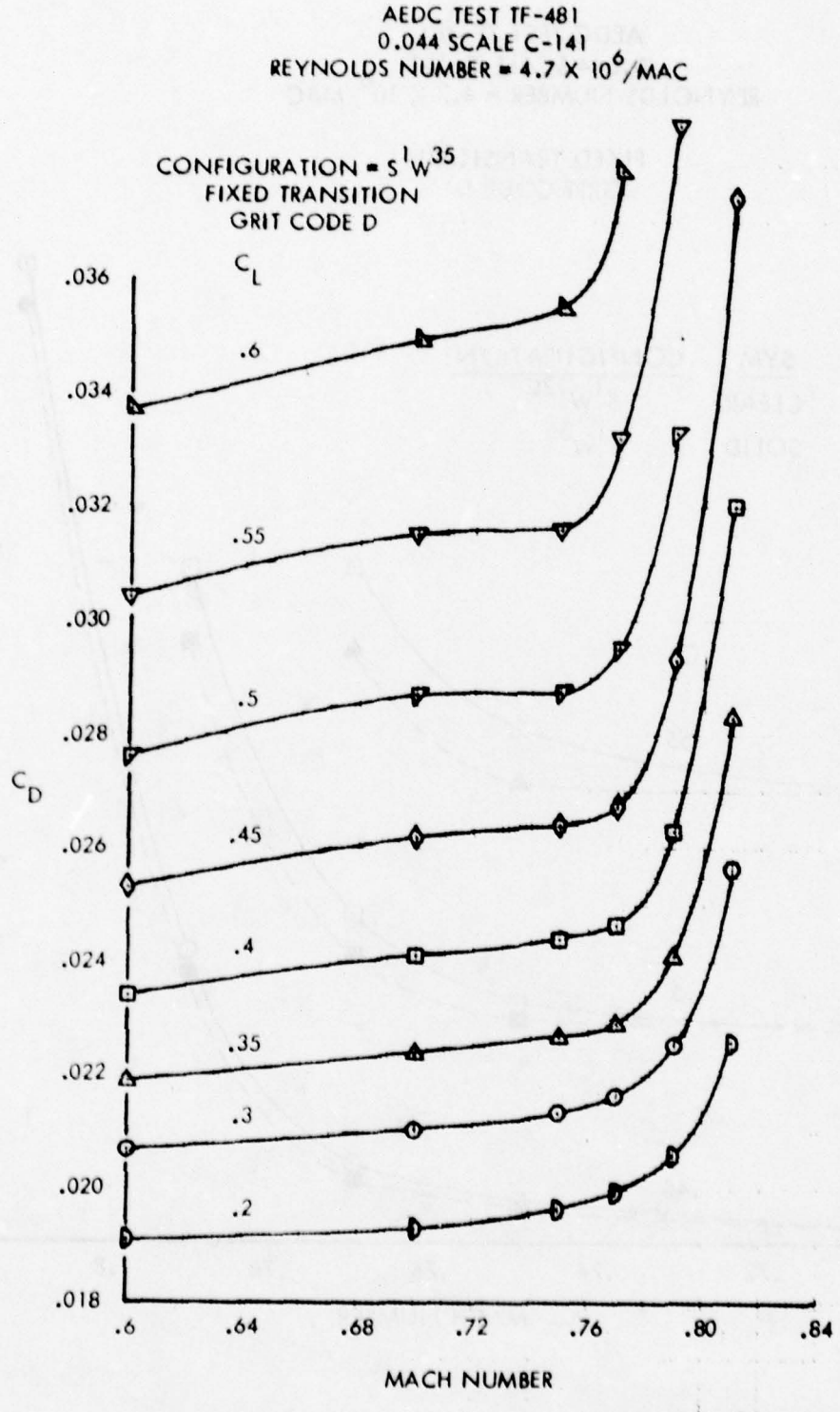

Figure 26. Drag Rise Characteristics for W^{35}, Grit Code D, Pylon/Nacelles On

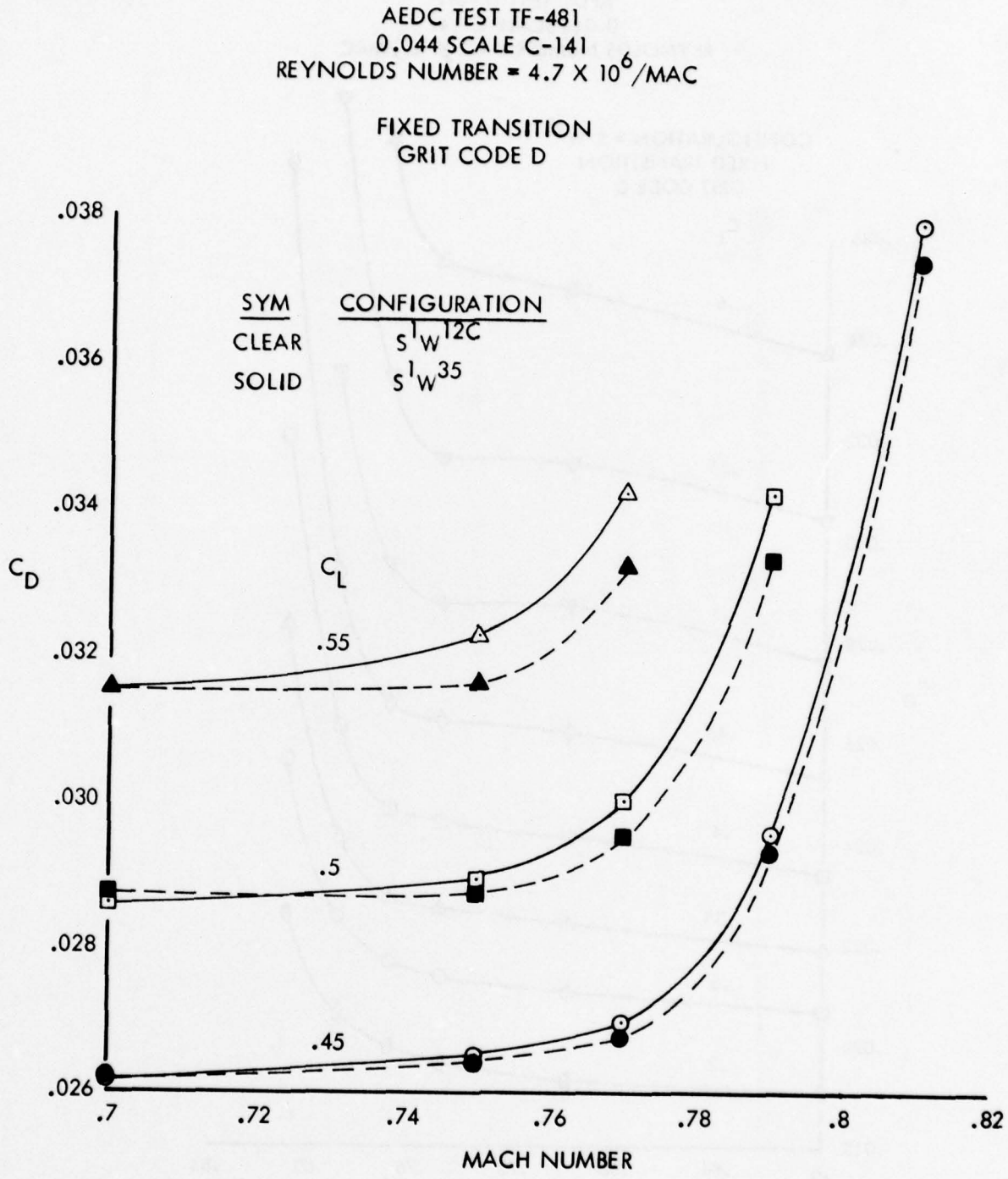

Figure 27. Effect of W^{35} on Drag Rise Characteristics, Pylon/Nacelles On

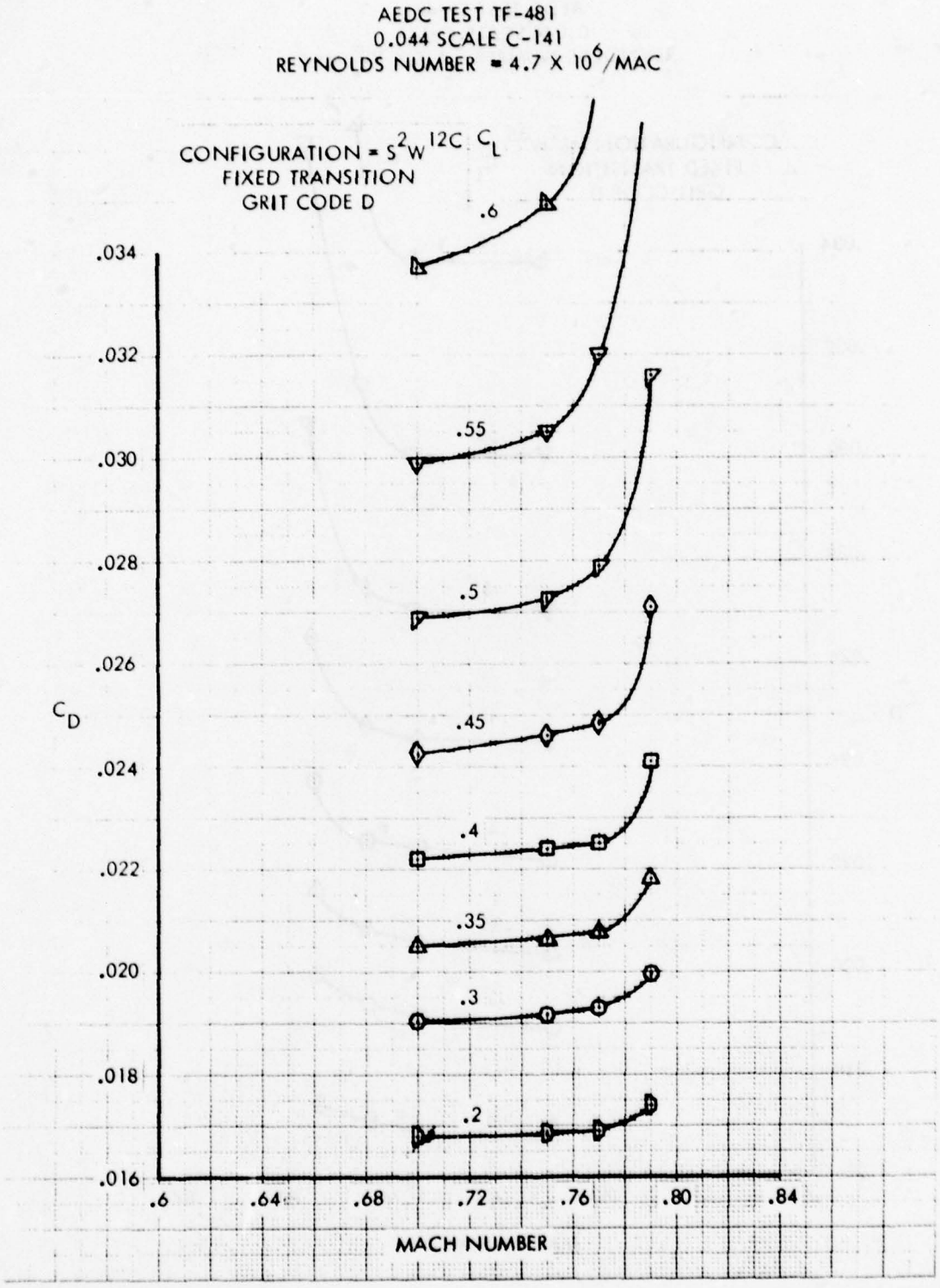

Figure 28. Drag Rise Characteristics for Baseline Leading Edge, Grit Code D, Pylon/Nacelles Off

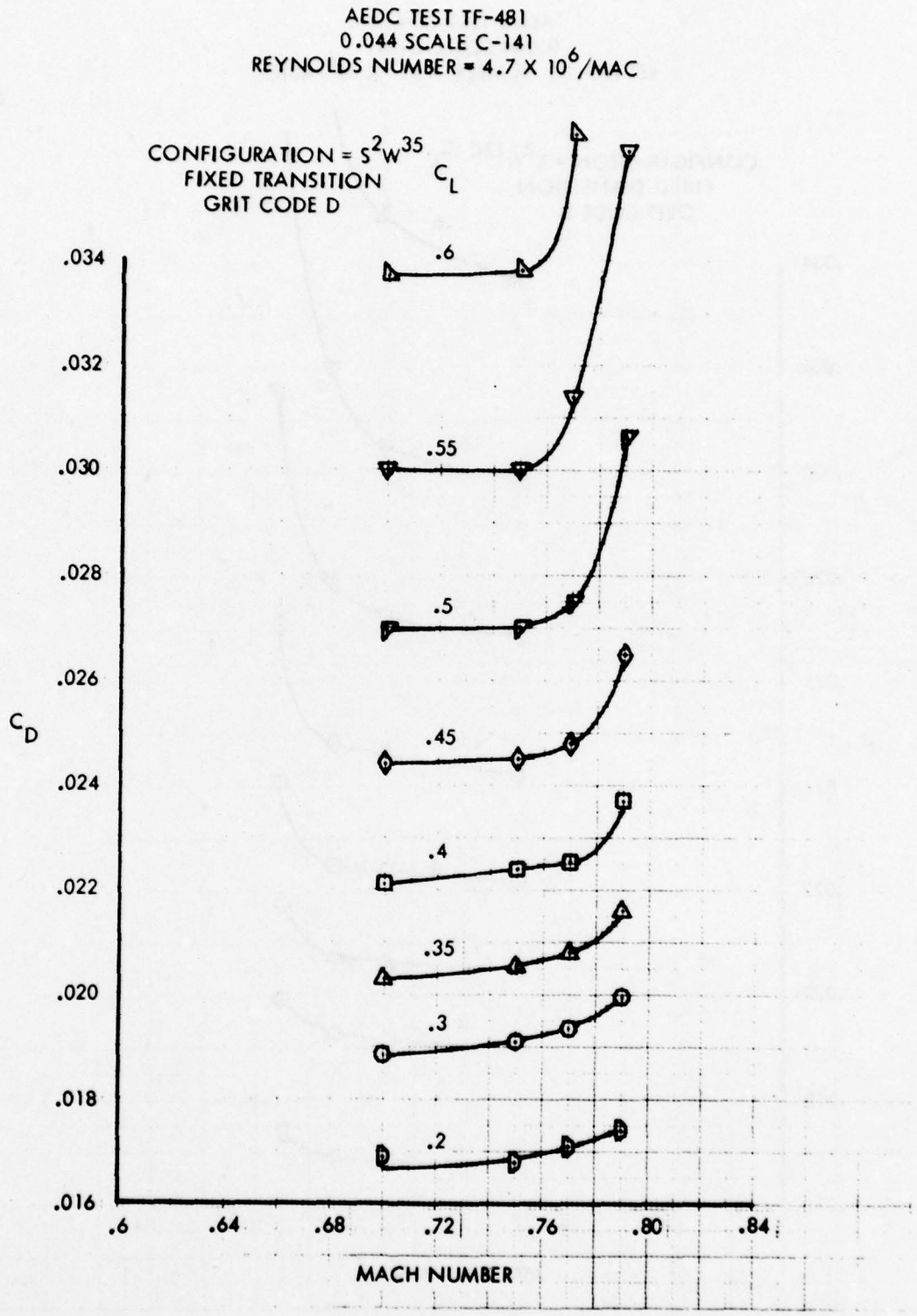

Figure 29. Drag Rise Characteristics for W^{35}, Grit Code D, Pylon/Nacelles Off

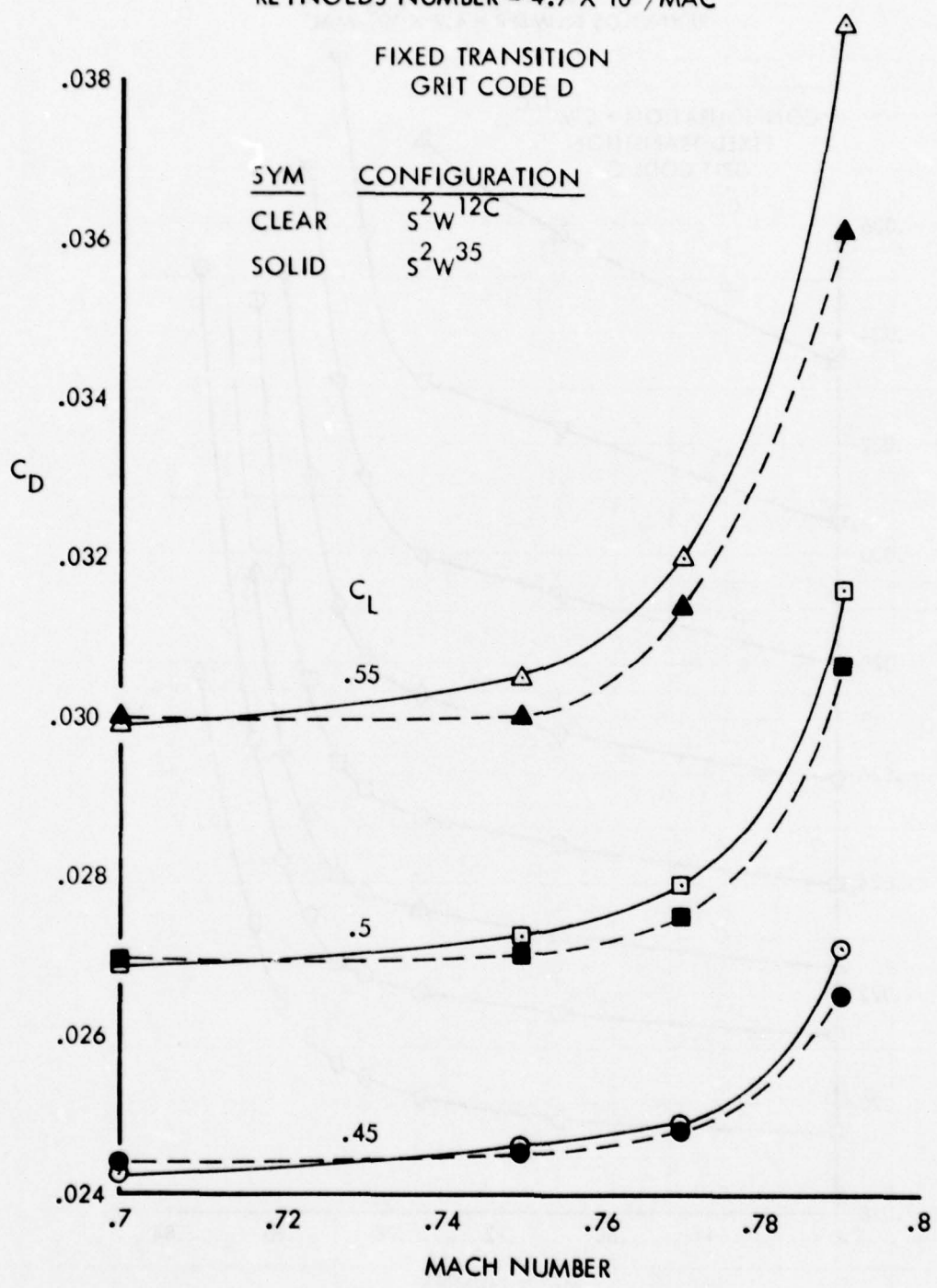

Figure 30. Effect of W^{35} on Drag Rise Characteristics, Pylon/Nacelles Off

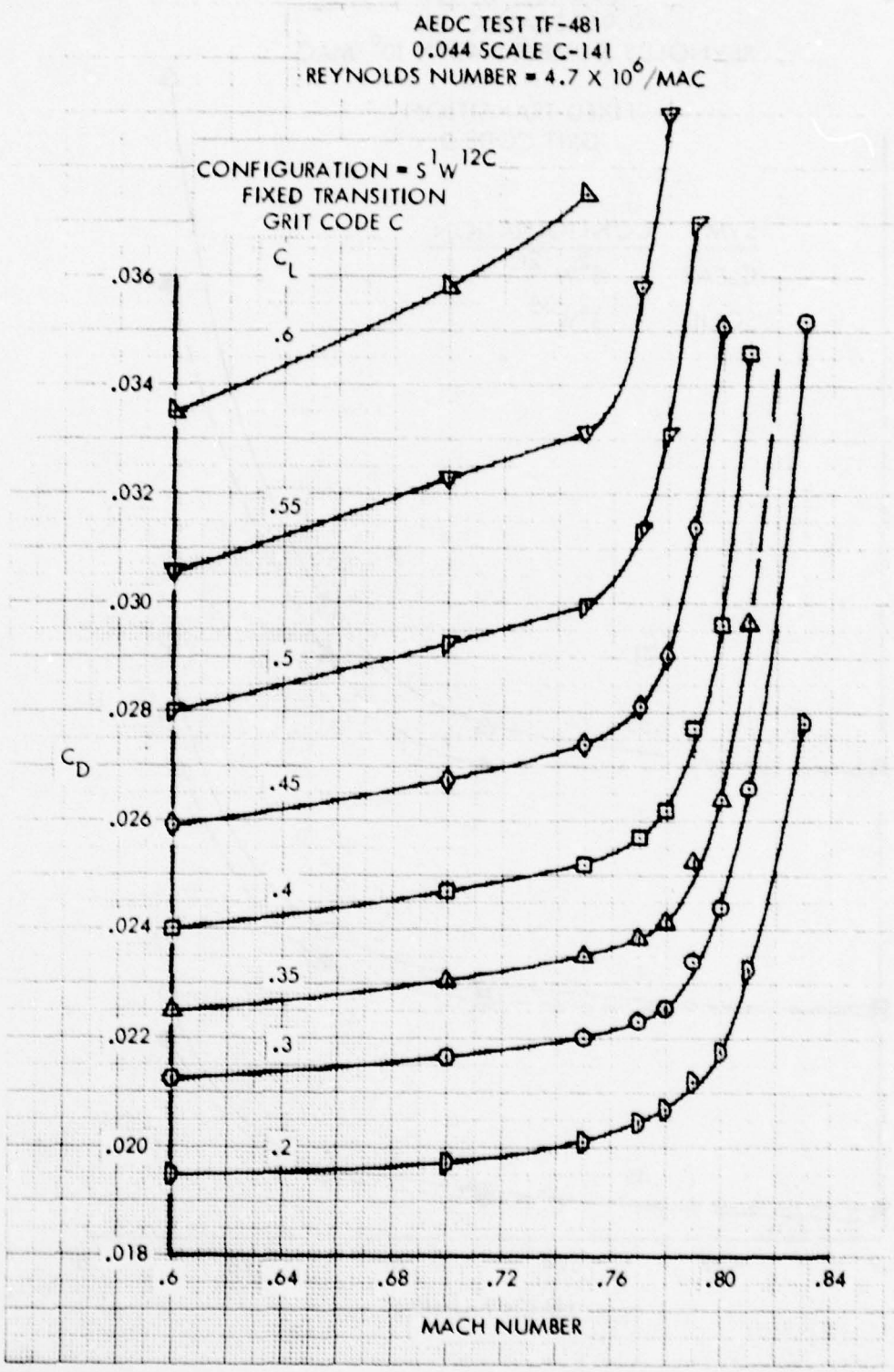

Figure 31. Drag Rise Characteristics for Baseline Leading Edge, Grit Code C

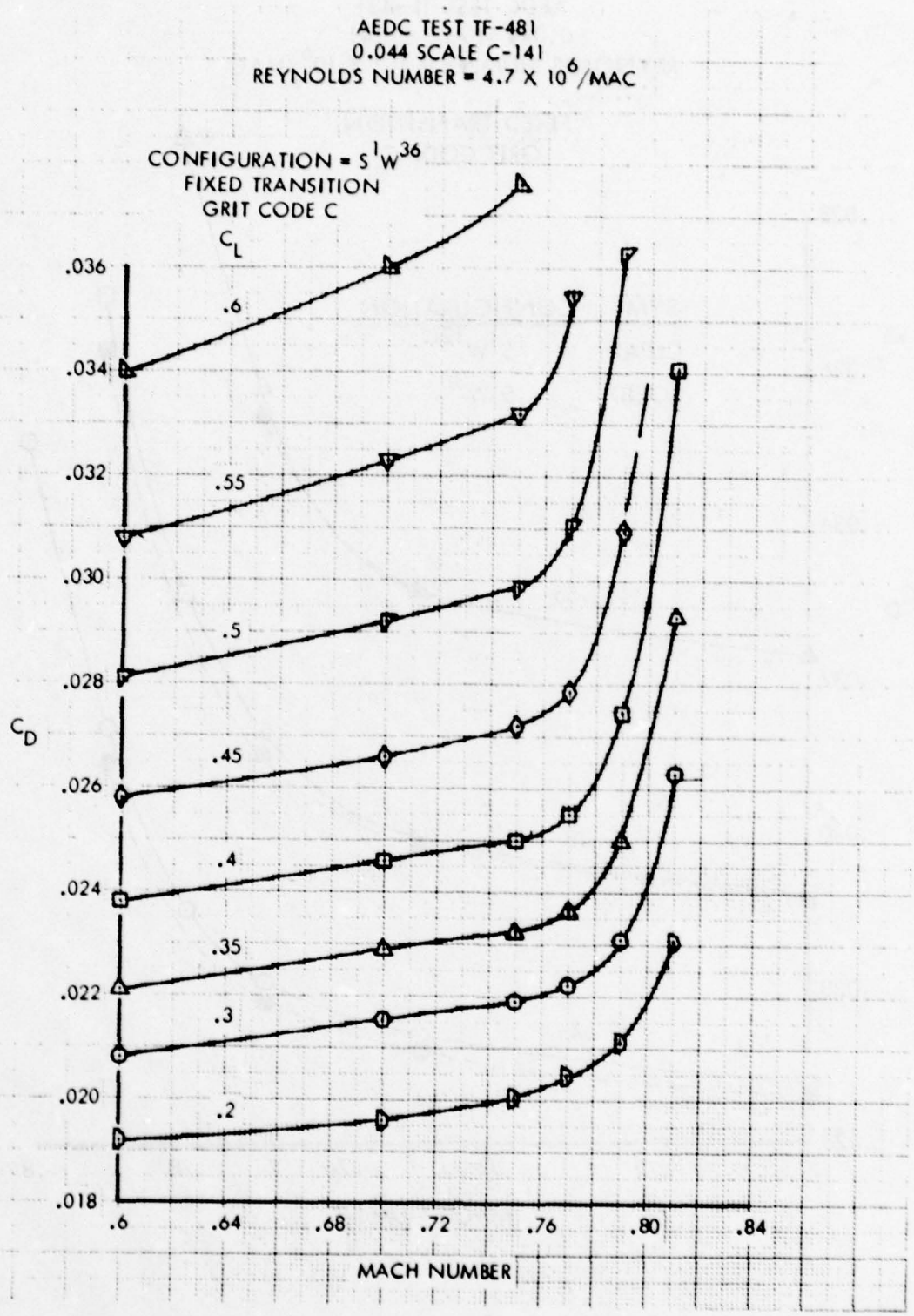

Figure 32. Drag Rise Characteristics for W^{36}, Grit Code C

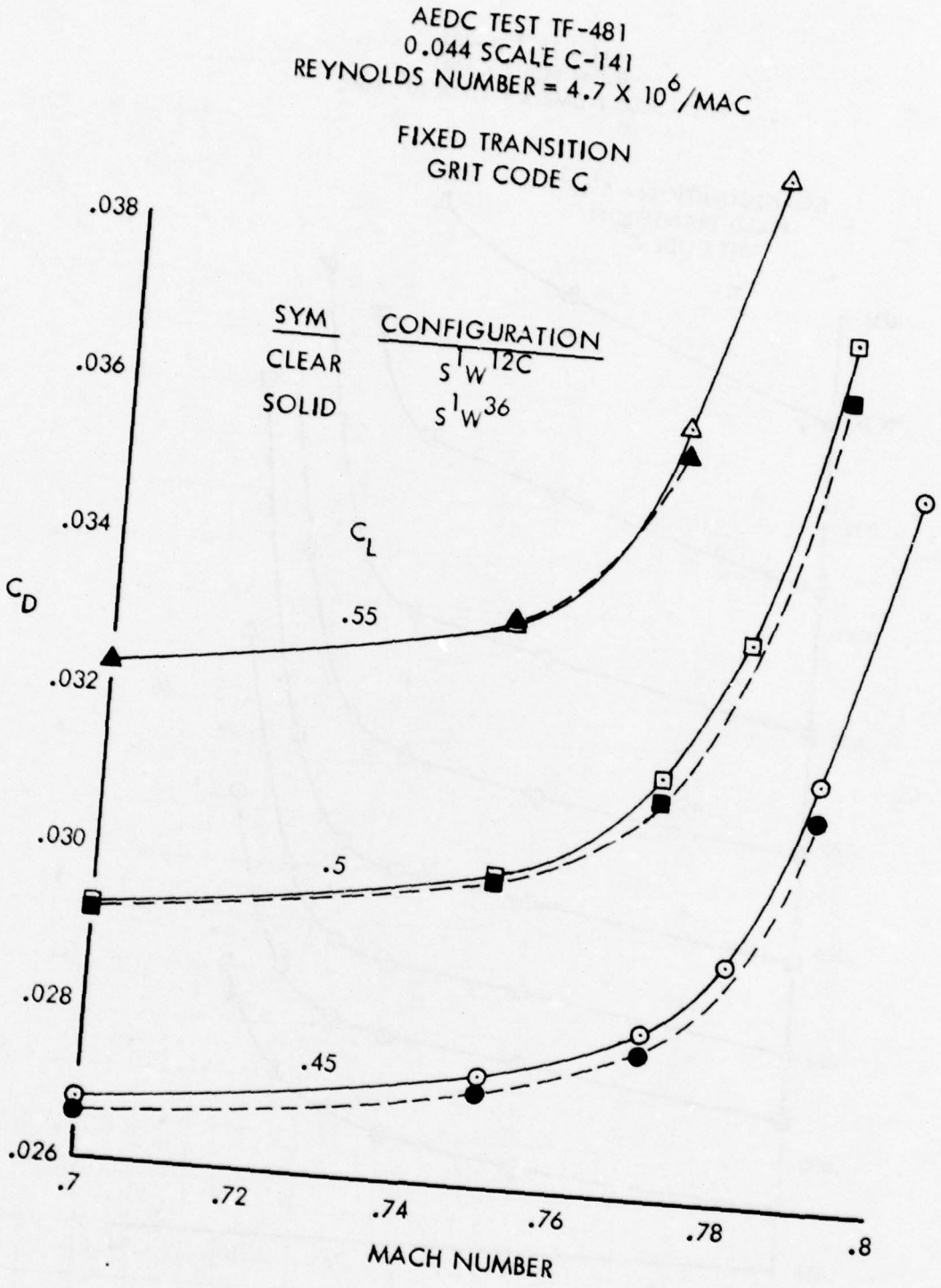

Figure 33. Effect of W^{36} on Drag Rise Characteristics

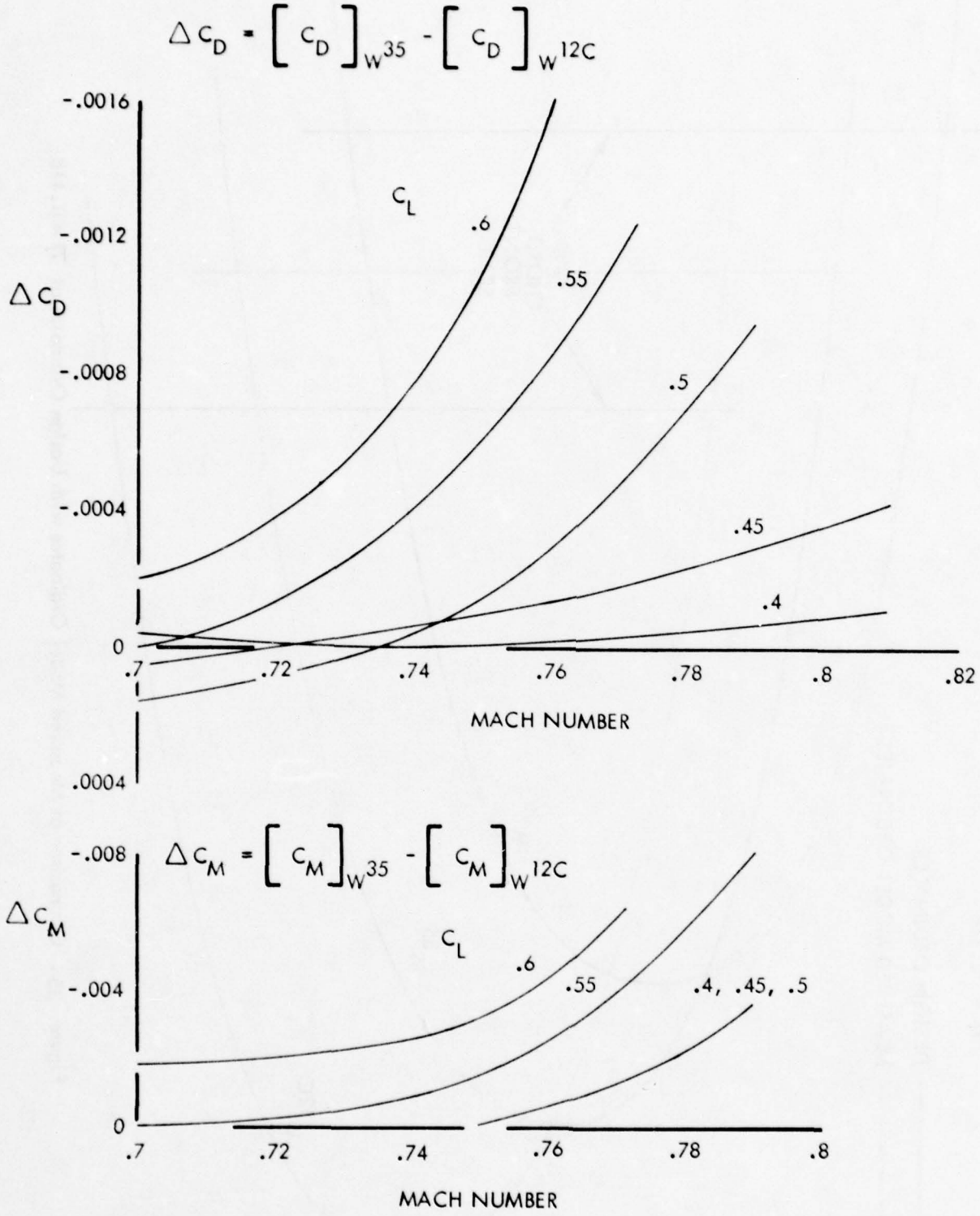

Figure 34. Incremental Drag and Pitching Moment Coefficients for W^{35}

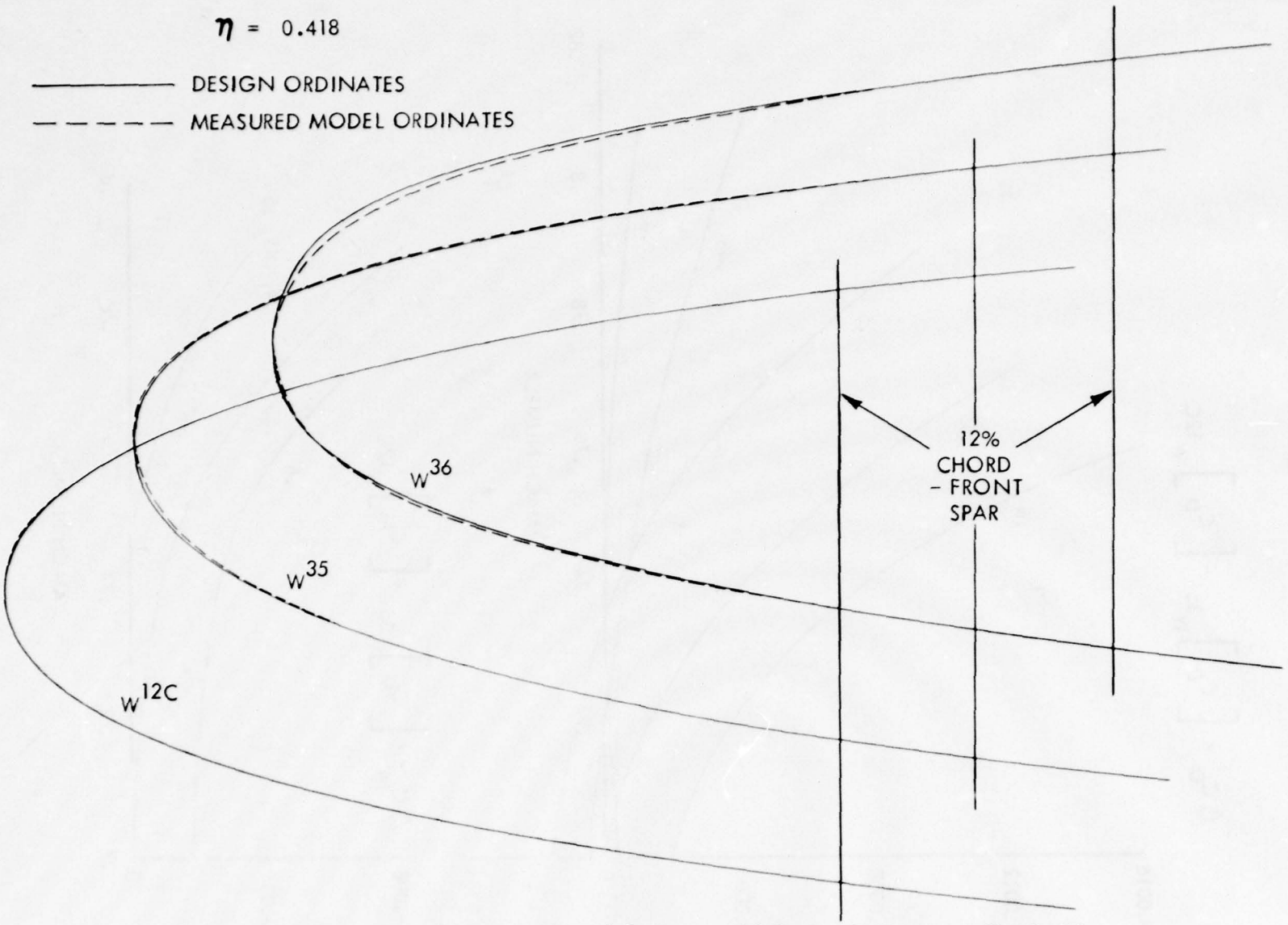

Figure 35. Comparison of Measured Model Ordinates with Design Ordinates at $\eta = 0.418$

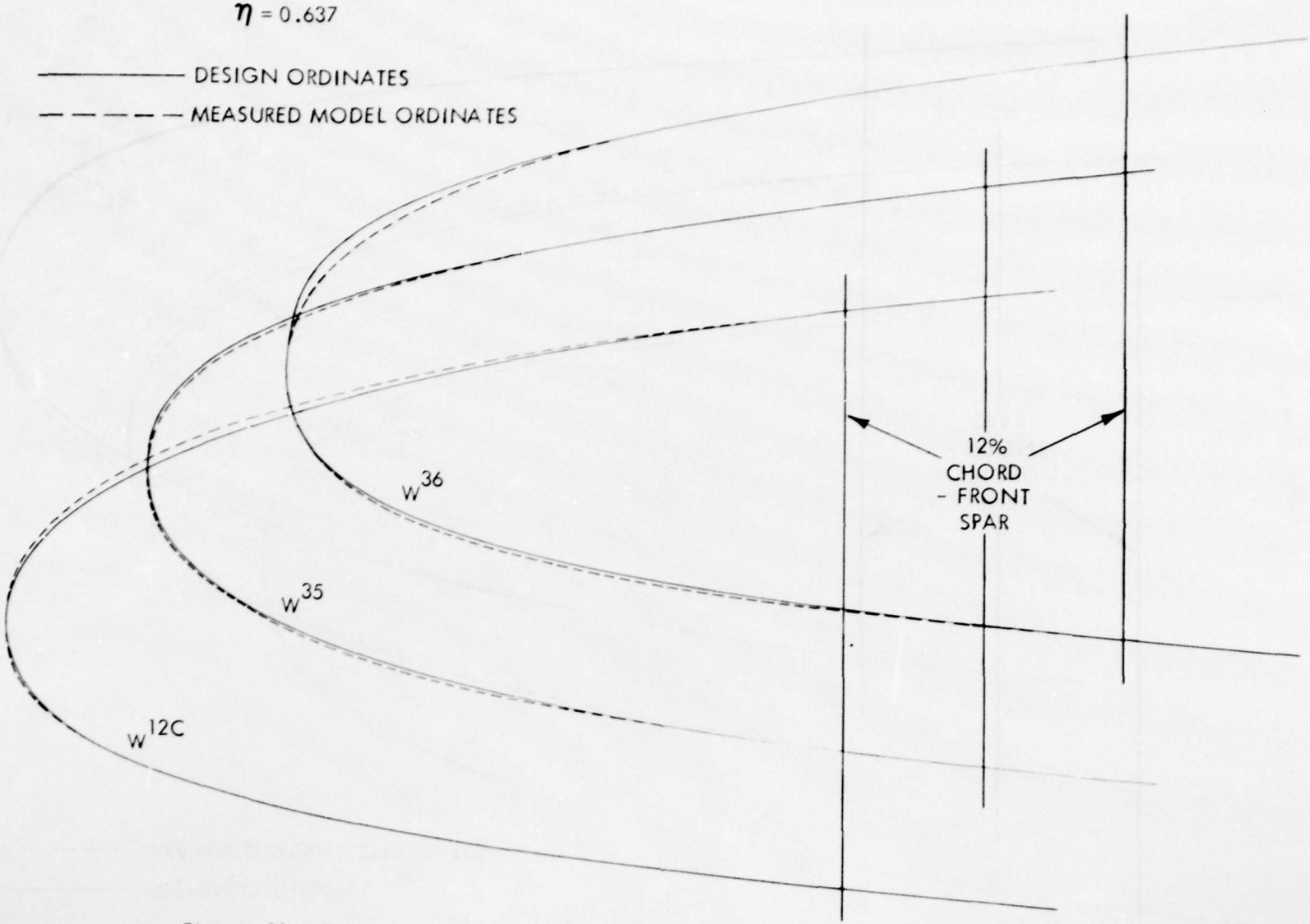

Figure 36. Comparison of Measured Model Ordinates with Design Ordinates at $\eta = 0.637$

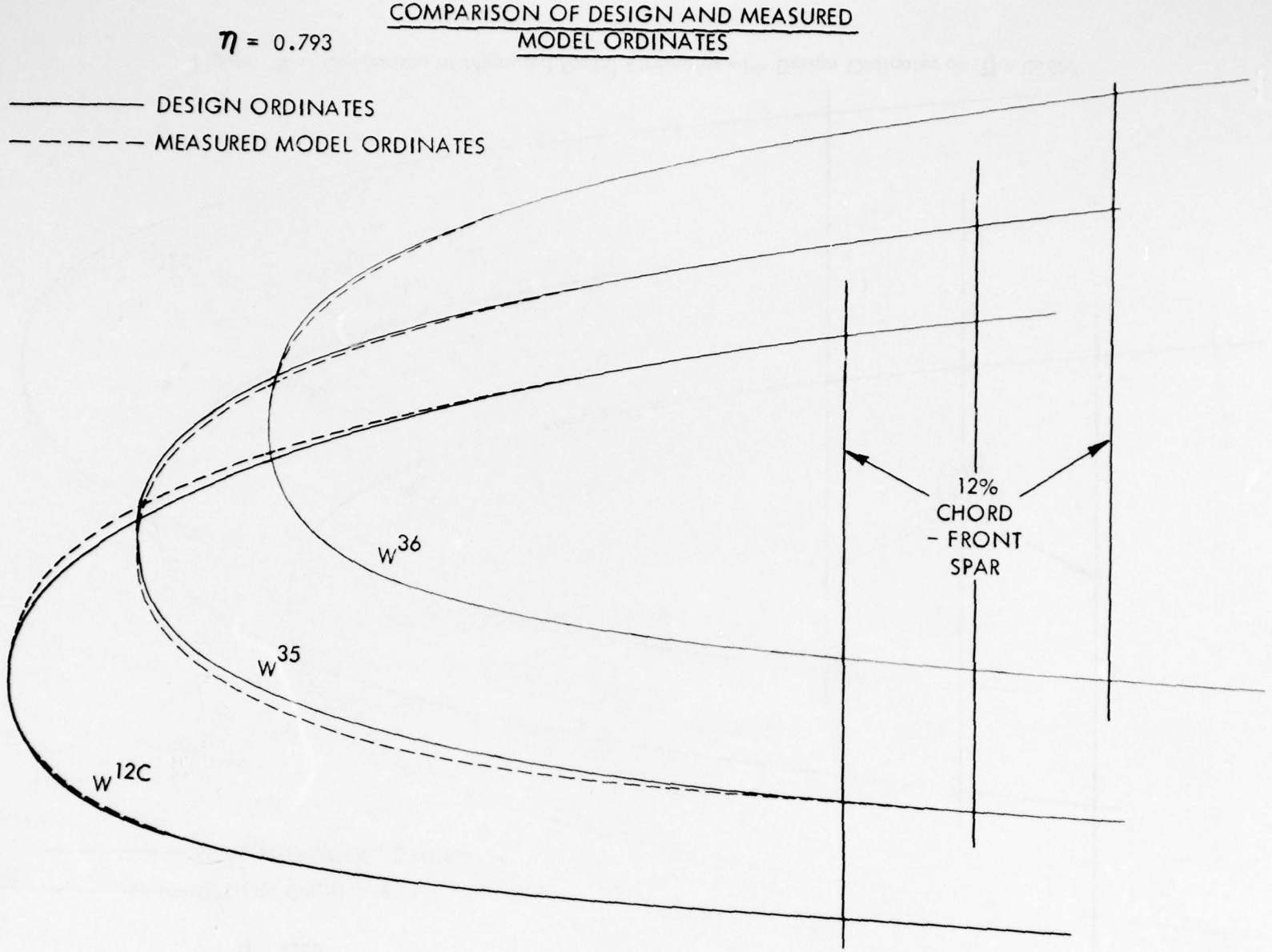

Figure 37. Comparison of Measured Model Ordinates with Design Ordinates at = 0.793

$\eta = 0.793$

COMPARISON OF DESIGN AND MEASURED MODEL ORDINATES

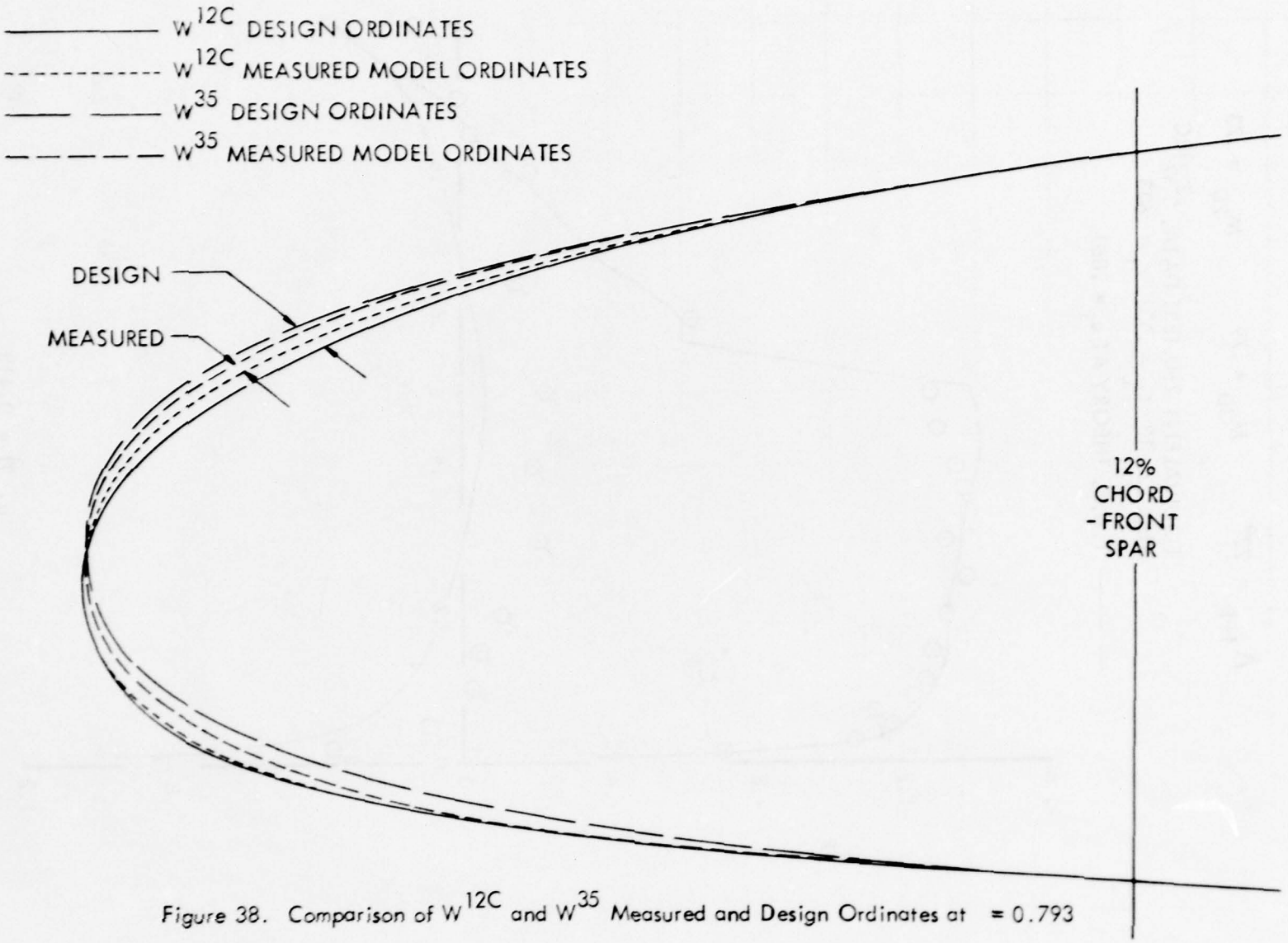

Figure 38. Comparison of W^{12C} and W^{35} Measured and Design Ordinates at $\eta = 0.793$

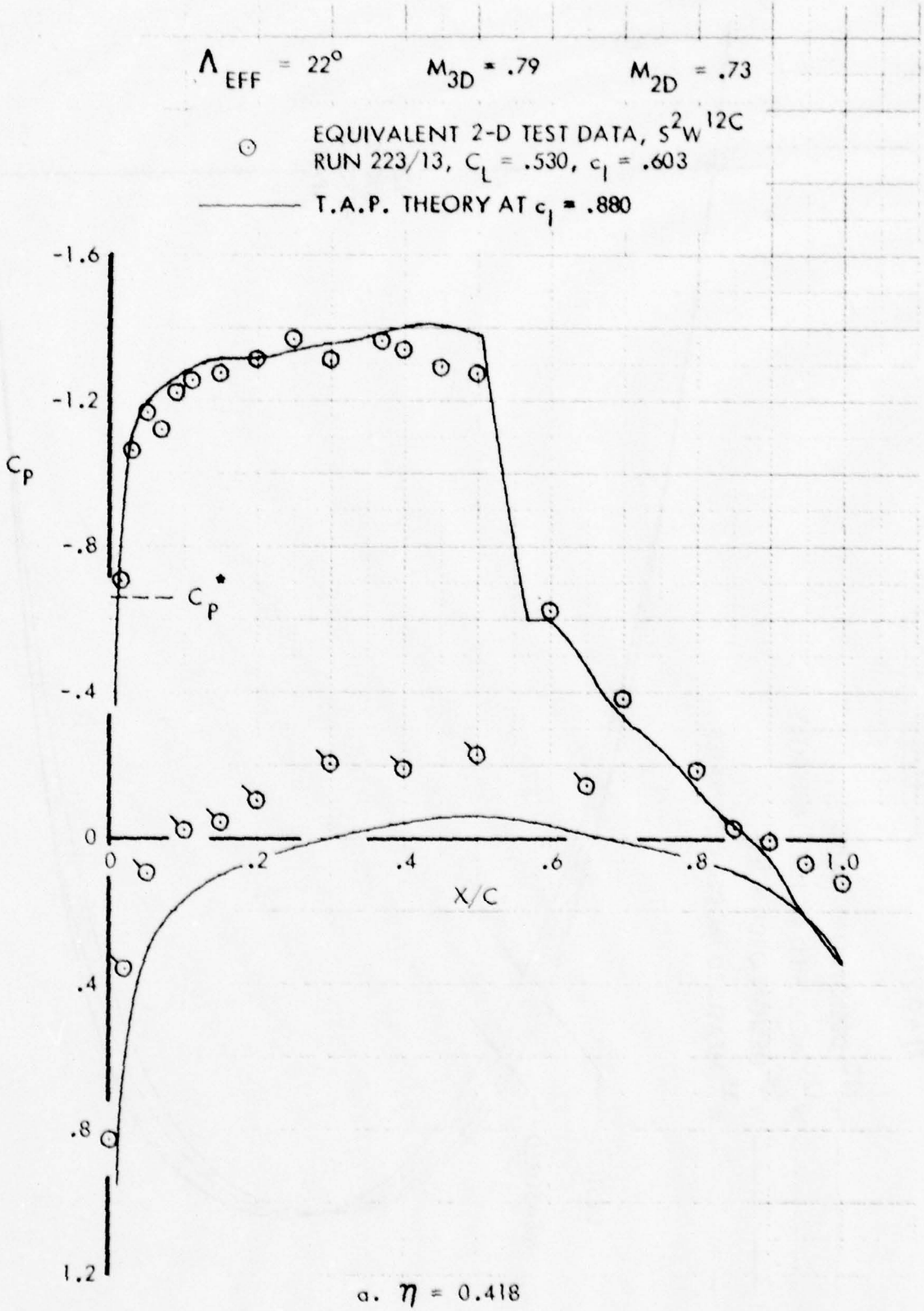

a. η = 0.418

Figure 39. Comparison of Design and Measured Pressure Distributions for W^{12C}

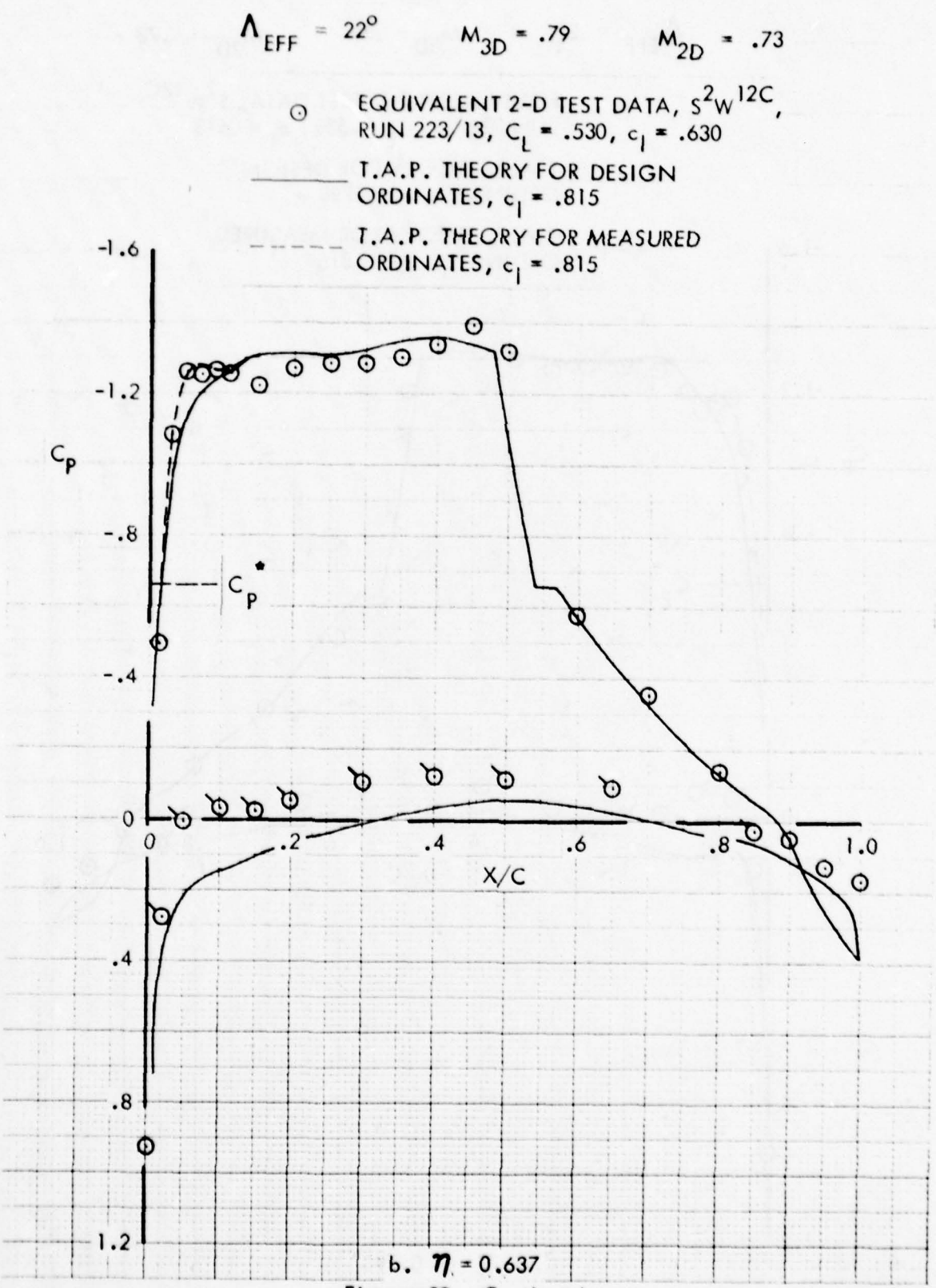

b. η = 0.637

Figure 39. Continued

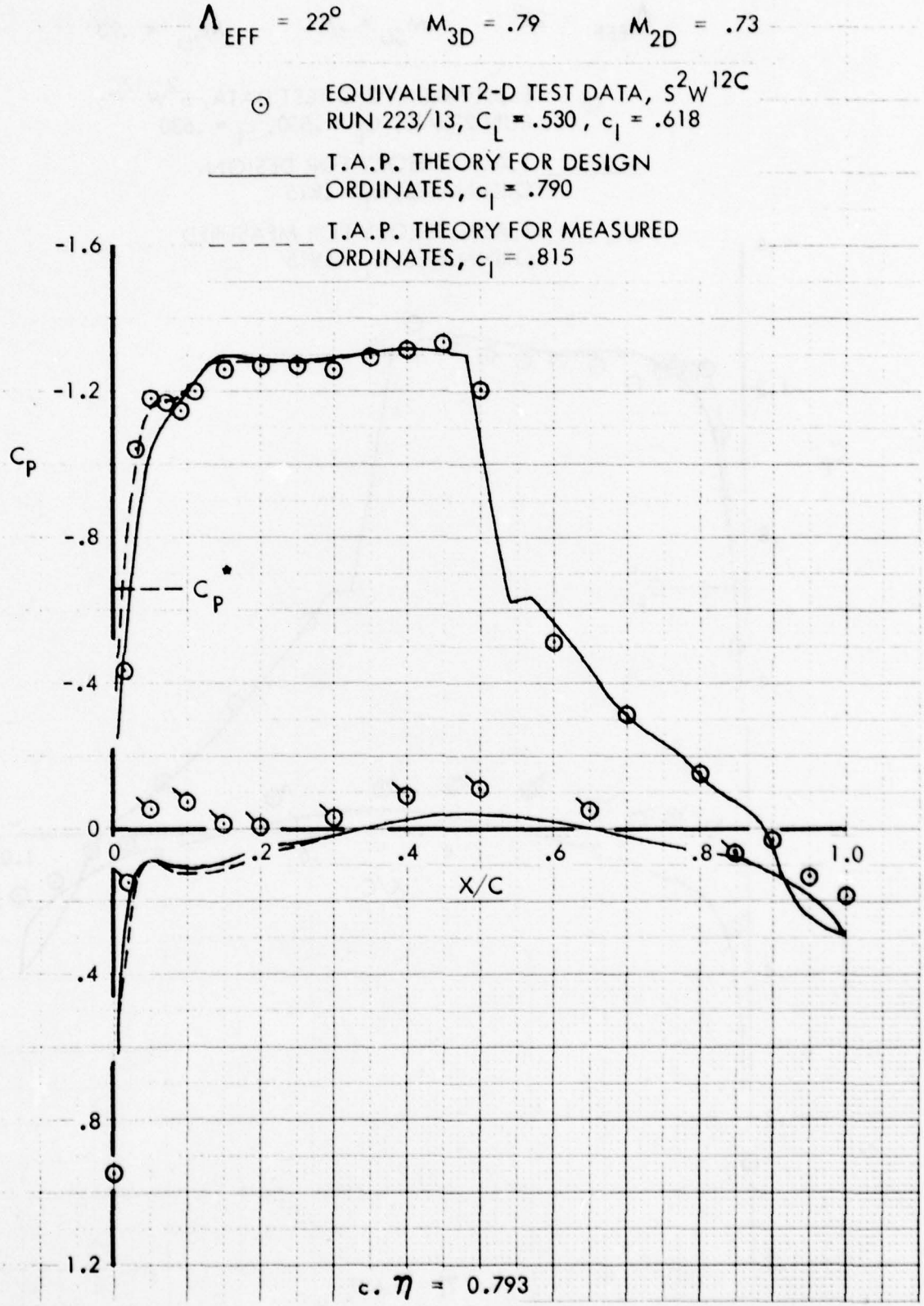

Figure 39. Concluded

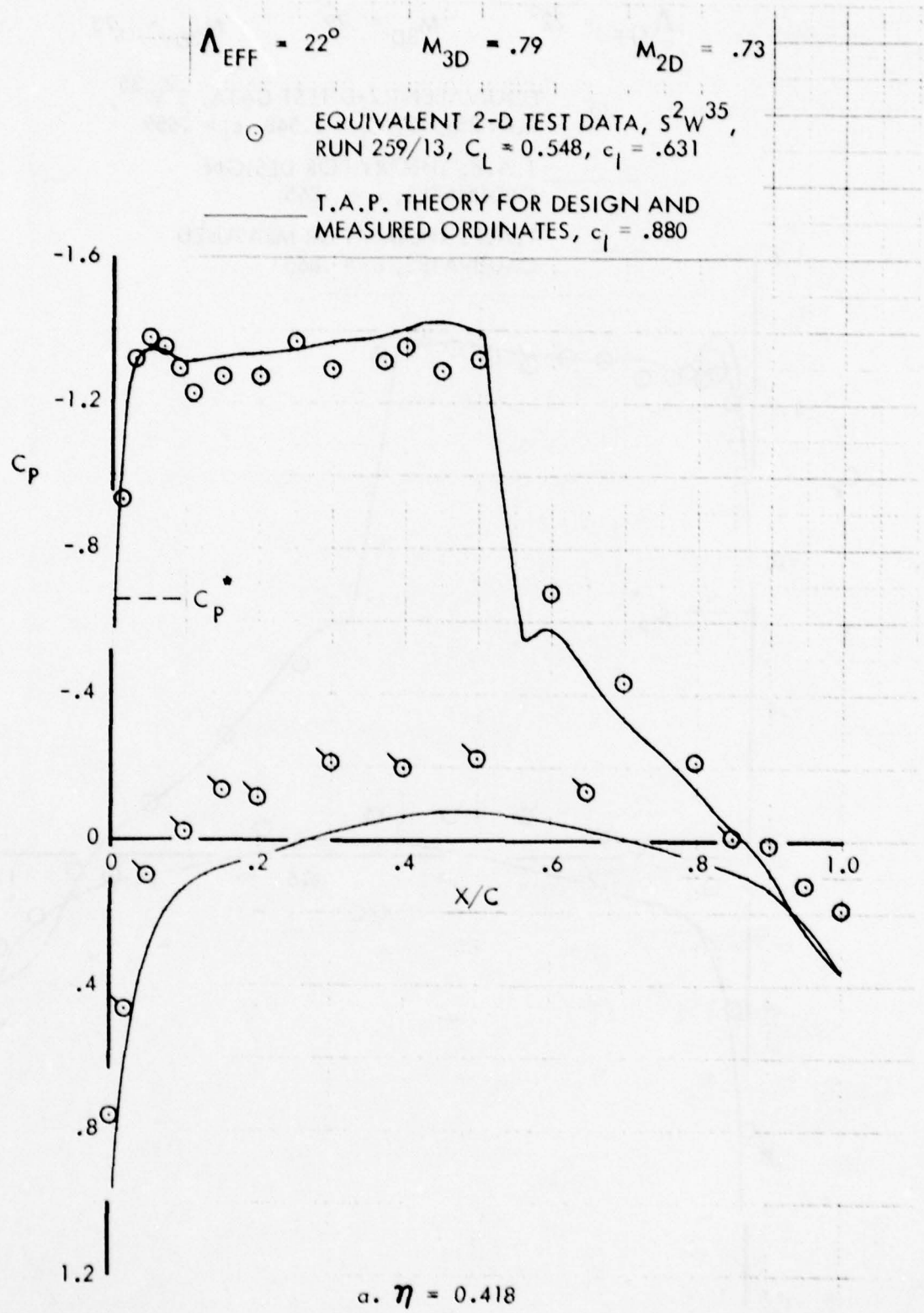

a. η = 0.418

Figure 40. Comparison of Design and Measured Pressure Distributions for W^{35}

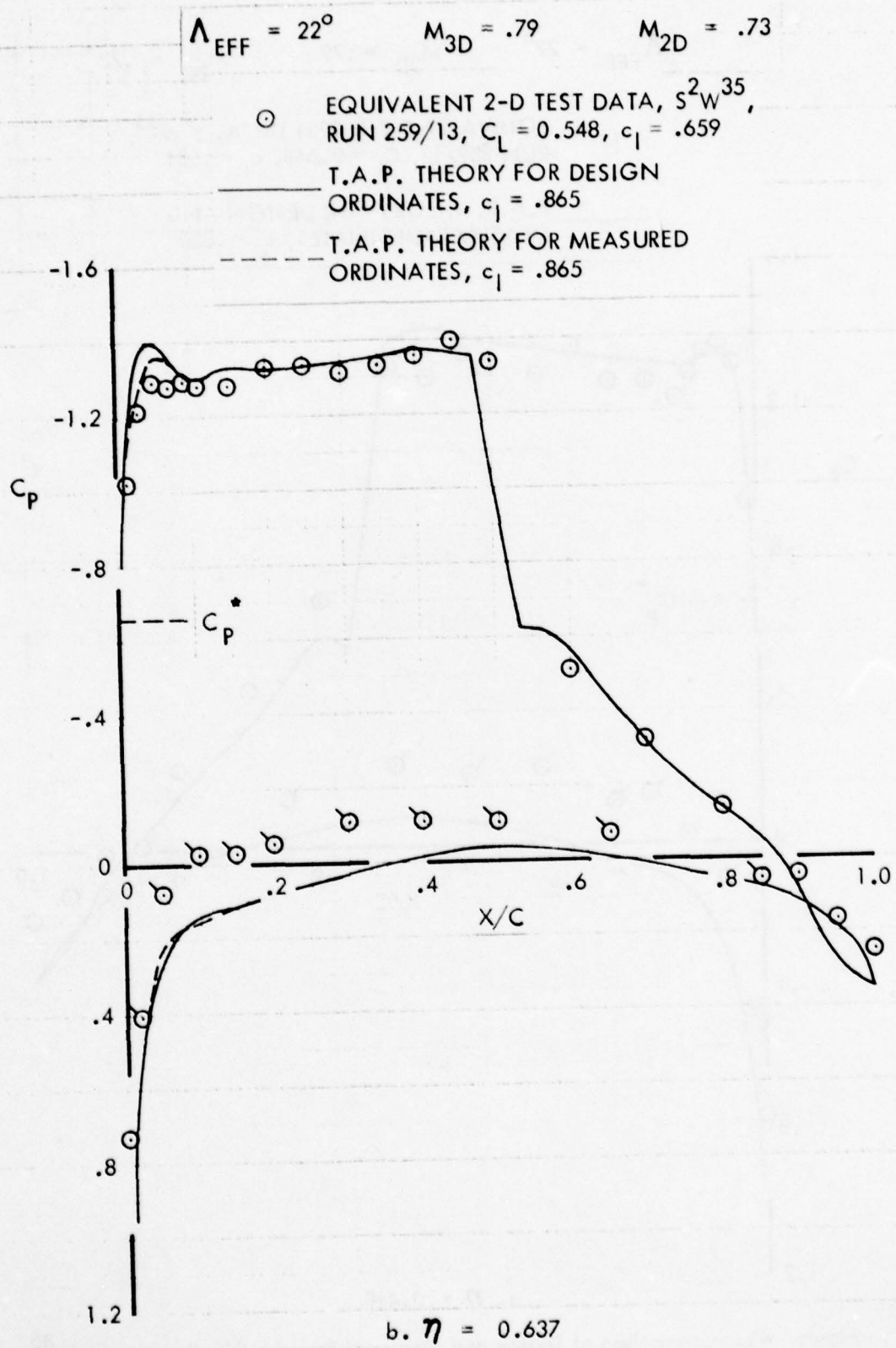

b. η = 0.637

Figure 40. Continued

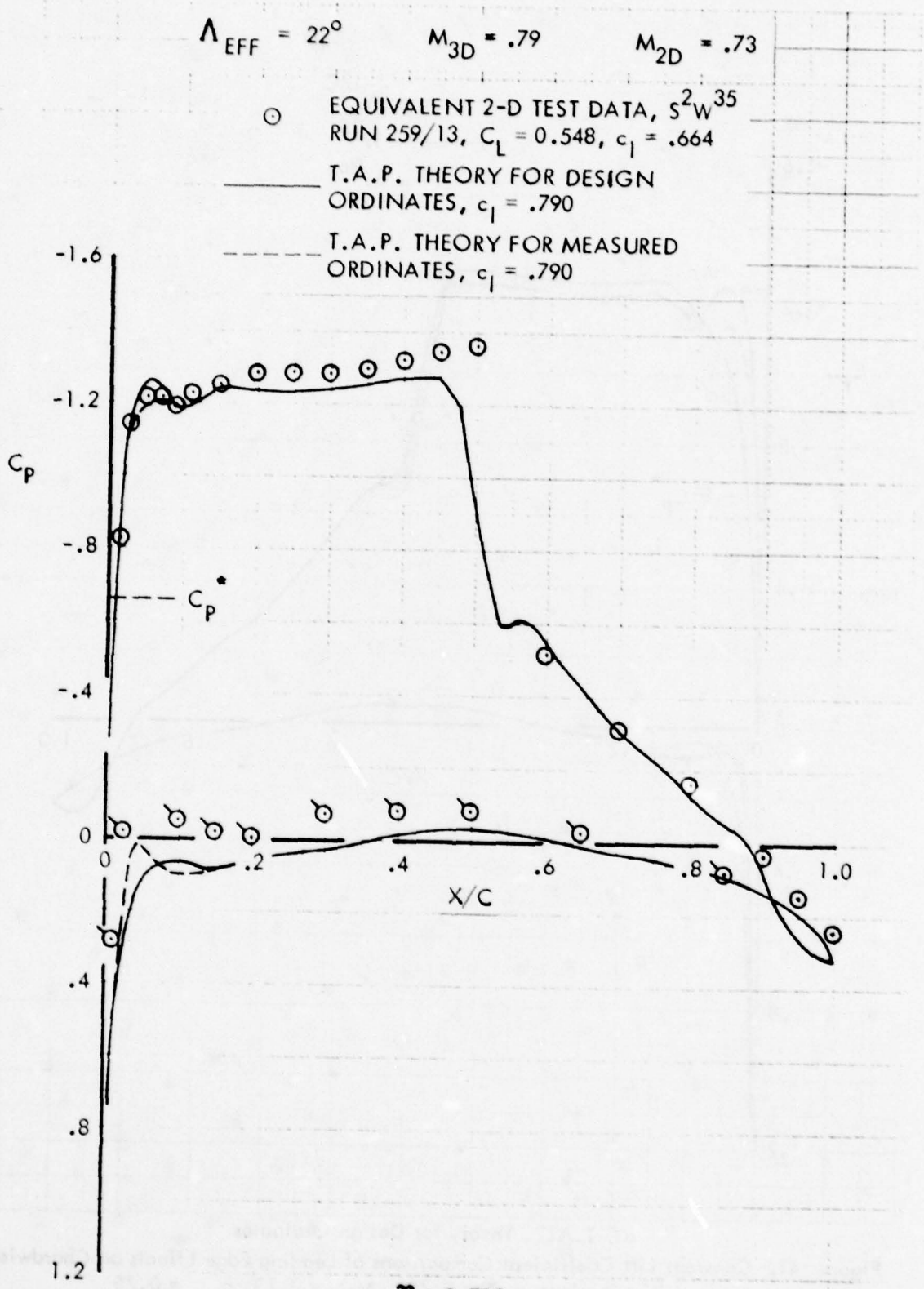

c. η = 0.793

Figure 40 . Concluded

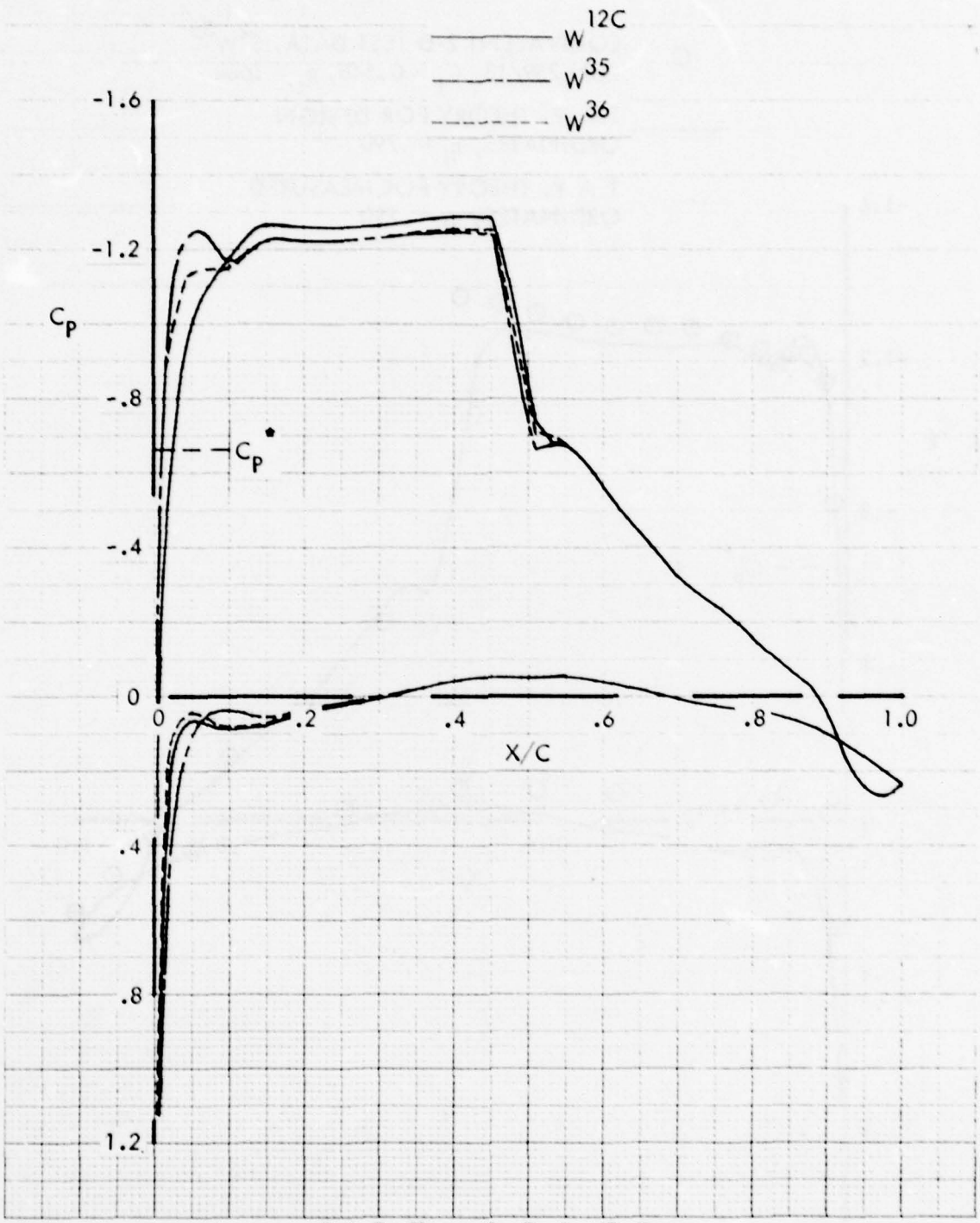

a. T.A.P. Theory for Design Ordinates

Figure 41. Constant Lift Coefficient Comparisons of Leading Edge Effects on Chordwise Pressure Distributions at $\eta = 0.793$, $M_{2D} = 0.73$, $c_{l_{2D}} = 0.75$

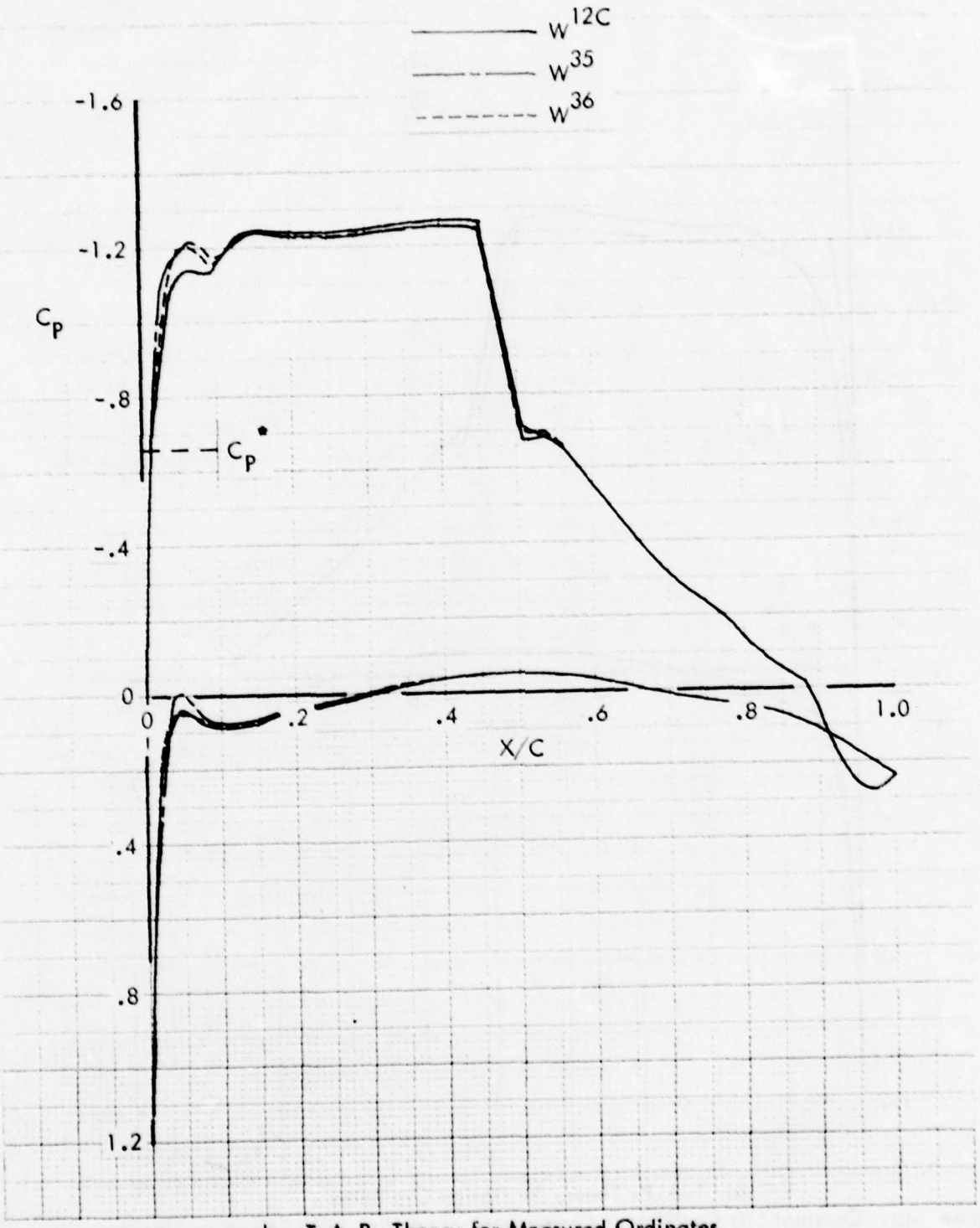

b. T.A.P. Theory for Measured Ordinates

Figure 41. Concluded

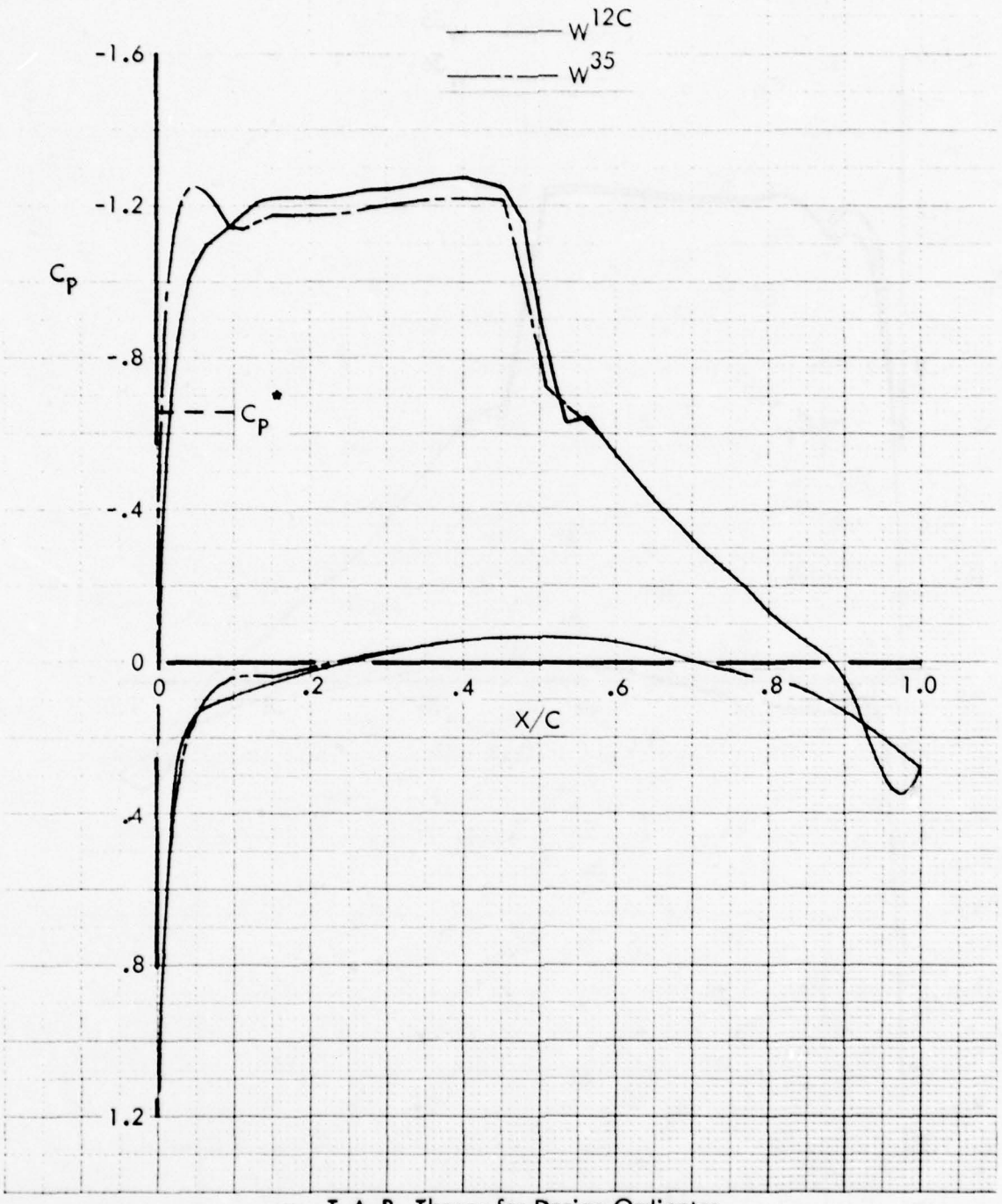

a. T.A.P. Theory for Design Ordinates

Figure 42. Constant Lift Coefficient Comparisons of Leading Edge Effects on Chordwise Pressure Distributions at $\eta = 0.637$, $M_{2D} = 0.73$, $c_{l_{2D}} = 0.75$

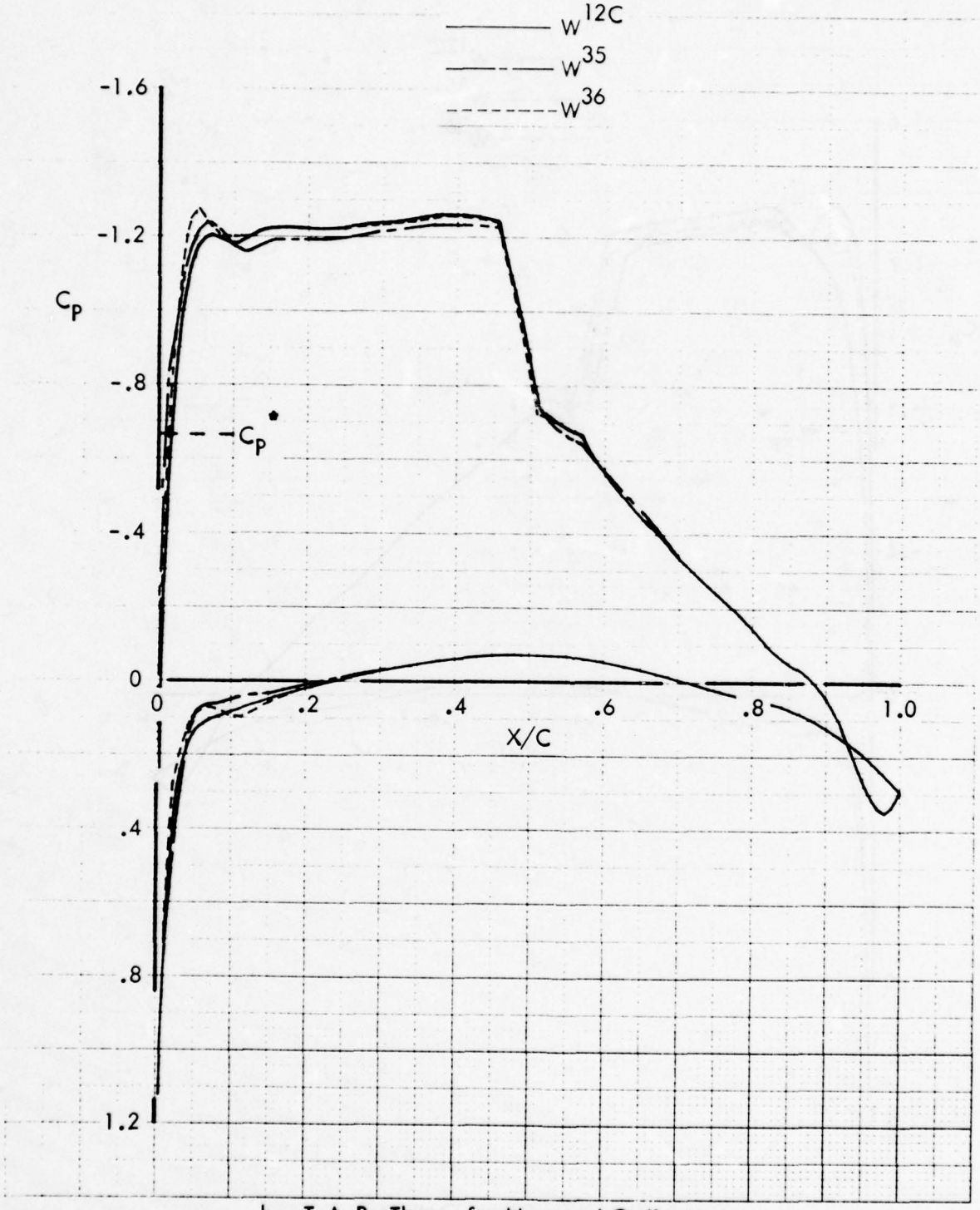

b. T.A.P. Theory for Measured Ordinates

Figure 42. Concluded

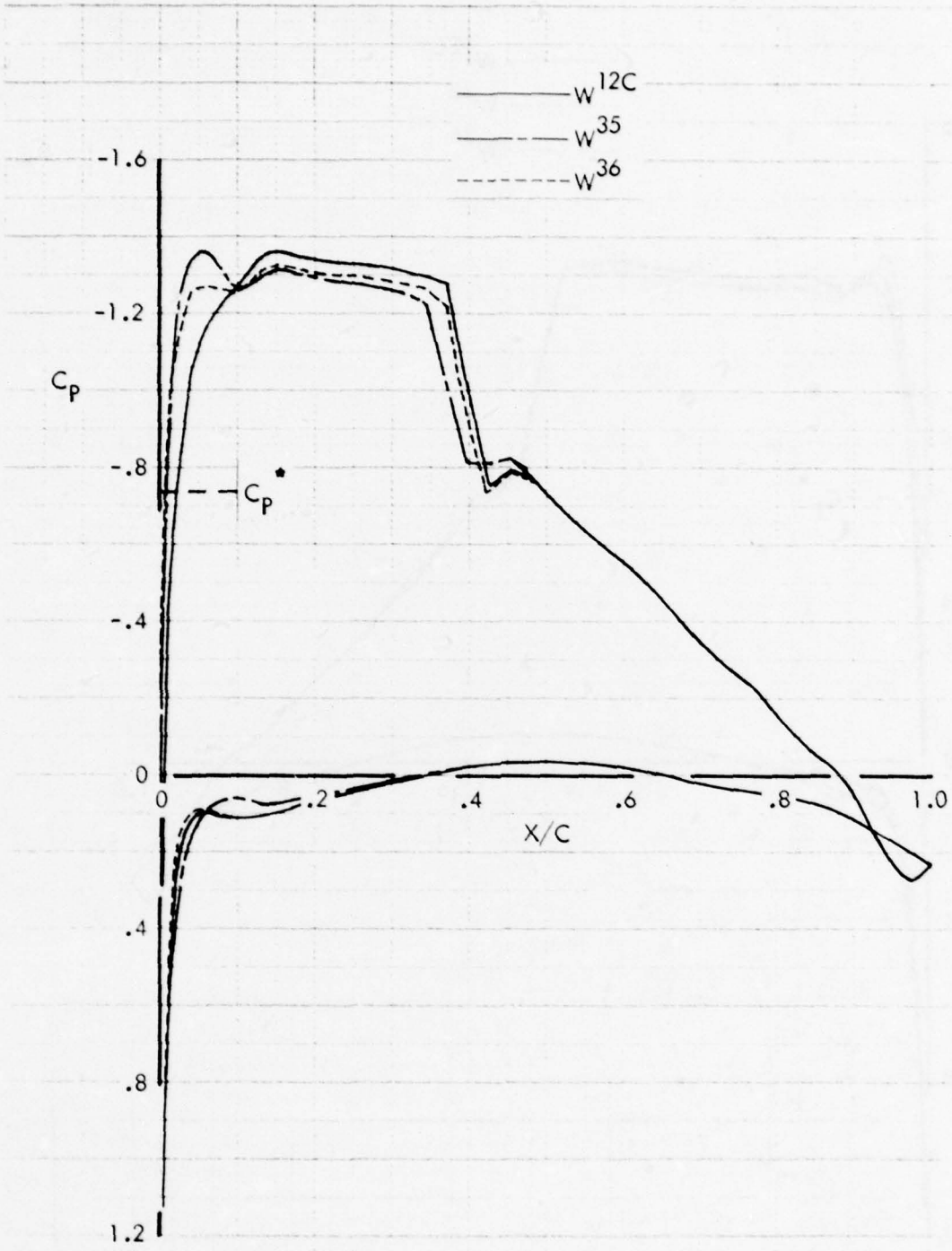

a. T.A.P. Theory for Design Ordinates

Figure 43. Constant Lift Coefficient Comparisons of Leading Edge Effects on Chordwise Pressure Distributions at $\eta = 0.793$, $M_{2D} = 0.71$, $c_{l_{2D}} = 0.75$

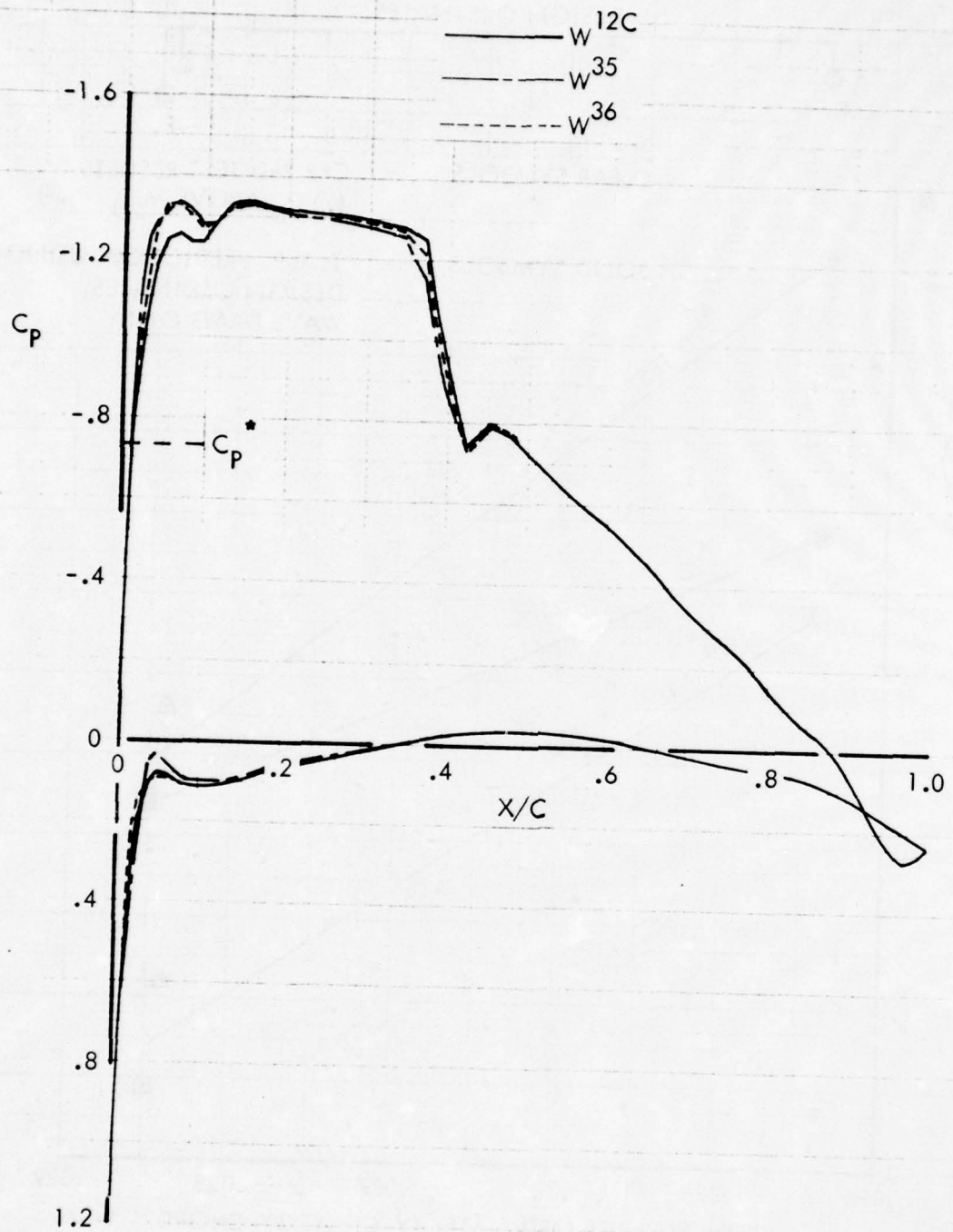

b. T.A.P. Theory for Measured Ordinates

Figure 43. Concluded

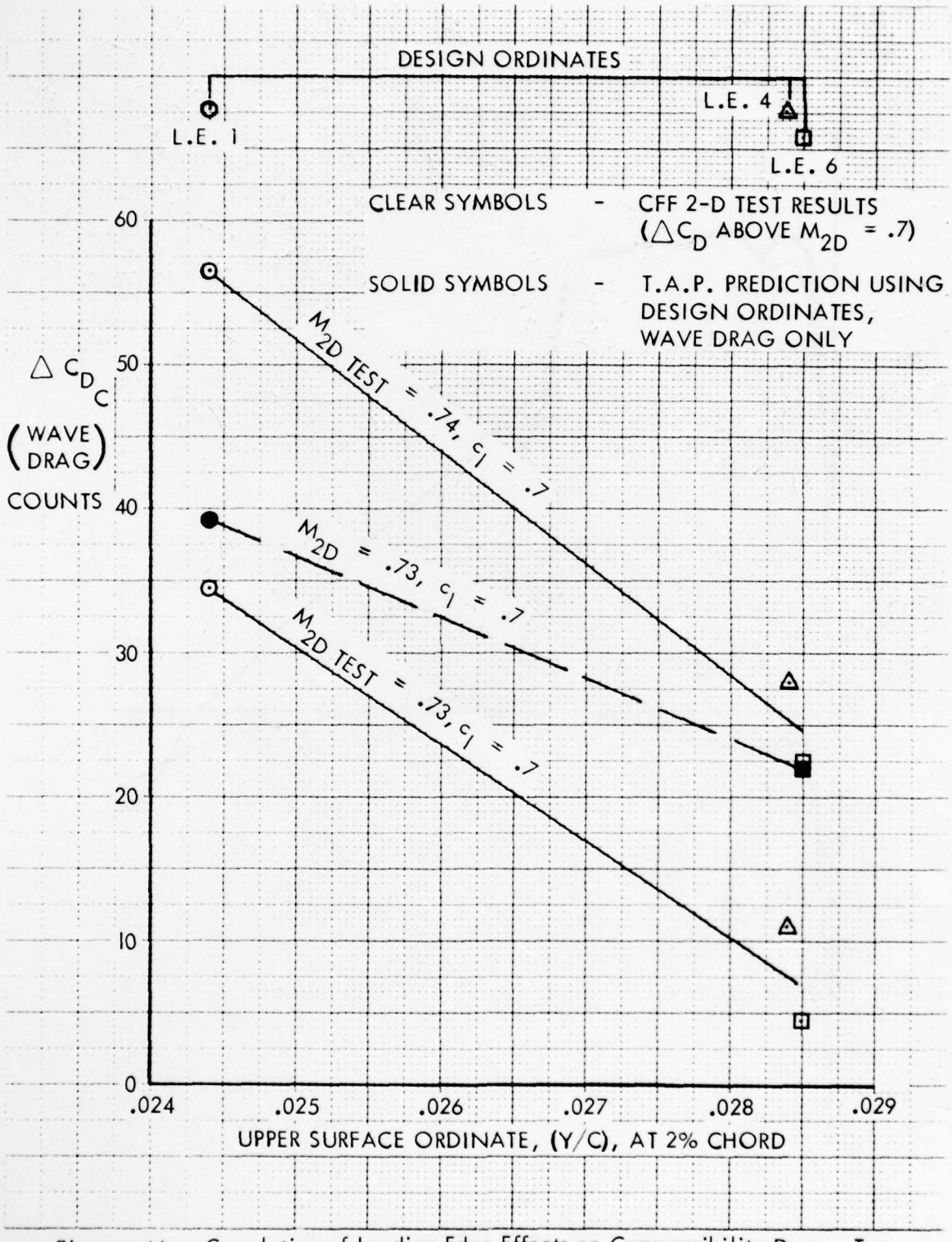

Figure 44. Correlation of Leading Edge Effects on Compressibility Drag - Two Dimensional C-141 Airfoil Test Results

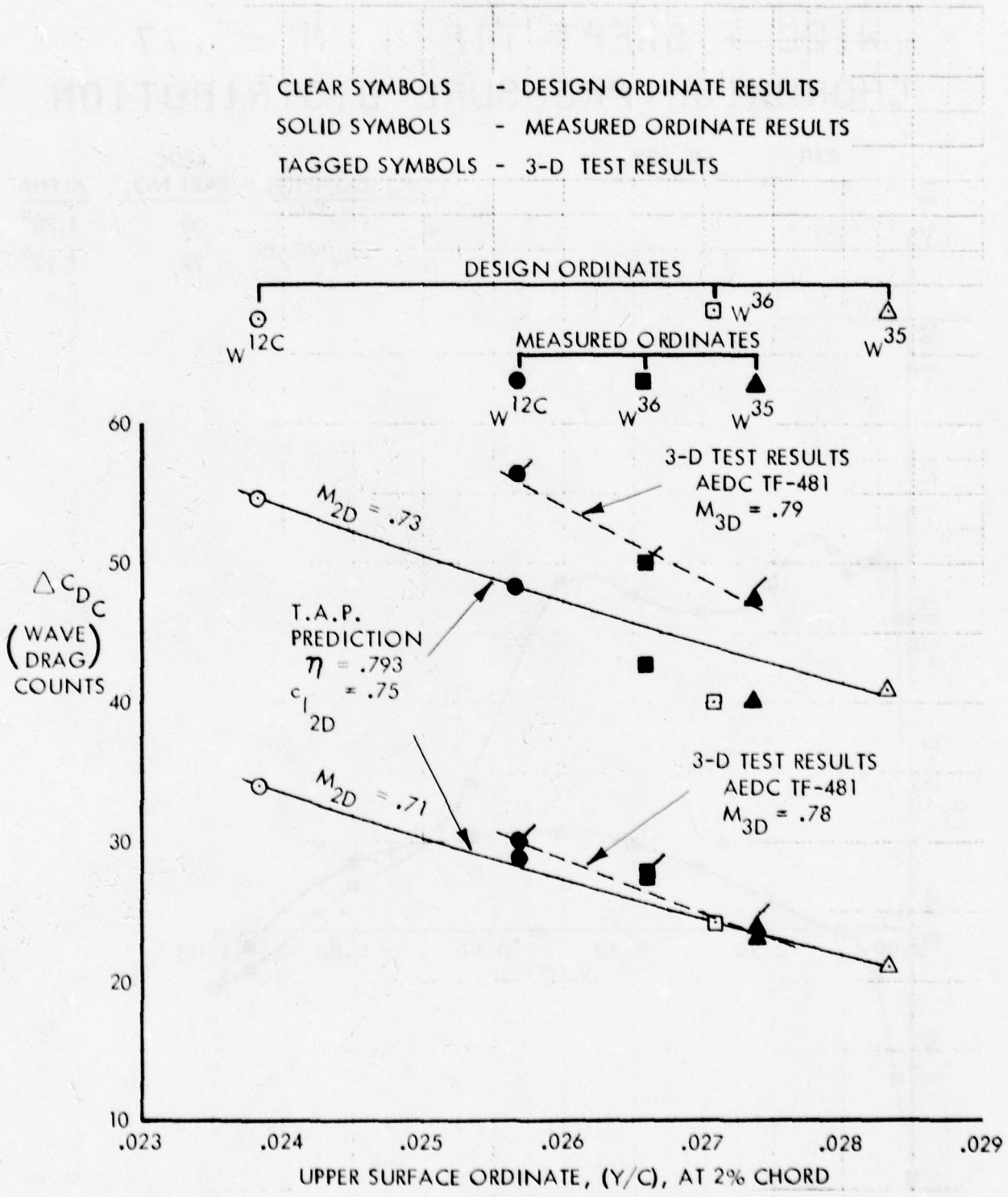

Figure 45. Correlation of Leading Edge Effects on Compressibility Drag - Three Dimensional C-141 Test Results and Equivalent Two Dimensional Predictions

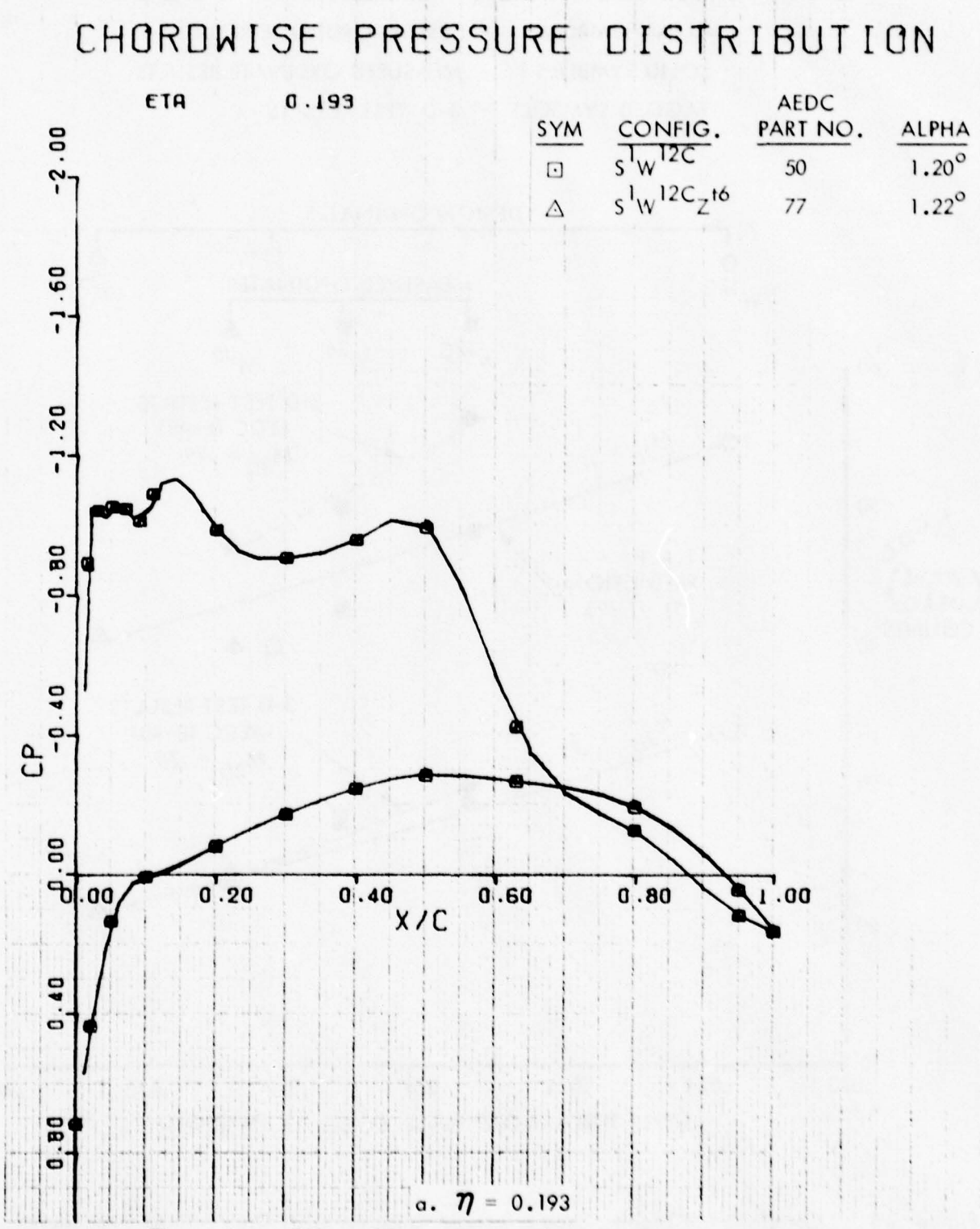

Figure 46. Effect of Swept Tips on Chordwise Pressure Distribution

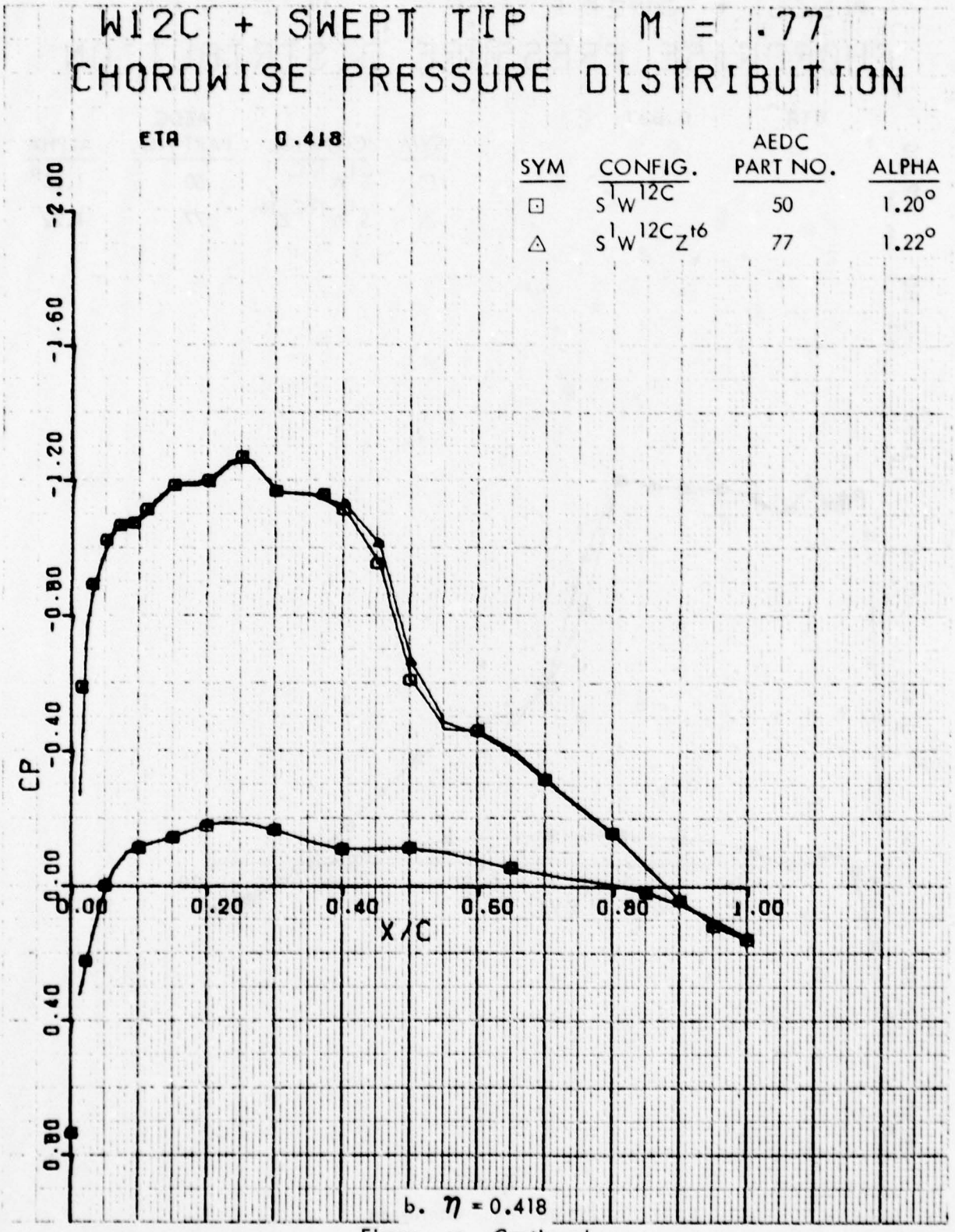

b. $\eta = 0.418$

Figure 46. Continued

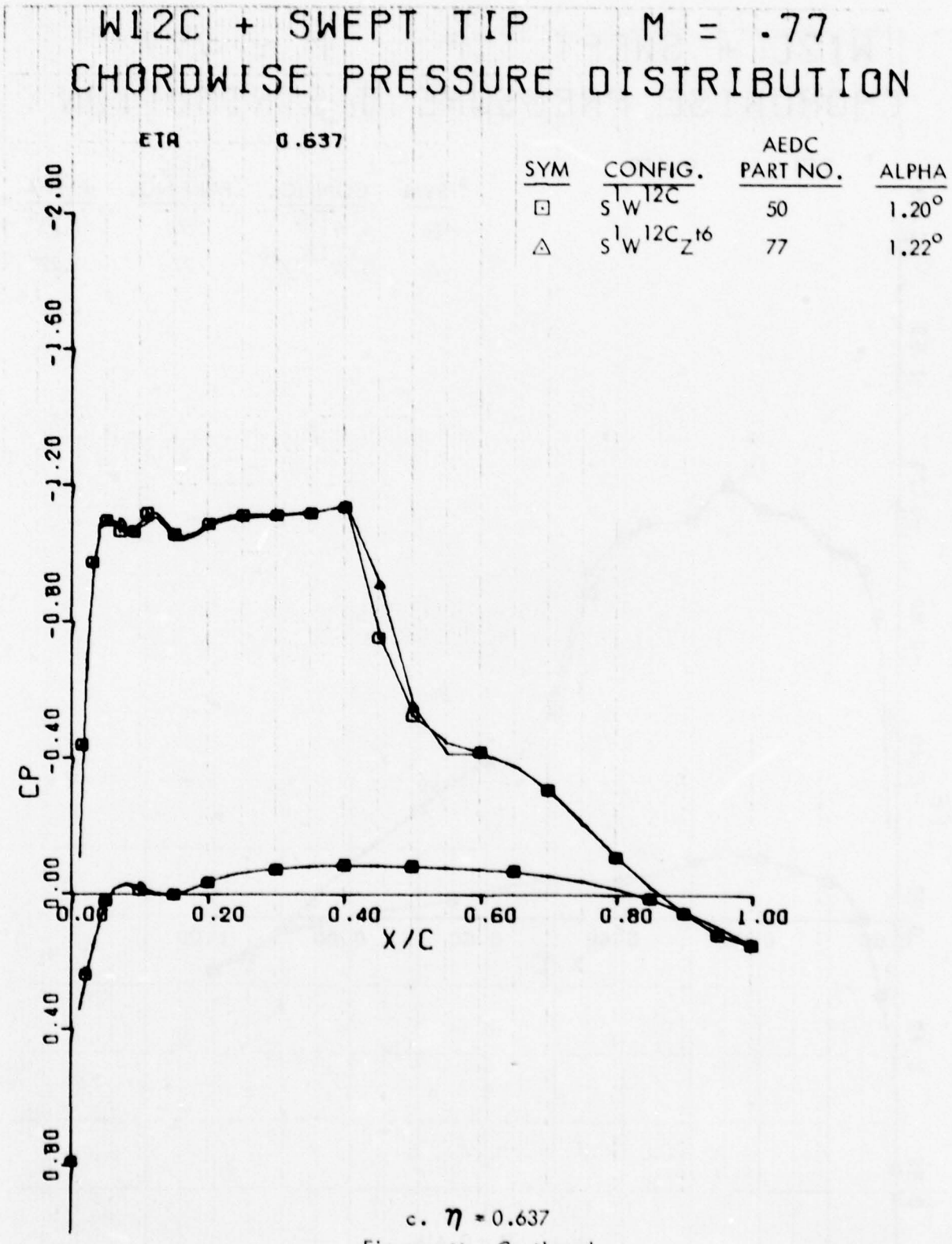

c. $\eta = 0.637$

Figure 46. Continued

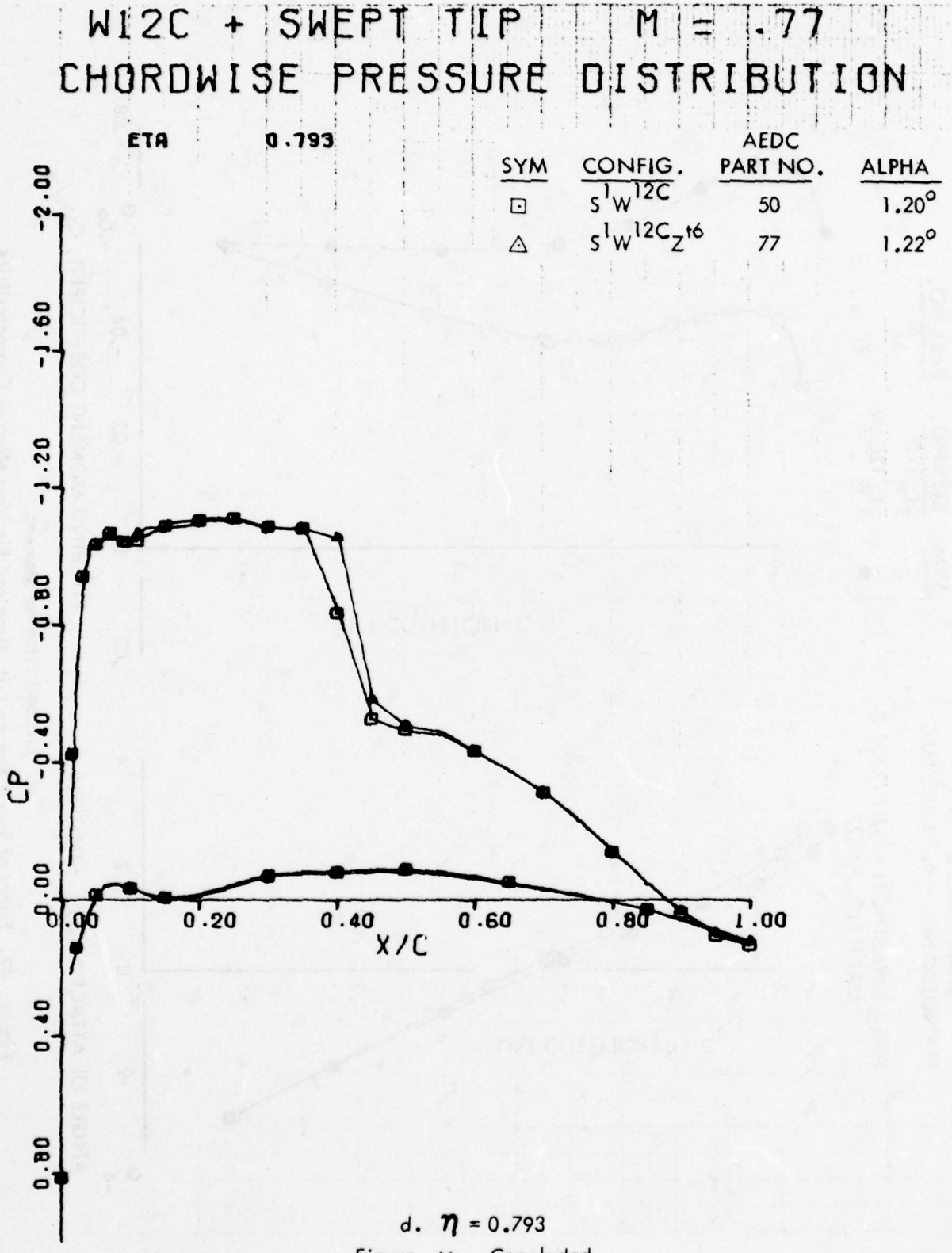

d. $\eta = 0.793$

Figure 46 . Concluded

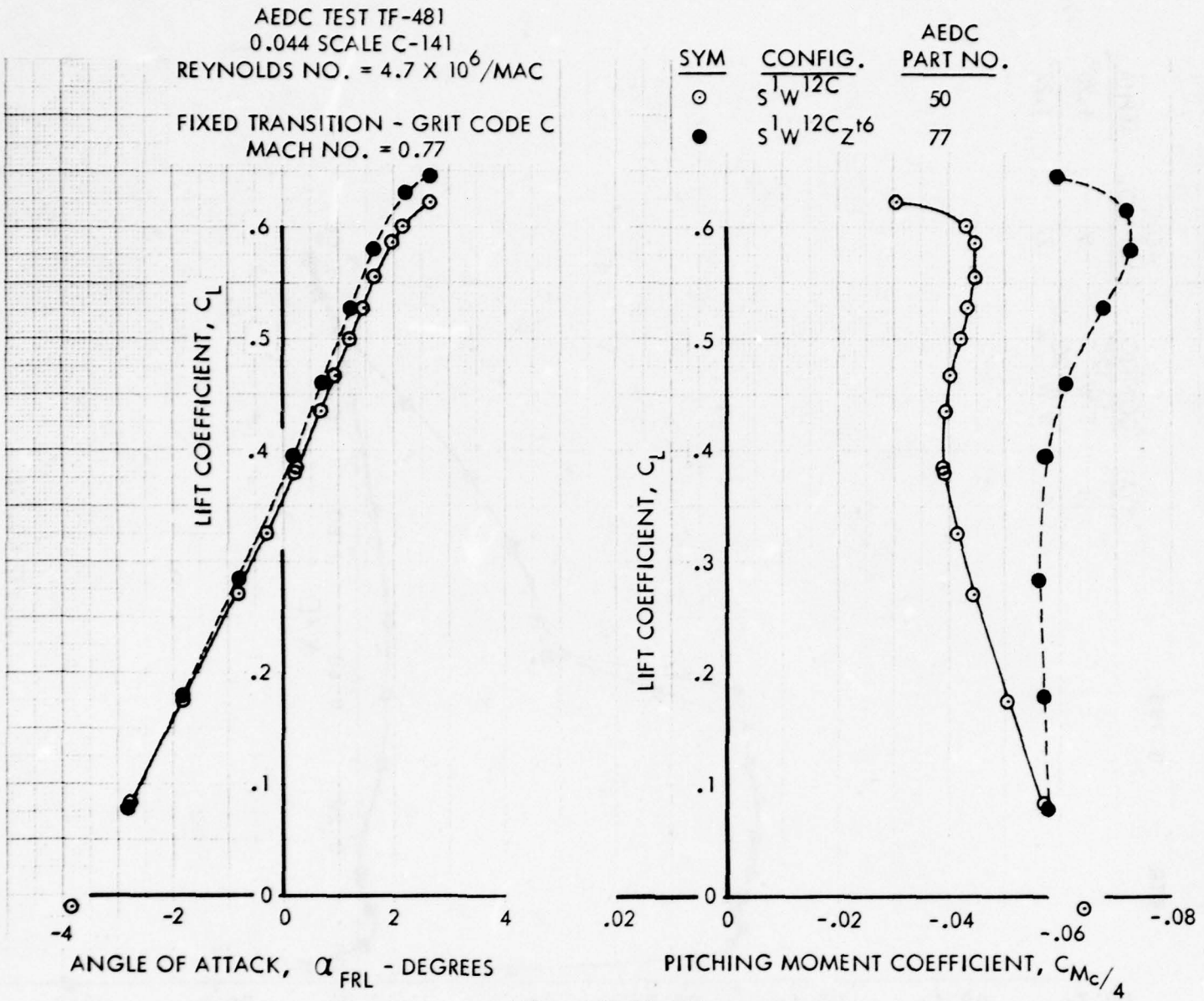

a. Lift and Pitching Moment

Figure 47. Effect of Swept Tips on Lift, Drag and Pitching Moment Characteristics

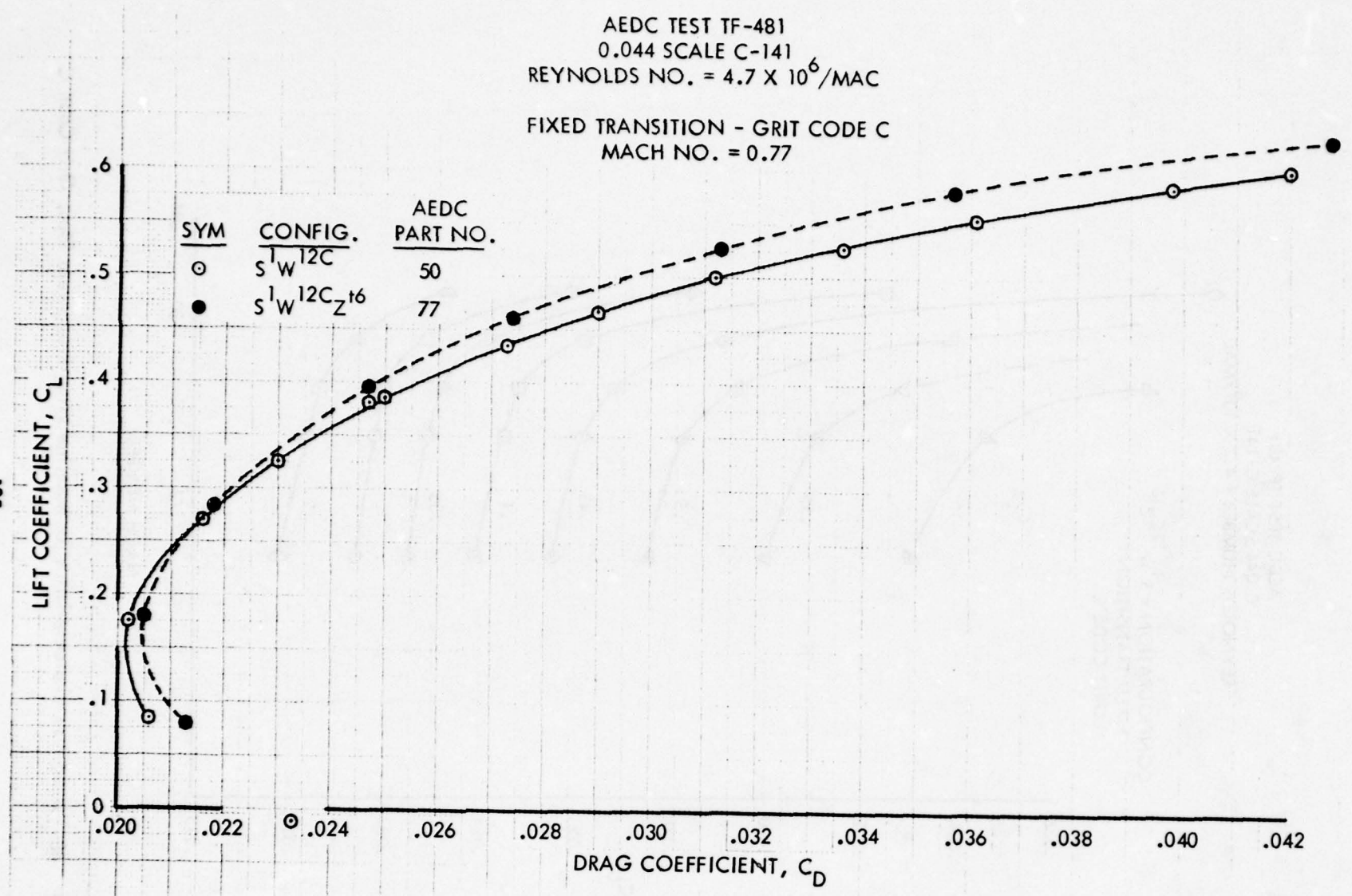

b. Drag Polar

Figure 47. Concluded

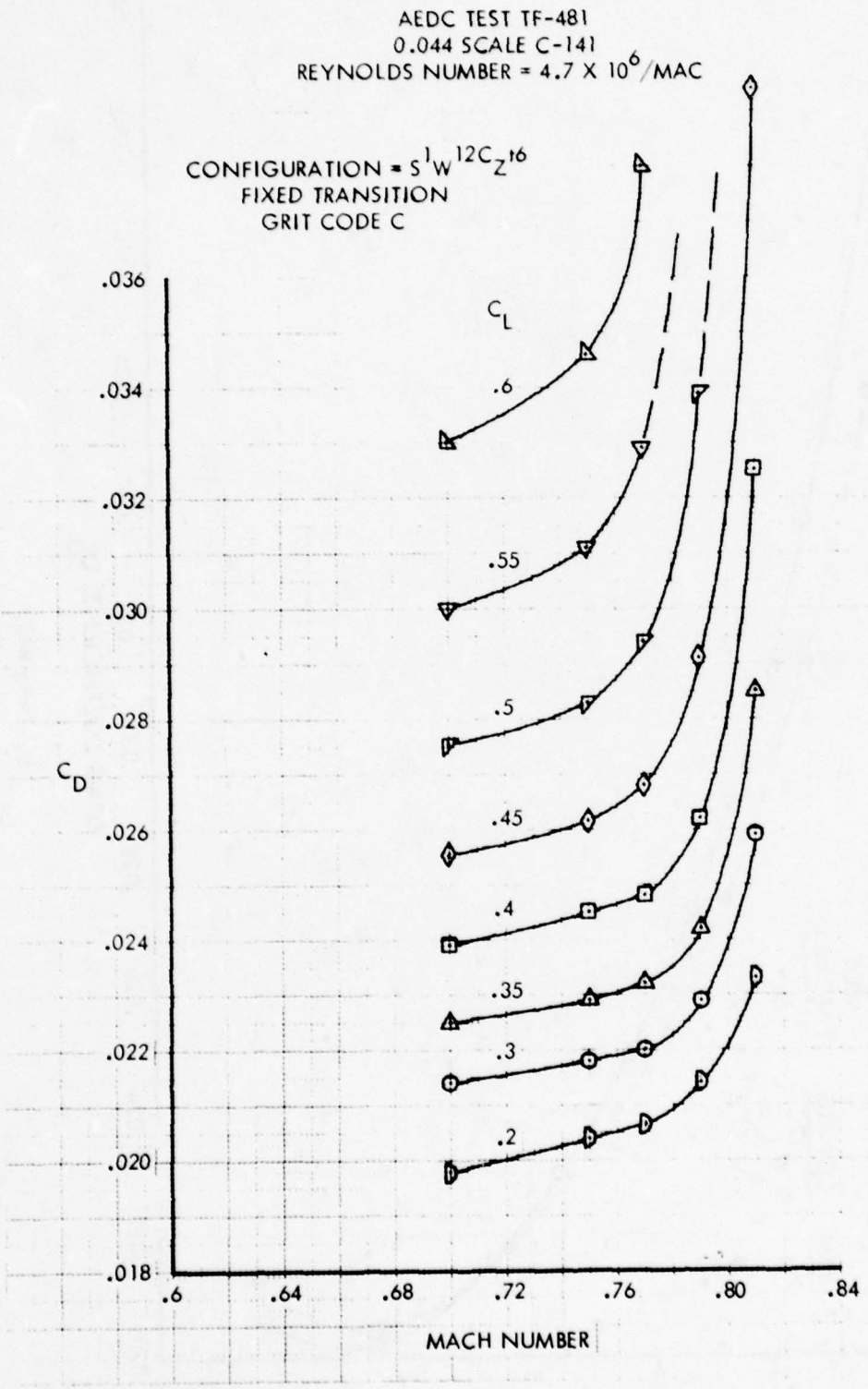

Figure 48. Drag Rise Characteristics for Baseline Wing Plus Swept Tips, Grit Code C

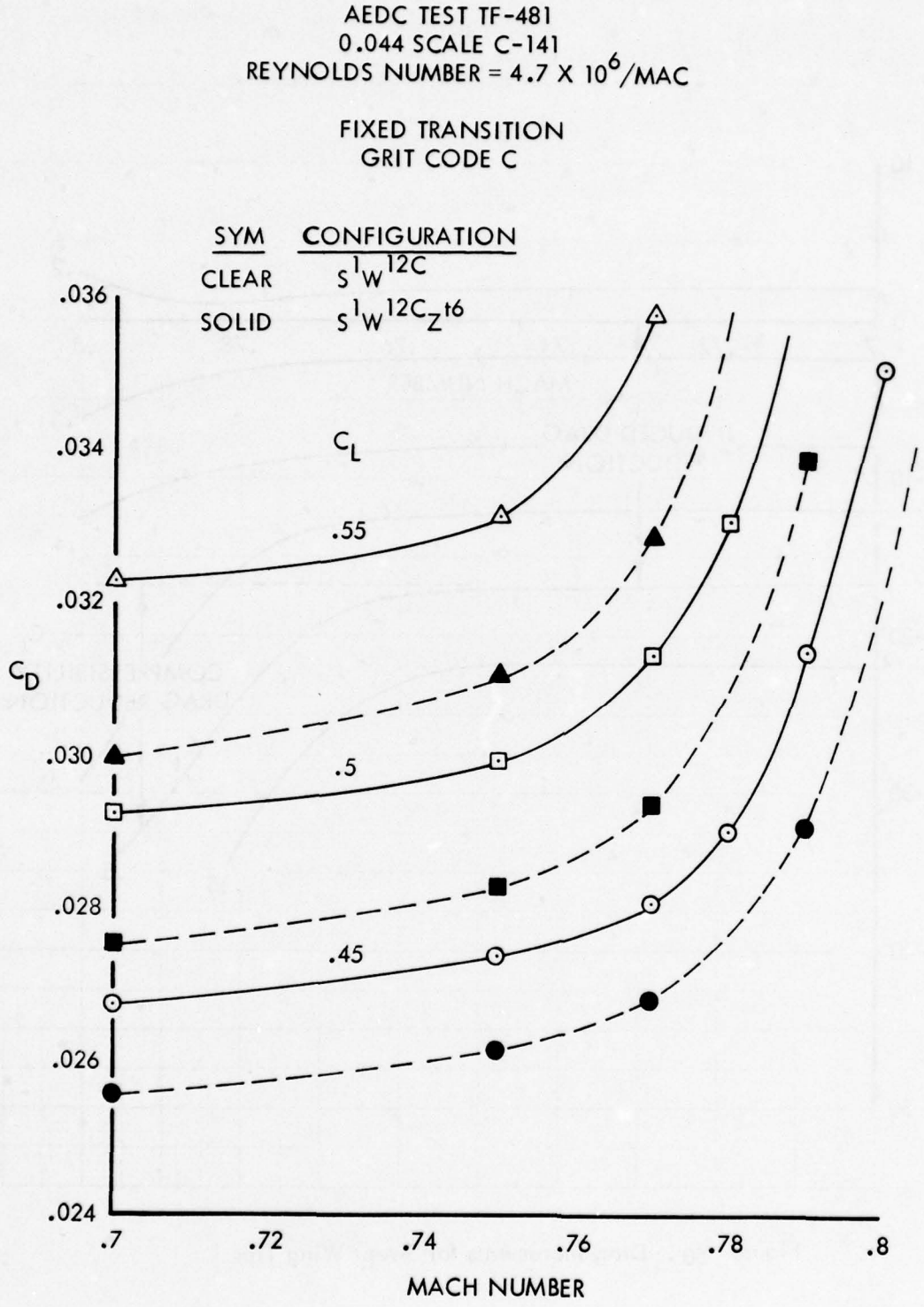

Figure 49. Effect of the Swept Tips on Drag Rise Characteristics

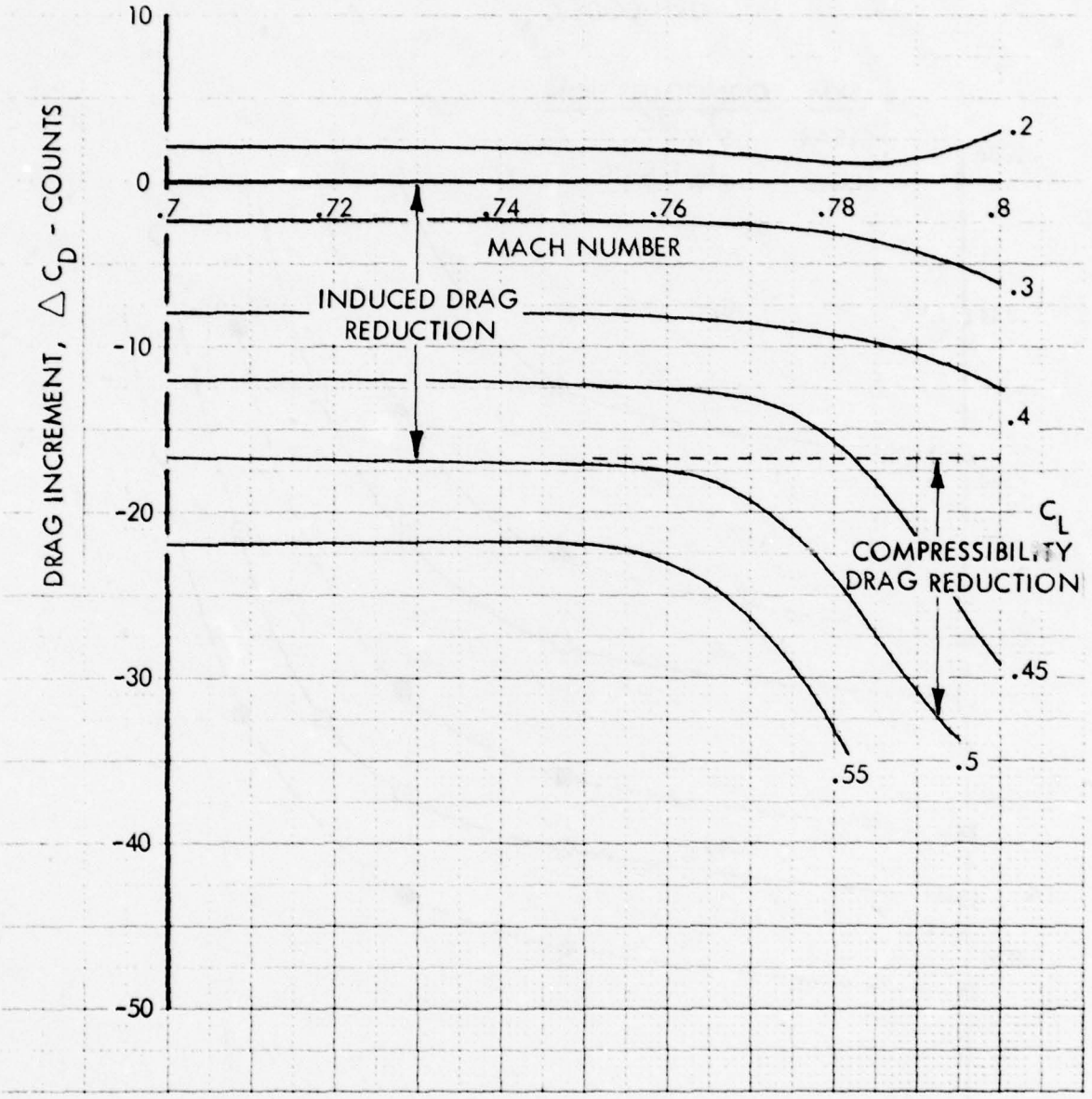

Figure 50. Drag Increments for Swept Wing Tips

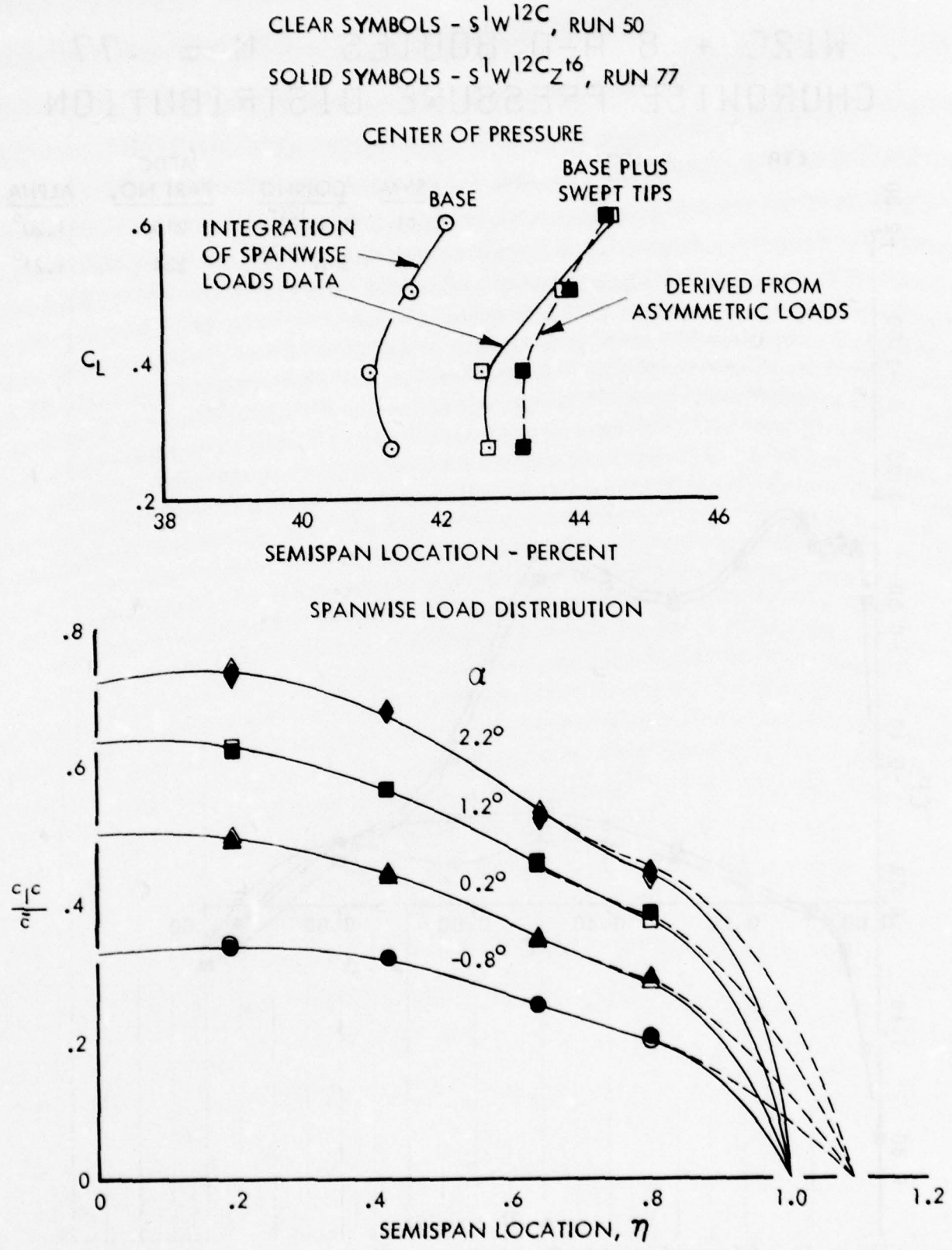

Figure 51. Effect of Swept Tips on Spanwise Load Distribution and Center of Pressure. M = 0.77.

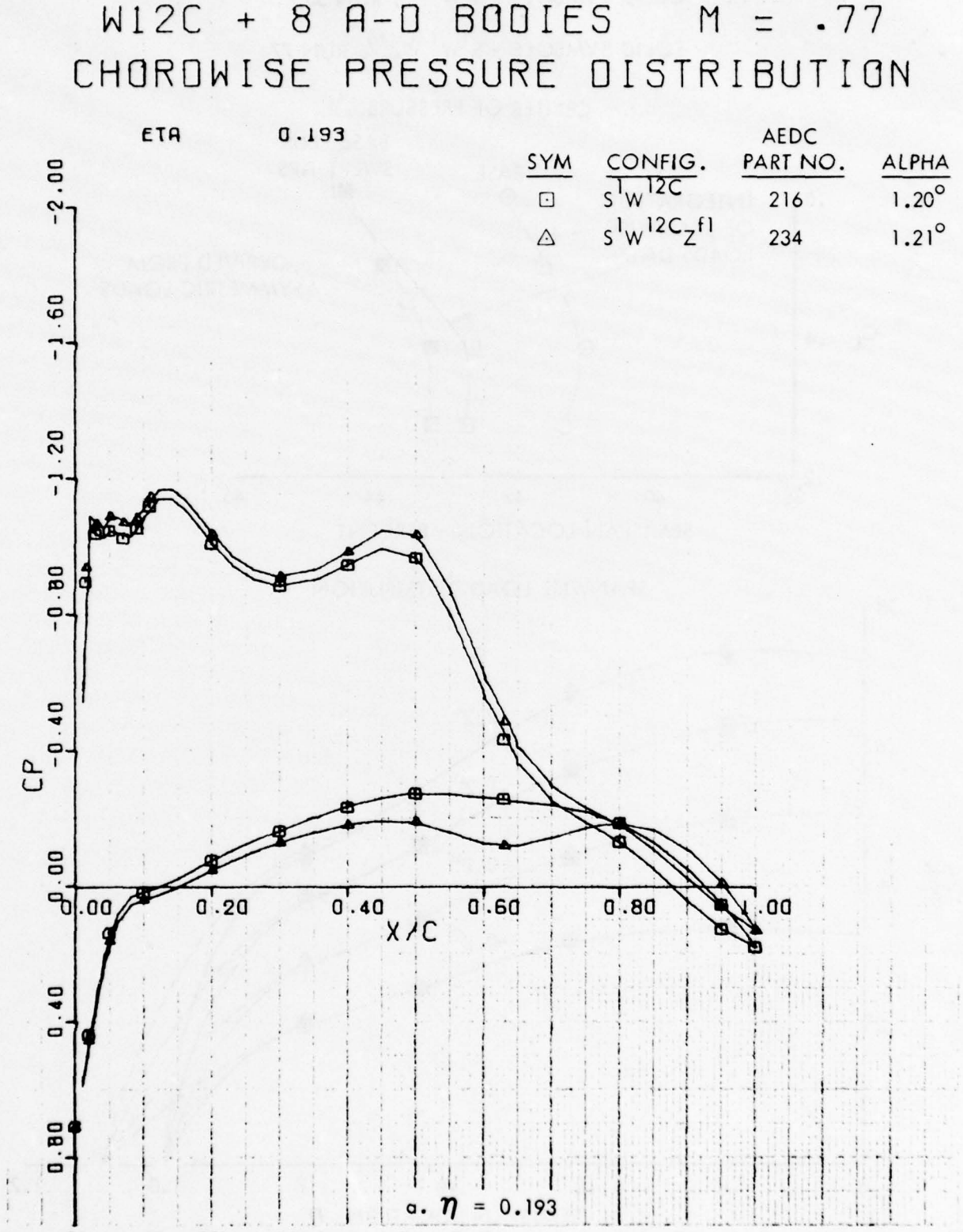

Figure 52 . Effect of Eight Anti-Drag Bodies on a Chordwise Pressure Distributions at Constant Alpha

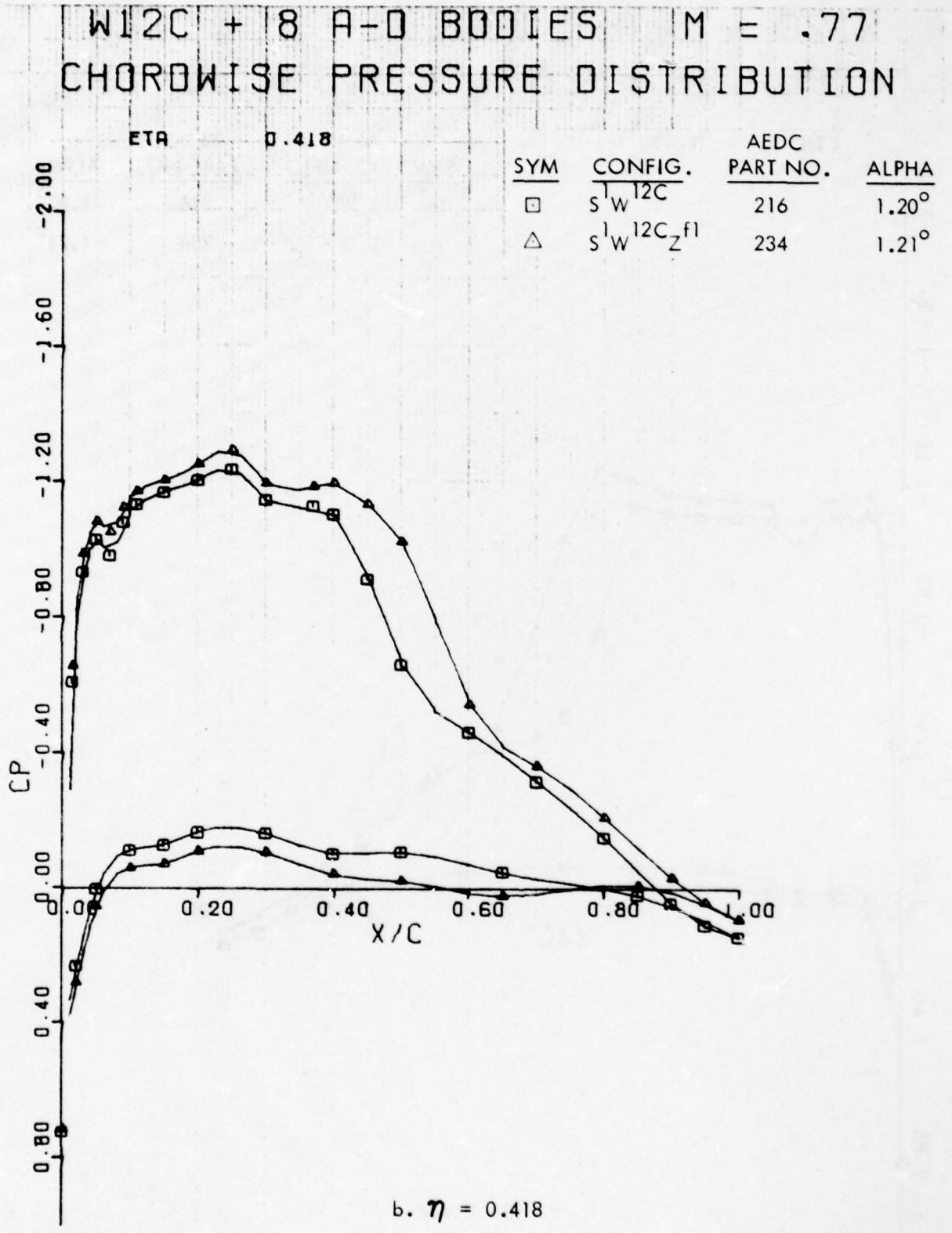

b. η = 0.418

Figure 52. Continued

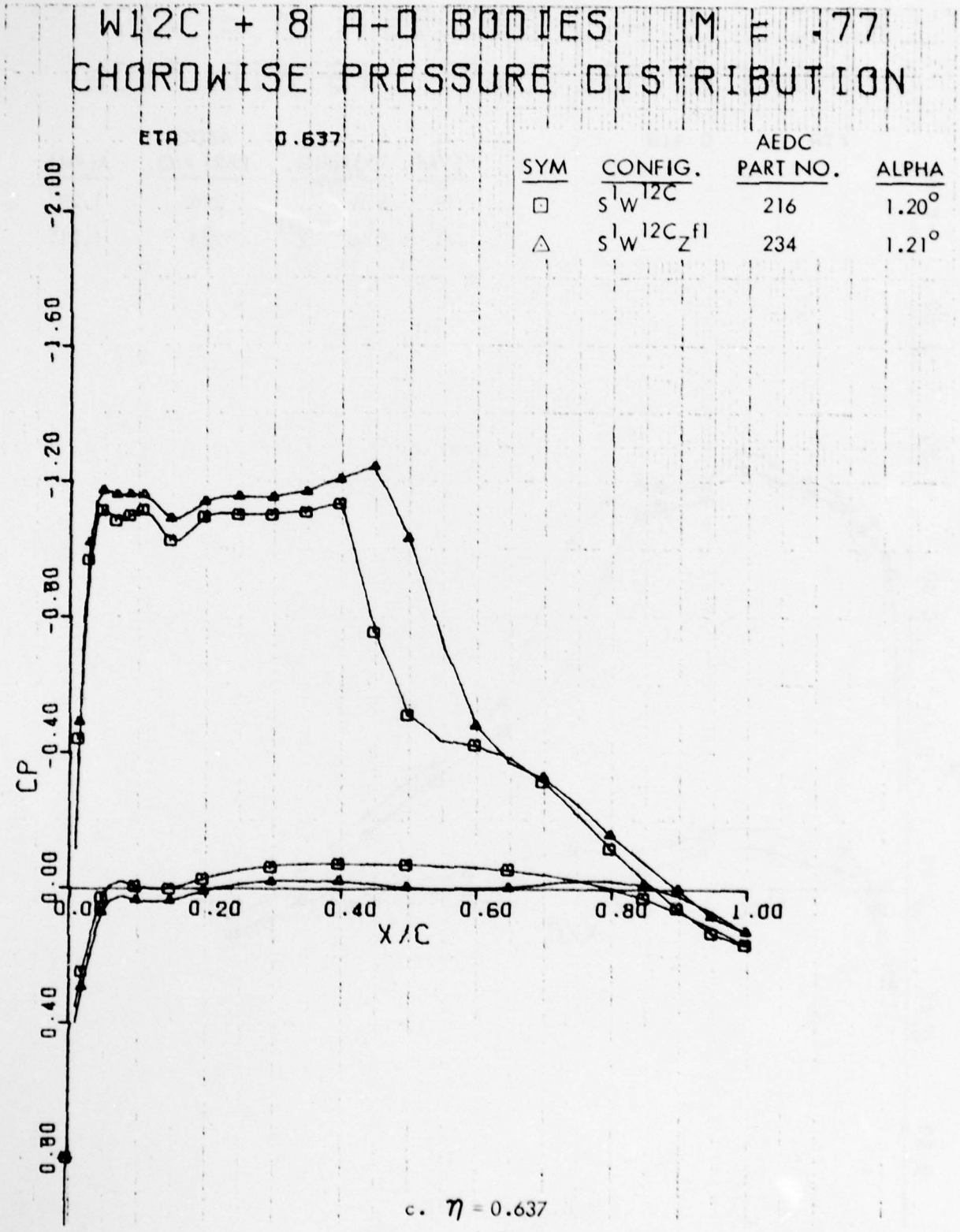

c. $\eta = 0.637$

Figure 52. Continued

W12C + 8 A-D BODIES M = .77
CHORDWISE PRESSURE DISTRIBUTION

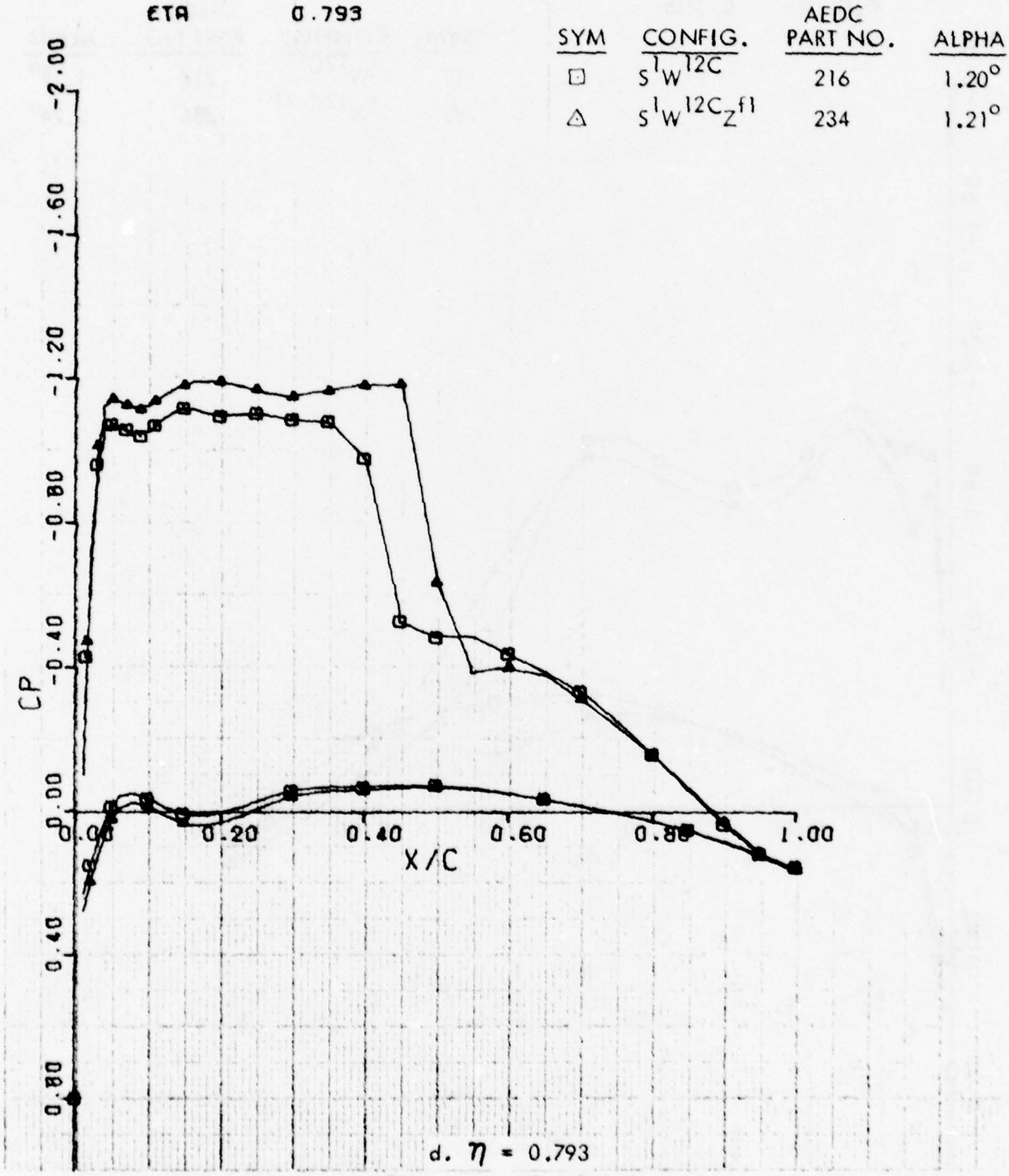

Figure 52 . Concluded

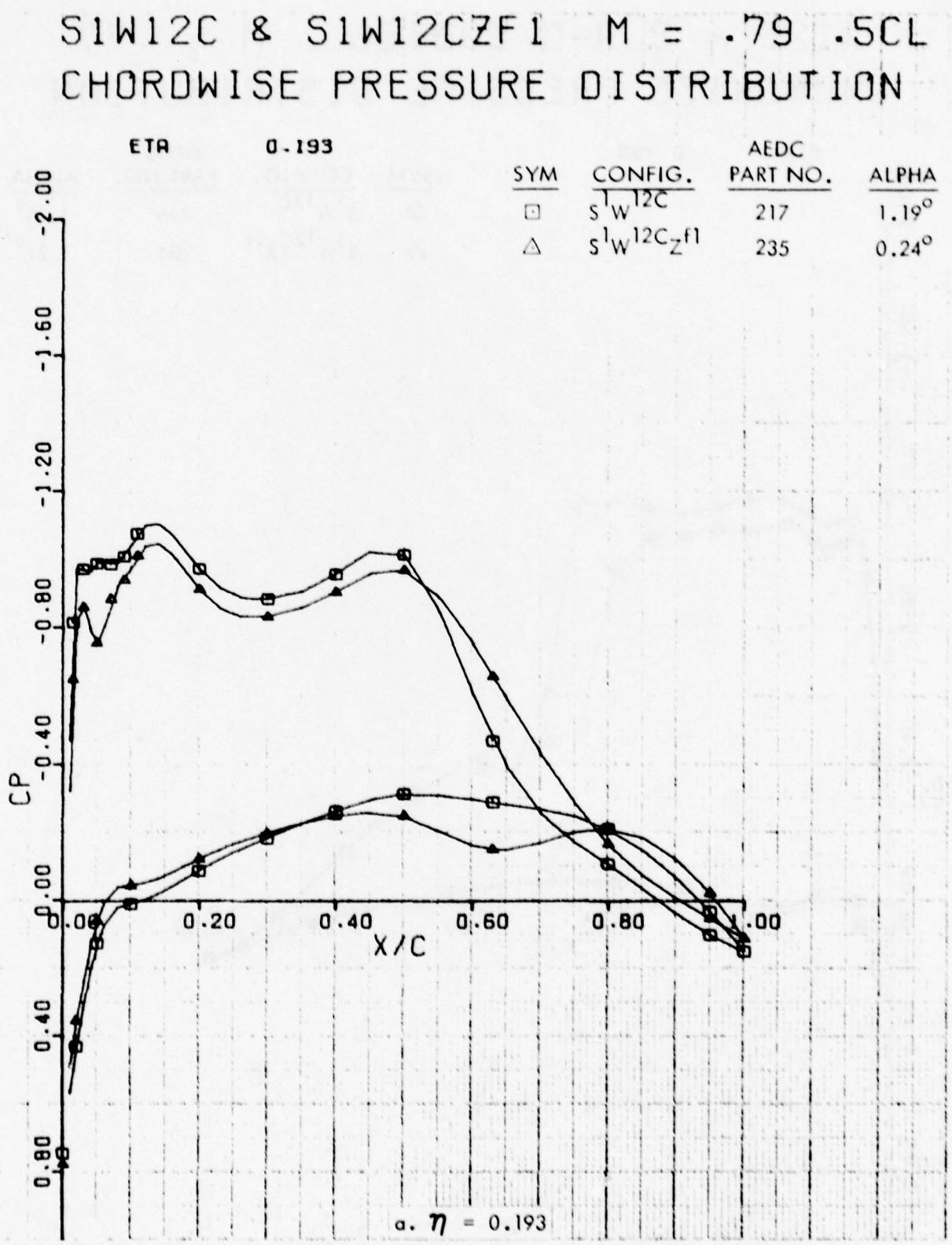

Figure 53. Effect of Eight Anti-Drag Bodies on Chordwise Pressure Distributions at Constant Lift

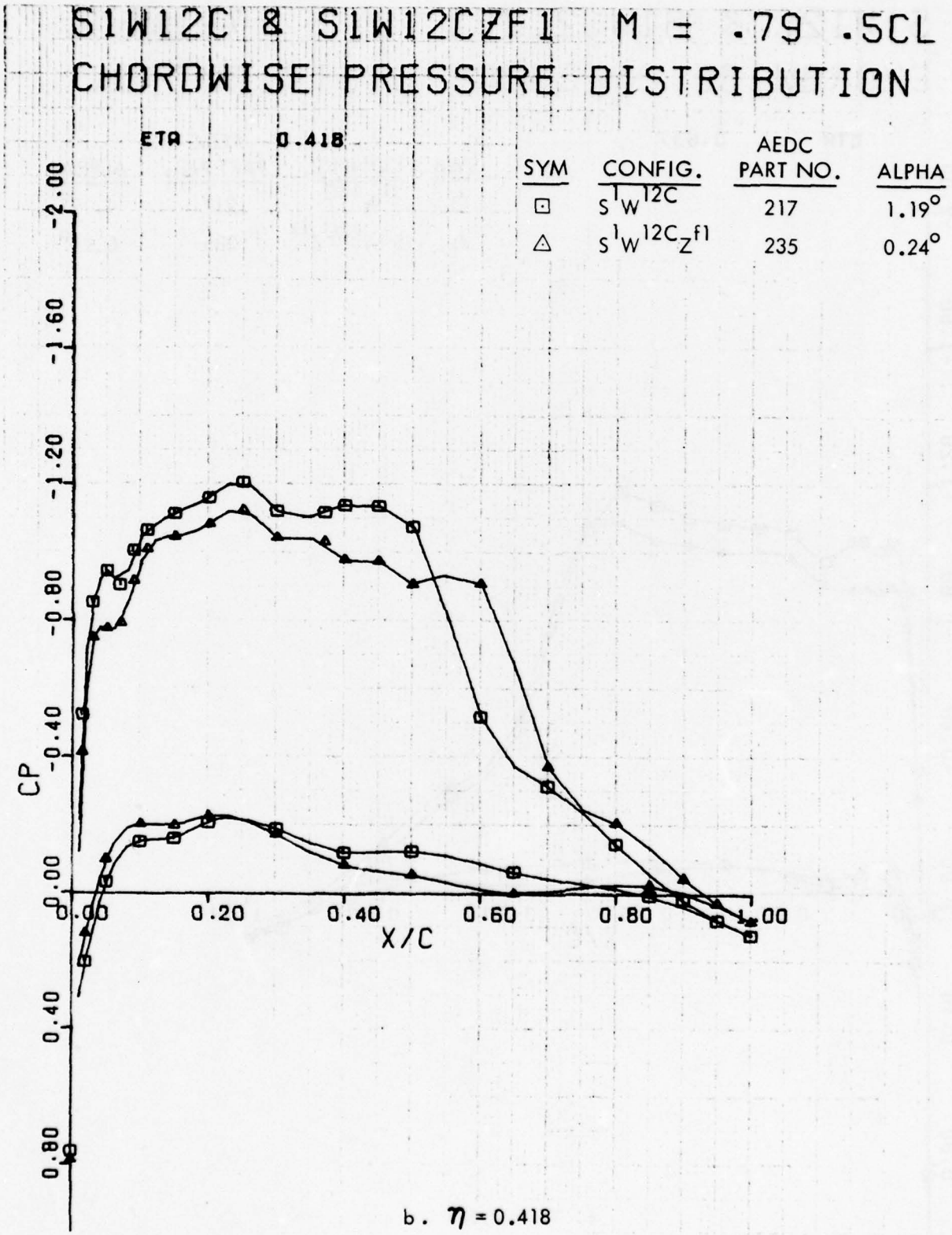

b. $\eta = 0.418$

Figure 53. Continued

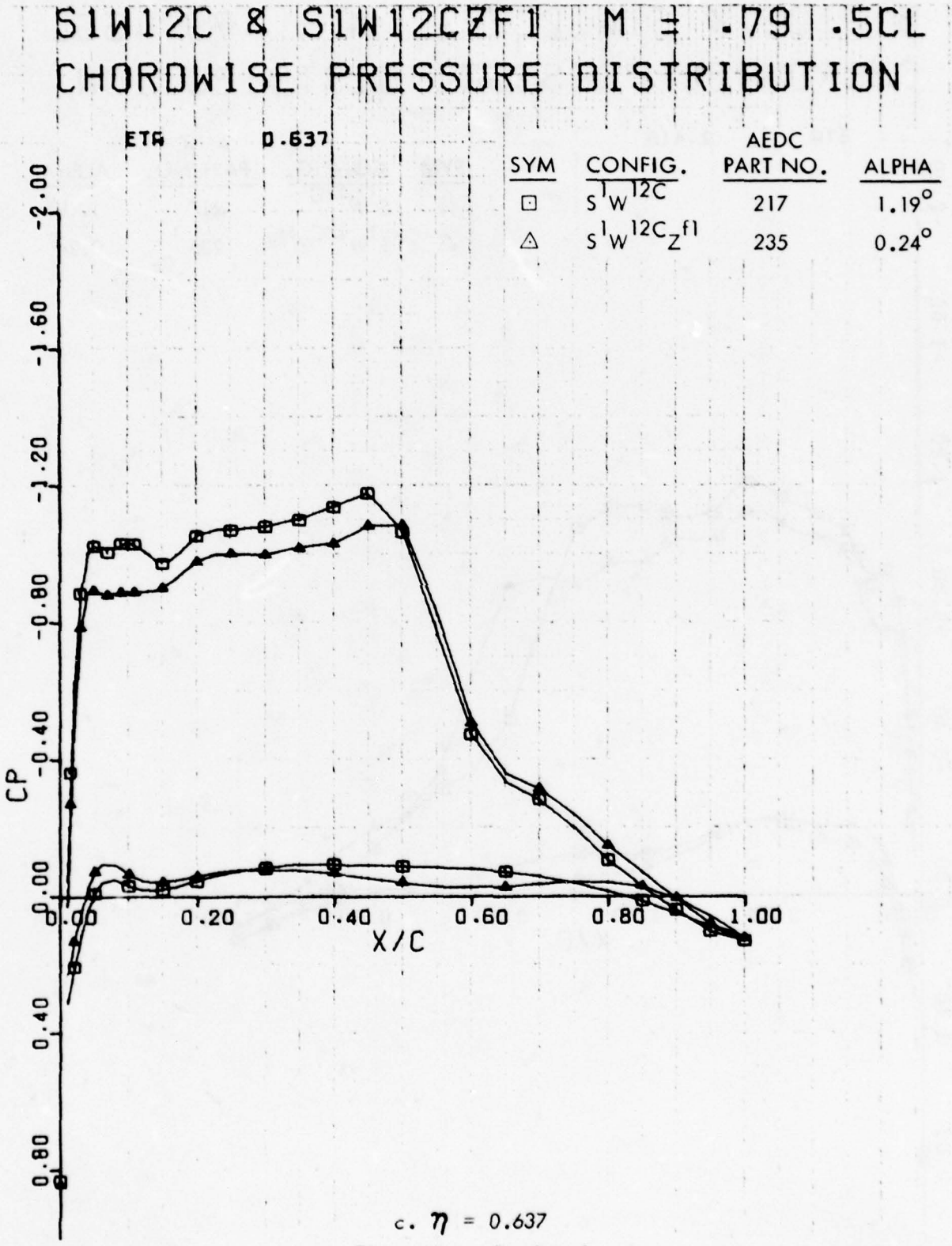

c. η = 0.637

Figure 53. Continued

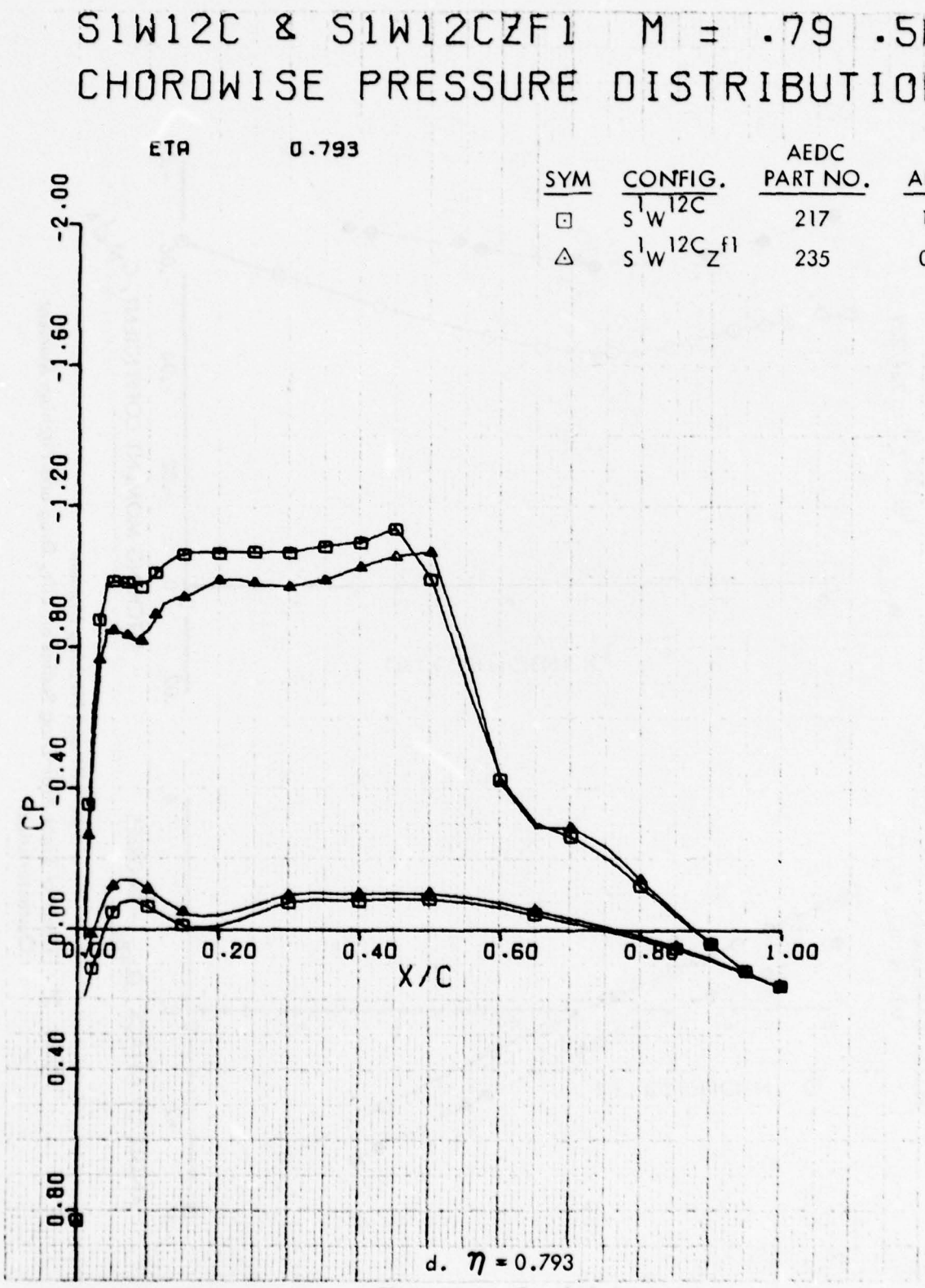

Figure 53. Concluded

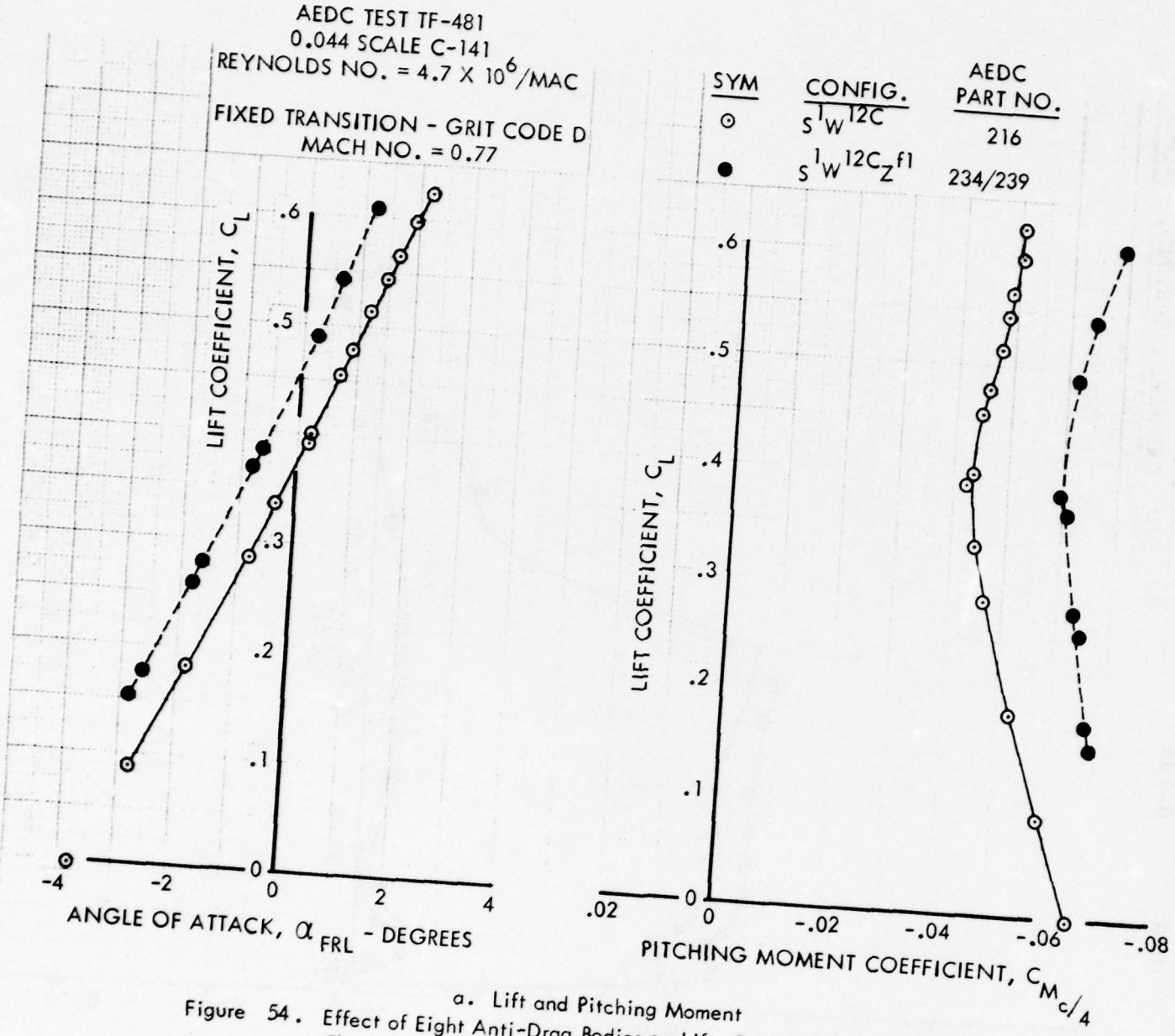

a. Lift and Pitching Moment

Figure 54. Effect of Eight Anti-Drag Bodies on Lift, Drag and Pitching Moment Characteristics

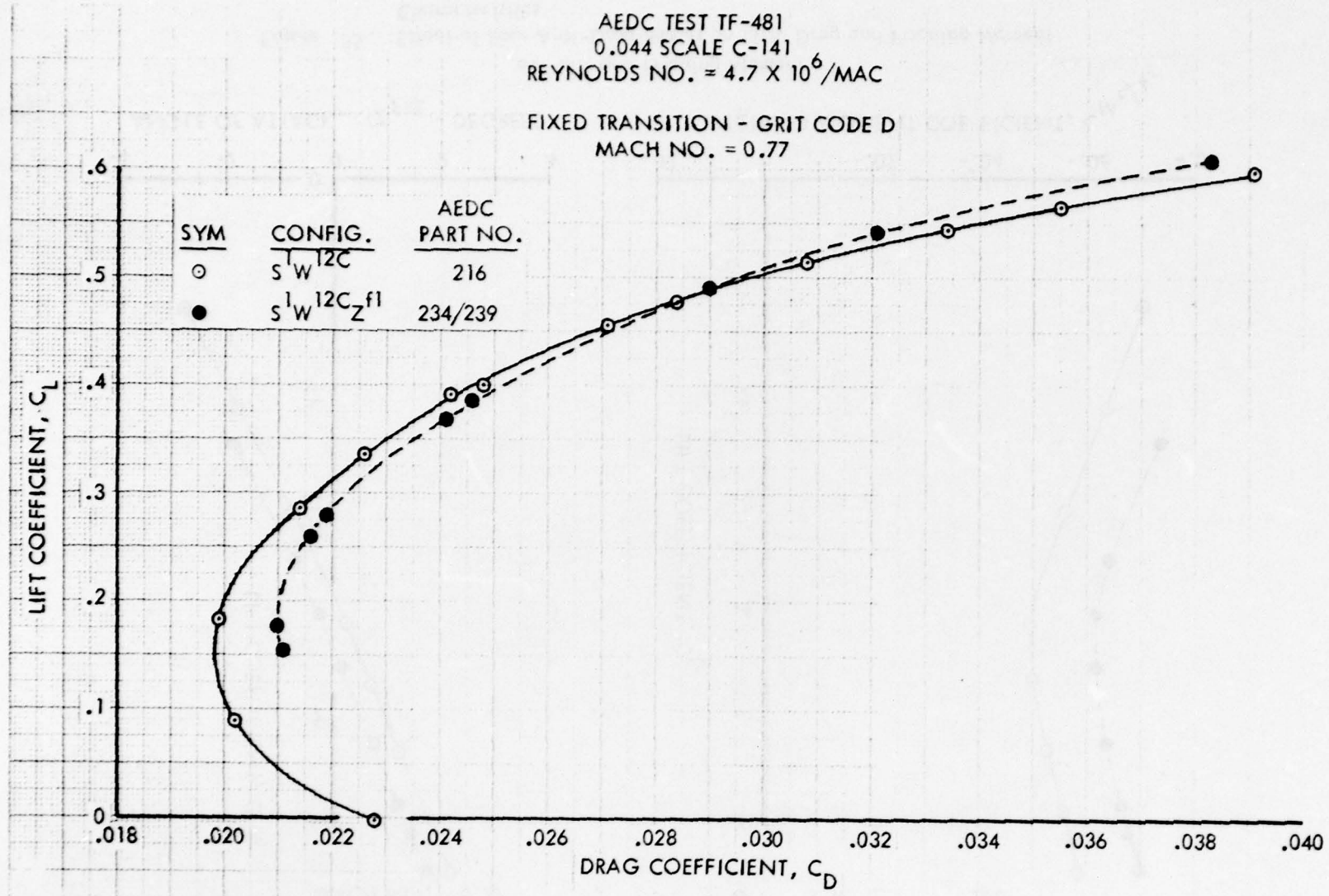

b. Drag Polar

Figure 54. Concluded

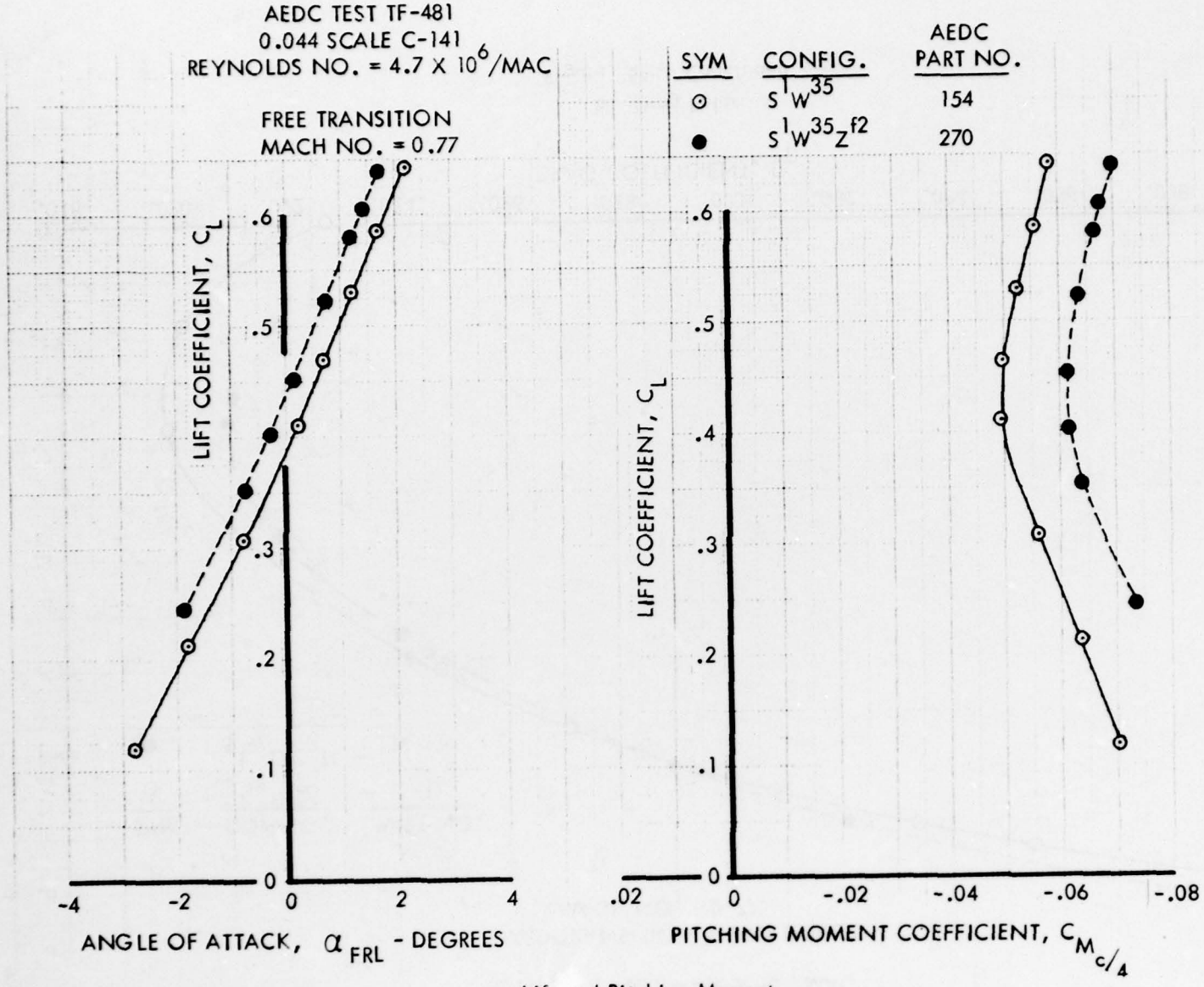

a. Lift and Pitching Moment

Figure 55. Effect of Four Anti-Drag Bodies on Lift, Drag and Pitching Moment Characteristics

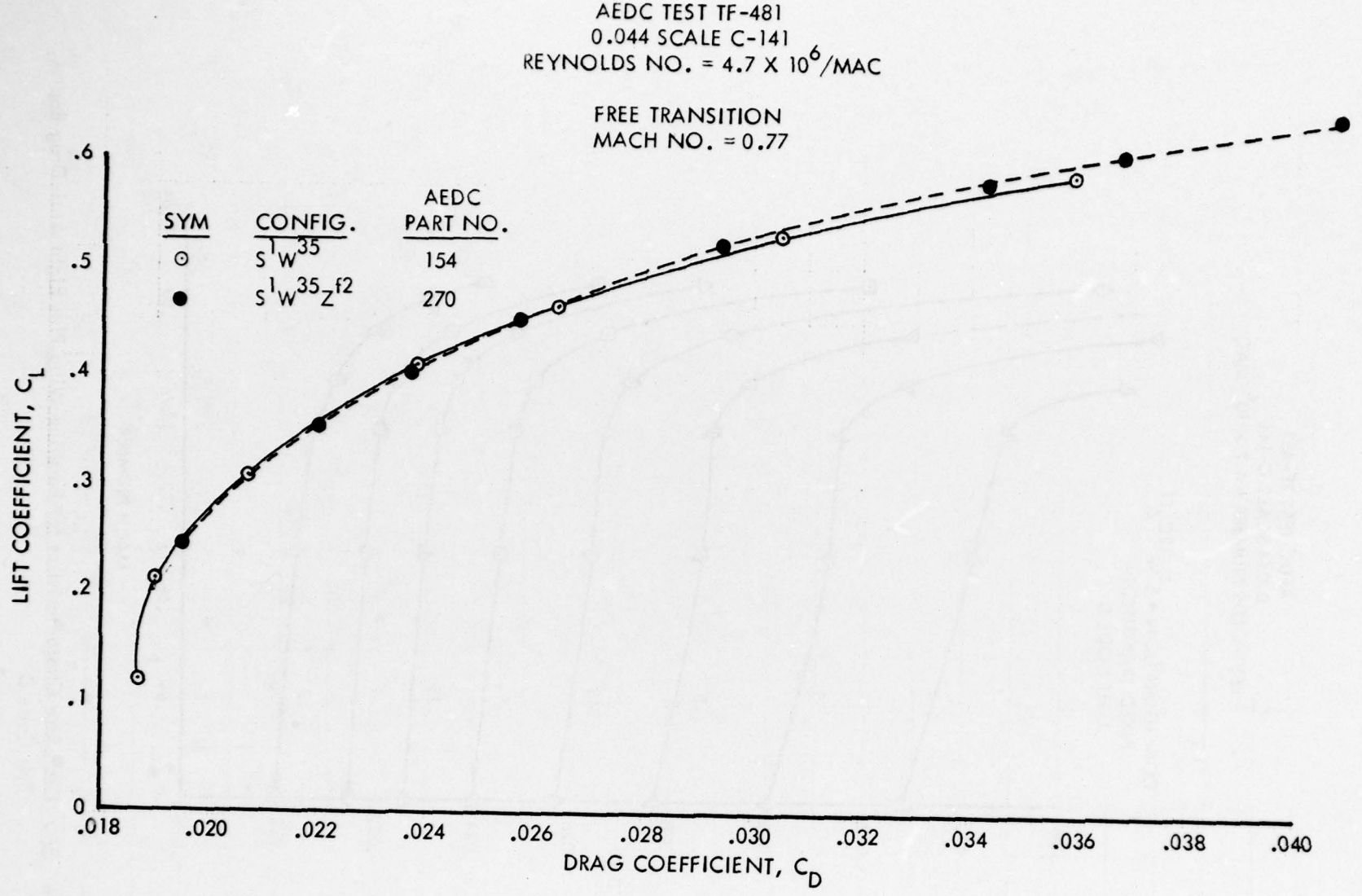

b. Drag Polar

Figure 55. Concluded

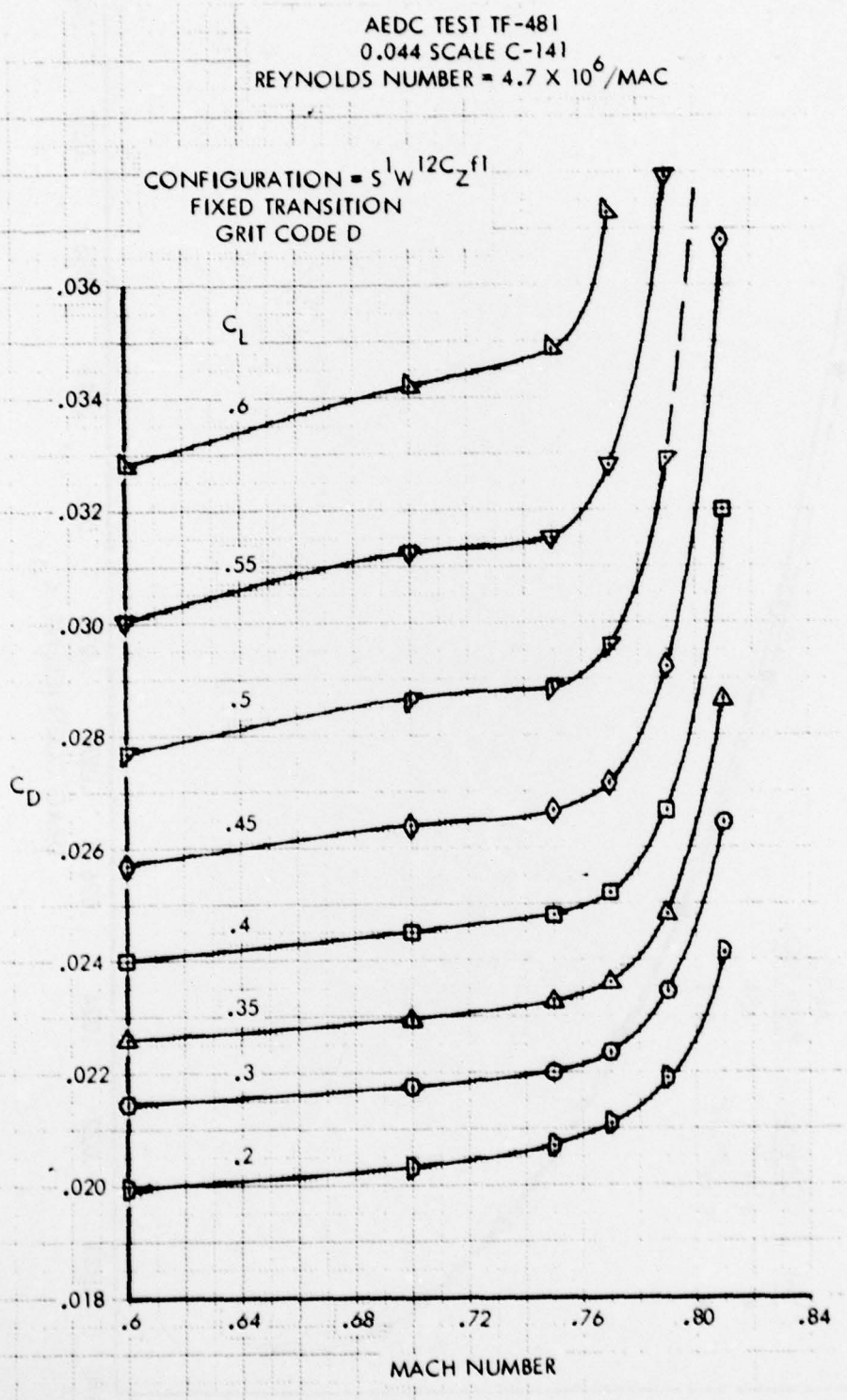

Figure 56. Drag Rise Characteristics for Baseline Wing Plus Eight Anti-Drag Bodies, Grit Code D

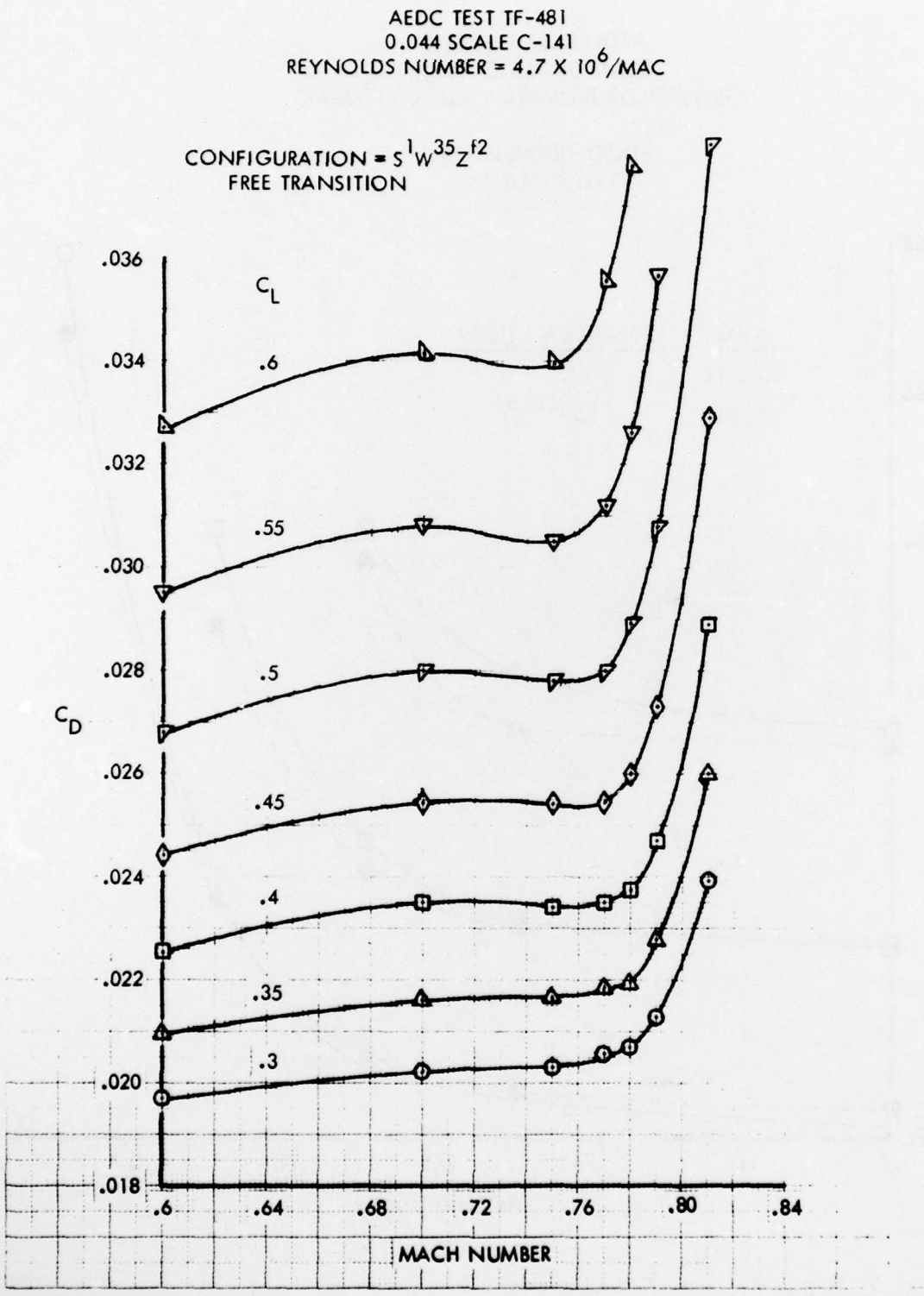

Figure 57 . Drag Rise Characteristics for W^{35} Plus Four Anti-Drag Bodies

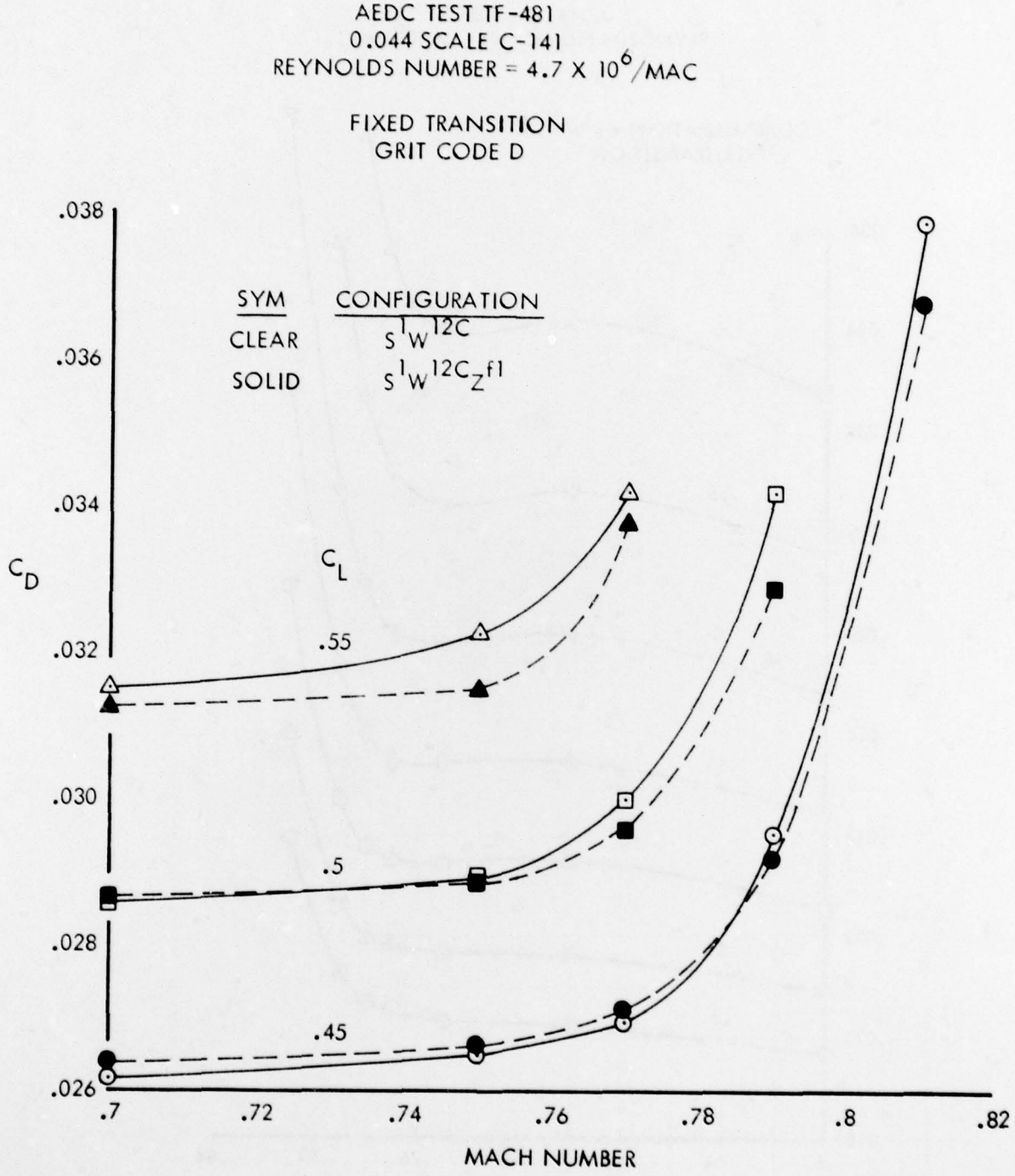

Figure 58. Effect of Eight Anti-Drag Bodies on Drag Rise Characteristics

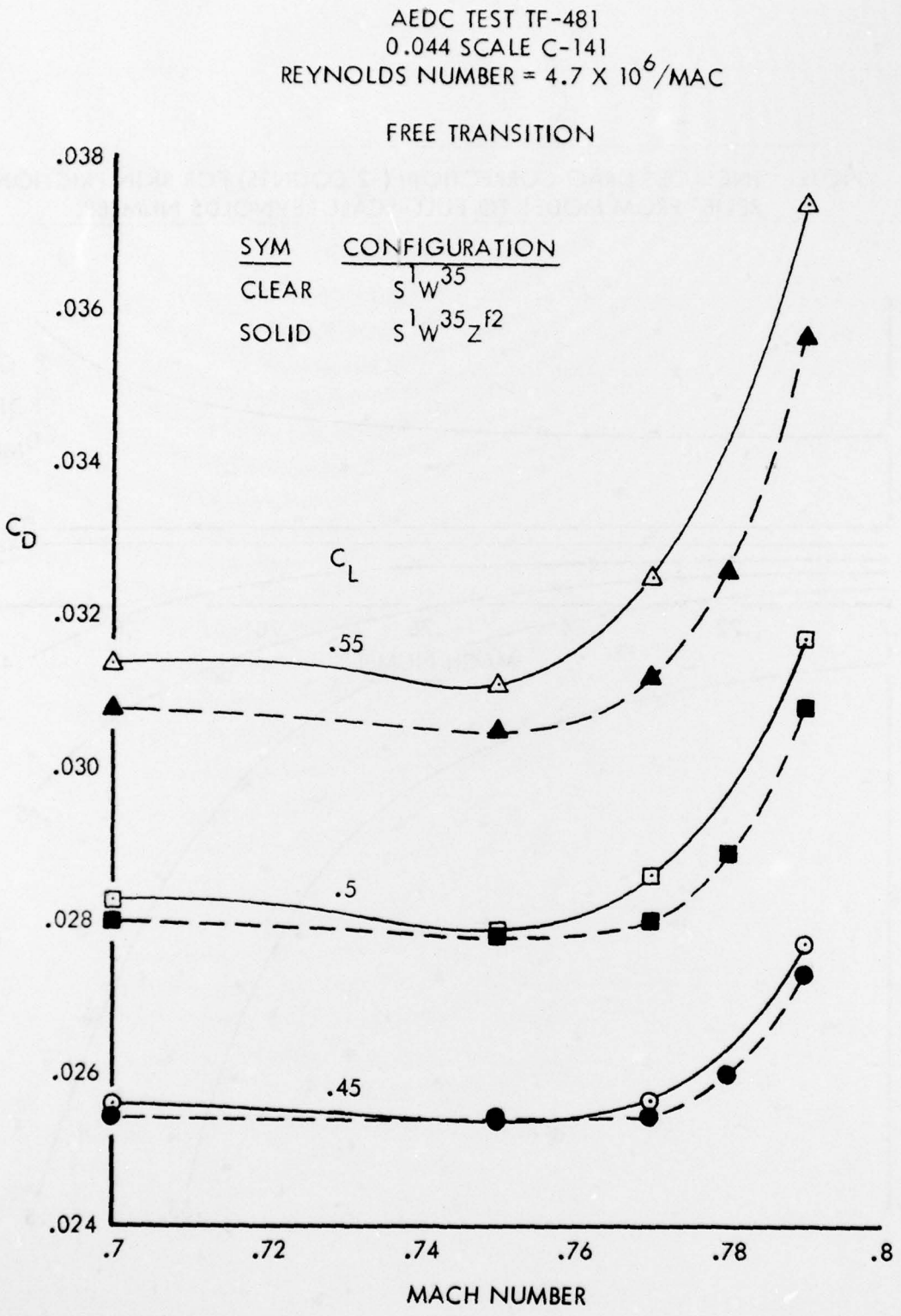

Figure 59. Effect of Four Anti-Drag Bodies on Drag Rise Characteristics

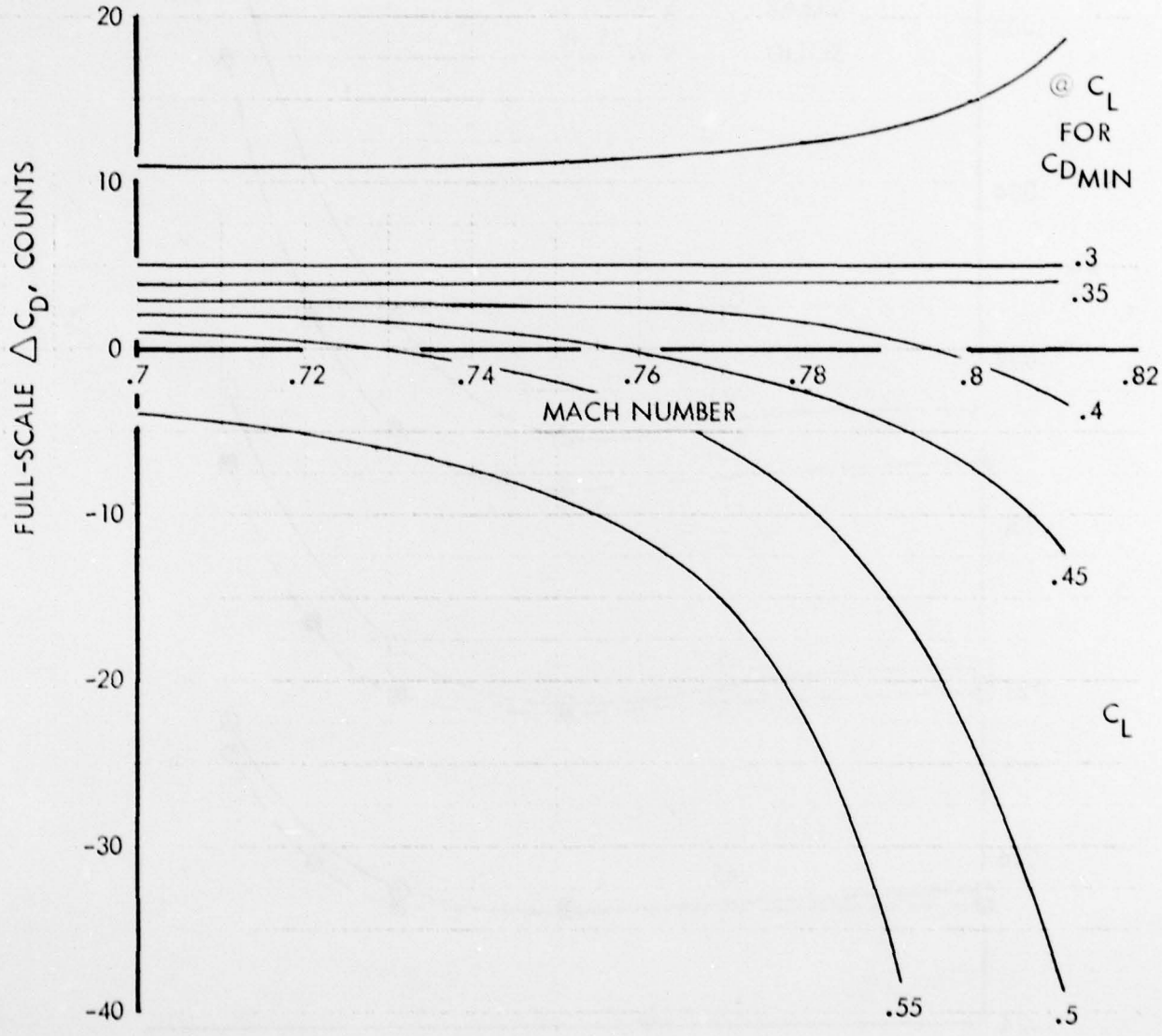

Figure 60 . Full-Scale Drag Increments for Eight Anti-Drag Bodies

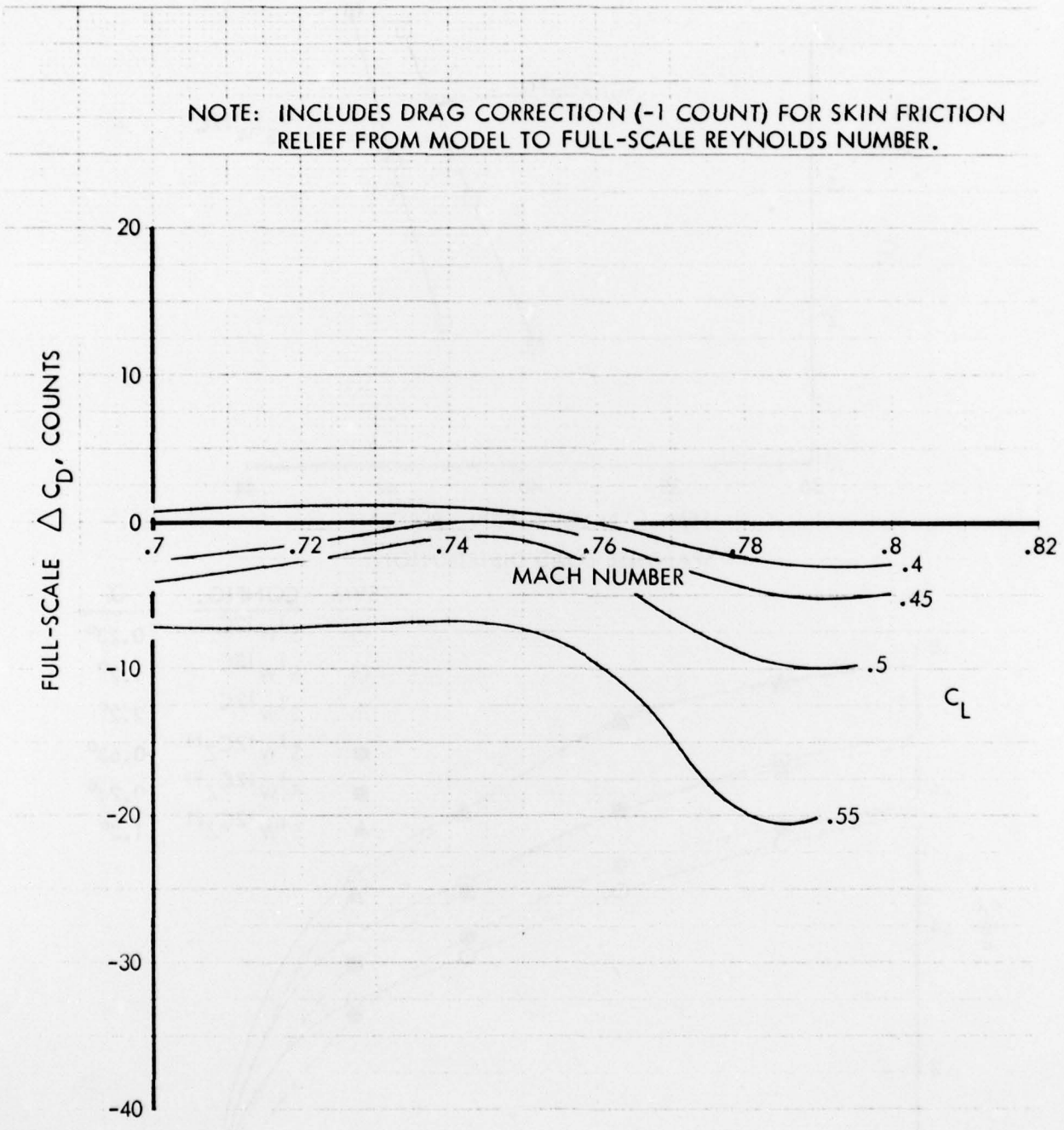

Figure 61. Full-Scale Drag Increments for Four Anti-Drag Bodies

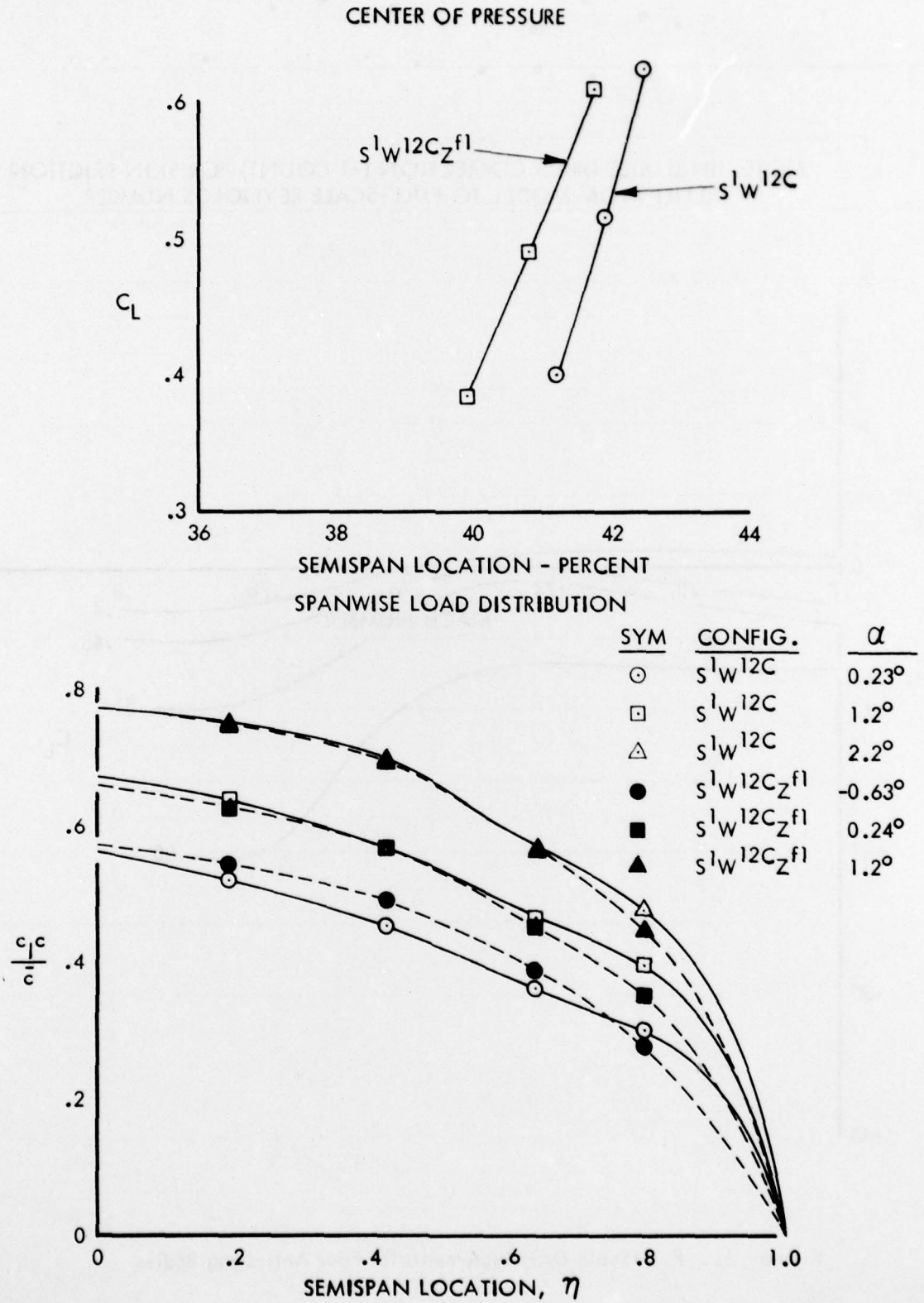

Figure 62. Effect of Anti-Drag Bodies on Spanwise Load Distribution and Center of Pressure. M = 0.77.

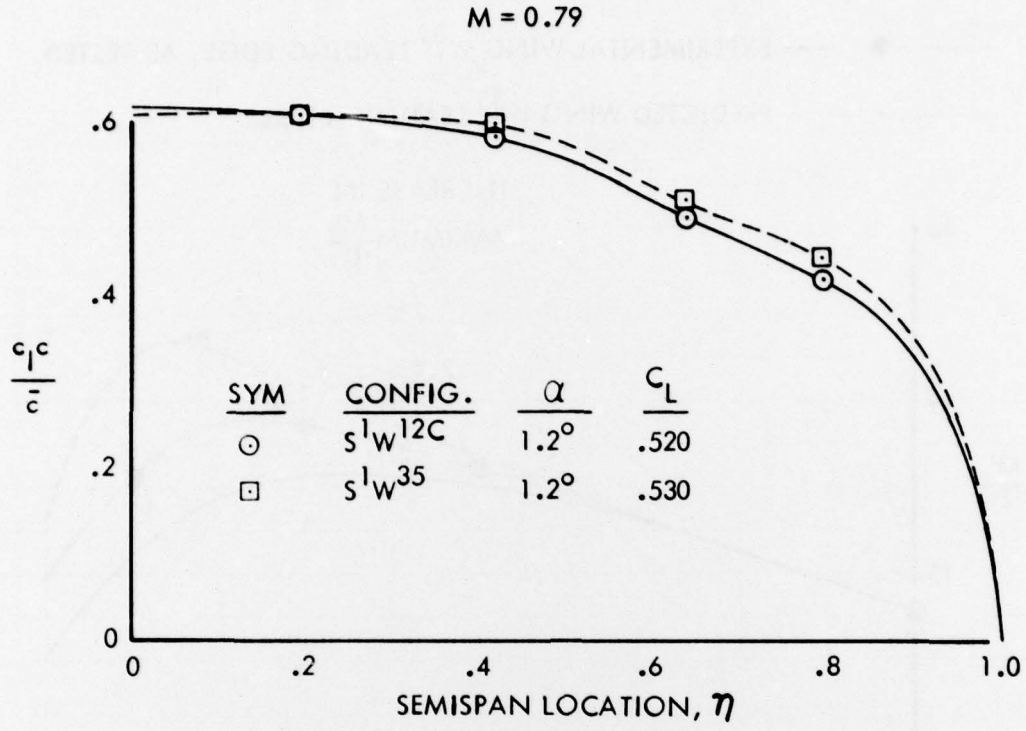

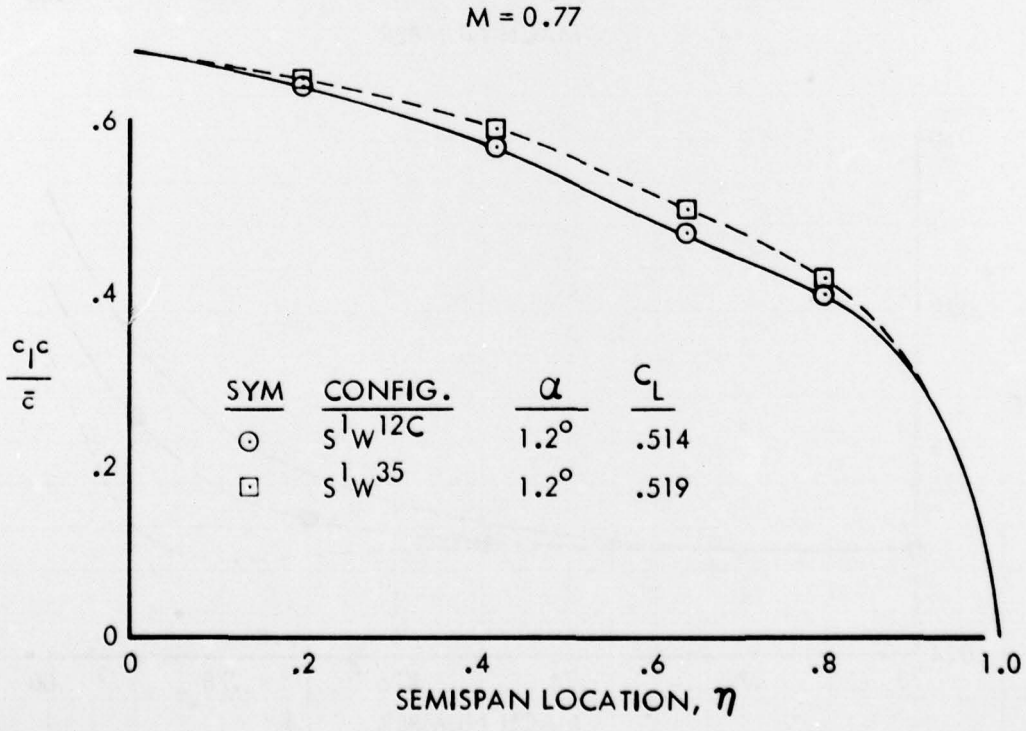

Figure 63. Effect of Leading Edge Modification on Spanwise Load Distribution

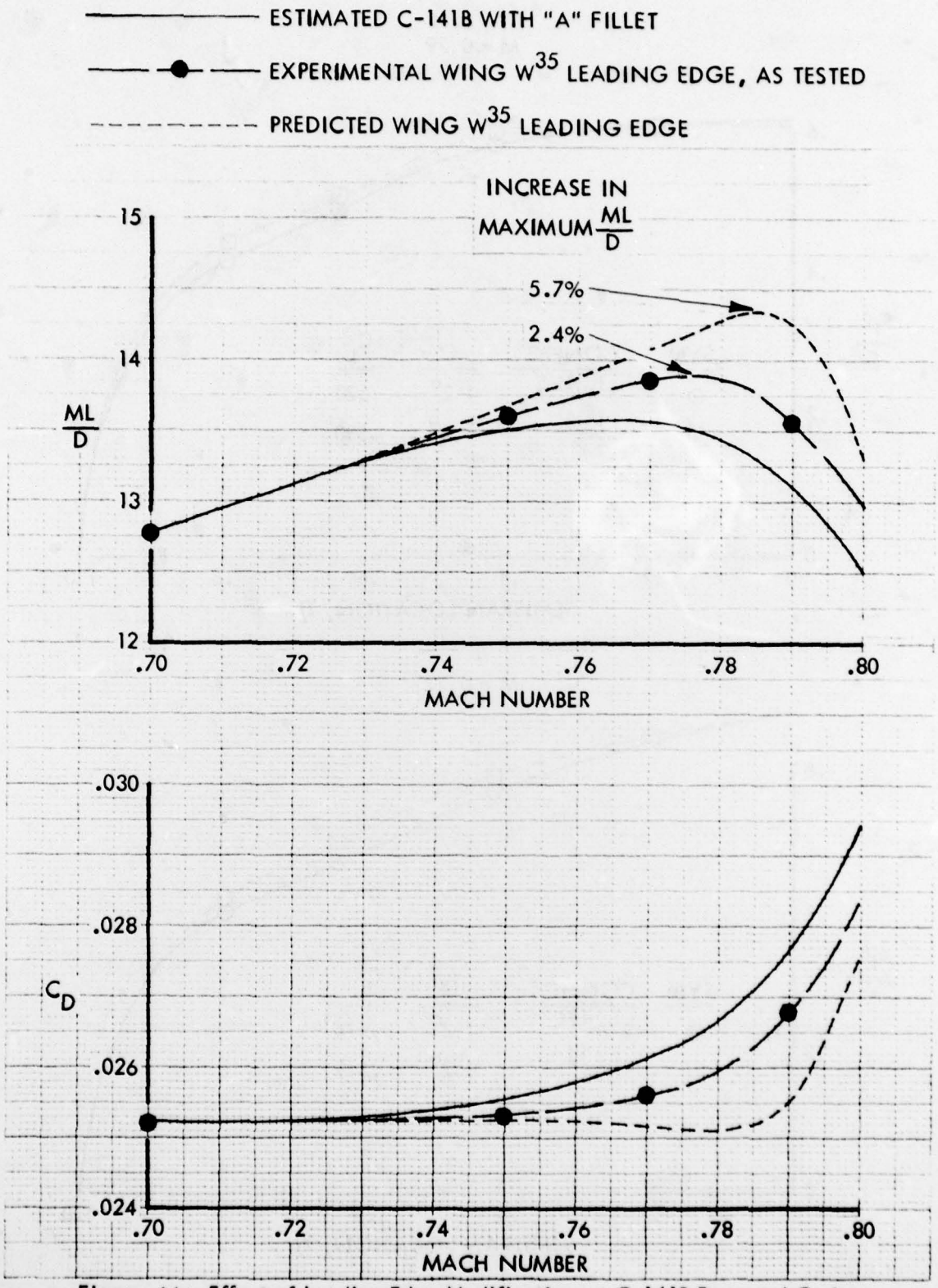

Figure 64. Effect of Leading Edge Modification on C-141B Drag and Cruise Range Parameter at Trim $C_L = 0.46$

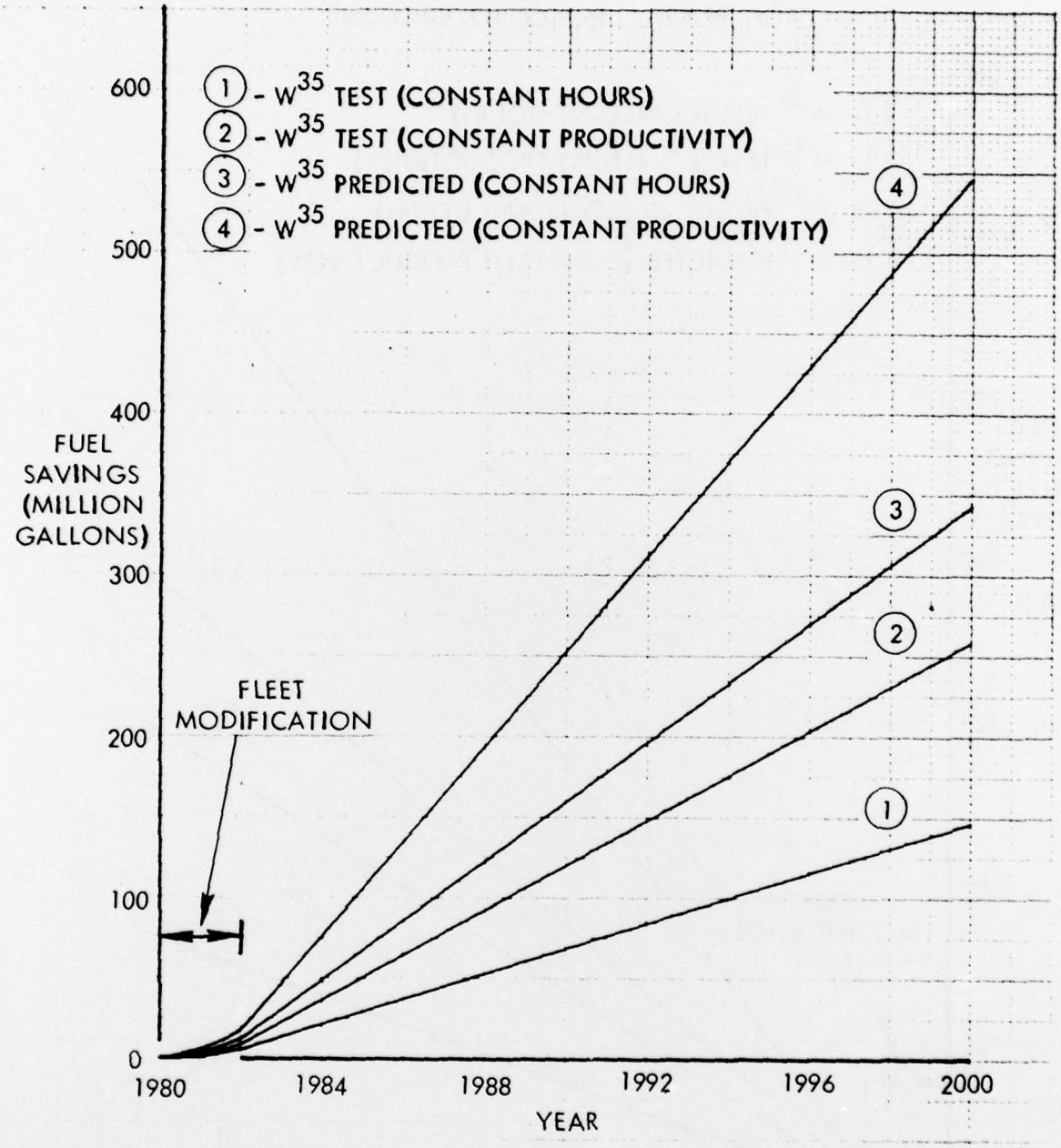

Figure 65. Projected Fuel Savings for Leading Edge Modification

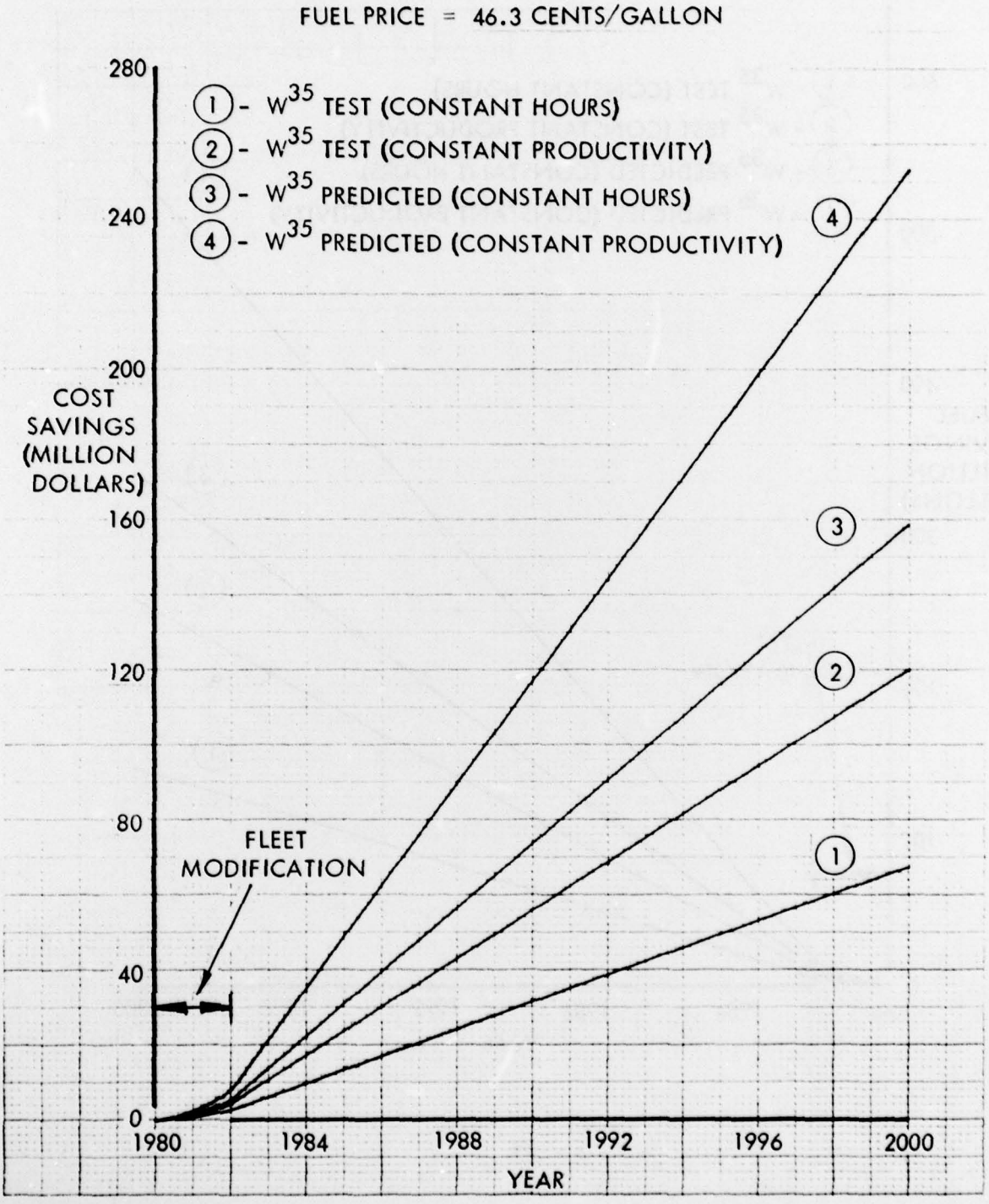

Figure 66. Projected Cost Savings for Leading Edge Modification

REFERENCES

1. F. Bauer, P. Garabedian, D. Korn, and A. Jameson, Supercritical Wing Sections II. Lecture Notes in Economics and Mathematical Systems, Vol. 108, Springer-Verlag, New York, 1975.

2. R. M. Hicks and G. N. Vanderplaats, Design of Low-Speed Airfoils by Numerical Optimization, SAE Business Aircraft Meeting, Wichita, April 1975.

3. R. M. Hicks, J. P. Mendoza, and A. Bandettini, "Effects of Forward Contour Modification on the Aerodynamic Characteristics of the NACA 64-212 Airfoil Section," NASA TM X-3243, September 1975.

4. L. A. Carlson, "TRANDES: A Fortran Program for Transonic Airfoil Analysis or Design," NASA CR-2821, June 1977.

5. R. M. Hicks and G. N. Vanderplaats, "Application of Numerical Optimization to the Design of Supercritical Airfoils without Creep Drag," SAE Paper 770440, April 1977.

6. G. H. Vanderplaats, "CONMIN - A Fortran Program for Constrained Function Minimization - User's Manual," NASA TMX-62282, August 1973.

7. J. M. Wright, "Development of Testing Technique Required to Duplicate Full Scale Wing Shock Location on a Wind Tunnel Model, Lockheed-Georgia Company Report LG1T6-1-16, May 1966.

8. R. M. Hicks, and P. A. Henne, "Wing Design by Numerical Optimization," AIAA Paper No. 77-1247, August 1977.

9. A. Jameson, "Iterative Solution of Transonic Flows Over Airfoils and Wings," Communications Pure Applied Math, Vol. 27, pp. 283-309, 1974.

10. A. L. Braslow, R. M. hicks and R. V. Harris, Jr., "Use of Grit-Type Boundary-Layer-Transition Trips on Wind Tunnel Models," NASA TN D-3579, 1966.

11. F. J. Keeney, Some Boundary Layer Flow Visualization Techniques Applicable to Large Continuous Wind Tunnels, University of Tennessee Thesis, December 1973.

12. C. J. Spurlin, "Documentation of Wind Tunnel Test Data from the AFFDL C-141B Wing Test," AEDC-DR-79-43, May 30, 1978.

13. R. J. Hart, A. W. Davis and P. C. Connor," YC-141B Preliminary Performance Substantiating Data Report Based on Phase I and II Flight Test Data," Addendum II to Lockheed-Georgia Company ER 8330, October 17, 1977.

☆U.S.Government Printing Office: 1979 — 657-002/116